UNIVERSITY OF SOUTHAMPTON
FACULTY OF PHYSICAL SCIENCES AND ENGINEERING
SCHOOL OF ELECTRONICS AND COMPUTER SCIENCE

Hybrid Automatic Repeat Request Assisted Cognitive Radios

by

Ateeq Ur Rehman
B.Eng

A doctoral thesis submitted in partial fulfilment of the
requirements for the award of Doctor of Philosophy
at the University of Southampton

November 2016

SUPERVISOR:
Prof. Lie-Liang Yang
BEng, MEng, FIET, FIEEE
and
Prof. Lajos Hanzo
FREng, FIEEE, FIET, EIC, EIC of IEEE Press, FEURASIP
Chair of Southampton Wirelss Group
School of Electronics and Computer Science
University of Southampton
Southampton SO17 1BJ
United Kingdom

𝔇edicated to my Grandmother

UNIVERSITY OF SOUTHAMPTON

ABSTRACT

FACULTY OF PHYSICAL SCIENCES AND ENGINEERING
SCHOOL OF ELECTRONICS AND COMPUTER SCIENCE

Doctor of Philosophy

Hybrid Automatic Repeat Request Assisted Cognitive Radios

by Ateeq Ur Rehman

It is widely known that the Cognitive Radio (CR) paradigm has the potential of improving the exploitation of the earmarked but momentarily unoccupied spectrum, which is exclusively allocated to the primary users (PUs) based on the conventional fixed spectrum allocation policy. The CR systems first have to sense, whether the PU's band is unoccupied and then dynamically access it. Naturally, CR systems suffer from the same propagation impairments as the traditional wireless communication systems, such as interference, fading and noise, which affect both the reliability and the attainable data rate. In order for the CR system to achieve both reliable data transmission as well as a high throughput and low delay, we propose novel CR-aided Hybrid Automatic Repeat Request (HARQ) protocols, which intrinsically amalgamate the CR functions with HARQ protocols and study their performance. Both perfect and imperfect spectrum sensing are considered.

Specifically, we propose the cognitive stop-and-wait-HARQ (CSW-HARQ), cognitive Go-Back-N-HARQ (CGBN-HARQ) as well as the cognitive selective-repeat (CSR-HARQ) schemes and study their throughput and delay both by analysis and simulation. To protect the PUs legal rights, we model their activity of occupying a primary radio (PR) channel as a two-state Markov chain consisting of 'ON' and 'OFF' states. In order to use the PR channel, the CR system first senses the presence of the PUs and once the PR channel is found to be free (i.e., in the OFF state), the CR system transmits its data packets relying on the principles of SW-HARQ, GBN-HARQ and SR-HARQ. Otherwise, the CR system continues sensing the channel until finding a free one. Naturally, the PR channel may be sensed erroneously, which results either in false alarm or in mis-detection. Therefore, the channel may be modelled by a two-state Markov chain, provided that sensing is ideal, or by a four-state Markov chain, if sensing is non-ideal. Here, the four states are determined by the actual state of the PR channel and the state sensed by the CR system. We analyse both the throughput and delay of CR systems relying on different HARQ schemes. We invoke a pair of analytical approaches, namely the probability based approach and the Discrete Time Markov Chain (DTMC) based approach. Closed-form expressions are derived for the throughput, average packet delay and the end-to-end packet delay. Furthermore, for the end-to-end packet delay, we derive both the probability distribution and the average end-to-end packet delay. In the DTMC-based approach, we propose a state generation algorithm for eliminating the illegitimate states, which helps reduce both the dimensionality of the related state transition matrices and the associ-

ated computational complexity. All the equations obtained by analysis are validated by numerical simulations.

Our performance results reveal that both the achievable throughput and delay of the CSW-HARQ, CGBN-HARQ and the CSR-HARQ schemes are substantially affected by the activity of the PUs, by the reliability of the PR channels, by the unreliable sensing decisions and by the number of packets transmitted per time-slot (TS). Specifically, when the probability of the PR channel being busy is high and/or its reliability is relatively low, the throughput attained by these HARQ schemes becomes relatively low and their packet delay increases. Furthermore, for the CGBN-HARQ and CSR-HARQ, our results show that when the propagation environment is time-variant, the number of packets transmitted within a TS should be adapted accordingly, in order to attain the highest throughput and the shortest average transmission delay.

Declaration of Authorship

I, **Ateeq Ur Rehman**, declare that the thesis entitled **Hybrid Automatic Repeat Request Assisted Cognitive Radios** and the work presented in it are my own and has been generated by me as the result of my own original research. I confirm that:

- This work was done wholly or mainly while in candidature for a research degree at this University;
- Where any part of this thesis has previously been submitted for a degree or any other qualification at this University or any other institution, this has been clearly stated;
- Where I have consulted the published work of others, this is always clearly attributed;
- Where I have quoted from the work of others, the source is always given. With the exception of such quotations, this thesis is entirely my own work;
- I have acknowledged all main sources of help;
- Where the thesis is based on work done by myself jointly with others, I have made clear exactly what was done by others and what I have contributed myself;
- Parts of this work have been published.

Signed: ..... Date: .....

Acknowledgements

First of all, I would like to give the greatest gratitude to both of my supervisors Professor Lie-Liang Yang and Professor Lajos Hanzo. I really appreciate their generous and insightful guidance as well as wise advice in the past four years of my PhD study, which encouraged me to build my own career that I am so passionate about. I appreciate that they shared with me their valuable experiences, not only in science, but also in life.

Secondly, I am deeply grateful to Dr. Chen Dong, Dr. Varghese Antony Thomas, Dr. Rakshith Rajashekar, Dr. Jie Hu, Abbas Ahmed, Shruti Gupta and Dr. Halil Yetgin. Their presence has helped me endure the ups and downs of being a researcher.

The support and kindness of many friends and colleagues whom I have made throughout these past few years have been invaluable to me. Although there are too many names to mention, I would like to express my gratitude to all those, who have been at least once with Southampton wireless, both past and present. I want to particularly thank Dr. Mohammed El-Hajjar, Dr. Soon Xin Ng, Dr. Rob Maunder, Dr. Rong Zhang, Ibrahim Hemadeh, Dimitrios Alanis, Dr. Zunaira Babar, Dr. Abdulah Jeza Aljohani, Dr. Liang Wei, Dr. Xuan Li, Dr. Li Li, and all other colleagues and staff, too numerous to mention here explicitly.

Without the support, patience and guidance of the following people, this study would not have been completed, Hassan Younas, Faheem Tanoli, Brekhna Faheem, Kelsey Glass, Gao Quinn, Faheem Wali, Azmat Ali Shah, Arshad Khan, Uzair Khan, Palwasha Sajjad, Mouzzam Khattak, Gulaly Khan, Saad Balooch, Saad Rahoojo, Zia Noori, Muhammad Khan, Ziggrawer Muneir. Southampton has always been better with them.

I owe my deepest gratitude to my father, Hidayat Ullah and my mother, my lovable uncles, brothers and sisters for their love, support and care for me, and Thank's To ALLAH for every thing.

The financial support of Abdul Wali Khan University Mardan, Pakistan is also gratefully acknowledged.

List of First-Author Publications

Journal Paper

1. **A. U. Rehman**, C. Dong, L. L. Yang and L. Hanzo, "Performance of Cognitive Stop-and-Wait Hybrid Automatic Repeat Request in the Face of Imperfect Sensing", *IEEE Access*, vol.4, pp.5489-5508, July 2016.

2. **A. U. Rehman**, C. Dong, V. A. Thomas, L. L. Yang and L. Hanzo, "Throughput and Delay Analysis of Cognitive Go-Back-N Hybrid Automatic Repeat reQuest Using Discrete-Time Markov Modelling", *Accepted in IEEE Access*, November 2016.

3. **A. U. Rehman**, V. A. Thomas, L. L. Yang and L. Hanzo, "Performance of Cognitive Selective-Repeat Hybrid Automatic Repeat Request", *Accepted in IEEE Access*, November 2016.

4. **A. U. Rehman**, L. L. Yang and L. Hanzo, "Throughput and Delay Analysis of Cognitive Go-Back-N Hybrid Automatic Repeat reQuest Using Discrete-Time Markov Modelling in the Face of Imperfect Sensing", *Submitted to IEEE Access*.

Conference Paper

1. **A. U. Rehman**, L. L. Yang and L. Hanzo, "Performance of Cognitive Hybrid Automatic Repeat reQuest: Stop-and-Wait", *IEEE 81st Vehicular Technology Conference (VTC Spring)*, Glasgow, Uk, May 2015.

2. **A. U. Rehman**, L. L. Yang and L. Hanzo, "Performance of Cognitive Hybrid Automatic Repeat reQuest: Go-Back-N", *IEEE 83rd Vehicular Technology Conference (VTC Spring)*, Nanjing, China, May 2016.

Contents

List of Symbols

General Conventions

- The superscript $\underline{(.)}$ indicates the symbol sequences.
- The superscript ^{T} is used to indicate matrix transpose operation. Therefore, $\mathbf{a}^T$ represents the transpose of the matrix $\mathbf{a}$.
- The $max()$ is used for finding the highest number in a vector.

Mathematical Operators and Functions

$[\cdot]_{a\times b}$	The matrix having a rows and b columns.
$\lfloor . \rfloor$	Represents floor function.
$\binom{N}{k}$	Represents the number of k different combinations from set N.
$\sum$	The sum operation.
E	Average.
$\mathbf{P}$	Boldface uppercase letters denote matrix.
$\mathbf{p}$	Boldface lowercase letters denote column vectors.
P_{ij}	Element of the matrix $\mathbf{A}$ at row i, column j.
$\mathbf{1}$	Column vector containing 1.
$\boldsymbol{\pi}$	Express steady-state probabilities.
π_i	ith element of steady-state vector.
$\mathbb{S}$	Sample set.
S_i	Represents state i.

Special Symbols

α	Transition probability from 'ON' to 'OFF' state.
β	Transition probability from 'OFF' to 'ON' state.
δ	Delta function.
$\mathcal{H}_0$	Channel occupied by PUs.
$\mathcal{H}_1$	Channel free from PUs.
λ	Rational Constant.
μ	Real status of the PR channel.
ν	Status of the PR channel sensed by the CU.
$\mathbf{\Phi}$	Steady-state vector.
Φ_i	ith element of a steady-state vector.
$\mathcal{T}$	Decision-making statistics obtained from the received signal.
$\mathcal{T}_h$	Predefined threshold for detection.
ξ	Status of a specific packet.
S_{cur}	Current state of the Algorithm.
S_l	Symbol used for lth state.
ρ	Degree of correlation between two variables.
	σ Variance
X_n	Gaussian Random Process.
$\mathbb{Q}$	Q function.

Specific Symbols

B	Number of busy TSs between first and last transmission of a packet.
c	Normalization factor for obtaining PMF.
G	Number of retransmissions of a packet.
k	Duration for sensing the time-slot.

K_d	Information Bits.
L_i	Represents number of new packets transmitted using state S_i.
$l_{i,j}$	Number of packets transmitted in S_i are successfully received in S_j.
M_c	Total number of packets to be transmitted.
M_T	Maximum delay.
N	Number of packets in a time-slot.
N_d	Coded symbols.
N_{DP}	Average delay due to busy channel occurring before transmission.
$n_p(S_i)$	Function for storing number of new packets associated with state S_i.
N_s	Total number of successfully transmitted packets.
N_t	Total number of TSs used for transmitting N_s packets.
$\boldsymbol{P}$	Transition matrix .
P_A	Probability that time-slot is actually free.
P_B	Probability that time-slot is found free due to mis-detection.
P_{bs}	Probability of finding a busy time-slot.
P_{cd}	Probability of detection.
$\boldsymbol{P}_d$	PMF of end-to-end delay obtained through simulation.
P_e	Packet error probability.
P_{fa}	Probability of false-alarm.
P_{fr}	Probability of finding a free time-slot.
P_{md}	Probability of mis-detection.
P_{MF}	Probability distribution of end-to-end packet delay.
P_{off}	Probability of the PR channel being free from the PUs.
P_{on}	Probability of the PR channel being occupied by the PUs.
$\mathbb{S}_N$	Subset of $\mathbb{S}$ in which new packets are transmitted.
$\mathbb{S}_i$	Subset of $\mathbb{S}_N$, which contains states associated with new packets.

R_T	Throughput by theory.
R'_T	Normalized throughput by theory.
R'_S	Throughput by simulation.
T	Duration of the TS.
T_d	Data transmission epoch.
T_D	Total average packet delay obtained from theory.
T_{DP}	Delay due to busy channels.
T_{DS}	Total average packet delay obtained by simulation.
T'_{DS}	Normalized average packet delay obtained by simulation.
T_p	Duration of packet transmission.
T_s	Sensing epoch.
T_w	Waiting epoch.
τ	Average end-to-end packet delay.
τ_s	Average end-to-end packet delay obtained by simulation.

Chapter 1

Introduction

Cognitive Radio (CR) has attracted a lot of attention since it was proposed in 1999 by Mitola [2,3]. It has emerged as a promising technique of improving the exploitation of the spectrum. This thesis is focussed on improving the data transmission integrity in CR. Specifically, we conceive and analyse automatic repeat request (ARQ) aided data transmission schemes operated in CR environments. We commence by outlining the motivation of the research, the problems to be solved as well as the contributions made by the thesis.

1.1 Motivation and Research Challenges

Wireless communications pervaded our daily lives. As a result, the world has witnessed an exponential increase of wireless tele-traffic, which has imposed a significantly increased demand on the electromagnetic spectrum, especially in the most desirable sub $-$ 2 GHz frequency bands [4]. In order to identify the cause of spectrum shortage and to conceive corresponding solutions, the Federal Communication Commission (FCC) of the United States (US) and the European Telecommunications Standards Institute (ETSI) have conducted surveys in different parts of the world and at different times [5–8]. These studies demonstrated that the inefficient spectrum utilization stems primarily from the classic static spectrum allocation policy, which exclusively allocates the spectrum bands to different networks, which are only allowed to be utilized by the authorized users, known as primary users (PUs). For example, the TV stations and cellular users are considered as PUs. By contrast, for the sake of improving the exploitation of the spectrum, CR systems rely on dynamic spectrum access (DSA), which allows the cognitive radio users (CUs) to share the licensed spectrum owned by PUs. This is achieved by sensing and then exploiting the earmarked, but momentarily unoccupied licensed spectrum [9–12]. For example, TV stations and cellular users are considered to be the primary users of the TV bands and cellular bands, respectively [13]. On the other hand, the CUs can be any users, who do not have or require licence for accessing the PUs spectrum. Therefore, the CUs perform continuous spectrum sensing to identify the unoccupied

slices of the spectrum (also known as spectrum holes) in the licensed spectrum and then utilize it for their own data transmission [9, 10, 14]. In order to avoid the degradation of the performance of authorized PUs, CUs have to evacuate the occupied spectrum, as soon as the PUs need it. These capabilities of CR have encouraged the regulatory bodies around the world to officially allow the operation of CR systems in order to increase the efficiency of the overall spectrum utilization, without having to make substantial changes of the legal system/devices operated under the conventional fixed spectrum allocation policy [5, 12, 15].

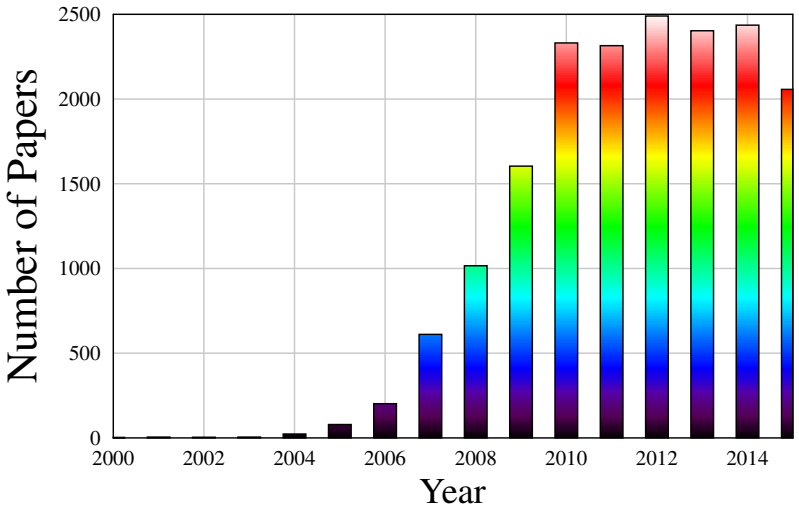

Figure 1.1: The number of contributions performed in the context of CR per year as per IEEE Xplore database.

Since its invention, CR has attracted intensive research, as evidenced by the contributions summarized in Fig. 1.1 [9–11, 14, 16, 17]. Specifically, Haykin in [14] has extensively appraised the fundamental principles of CR, elaborating on the issues of spectrum sensing, channel estimation, cooperative communications, power control and dynamic spectrum management. The detection of unoccupied spectrum and the ensuing resource allocation have been explored by elaborating on a range of attractive detection and tracking techniques in [9–11]. The architecture of CR networks and its impact on dynamic resource allocation have been addressed in [16], whereas in [17] Tragos *et al.* investigated the problem of resource allocation both in centralized and in distributed networks, when considering the effects of interference, power, delay, etc.

Following the detection of unoccupied spectrum slots, during data transmission the CUs also face similar challenges to those of the conventional PUs in wireless communication systems. In order to achieve reliable communication in CR systems, powerful error correction/decoding codes are also required [18, 19]. As in conventional wireless systems, ARQ constitutes an efficient technique conceived for reliable data transmission over noisy channels. As shown in [20], the ARQ schemes may be classified into three popular ARQ protocols, namely the Stop-and-Wait ARQ (SW-ARQ), Go-Back-N ARQ (GBN-ARQ) and the Selective-Repeat ARQ (SR-ARQ) [18, 21, 22]. The general principles of ARQ are appealingly simple. After transmitting a packet, if the transmitter node's control-channel receiver fails to receive a positive acknowledgement within a predefined time du-

ration or if it receives a negative acknowledgement, the packet is retransmitted. The ARQ protocols are usually capable of achieving high-reliability data transmission, provided that the channel-induced error rate remains moderate. However, beyond a certain error rate, both the throughput and delay may become inadequate owing to the excessive number of retransmissions. Hence, for the sake of enhancing the performance, sophisticated combinations of Forward Error Correction (FEC) and ARQ may be employed, which are termed as Hybrid ARQ (HARQ) schemes [23, 24], where the ARQ mechanism is only activated for the retransmission of a packet, when the number of errors encountered is beyond the error-correction capability of the FEC scheme. As a benefit, HARQ schemes are typically capable of providing a better throughput/delay performance than the corresponding pure ARQ schemes. Hence, they have been widely employed in wireless communication systems [25, 26]. This motivates us to study and incorporate the HARQ schemes in CR systems. In Chapter 2, we will provide a more comprehensive review of both ARQ and HARQ.

The main objective of CR is to maximize the utilization of the sparsely used licensed spectrum by efficiently sensing as well as detecting free spectrum holes and then exploiting them. Hence, it is important to design flexible CR systems that are capable of supporting high-reliability data transmission. It is well-known that wireless links are error-prone and location dependent. The factors influencing the reliability of data transmission include path-loss, shadowing, multi-path fading, noise, interference, etc., which are encountered by all types of wireless systems. However, in addition to these factors in CR systems, the reliability of data transmission is also affected by the dynamic nature of the spectral bands due to the activity of PUs owing to unreliable sensing, which makes communication in CR systems more challenging. In this thesis, we propose to introduce HARQ schemes for the protection of data transmission in CR systems, because they constitute a promising and efficient paradigm for achieving reliable communication in conventional wireless systems. However, due to the dynamic occupancy of the communication spectrum in CR systems, the HARQ schemes operated in CR face more grave challenges than those operated in conventional wireless systems. The design of high-efficiency HARQ schemes for CR and their theoretical analyze performance analysis constitute the main research issues of this thesis.

To be more specific, the main goals of this thesis include the modelling of the communication between a CR transmitter and receiver based on idealized perfect and realistic imperfect sensing, to model the activity of the PUs of a PR system and to model the channel between the CR transmitter and receiver. Based on the results, we then design attractive HARQ schemes and study in detail the performance of the various HARQ schemes invoked. We provide answers to the following research problems.

1.2 Summary of Contributions

In order to address the above-mentioned challenges, in this thesis, we propose novel cognitive protocols, which intrinsically amalgamate CR with HARQ protocols for achieving reliable communi-

cation, when both perfect and imperfect sensing scenarios are considered. Our proposed schemes are inspired by the classic HARQ protocols. However, they require significant advances for reformulating the transmission principles of the classic HARQ protocols, when they are operated in the context of CR systems. After outlining the various HARQ schemes considered, we theoretically model and analyse the protocols by relying on a pair of distinctive approaches, namely a probability-based approach and a Discrete Time Markov Chain (DTMC) based approach. Furthermore, we study both the throughput and delay of the CR systems supported by the different HARQ protocols in terms their parameters. These theoretical results are then finally verified by our simulation based study. Specifically, in Fig. 1.2 we graphically illustrate the structure of this thesis, where the relationship between the chapters is captured.

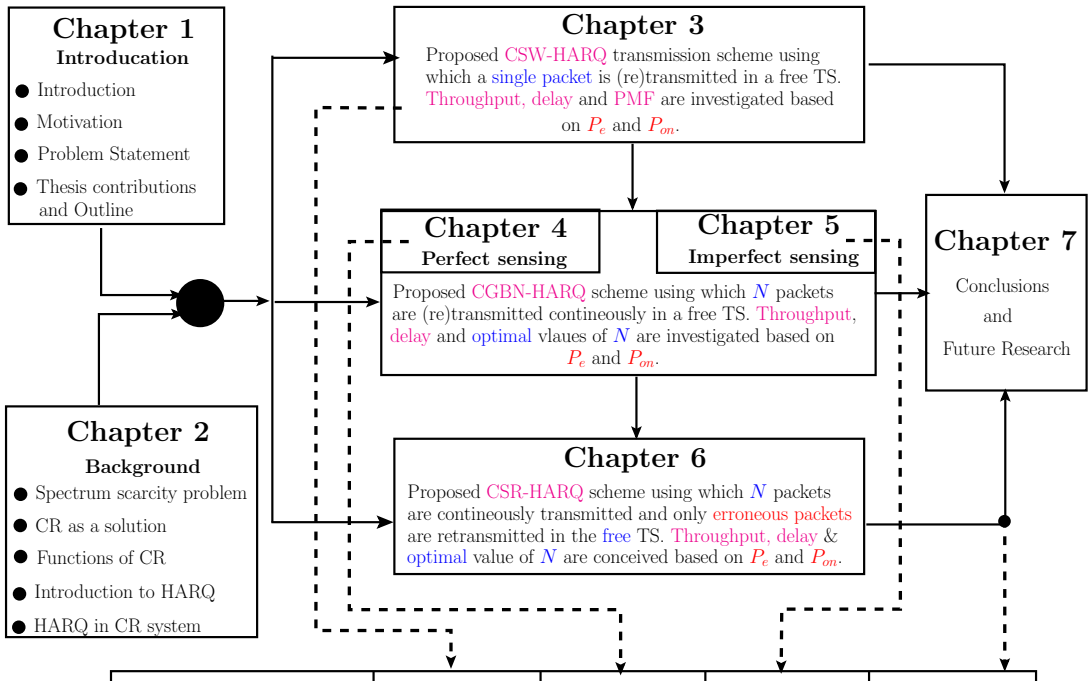

Characteristics	Chapter 3	Chapter 4	Chapter 5	Chapter 6
Probabilitic-based analysis	✓	✗	✗	✓
DTMC-based analysis	✓	✓	✓	✓
Perfect Sensing	✓	✓	✓	✓
Imperfect Sensing	✓	✗	✓	✗
Throughput	✓	✓	✓	✓
Average Packet Delay	✓	✓	✓	✓
Optimal value of N	✗	✓	✓	✓

Figure 1.2: Organization of the thesis showing the connection between chapters and their characteristics. N represents the number of packets, P_e and P_{on} represents the packet error probabilities and probabilities of channel being busy, respectively.

In more detail, in Chapter 2, we provide a rudimentary overview of the CR, ARQ and of the ARQ protocols designed for CR. Among many alternatives conceived for circumventing the spec-

trum scarcity issues, our point of interest is the widely known CR paradigm. Therefore, in this chapter, we first briefly elaborate on the concept of CR systems in terms of their design, architecture, functions and recent advances. Then, we focus our attention on the techniques conceived for achieving reliable communication. We first provide a brief introduction to the implementation of HARQ protocols in the context of conventional wireless systems and address their challenges in CR communications.

In order to support the process of spectrum reuse, in Chapter 3, we consider a CR communication scheme, which senses and opportunistically accesses a PR spectrum for the sake of implementing communication between a pair of nodes relying on the stop-and-wait hybrid automatic repeat request (SW-HARQ) protocol. This arrangement is represented by the cognitive SW-HARQ (CSW-HARQ) scheme, where the availability/unavailability of the PR channel is modelled as a two-state Markov chain having 'OFF' and 'ON' states, respectively. Once the CU finds that the PR channel is available (i.e., in 'OFF' state), the CU transmits its data packet over the PR channel's spectrum, whilst relying on the principles of SW-HARQ. In this Chapter 3, we investigate both the throughput and delay of the CSW-HARQ protocol, with a special emphasis on the impact of the various system parameters involved in the scenarios of both perfect and imperfect spectrum sensing. Furthermore, we analyze both the throughput as well as the average packet delay and the end-to-end packet delay of the CSW-HARQ system. We propose a pair of analytical approaches: 1) the probability-based approach and 2) the Discrete Time Markov chain (DTMC)-based approach. Closed-form expressions are derived for both the throughput and the delay under both idealized perfect or realistic imperfect sensing environments, which are validated by our simulations. We demonstrate that the activity of the PUs, the transmission reliability of the CU as well as the specific sensing environment encountered have a significant impact on both the throughput and the delay of the CR system.

For the sake of improving the attainable spectrum exploitation, in Chapter 4 we propose a cognitive Go-Back-N-HARQ (CGBN-HARQ) scheme for data transmission in a CR system. As in Chapter 3, we model the activity of PUs as a two-state Markov chain having 'ON' and 'OFF' states. Once, the CU finds that there are no active PUs (i.e., they all are in the 'OFF' state), on a considered channel, the CR transmitter transmits some data packets following the modified GBN-HARQ protocol. Otherwise it waits and senses the channel again. In this chapter, the proposed CGBN-HARQ scheme is theoretically analysed with the aid of DTMC, where an attractive algorithm is proposed for generating all possible states in which the transmitter may reside in a given time-slot (TS). Furthermore, based on the DTMC modelling, we derive a range of closed-form expressions for evaluating the throughput, the average packet delay and end-to-end packet delay only in idealistic perfect sensing environments, which are verified by a simulations.

Then in Chapter 5, we implement the CGBN-HARQ in a realistic imperfect sensing environment. The presence/absence of the PU in a particular channel is again modelled by a two-state Markov chain. However, the CR system may wrongly identify the PR channel's state due to unreli-

able sensing, which may result in false-alarm or mis-detection. In this case, the channel perceived by the CR system can be described as a four-state Markov chain by considering the actual state of the PR channel and the sensed state of the CR system. In contrast to the state definition and analytical modelling used in Chapter 4, in this chapter, we modified the analytical modelling for the sake of capturing the effect of incorrect sensing decisions. Similarly, the state generation algorithm is also redesigned for the sake of illuminating the illegitimate states. Furthermore, closed-form expressions are derived for the achievable throughput and delay based on our analytical modelling, which are then also validated by simulations. The performance results demonstrated that both the achievable throughput and delay are significantly affected by the activity of the PUs, by the reliability of the PR channel, by the unreliable sensing decision and by the number of packets transmitted per TS. To attain the maximum throughput and to reduce the transmission delay, the number of packets transmitted within a TS should be carefully adapted based on both the activity level of the PUs and on the quality of the PR channel.

It is widely recognized that the SW-HARQ scheme is simple to implement, but may become inefficient, when the channel is relatively reliable. In this case, the GBN-HARQ scheme is capable of significantly enhancing the performance at the cost of an increased complexity. Furthermore, at a modest further increase of the complexity, the Selective-Repeat-HARQ (SR-HARQ) is capable of providing some further performance gains. Therefore, in Chapter 6 we introduced a novel transmission protocol based on the classical SR-HARQ protocol for accessing a PR channel, which is referred to as the CSR-HARQ. As in Chapter 3 and 4, we assume that the PUs transmit information is scheduled on the basis of TSs. During a TS, the CR transmitter first senses the PR channel. Once a free TS is found, the CR transmits a number of packets to the CR receiver based on the principles of the SR-HARQ. In this chapter, we analyze the throughput, the average packet delay and the end-to-end packets delay of the CSR-HARQ. Furthermore, we proposed a pair of approaches for performance analysis. The first one is the probability based approach, while the second one relies on the DTMC principles. Finally, we study the attainable throughput, the average packet delay as well as the end-to-end packet delay performance of the CSR-HARQ by both simulations and based on of our derived formulas. Our performance results show that the performance of the CSR-HARQ systems is significantly impacted both by the activity of the PR channel and by the reliability of the sensed free channels.

Finally, in Chapter 7, the salient findings of this thesis are summarized, along with the description of potential future research ideas.

Chapter 2

Background Overview

This chapter is organized in four Sections. In Section 2.1, we present an overview of CR systems, where the basic principles of DSA are provided in Subsection 2.1.1, while the concept and the well-known definitions of CR are outlined in Subsection 2.1.2. In Subsection 2.1.3, the specific modes through which the CR system accesses and utilizes the spectrum are discussed, whereas Subsection 2.1.4 elaborates on the spectrum sensing algorithms. After identifying the unoccupied spectrum, the CR transmits its own data, which is subjected to the usual wireless channel impairments. In Section 2.2, the classic ARQ and HARQ based transmission scheme are discussed, while in Section 2.3, we highlight the state-of-the-art and the open challenges in the context of achieving reliable data transmission in CR systems. Finally, we summarize this chapter in Section 2.4.

2.1 Cognitive Radio Evolution

The radio spectrum constitutes the key resource of supporting wireless applications. Usually, different frequency bands have a different propagation properties, therefore they are only suitable for specific wireless applications. In order to officially allocate a suitable frequency band to a specific application, in 1934, the United States (US) congress passed a communication act for establishing a commission known as the Federal Communication Commission (FCC) which was tasked with consolidating rules for interstate telecommunication. Among the numerous responsibilities of the FCC, the management and licensing of the spectrum were the most important aspects in the US. Therefore, the USA and the European countries embarked on regulating the electromagnetic radio spectrum with the objective of avoiding interference between users of the adjacent frequencies and between geographical locations in each other's close proximity, especially in maritime communication, security and defence [27, 28].

The first step towards spectrum management was to organize the spectrum into well-defined spectral bands under the existing command-and-control regulatory structure [27, 28]. The regula-

tory bodies, e.g. such as FCC in USA and the European Telecommunication Standard Institute (ETSI) in Europe, then allocated these spectral bands to the highest bidder with the goal of exploiting the spectrum and increasing the revenues for the government. Under these regulations, the spectral bands are statically allocated with the full right given to the specific wireless services in short-term or long-term over wide geographical areas [5]. These frequency bands are known as licensed bands and their users are licensed users or primary radio users (PUs). In 2003, the National Telecommunication and Information Administration (NTIA) presented a chart showing the exclusively allocation of frequency bands based on the static spectrum allocation approach to specific networks. For instance, as shown in Fig. 2.1, the FCC exclusive allocated the very-high frequency (VHF) and ultra-high frequency (UHF) bands to broadcast television (TV) stations [29]. As a result, only PUs i.e. TV stations were allowed to use these spectral bands. Under this approach, the interference between different systems was mitigated. However, this rigid allocation does not support innovative wireless services.

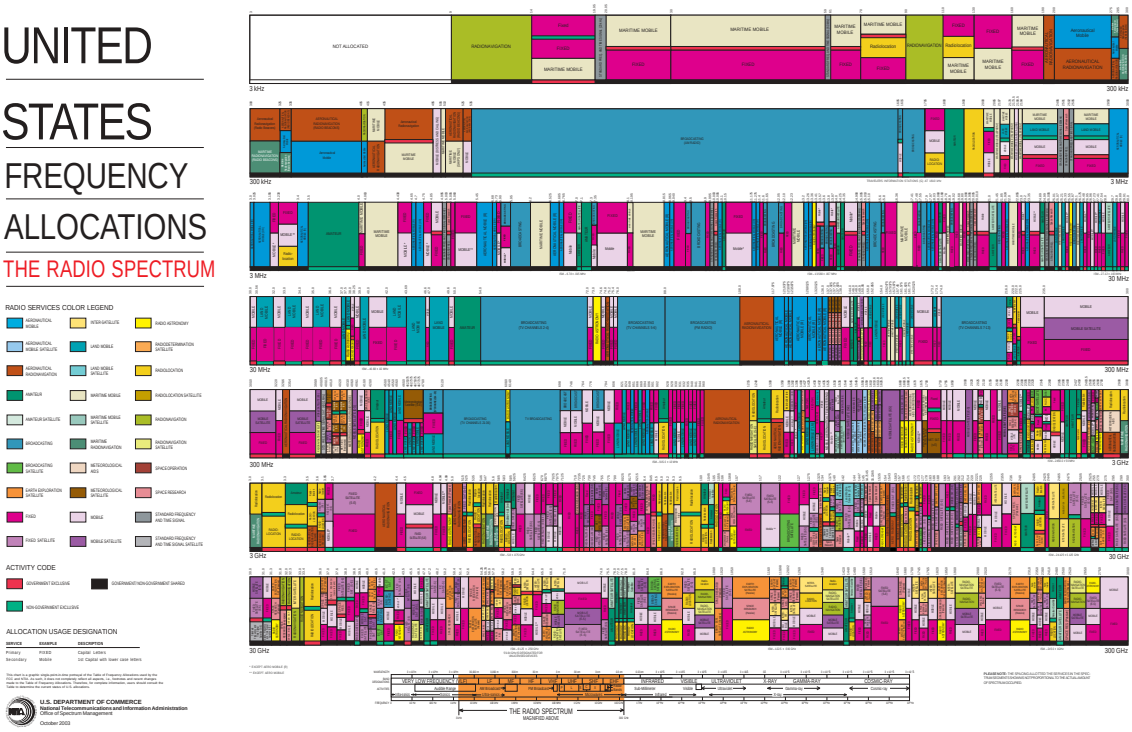

Figure 2.1: U.S. Frequency allocation chart Oct 2003 by ©NTIA.

In order to support novel wireless applications, the regulatory bodies have dedicated a specific portion of the radio spectrum to low-power operations without requiring licence. These bands are known as unlicensed bands, as exemplified by the Industrial, Scientific and Medical (ISM) and Unlicensed National Information Infrastructure (UNII) bands. Owing to the benefits of free access, the world has witnessed a tremendous growth in the development of wireless applications, such as cordless phones, smart watches, Wi-Fi, Blue-tooth, WiMAX and Zigbee [10, 11, 30], which results in congestion in these spectral bands, as shown in Fig. 2.2. This situation is further aggravated by

other wireless devices, such a wireless PDAs, keyboards, wireless headsets etc that are operated in these bands. Table 2.1 summaries the situation of unlicensed frequency bands used by the ISM applications [31]. Moreover, the recent studies in [32–34] have predicted that the mobile data traffic will increase from 3.7 exabytes to 30.6 exabytes per month, while the number of subscribers will be increased from 4.7 billion to approximately 6 billion in next few years, further congesting the radio spectrum.

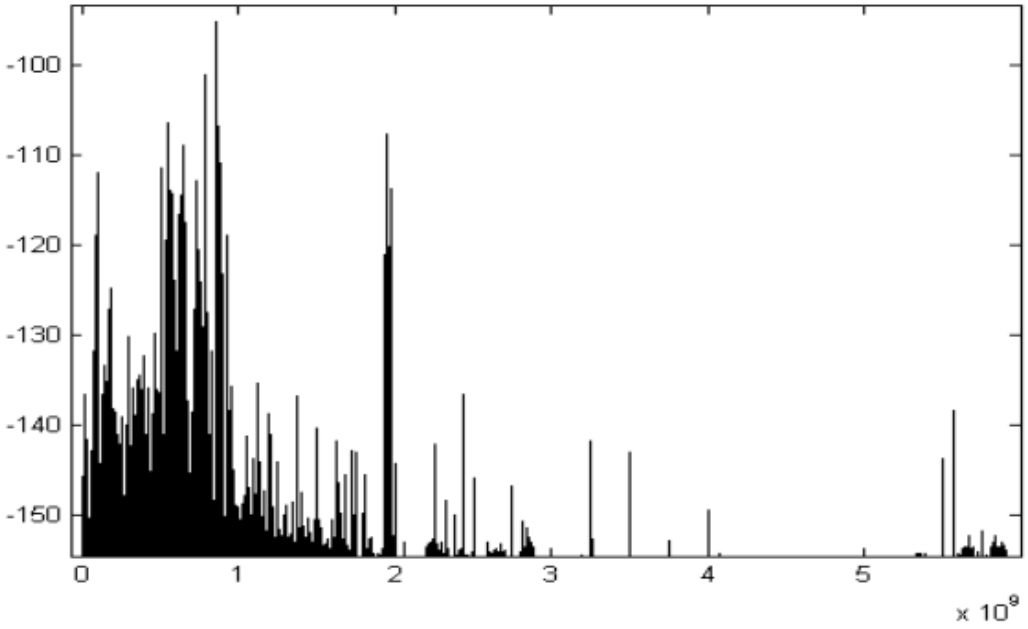

Figure 2.2: Measurement of $0-6$ GHz spectrum utilization ©Yang 2005 [7] and ©Cabric 2007 [35].

It is widely known that in most countries the valuable frequency bands exhibiting friendly propagation properties have already been allocated, as shown in Fig. 2.1, whereas the unlicensed bands are over-utilized, which results in the widely recognized spectrum scarcity problem [6, 10]. Thus, in order to mitigate the spectrum scarcity, research communities around the globe have proposed different solutions, among which the concept of spectrum reuse has attracted the most attention. Simultaneously, the spectrum shortfall has also motivated the spectrum regulatory bodies including the FCC in the US and ETSI in Europe, to find the root cause of the spectrum shortage and to devise efficient solutions. Hence, they have conducted statistically relevant studies during different time intervals in different geographical areas [5–8, 35–37]. The results of these studies reveal that under the conventional static spectrum allocation policy, substantial segments of the earmarked electromagnetic spectrum are actually under-utilized. For example, the spectrum measurements of [8] demonstrated that the typical spectrum occupancy in the US varies between 15% to 85%, whereas the measurements taken in the downtown area of Berkley, suggested that the spectrum utilization below 3 GHz is approximately 30%, while in the range of $3-6$ GHz is only 0.5% [7, 35], as illustrated in Fig. 2.2. The outcome of these surveys questioned the sustainability of the existing inefficient and inflexible spectrum allocation approach.

Frequency Range	Carrier Frequency	Availability	Licensed users
6.765 MHz - 6.795 MHz	6.78 MHz	Depends on local acceptance	Fixed service and Mobile service users
13.553 MHz - 13.567 MHz	13.56 MHz	Worldwide	Fixed and Mobile services except Aeronautical mobile (R) service
26.957 MHz - 27.283 MHz	27.12 MHz	Worldwide	Fixed and Mobile services except Aeronautical mobile (R) service
40.66 MHz - 40.7 MHz	40.68 MHz	Worldwide	Fixed, Mobile services as well as Earth exploration-satellite service
433.05 MHz - 434.79 MHz	433.92 MHz	Available in Region 1 based on local acceptance	AMATEUR SERVICE and RADIO LOCATION SERVICE
902 MHz - 928 MHz	915 MHz	Available in Region 2	FIXED, Mobile except aeronautical mobile and Radio location service; in Region 2 additional Amateur service
2.4 GHz - 2.5 GHz	2.45 GHz	Worldwide	FIXED, MOBILE, RADIO LOCATION, Amateur and Amateur-satellite service
5.725 GHz - 5.875 GHz	5.8 GHz	Worldwide	FIXED-SATELLITE, RADIO LOCATION, MOBILE, Amateur and Amateur-satellite service
24 GHz - 24.25 GHz	24.125 GHz	Worldwide	AMATEUR, AMATEUR-SATELLITE, RADIO LOCATION and Earth exploration-satellite service (active)
61 GHz - 61.5 GHz	61.25 GHz	Depends on local acceptance	FIXED, INTER-SATELLITE, MOBILE and RADIO LOCATION SERVICE
122 GHz - 123 GHz	122.5 GHz	Depends on local acceptance	EARTH EXPLORATION-SATELLITE (passive), FIXED, INTER-SATELLITE, MOBILE, SPACE RESEARCH (passive) and Amateur service
244 GHz - 246 GHz	245 GHz	Depends on local acceptance	RADIO LOCATION, RADIO ASTRONOMY, Amateur and Amateur-satellite service

Table 2.1: Frequency band allocation for applications using the ISM band defined by ITU-R [31]

In order to find solutions for overcoming the spectrum scarcity, in the late of 1990s, the authors of [38–42] studied the spectrum sharing approach for the first time. They showed that by invoking cooperation, the capacity of the overall network and exploitation of the spectrum can be significantly improved. The fundamental work on dynamic spectrum management was presented in [43], where three allocation techniques were discussed. Following that, in [44, 45] the authors studied channel allocation based on the user's demand, with the objective of increasing the spectral efficiency, provided that no collisions occur and that the level of interference is kept sufficiently low. Furthermore, it is impractical to introduce a new spectrum allocation chart based on the actual spectrum usage, because it is impossible to predict whether the new spectrum allocation approach is suitable for the development of future wireless applications. On the other hand, adjusting or reallocation spectrum slices based on usage may not be acceptable to the PUs. Note that for the sake of devising new solutions, it is always important to satisfy the legal rights of PUs, hence high priority have to be given to them. Hence, the FCC [36], has issued a legal declaration, proposing dynamic spectrum access (DSA), which allows the unlicensed users to find free holes in the sparsely used licensed spectrum and to use them for their own transmission, provided that no harmful interference is imposed on the PUs [2, 3, 9, 14].

2.1.1 Dynamic Spectrum Access

The concept of Dynamic Spectrum Access (DSA) relies on *analysing the spectral resources by ensuring that changes in the environment and resources does not affect the communication and make the spectrum utilization more effective and robust* [9, 10, 46]. DSA enables unlicensed users, known as cognitive radio users (CUs) or secondary users (SUs), to search for unoccupied segments of the earmarked licensed spectrum and to use them temporarily for their own communication [9, 10, 46]. In order to avoid inflicting interference upon the PUs, in DSA systems the CUs must continuously monitor the activity of the PUs over the spectrum.

The concept of DSA was first presented in the IEEE Symposium on Dynamic Spectrum Access Network (DySPAN) in 2005, which can be categorized into three main models, the common-use model, shared-use model and the exclusive-use model [13, 30], which have the characteristics described as follows.

- **Commons-use Model**: This model is also known as the open spectrum sharing model [47, 48]. Under this model, some specified spectrum may be freely used by any users without requiring a license. For example, the model of accessing the ISM band belongs to the common-use model. The ISM band is a licence-free band which is suitable for low-power and short range applications such as Wi-Fi (802.11), Bluetooth (802.15.1), cordless phones and medical devices etc. As shown in Fig. 2.2, the over-crowdedness may increase the level of interference. Hence, by allowing CUs for example COCast [49] and CORoute [50] in ISM bands, the over-crowdedness and the interference may be reduced by exploiting the unoccupied channels and/or by determining the channels having minimum or no tele-traffic.

- **Shared-Use Model**: This model adopts a hierarchical access approach, which allows CUs to access the licensed spectrum, provided that no performance degradation is imposed on PUs transmission. In order to share the spectrum, various sharing approaches [51], including *spectrum underlay* and *spectrum overlay* approaches have been proposed [4, 16], which will be discussed in more detail in the following section.

- **Dynamic Exclusive Use Model**: This model follows the classic static spectrum allocation policy with the spectrum being licensed to the specific wireless services for their exclusive use. With the objective of maximizing the spectrum utilization and efficiency [9], two models, namely the spectrum property rights and dynamic spectrum allocation model, have been proposed [52–54]. The former model allows the PUs to sell and trade their spectrum to the unlicensed users, when they do not use them. Although the PUs have full right to earn profit by sharing or selling the spectrum, it might not be officially allowed by the regulation policy. The latter approach was introduced by the European DRiVE project [54] with the objective of improving the spectral utilization by dynamically allocating the spectrum based on the time, space and geographic region.

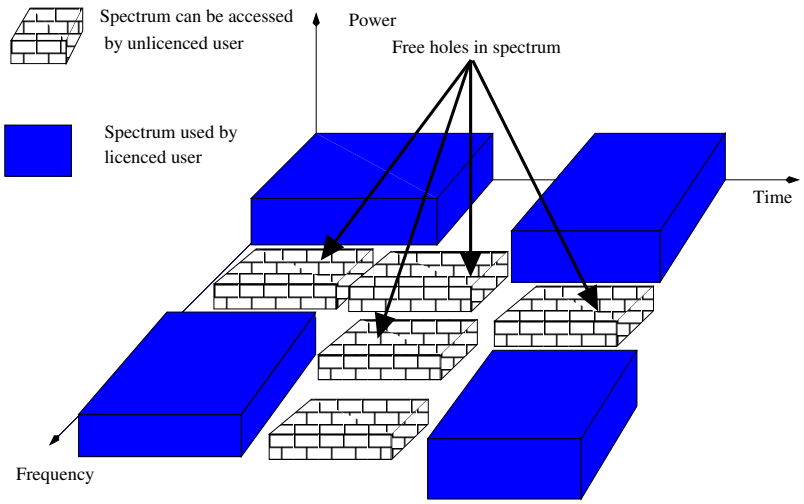

Figure 2.3: An illustration of spectrum holes [10, 55].

2.1.2 The Concept of Cognitive Radio

In order to implement DSA, the concept of cognitive radio (CR) has been proposed [2, 3], "as a foundation of a software defined radio (SDR) that employs a model-based learning with an objective of achieving a specified level of competence in a radio related domains". According to Haykin [14], a CR node is an intelligent sensor node having the capability of continuously sensing the operating environment with the objective of learning and dynamically modifying and/or adjusting its transmission parameters such as its waveform, spectrum access, carrier-frequency and networking protocol, which are essential for achieving a stable network and application performance. Since its invention, CR has been considered to be one of the key enabling techniques of DSA and it has been recognised by different organizations, including the FCC [5] and the International Telecommunication Union (ITU) [31].

- FCC: CR is a smart radio that can modify and adjust its transmission parameters based on the operational environments.
- ITU: A CR node is a wireless sensor node that has the capability to sense its operational environment as well as the capability to dynamically adjust its operating parameters.

Hence a CR system has the capability to sense and detect the unoccupied portions of the spectrum and then exploit them for its own transmission, as depicted in Fig. 2.3. The unoccupied portion of the licensed spectrum is also known as spectrum hole [10, 55]. Moreover, a CR system has to adjust its parameters in response to the time-varying environments. Due to these capabilities, CR has been considered as a promising paradigm of improving the bandwidth efficiency of the classic wireless system over that of the static spectrum allocation [46, 71–73]. As a result, the CR concept has been incorporated into the various IEEE standards for wireless communications which include the 1900 and 802.22 standards series [74, 75] discussed in [76, 77].

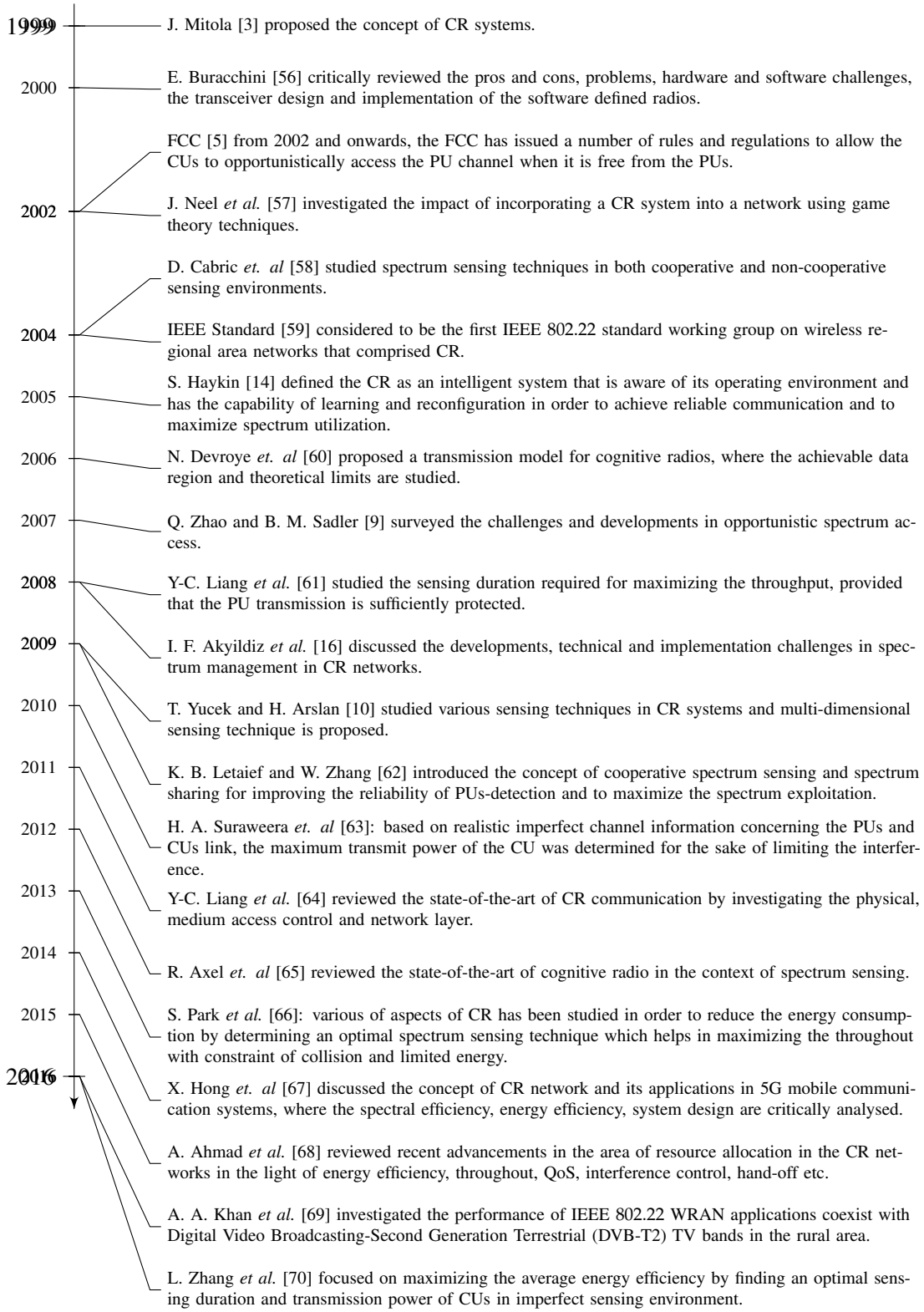

Figure 2.4: Timeline showing the milestione achieved in the direction of cognitive radio implementation.

2.1.3 Design and Architecture of Cognitive Radio Systems

In this section, an overview of the CR system concept is presented, including its access to the licensed bands. Specifically, based on the information about the PR network, a CR system may ac-

cess the PR spectrum in the underlay, overlay or interweave mode, which are discussed as follows.

2.1.3.1 Cognitive Radio Access Paradigms

In CR networks, the CUs are allowed to access the PR spectrum, provided that they do not impose harmful interference on the PUs communications. From literature [4, 13], there are three typical paradigms for CUs for accessing the PR spectrum, which are the underlay, overlay and interweave modes.

- **Underlay Mode**: In this mode, the CUs are allowed to utilize the PR spectrum, provided that the interference imposed by CUs on the PUs is below a pre-set threshold [4, 78]. Since in this mode the interference constraint is strict, this approach is mainly suitable for short-range communications, which relies on transmitting signals over a wide frequency band with a very low transmission power. The underlay approach is also favourable in the specific scenarios, where the PUs are always active. In this case, the CUs do not have to find the spectrum holes, but they always send their signals at a power below the threshold [4, 13, 30].

- **Overlay Mode**: In the overlay mode, the CUs are allowed to concurrently transmit signals with the PUs which is achieved by exploiting the available information about the PUs signal format and possibly some further information. The information may be determined for example, if the PUs either use publicized codewords based on the uniform standard for transmission or periodically broadcast their coded information [4]. For instance, the CUs may overhear the PUs ARQ feedback flags and transmit their data during the retransmission process of the PUs [79]. Specifically, the CUs can carry out their communication via, for example, dirty paper coding at the transmitter and invoke interference cancellation at the receiver [4]. On the other hand, when operated in geographic areas, where the PR signals are weak, the CUs may invoke some of their resources to assist the PUs, while use the remaining resources to transmit their own data [78]. This will ensure that the PUs transmission is protected, while the CUs transmit their own data [78].

- **Interweave Mode**: The interweave mode is based on the concept of opportunistic spectrum access as envisioned by Mitola [3]. When operated under this mode, a CU periodically senses the radio environment for the sake of spotting free spectrum holes. If a spectrum hole is discovered, the CU uses it for the transmission of its data [4, 9–11]. Therefore, in the interweave mode, the band has to be uncontaminated in order to avoid imposing severe interference on the PUs due to mis-detection or to avoid wasting the available resources due to false-alarm.

2.1.4 Cognitive Radio Functions

In order to make efficient use of the spectrum, but not to degrade the performance of the CUs, a dynamic spectrum management framework has been proposed [11], which carries out the following operations: 1) Identification of unoccupied spectrum; 2) Channel selection; 3) Information exchange with other CUs; and 4) Relinquishing a channel as soon as it is required by a PU. Correspondingly, the dynamic spectrum management of CR systems may be divided into four functions, namely [11, 16]: 1) *spectrum sensing*; 2) *spectrum decision*; 3) *spectrum sharing*; and 4) *spectrum mobility*, which are illustrated in Fig. 2.5. Below, we provide a rudimentary overview of these functions.

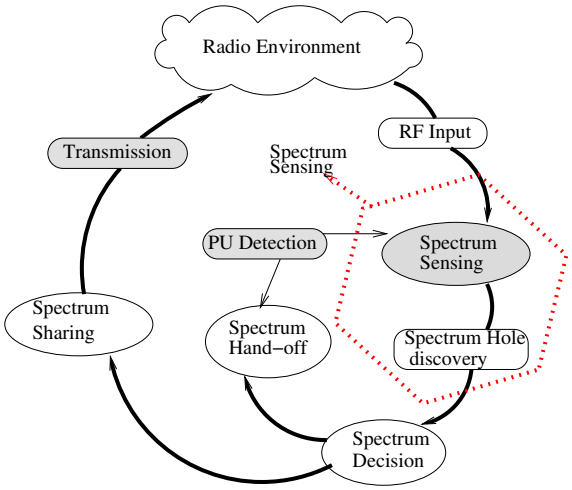

Figure 2.5: Spectrum management tasks in CR systems.

2.1.4.1 Spectrum Sensing

For a CR system to work efficiently, an essential first step is to identify the spectrum holes that are not occupied by the PR systems with the aid of spectrum sensing. In CR, reliable spectrum sensing is not easy to achieve, since some CR systems are operated in the weak signal region of PR systems. Furthermore, there may be simultaneous transmissions from both the PUs and CUs. Therefore, a wide-range of sophisticated spectrum sensing approaches have been proposed [11, 80]. Below, we consider a generic model of spectrum sensing in CR, based on which both non-cooperative and cooperative sensing are reviewed.

2.1.4.1.1 Spectrum Sensing Model

Spectrum sensing can be modelled as a binary hypothesis problem, with $\mathcal{H}_0$ and $\mathcal{H}_1$ representing that the spectrum considered is occupied or not, respectively. Let $\mathcal{T}$ represent the associated decision-making statistics obtained from the received signal as well as relying on any *a-priori* knowledge. Furthermore, let $\mathcal{T}_h$ be a predefined detection threshold. Then, the decision of spec-

trum sensing can be made according to the rules of

$$\begin{cases} \mathcal{H}_0, & \text{if } \mathcal{T} \leq \mathcal{T}_h, \\ \mathcal{H}_1, & \text{if } \mathcal{T} > \mathcal{T}_h \end{cases} \tag{2.1}$$

The performance of a spectrum sensing algorithm can be quantified in terms its sensitivity, probability of correct detection (P_{cd}) and probability of false-alarm (P_{fa}), etc. Specifically, the P_{cd} represents the chances that the PU is correctly detected, when it wants to use the spectral band, which can be formulated as

$$P_{cd} = \Pr\{\mathcal{T} > \mathcal{T}_h | \mathcal{H}_1\}. \tag{2.2}$$

By contrast, the P_{fa} is the probability that a PU is deemed to be present, when the spectrum is in fact free to use. Hence, P_{fa} can be expressed as

$$P_{fa} = \Pr\{\mathcal{T} > \mathcal{T}_h | \mathcal{H}_0\}. \tag{2.3}$$

By contrast, the CR system may fail to identify the ongoing transmission within a band, hence declaring that the spectral band is free from PUs, which is known as the mis-detection. Correspondingly, the mis-detection probability (P_{md}) can be expressed as,

$$P_{md} = \Pr\{\mathcal{T} < \mathcal{T}_h | \mathcal{H}_1\} = 1 - P_{cd}. \tag{2.4}$$

In order to maximize the exploitation of band that imposes negligible interference on the PR systems, spectrum sensing is generally motivated to maximize P_{cd} and simultaneously minimize P_{fa}, or maximize P_{cd} for a given P_{fa} [61, 81]. This is because minimizing P_{fa} maximizes the exploitation of the spectrum, when it is free from the PUs [61], whereas, maximizing P_{cd} minimizes the collisions between the CUs and PUs. Therefore, in order to achieve the highest possible spectrum sensing efficiency, the decision statistics as well as the sensing parameters have to be carefully designed [61, 81–83]. Correspondingly, various spectrum sensing techniques have been proposed in the literature [16, 83–85], which may be classified into three main categories: 1) non-cooperative sensing 2) cooperative sensing, and 3) interference-based sensing, as summarized in Fig. 2.6 [10].

2.1.4.2 Non-Cooperative Sensing

In the context of non-cooperative sensing, a CU does not interact with the PUs and the other CUs in the network. In order to find a spectrum hole suitable for communication, a CU measures the activity of the both PUs and of the other CUs based on their transmitted signals with aid of local observations [86]. Since a channel may be occupied by the PU or any other CU, sometimes, it is important to distinguish them by determining whether the signal is from a PU or a CU [87]. In

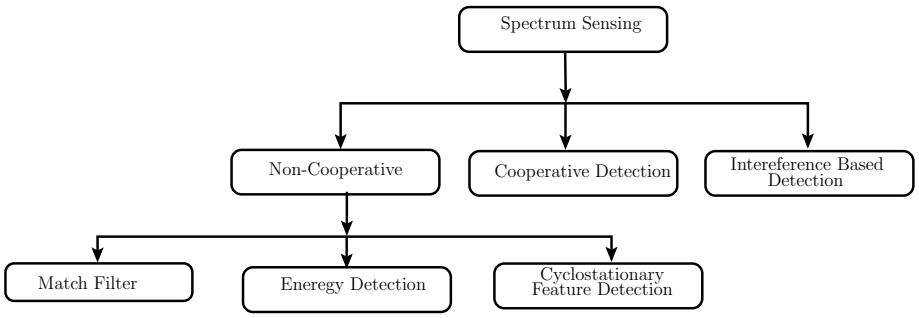

Figure 2.6: Different types of spectrum sensing techniques.

CR, non-cooperative sensing techniques include matched filtering (MF), energy detection (ED), cyclostationary feature detection, waveform based sensing and radio identification based detection [11, 71, 80, 87–89]. Their pros and cons are summarized in Table 2.2, accompanied by the discussions below.

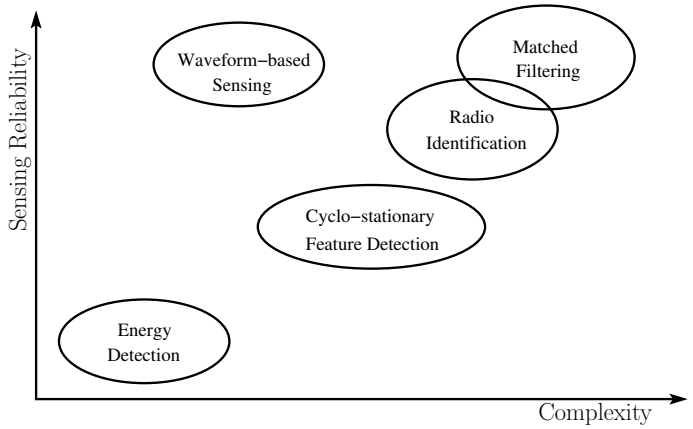

Figure 2.7: Comparison of spectrum sensing methods based on complexity and accuracy ©Yucek and Arslan [80].

Comparisons of the Non-Cooperative Sensing Methods

Sensing algorithms are characterized by their implementation cost, sensing reliability, complexity, etc. In Fig. 2.7 we show the trade-off between the sensing reliability and the complexity of some popular non-cooperative sensing schemes, which are also summarized in Table 2.2. Among the spectrum sensing approaches considered, the waveform-based sensing algorithm [95, 101] is capable of attaining a higher sensing reliability than the energy detection [80, 94] and the cyclostationary scheme [87, 100]. On the other hand, in the waveform-based sensing [95], the PUs have to transmit signal patterns known to the CUs, which results in a high complexity, since the CUs may require extra circuitry and power for obtaining the *a-prior* information about the PUs [80, 101]. As shown in Fig. 2.7, when no information is known about the PUs, the energy detection has a lower complexity than the other. However, its reliability is the worst among the schemes considered.

The cyclostationary feature detection exploits known *a-prior* information about the PUs (for

Sensing Technique	Definition	Pros and Cons
Matched Filter (MF) Detection	The CR system may detect the PU's signal by comparing a known PU template signal (pilot, preambles, spreading codes) with the unknown input signal [13, 80, 90, 91].	**Pros**: Sensing time is lower, low false-alarm and miss-detection probabilities, low implementation cost and provides optimal performance. **Cons**: MF requires perfect and prior knowledge of the PU signal. It has higher power consumption and complexity as well as it requires extra circuitry [11, 13, 58, 80, 91, 92].
Energy Detection (ED)	PUs signals are detected by comparing the received signal with threshold which depends on the noise [80, 90, 93, 94].	**Pros:** ED does not require prior PU signal information, it has low computational complexities, circuitry, processing and low implementation cost. **Cons:** Requires larger sensing time, the detection is based on the uncertainty of the noise power and setting an optimal threshold is difficult in practise. It can not distinguish between PUs and CUs signals [58, 86, 87, 89, 95–97]
Cyclostationary Feature Detection	By exploiting the cyclostationary feature of the received signal, the activity of the PUs can be determined. The PU signals has a periodic pattern, which may be used by the CU to detect the activity of PU [58, 80, 98–100].	**Pros:** Differentiate noise from PUs signal, it can recover various modulation schemes used by the PUs, robust against changes in noise and low SNR, it has less hidden node problem, and having high detection probability than ED. **Cons:** Requires larger sensing time, the computational complexity is higher, required partial information of PUs signal [13, 58, 80, 87, 100].
Waveform Based Sensing and Detection	Applicable only when PUs patterns, such as preambles, mid-ambles, pilot pattern, spreading sequences, are known. The signal received by CU are compared with the known patterns, through which the presence of PU is detected [80, 87, 95, 101].	**Pros:** Complexity is lower than matched filter. It performs better than ED [95], effective in terms of reliability and convergence time. **Cons:** Requires demodulation before detection for which PU transmission parameters like bandwidth carrier frequency, modulation type, frame formate are needed. Its performance degrades significantly when PUs information are inaccurate [58, 80, 87, 101].
Radio Identification Based Detection	CUs determine the transmission technologies of PUs through which complete information is achieved. For example, channel bandwidth, shape, range, cyclic frequencies, detected energy and correlation characteristics can be used for identification and CUs use it for their own transmission [80, 96, 102].	**Pros:** Accuracy is higher than both the ED and cyclostationary feature detection. **Cons:** Implementation cost and complexity is higher [80, 102].

Table 2.2: Non-cooperative spectrum sensing techniques.

example, sine wave carriers, pulse trains, cyclic prefixes, the periodicity of the signal, which makes them cyclostationary) to detect the spectrum holes [80, 87]. The cyclostationary feature detection imposes a higher complexity than the ED, but achieves a higher reliability [80, 87, 91]. As shown in [91, 103], the cyclostationary feature detection tends to fail in fading scenarios, which typically results in an SNR cliff. Furthermore, the cyclostationary feature detection based sensing was also shown to be sensitive to to the sampling clock offsets [80]. In contrast to the ED and cyclostationary feature detection, the radio identification based sensing [96, 102] and MF-based sensing are capable of attaining a higher reliability sensing, because complete knowledge about PU signal is achieved [96]. However, MF based sensing has higher complexity than the waveform based sensing, ED-based and cyclostationary feature detection based sensing, because in practice, it is challenging to obtain complete information about the the PU signals. [87].

2.1.4.3 Cooperative Sensing

In practice it is hard for a non-cooperative sensing algorithm to identify a channel carrying a weak PU signal, especially in the face of multi-path fading, shadowing, noise, etc [86]. Furthermore, the

ubiquitous hidden terminal problem may be encountered [58, 80]. These problems may be avoided with the aid of cooperative sensing relying on information sharing amongst the neighbour sensing nodes, in order to increase both the reliability and the accuracy of spectrum sensing [71, 80, 104]. In cooperative sensing, the CR sensing nodes share their sensing information with each other, which assists in providing more accurate and reliable information as well as in carrying out more reliable decisions about the activity of the PUs. Specifically, the cooperation schemes may be designed with the motivation 1) to maximize the probability of detection, 2) to minimize the probability of false-alarm and miss-detection and/or 3) to mitigate the hidden node problem [80, 105]. Despite the above-mentioned advantages, cooperative sensing also faces some challenges, such as conceiving efficient information sharing algorithms, which increases its complexity [106].

In the literature, the cooperative sensing schemes are divided into centralized and distributed sensing [11, 71, 80, 87, 107]. In the centralized sensing schemes, control channels are required for conveying local sensing information to the central decision unit [108, 109]. By contrast, in the distributed sensing schemes, the control channels are used for transmitting the local sensing information from one node to another, in order to reliably detect the spectrum holes [110, 111].

2.1.4.4 Interference Temperature

The FCC [5] has introduced a concept for measuring the level of interference, which known as interference temperature. The CUs are allowed to use the licensed band, provided that the interference temperature is below the interference limit [13].

2.1.5 Spectrum Decision

Following the sensing process, the CUs may observe a number of free channels for their use. Then, a spectrum decision process is activated for selecting the best possible channels among the available ones for satisfying the required QoS [16, 112]. Spectrum decision can be made either in a *centralized* or *distributed* form. In the context of centralized decision making, a CR base station (BS) receives the local sensing information from the individual sensing nodes, then it decides and selects the best channels to use. Centralized decision making is efficient, but increases the communication overhead. By contrast, in *distributed* decision making, a node makes its decision by only sharing information with its local neighbours in a small cluster [113]. This approach is efficient both for operation in *ad hoc* and mobile topologies, since it consumes a low power and imposes a low communication overhead [16, 71]. However, there are challenges in terms of designing efficient schemes for making accurate decisions as well as conceiving efficient algorithms for the scenario, when the different nodes have different dynamic parameters. Furthermore, it is challenging to efficiently distribute the control channel information.

2.1.6 Spectrum Mobility and Hand-off

Following spectrum sensing and decision, a CU may camp on a particular channel for transmitting its data. However, there is a realistic chance that a PU becomes active and hence requires the channel that is currently being used by the CU. In this case, the CU has to relinquish the channel for the PU to use and switch to another channel. This process is known as spectrum mobility or spectrum hand-off. In CR, spectrum hand-off must be performed promptly and efficiently, so that the transmission of PUs is not hampered, and the QoS is not affected [71, 114]. Note that it is important for the spectrum mobility and hand-off protocols to know about the switching time required for finding the best channel to avoid long delays [16, 115]. In the context of spectrum hand-off, there are some open research issues, which include 1) mobility in the time- and spatial-domain; 2) design of efficient spectrum hand-off and management algorithms in order to reduce the hand-off delay [11, 16].

2.1.7 Spectrum Sharing

Finally, a CR system may simultaneously support multiple CUs. Spectrum sharing allows CUs to cooperate with each other for optimally exploiting the resources, without imposing excessive interference on the PUs [116]. In CR, the protocols conceived for spectrum sharing have similar functionalities to those of the medium access control (MAC) protocols. However, the coexistence of CUs and PUs, as well as dynamic assignment of spectral bands imposed a lot of challenges in the context of power allocation, topology, spectrum coordination and access, etc [51].

2.1.8 Recent Advances in Cognitive Radio Systems

In this section, we briefly review the recent spectrum management issues and standardization efforts in the context of CR systems.

2.1.8.1 Spectrum Management Initiatives in the US

2.1.8.2 TV Band

In 2010, the FCC officially defined the rules and policies introduced for authorizing CUs to utilize the unoccupied TV channels, which are also known as TV white spaces [117]. The so-called database-driven approach was introduced, which provides the information about what frequencies can be accessed during what time periods. The database-driven approach simplifies the sensing task and avoids interference. Based on this approach, two IEEE standards, namely 802.22 and 802.11af, were formed for communication using the unoccupied TV channels.

2.1.8.3 Advanced Wireless Services (AWS)-3 Band

In January 2015, FCC arranged an auction for the bands of $1695 - 1710$ MHz, $1755 - 1780$ MHz, and $2155 - 2180$ MHz, jointly known as the AWS-3 bands [118]. As a result, a limited number of federal systems share the AWS-3 spectral bands with non-federal system users.

2.1.8.4 3.5 Ghz Band

The FCC opened the $3550 - 3700$ MHz band for CUs to utilize for providing Cognitive Broadband Radio Services [119]. Based on the regulations, the spectrum is accessed based on a three-tier model, comprised of the incumbent users, priority access users and general authorized access users [119].

2.1.8.5 5 Ghz Band

The FCC announced a change in the UNII band, attaching an additional 195 MHz of spectrum to the 5 GHz band [120]. Moreover, in 2014, the FCC proposed to modify the UNII based bands, in order to improve the utility of the 5 GHz band, provided that no interference is imposed on the licensed users operating within this band [121].

2.1.8.6 Millimetre Wave Bands

To improve the performance of unlicensed users in terms of capacity and short-range outdoor backhaul, the FCC made a few of amendments, in order to allow the ISM band devices to be operated in the $57 - 64$ GHz band, which is known as the 60 GHz band.

2.1.9 Spectrum Management in the Other Nations

In 2015, the European Conference of Postal and Telecommunications Administration defined the regulations for CR to operate over the 5 Ghz band, and examined the option of allowing WiFi to share the bands of $55350 - 5470$ MHz, $54725 - 5850$ MHz and $5850 - 5925$ MHz with PUs for the sake of establishing a European Common position [122]. The United Kingdom's Office of Communication (OFCOM) decided to permit unlicensed users to access the unoccupied part of the $470 - 790$ MHz band, based on the spectrum database approach [123]. In France, the 2.3 GHz, 5.8 GHz and $17.7 - 19.7$ GHz bands were released for sharing with unlicensed users.

In 2012, the Canadian spectrum management body, namely Industry Canada (IC), introduced the regulations to be observed by unlicensed users to access the TV white space [124]. Recently, the IC published the regulations, which elaborate on the operational and technical requirements of the devices using the TV white space [125]. Similarly, the Infocomm Development Authority

of Singapore (IDA) allowed CR devices to use the TV white spaces. The research community in China is working on finding the amount of spectrum required for supporting the 5G systems. More particularly, the IMT-2020 group has been created for defining and developing the relevant standards and requirements for the development of 5G in China. So far, the IMT2020 has identified that the $450-470$ MHz, $698-806$ MHz and $3400-3600$ MHz bands as being suitable for 5G [126].

2.2 Overview of Automatic Repeat reQuest Schemes

Supporting reliable data transmission over wireless links is a challenge due to the hostility of wireless channels. Hence powerful error-correction and error-detection techniques are required. Automatic Repeat reQuest (ARQ) [127] and Forward Error Correction (FEC) [19] constitute the most popular techniques invoked for improving the transmission reliability. Furthermore, the ARQ and FEC techniques can be appropriately combined for the sake of maximizing the throughput and transmission reliability, which results in the family of Hybrid ARQ (HARQ) techniques, which have found numerous applications [128, 129]. For example, HARQ protocols have been conceived for achieving reliable communications in underwater acoustic networks [130], in satellite communications [131], in audio and video transmission over the Internet [132] and in multi-relay communications [133]. Zhang and Hanzo [134] have proposed the HARQ-aided superposition coding both for improving the cell-edge coverage and the energy efficiency. Chen *et al.* [135–137] have proposed multi-component turbo coded MCTC HARQ schemes, relying on the so-called deferred interation philosophy, which reduce the complexity by postponing the activation of the turbo iterations until the reception of sufficient redundancy for ensuring reliable decoding. In [138] De *et al.* have proposed channel-adaptive stop-and-wait retransmission schemes for short-range wireless communications, in order to reduce the energy dissipation. Moreover, HARQ has also been proposed for a range of IEEE standards [139–141], as noted in Table 2.3.

In the following subsections, the family of ARQ techniques is discussed in the context of their pros and cons.

The concept of ARQ was introduced by Chang in [20] and Harris *et al.* in [142], as a mechanism that uses a feedback channel to inform the transmitter, whether a transmitted packet is correctly received or not. Later Shannon [143] analysed the theoretical limits of the feedback assisted channel and stated that the capacity of the memoryless channel cannot be increased by a feedback channel. However, the reliability of the channel at a rate below its capacity can indeed be enhanced by ARQ [143].

In the different ARQ schemes, either positive acknowledgement (ACK), or negative acknowledgement (NACK) flags are used [18, 21, 22]. In order for a receiver to determine, whether a received packet is correct and take the corresponding action, the pure ARQ schemes use cyclic

redundancy check (CRC) codes, which encode each packet by concatenating parity bits to form a codeword that is transmitted to the receiver over a wireless channel. Once, the receiver receives a codeword, it decodes it by performing parity checking. If the codeword passes the parity checking, the received packet is considered to be error-free. Then, the receiver informs the transmitter by sending an ACK signal. By contrast, if the received packet is found to be erroneous, the receiver feeds back a NACK signal to the transmitter to ask for retransmission. At the transmitter, when it receives an ACK signal, it transmits a new packet. By contrast, if a NACK signal is received, the erroneous packet is retransmitted. Moreover, if the transmitter fails to receive the feedback (ACK or NACK) after some given time, the transmitter also retransmits the packet, regardless of its status. The process of the above retransmissions continues until the successful reception of the packet.

The following the basic ARQ techniques have been proposed: 1) Stop-and-Wait (SW), 2) Go-Back-N (GBN) and 3) Selective-Repeat (SR) [18, 144–147]. The performance of ARQ schemes is typically quantified in terms of packet loss rate, throughput, delay, etc. [146–149]. They may be implemented either at the MAC layer or the Transport layer. ARQ is capable of providing a high reliability, albeit at the cost of an increased transmission delay and throughput. When the SNR is low, a high delay is imposed, due to the significant increase of retransmissions [128]. Hence, in order to reduce the number of retransmissions, reduce the delay and increase the throughput of the system, hybrid FEC and ARQ (HARQ) may be invoked, where the FEC scheme cleans up most the error-infested packets, as discussed in [129, 150].

2.2.1 Stop-and-Wait ARQ Protocol

The Stop-and-Wait Automatic Repeat reQuest (SW-ARQ) [18] protocol enables a transmitter to send a single packet to its receiver. Then the transmitter's control channel receiver waits for the acknowledgement, which is expected to be received after the round-trip-time (RTT) defined as the time duration from the instant of packet transmission to the reception of its feedback. Under the SW-ARQ, both the transmitter and receiver require a buffer size of one packet for storing the index of the packet the transmitter transmitted and the receiver is expecting to receive. Specifically, the buffer at both side is used for storing the index of the packet. The operational principles of the SW-ARQ are highlighted below with the aid of Fig. 2.8.

Operation of the transmitter: The transmitter sends a packet and waits for its acknowledgement. During the waiting time, the transmitter does not transmit any other packet until the feedback is received, as shown in Fig. 2.8. This is due to the fact that the transmitter only has a buffer size of one packet. Hence, only a single packet can be transmitted at a time. Furthermore, the transmitter's buffer is updated based on the reception of feedback flags as follows:

- If an ACK is received, the buffer index is increased by one and the copy of the acknowledged packet is replaced by a new packet, which is transmitted immediately.

- If a NACK is received, the buffer remains unchanged and the same packet is retransmitted.

Operation of the receiver: Upon receiving a packet, the receiver checks whether the packet is received with or without errors, based on which the receiver updates its buffer as follows:

- If an error-free packet is received, the receiver's buffer index is increased by one and the receiver's control channel transmitter sends transmits an ACK flag to the transmitter's control channel receiver.
- Otherwise, if an erroneous packet is received, the receiver's buffer remains unchanged and the receiver's control channel transmitter sends a NACK flag to request the transmitter's control channel receiver for retransmission of the erroneous packet.

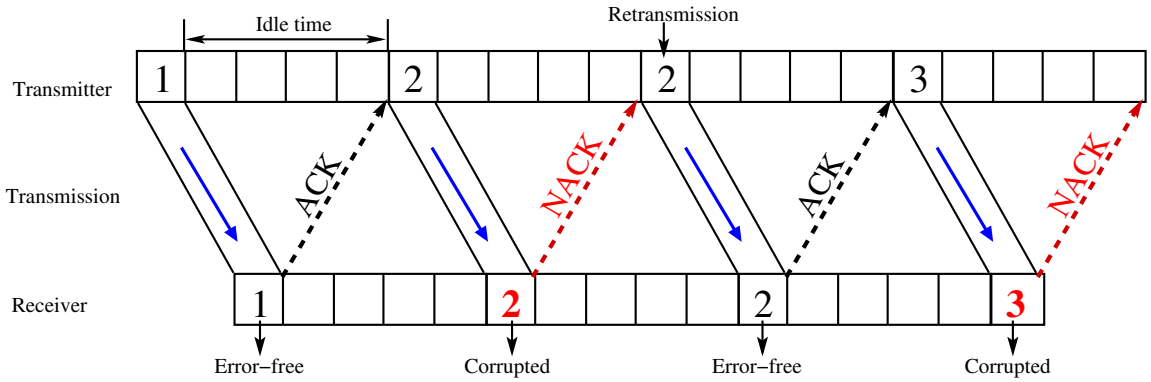

Figure 2.8: Transmission flow of packets using SW-ARQ scheme with a RTT of five packet duration.

Fig. 2.8 shows an example of data transmission based on the SW-ARQ scheme. As depicted in Fig. 2.8, the transmitter starts its transmissions by sending packet 1 to the receiver and waits for the associated feedback. After receiving packet 1, the receiver finds that packet 1 is correctly received. Therefore, it sends an ACK flag to inform the transmitter of the correct reception. Upon receiving an ACK for packet 1 from the receiver, the transmitter transmits the newly added packet 2. However, the receiver detects that packet 2 is corrupted. Therefore, it discards the packet and transmits a NACK signal to the transmitter to request a retransmission. After the reception of the NACK, the transmitter retransmits packet 2. The above process continues until all the packets are transmitted correctly.

The SW-ARQ has the advantage of a low-complexity implementation, but it imposes a long delay waiting for receiving the ACK and NACK [18, 21, 22]. When the channel has a high SNR, the throughput of SW-ARQ is much lower than that of the GBN and SR-ARQ schemes.

2.2.2 Go-Back-N ARQ Protocol

To overcome of long idle time of the SW-ARQ, the GBN-ARQ protocol was proposed and studied in [18, 21, 22]. Under the GBN-ARQ, the transmitter continuously transmits packets one after

another without waiting for their acknowledgements, until it receives a negative feedback from the receiver. To support this operation, a buffer size of N packets is used at the transmitter, while a buffer size of one packet is used at the receiver, where N is determined by the transmission rate and the RTT [18, 21, 22]. The operation of the GBN-ARQ can be highlighted with the aid of Fig. 2.9 as follows.

Operation of transmitter: The transmitter keeps sending packets with the aid of a buffer having the capacity of N packets, which is updated based on the reception of feedback flags as follows:

- If an ACK is received for a packet, the transmitter sends a new packet, which is also added at the end of the buffer;
- If a NACK is received for a packet, the transmitter buffer remains unchanged and both the erroneous packet as well as the packets sent after the erroneous packet are retransmitted.

Operation of receiver: At the receiver, the following operations are executed:

- If the received packet is found to be error-free, then the index of the receiver buffer is increased by one and correspondingly, an ACK flag is returned to the transmitter.
- On the other hand, if an erroneous packet is received, then the receiver keeps the index of the receiver buffer unchanged and discards all the $(N-1)$ packets received after the erroneous packet. Simultaneously, the receiver feeds back a NACK to the transmitter.

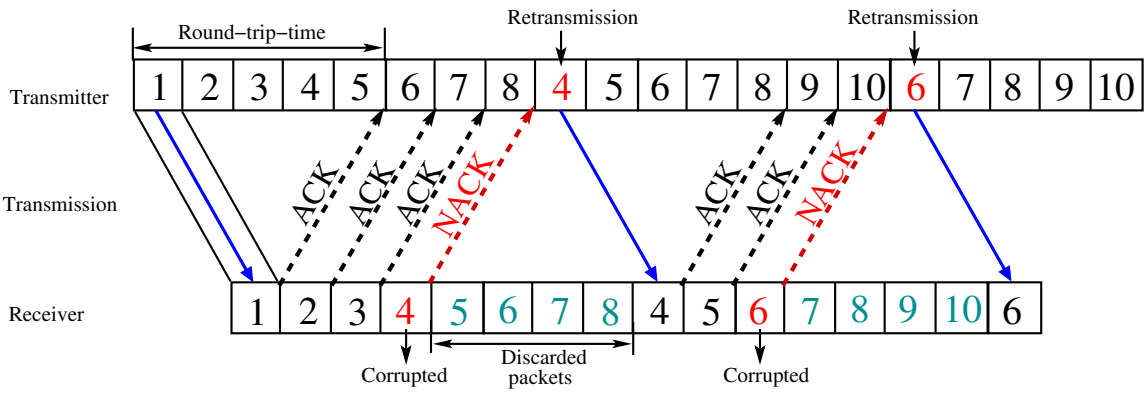

Figure 2.9: Transmission flow of packets using the GBN-ARQ scheme, when the buffer size and RTT are $N = 5$.

As an example, Fig. 2.9 shows the principles of GBN-ARQ. The transmitter transmits packet 1 and during its RTT, followed by transmitting packets $2, 3, 4$ and 5, until it receives the relevant feedback from the receiver. As shown in Fig. 2.9, packets $1, 2$ and 3 are correctly received as indicated by the ACKs. Therefore, the transmitter keeps sending packets $6, 7$ and 8. Then, packet 4 is received in error, which is signalled back to the transmitter using a NACK. Therefore, the transmitter retransmits packets $4-8$. At the receiver, according to the GBN-ARQ protocol, packets

$4-8$ are all discarded, since the receiver is still waiting for receiving packet 4. The above process continues until all packets are correctly received.

At relatively high SNRs the GBN-ARQ scheme is more efficient than the SW-ARQ, due to the fact that it keeps on transmitting packets without having to wait for the acknowledgement. Therefore, the GBN-ARQ usually achieves a higher throughput and lower average delay than the SW-ARQ arrangement. However, to carry out the operations of the GBN-ARQ, the transmitter requires a buffer for storing all the copies of the hitherto unacknowledged packets, whereas the receiver has a buffer of size one packet for storing the index of the expected packet. Therefore, the receiver has to discard the unexpected packets and hence their retransmissions becomes mandatory.

2.2.3 Selective-Repeat ARQ Protocol

Similar to the GBN-ARQ, in the Selective-Repeat ARQ (SR-ARQ), the transmitter also continuously transmits its packets without waiting for their feedback flags. However, in the SR-ARQ, the transmitter only retransmits those packets, which are negatively confirmed. Therefore, it can avoid the unnecessary retransmission of packets. In addition to using a buffer size of N packets at the transmitter as GBN-ARQ, we assume that a buffer of size N is used the receiver of the SR-ARQ for storing the index of the expected packets [18, 21, 22]. Then, the operational principles of the SR-ARQ can be explained below with the aid of Fig. 2.10.

Operation of transmitter: The transmitter continuously sends N packets and then its buffer is modified based on the occurrence of one of the following events:

- If an ACK is received for a packet, the transmitter updates its buffer by adding a new packet at the end of the buffer, while the copy of the positively acknowledged packet is deleted. Simultaneously, a new packet is transmitted.
- On the other hand, if a NACK is received for a packet, the transmitter does not change its buffer content at that specific position, but immediately retransmits the packet that was negatively confirmed.

Operation of receiver: When the receiver receives a packet, it first checks whether the index of the received packet matches the index number in its buffer. If it matches, then the receiver generates an acknowledgement flag for the received packet and updates its buffer based on the status of the packet. Specifically, if the packet is correctly received, the receiver sends an ACK to the transmitter, while the buffer index is increased by N. Otherwise, the receiver sends a NACK, while the buffer remains unchanged.

For example, as shown in Fig. 2.10, the receiver accepts only the packets having the same index as those expected by the receiver and only those positions of the receiver buffer are updated, when error-free packets are received. Otherwise, the receiver's buffer remains unchanged. Note that

although the receiver may receive its packets out of the order, it can still delivers the packets in a chronological order to the upper layers [18, 21, 22].

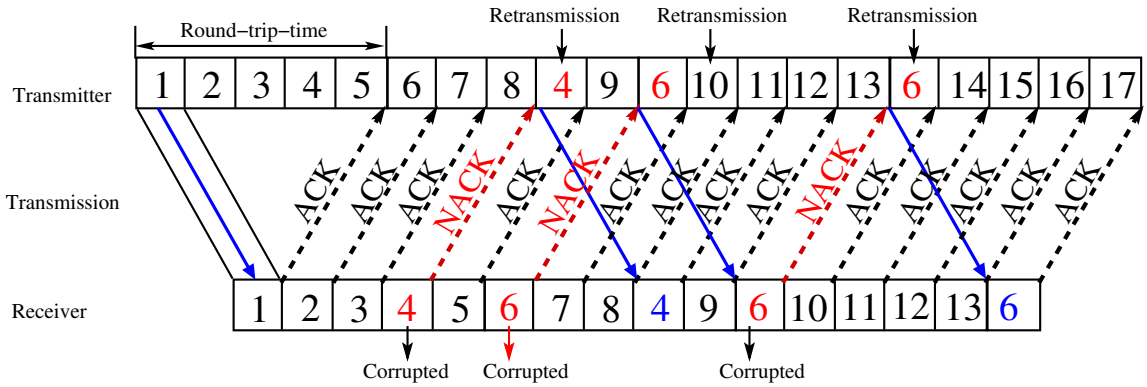

Figure 2.10: Transmission flow of packets using the SR-ARQ scheme, when buffer size and RTT are $N = 5$.

Fig. 2.10 depicts the transmission flow of packets based on the SR-ARQ protocol. When comparing Fig. 2.10 and Fig. 2.9, both of which have the same transmitter buffer size, RTT and error pattern, we can observe that in Fig. 2.10, only the erroneously received packets are retransmitted. By contrast, in Fig. 2.9 the erroneously received packet and the subsequent ($N - 1 = 4$) packets are all retransmitted, regardless whether they are error-free or not.

The SR-ARQ is capable of achieving a higher throughput and lower average delay than the SW-ARQ and GBN-ARQ protocol, since it can continuously transmit packets and only the erroneously received packets are retransmitted, Therefore, both the transmitter and receiver require a buffer for storing the packets, which results in a more complex transmitter and receiver. When the channel SNR is low, both buffers may be large, due to the high large number of retransmissions.

2.2.4 Hybrid Automatic Repeat reQuest

Again, implementation of either ARQ or FEC in isolation may become inefficient for many applications. Therefore, a carefully designed combination of ARQ and FEC may be required, forming the hybrid ARQ (HARQ) scheme [23, 24]. In HARQ, the packets are encoded using an error-correction/detection code which has both error-correction and error-detection capability. Therefore, upon the reception of a codeword, the receiver first makes an attempt to carry out error-correction decoding. If error-correction decoding is successful, the receiver sends the ACK flag to the transmitter. However, if the number of errors exceeds the correction capability of the code, then the receiver sends a NACK flag to the transmitter to request the retransmission of the packet. In the HARQ schemes, the FEC helps in rectifying the errors, but upon receiving uncorrectable error patterns, packet retransmissions are requested by relying on the ARQ approach. As a result, both the throughput and reliability of the system is improved by the joint employment of error-correction and ARQ [18, 128, 147, 151].

With the aid of FEC schemes, the HARQ schemes evolved further into Type-I, Type-II and Type-III HARQ arrangements [18, 128]. The Type-I HARQ is suitable for the systems operating in the face of a constant noise and interference level. In this Type-I HARQ, the receiver first makes an attempt to rectify the errors when the codeword is detected in error. If the errors are within the error-correcting capability of the code, the errors are corrected and the decoded message is transmitted to the upper layers. By contrast, if uncorrectable error patterns are received, the receiver discards the codeword and requests for its retransmission by sending a NACK flag, which is akin to ARQ. After receiving the NACK flag, the transmitter retransmits the same codeword. The receiver carries out the same processing as mentioned above. These operations continue until all packets are correctly received. The Type-I HARQ usually requires a large number of parity bits, since it performs both error-correction/decoding and error-detection, which result in a high overhead. Moreover, the Type-I HARQ may result in a lower throughput than the simple ARQ, when operating in a high-SNR environment. However, when the channel is less reliable, the Type-I HARQ may attain a significantly higher throughput than the simple ARQ, due to the reduced number of retransmissions.

To mitigate the deficiencies of Type-I HARQ, Type-II HARQ has been proposed [18, 128, 152]. In the Type-II HARQ, when the channel is reliable, it operate just like the pure ARQ with the aid of error-correction only decoding. However, when the channel becomes less reliable, then extra parity bits are transmitted for error-correction. In more detail, the information bits combined with the error-detection bits (similar to pure ARQ) are firstly transmitted without being encoded by FEC. If a packet is received without any errors during its first transmission, then the transmission of the packet is deemed to be completed. Otherwise, the receiver requests its retransmission. Then, during the second transmission, the transmitter sends only a limited number of extra some parity bits, rather than sending the whole codeword again. After the reception of the extra parity bits, the receiver performs error-correction decoding by combining the new parity bits with the previously received erroneous packets stored in its buffer. If decoding is successful, the receiver sends an ACK flag. By contrast, if the receiver fails to correct the errors, it requests another retransmission. This time, depending on the specific retransmission approach, either the original codeword is retransmitted or a new block of parity bits is transmitted. The above process continues, until the packet is correctly received. The Type-II HARQ is also known as the Incremental Redundancy based HARQ (IR-HARQ) [152].

Finally, the Type-III HARQ is a special case of Type-II HARQ, where each transmission is self-decodable. Specifically, in the Type-III HARQ, the FEC decoder extracts the information bits either from all the previously received sequences or from only the last sequence received. The ability of self-decodability used by the Type-III HARQ improves the probability of error-free transmissions of the information bits in the Type-II HARQ approaches. According to [153–155], the Type-III HARQ schemes are capable of performing better than the Type-I and Type-II HARQ, due to the property of self-decodability. Moreover, a comprehensive overview and performance

comparisons of various types of HARQ are presented in [18, 128, 156] and the references therein. Type-I and Type-II HARQ schemes have widely been studied in the context of both Reed-Solomon (RS) codes and the rate compatible punctured convolutional (RCPC) codes [157]. In [158], Zhang and Kassam proposed a selective combined HARQ scheme based on the family of RCPC codes for improving the attainable video quality by allowing the decoder to have various combining choices. In [159], Malkamaki and Leib investigated truncated Type-II HARQ in block fading environments. Marcille *et al.* [160] studied both bandwidth and power allocation in the context of Orthogonal Frequency-Division Multiple Access (OFDMA) based multi-user systems employing the Type-I HARQ transmission scheme. In order to enhance the spectral efficiency and reduce the number of retransmissions, a combination of network coding and turbo-coding has been proposed for a Type-III HARQ [161]. Additionally, in [162], Zhu *et al.* conceived an adaptive truncated HARQ scheme for reducing the video distortion imposed. In Table 2.3, we outlined the evolutionary time-like of HARQ schemes.

Table 2.3: Milestones of various HARQ protocols.

Year	Author(s)	Contribution
1970	E. Y. Rocher and R. L. Pickholtz [151]	analysed the performance of HARQ for transmission over an unreliable binary symmetric channel, where BCH codes were used for error detection and correction.
1972	H. O. Burton and D. D. Sullivan [148]	conceived a basic error control technique for dealing with errors imposed by telephone channels.
1975	A. R. K. Sastry [163]	modified the SW-ARQ and GBN-ARQ protocols for achieving an increased throughput over satellite channels.
1984	S. Lin *et. al* [164]	surveyed various ARQ and HARQ protocols.
1990	S. Kallel [165]	proposed code combining technique for improving the attainable throughput.
1995	L. Hanzo and J. Streit [166]	proposed video codes, where the robustness of the system was increased by employing ARQ.
1997	M. Zorzi *et al.* [167]	characterized the throughput of the GBN-ARQ and SR-ARQ protocols in fading mobile radio channels.
	H. Liu and M. E. Zarki [157]	amalgamated Type-I and Type-II HARQ schemes for video transmission using both Reed-Solomon and rate compatible punctured convolutional codes in order to achieve a high reliability and to maximize the video quality.
1999	Q. Zhang and S. A. Kassam [158]	conceived a HARQ aided selective combining approach, which achieved a better performance than Type-II HARQ in fading channel environments. Moreover, video quality is improved by using the RCPC codes.
2000	E. M. Sozer *et al.* [130]	studied ARQ protocols in underwater acoustic networks.
	H. Jianhua [131]	introduced a novel tandem broadcast SR-ARQ scheme for improving the performance of satellite communication.
2001	G. Caire and D. Tuninetti [168]	formulated an information-theoretic view of transmission protocols designed for achieving error-free transmission by employing HARQ over Gaussian fading channels and studied their throughput as well as average delay.
2003	A. C. K. Soong *et. al* [169]	formulated a new forward packet data channel aided Type-II HARQ scheme which helps in enhancing the efficiency of data transmission and improving the spectral efficiency.
2005	B. Zhao and M. C. Valenti [170]	designed a generalized framework for an *ad hoc* network that utilize the spatial diversity by introducing HARQ and relay techniques through which significant improvement is achieved in energy efficiency.
2007	K. C. Beh *et. al* [171]	studied the performance of HARQ in a third generation partnership project (3GPP) long term evolution (LTE) specification over OFDMA system.

Continuation of Table 2.3

Year	Author(s)	Contribution
2008	D. Kim *et. al* [172]	proposed a cross layer ARQ scheme in which the feedback of HARQ is used as ARQ feedback, due to which the overhead of ARQ feedback is removed and hence, the throughput and delay are improved.
2009	D. Nguyen *et al.* [173]	introduced the idea of allowing the transmitter to combine and retransmit the lost packets in such a way that the receiver recovers the packets from receiving a single copy.
	M. C. Vuran and I. F. Akyildiz [174]	studied HARQ and FEC codes in order to enhance the performance in terms of energy efficiency and latency under the constraint of a specific packet error rate.
2010	R. Zhang and L. Hanzo [134, 175]	proposed HARQ aided superposition coding for improving the cell-edge coverage, while improving the energy efficiency. In [175] multiplexed HARQ was invoked reducing the end-to-end delay by reducing the number of retransmissions.
2011	Y. I. Seo and D. K. Sung [176]	investigated the performance of a dedicated resource allocation scheme by employing a queuing system relying on HARQ for analyzing both packet delay distribution and the user capacity.
	H. Chen *et al.* [135–137]	proposed sophisticated multi-component turbo coded HARQ, where the complexity was reduced by postponing the activation of the turbo iterations until sufficient redundancy was received for triggering reliable decoding.
2012	J. So [177]	investigated the throughput and packet delay of the voice-over internet protocol (VOIP) in a mobile WiMAX system context using HARQ.
2013	H. Chen *et al.* [150, 178]	discussed the challenges of amalgamating HARQ with turbo codes for reducing the complexity. As a further advance, a distributed multiple component turbo code (MCTC) was also designed [178] for cooperative HARQ for the sake of reducing the decoding complexity compared to the classic twin-component parallel turbo code.
2014	H. A. Ngo and L. Hanzo [129]	surveyed the state-of-the-art of the HARQ in the context of cooperative wireless communication and a novel rely-switching technique was proposed for enhancing the system's throughput.
2015	H. Chen *et al.* [179]	proposed an improved Raptor code for enhancing the performance of fountain codes for reducing the packet loss probability. Moreover, improved Raptor codes were amalgamated with HARQ for constructing an adaptive HARQ scheme, which helps in choosing the appropriate coding rate.
	K. Xu *et al.* [161]	proposed network coding assisted and distributed turbo coding aided Type-III HARQ for improving the spectral efficiency through reducing the number retransmissions and by exchanging extrinsic information between the network coding and turbo decoder.
	M. Chitre and W. S. Soh [180]	studied the problem of reliable data transmission in point-to-point under-water acoustic communication. The results showed that juggling-like ARQ (J-ARQ) performs poorly when transferring small files. This deficiency was mitigated by proposing rate-less code-based J-ARQ.
2016	C. Zhu *et al.* [162]	introduced an adaptive truncated HARQ-aided system for reducing the video distortion, while controlling the delay imposed.
	N. D. K. Liyanage *et al.* [181]	analyzed both the throughput and the bit error performance of high speed downlink packet access (HSDPA) systems relying on adaptive modulation and coding. For reducing the radio resources occupied, an optimal value of the maximum number of retransmissions was found for the HSDPA system.
	B. Makki *et al.* [182]	analysed the performance of a relay-network by employing HARQ and adaptive power allocation.
2008-2012	IEEE standards 802.20, 802.16m and 802.16.1 [139–141]	all rely on HARQ.

2.3 HARQ Protocols in Cognitive Radio Systems

As argued before, data transmission in the CR systems faces the usual challenges of wireless communication, such as interference, fading, noise, etc. in addition to the dynamic nature of CRs [64, 183, 184]. Similar to the conventional wireless systems, the CR systems also require powerful error correction/detection techniques [18, 19]. For example, an anti-jamming coding technique was proposed in [185, 186]. Liu *et al.* in [187] proposed a network-coding approach for increasing the throughput of ARQ protocols operated in CR environments. Similarly, Makki *et al.* [188, 189] analyzed the throughput of CR systems. In [190], Liang *et al.* proposed an adaptive dynamic network coding technique for CR networks, where the PUs and CUs cooperated. Powerful near-instantaneously adaptive turbo trellis coded modulation (TTCM) was invoked for protecting the information without extending the bandwidth. Furthermore, in [64], Liang *et al.* reviewed the state-of-the-art in CR communication by investigating the physical, MAC and network layers.

However, there is a paucity of studies on the analysis of HARQ protocols in the context of CR systems. The dynamic nature of the PUs actions renders the analytical modelling of the HARQ protocols in the context of CR systems a challenging task. Hence the detailed theoretical analysis of the throughput and delay of CR systems employing HARQ protocols [185–197] has remained to a large extent unexplored. In the investigations disseminated in [191–193], it was assumed that the CUs sense the activity of the PUs via observing their feedbacks flags (ACK and NACK). Based on this feedback flag the CUs decided whether to transmit or not based on the principles of HARQ. As a further result, the throughput of the SR-ARQ protocol has been studied in [198], in the context of CR systems, while Ao and Chen [194] as well as Touati *et al.* [195] have provided a seminal performance analysis of ARQ assisted CR relay systems. Additionally, a hybrid of the spectrum interweave and underlay sharing paradigms was proposed in [196, 197] for improving the performance of CUs. On the other hand, in [64, 183, 184] the authors have offered comprehensive surveys for various data transmission techniques employed in CR systems. In Table 2.4, we summarize some of the contributions related to CR-aided HARQ.

Table 2.4: Milestones in CR-aided HARQ protocols systems.

Year	Author(s)	Contribution
2001	R. E. Ramos and K. Madani [199]	studied the protocol layer in the context of SDR systems.
2005	D. Cabric and R. W. Brodersen [200]	studied the physical layer design issues of CR and proposed a power control and spectrum shaping scheme for mitigating the interference imposed on the PUs.
	T. Fujii and Y. Suzuki [201]	proposed space time block coding-aided ARQ for data transmission in spectrum sharing environments for supporting reliable communication.
2006	N. Devroye *et. al* [202]	reviewed the communication limits of CR and investigated how to achieve these limits in the presence of low interference level.
	T. Fujii *et. al* [203]	introduced space-time-block-coding assisted distributed ARQ in *ad-hoc* CR networks, where reliable data transmission was achieved by retransmitting the erroneous packets using ARQ. A frequency table constructed at the source node for changing the channel after each retransmission.

Continuation of Table 2.4		
	P. Mähönen *et. al* [204]	conceived a cognitive resource manger, which assists in optimizing the network resources and managing cross-layer optimization.
2007	A. Baker *et. al* [205]	compared various low density parity check algorithms in terms of their error-correction capabilities, complexity, energy and power consumption in the context of CR systems.
	T. Weingart *et. al* [206]	characterized how the physical, network and application layer parameters interact with each other in order to maximize the spectrum efficiency, throughput and reliability.
2008	H. Su and X. Zhang [207]	proposed a cross-layer operation aided multi-channel MAC protocol for improving the throughput and delay of CR-based *ad-hoc* networks. Specifically, a pair of spectrum sensing policies were used for the detection of spectrum holes at the physical layer. The associated packet scheduling and MAC layer transmission were also considered.
	G. Yue [208]	studied various coding techniques designed for anti-jamming. It was found that both the rate-less coding and anti-jamming codes are effective in CR systems.
	H. Kushwaha *et. al* [209]	proposed a transmission scheme for distributed multimedia applications supported by CR networks with the aid of fountain codes.
	S. -L. Cheng, Y. Zhen [210]	a cross-layer operation assisted approach of the physical and MAC layer has been proposed for improving the overall throughput by jointly designing the power control modulation and truncated ARQ.
2009	K. B. Letaief and W. Zhang [62]	focused on space-time-frequency coding and adapted the coding structure in dynamic CR environments.
2009	S. Y. Jeon and D. H. Cho [198]	studied the performance of ARQ in multi-hop relaying aided cognitive systems through which the reliability of the system was improved. As a benefit of efficient resource sharing, the overall system performance was enhanced.
	G. Yue and X. Wang [211]	invoked an anti-jamming coding technique in the context of a CR system for achieving 1) reliable transmission, 2) increased throughput and 3) low redundancy with the aid of rateless coding.
2010	W. C. Ao and K.C. Chen [194]	proposed an end-to-end HARQ scheme based on amplify-and-forward cooperative relaying.
	L. Yang *et. al* [187]	proposed a network coding assisted ARQ scheme for improving the efficiency of conventional ARQ schemes.
	R. A. Roshid *et. al* [212]	reviewed various cooperative sensing and transmission techniques conceived for the CUs and PUs both for improving the throughput and for protecting the PUs transmission from collisions.
2011	Y. Qi *et. al* [213]	introduced a so-called H^2-ARQ relaying scheme for improving both the energy efficiency and throughput.
	S. M. Cheng *et. al* [214]	proposed an opportunistic interference mitigation strategy for improving the data rate of the CUs by listening to the PU's ARQ feedback.
	S. Akin and M. C. Gursoy [215]	studied the capacity of the CU's channel in the presence of both QoS as well as channel uncertainty and transmission power constraints. Based on these constraints, the optimal throughput was determined.
2012	J. Liu *et. al* [216]	introduced a pair of opportunistic spectrum sharing schemes for minimizing the average delay and for enhancing the QoS of CR in bursty-traffic CR environments.
	L. Musavian and T. L. Ngoc [217]	investigated the packet error rate and delay of a specific underlay spectrum sharing approach by proposing a cross-layer resource allocation technique.
2012	B. Makki *et. al* [188]	analyzed the performance of spectrum sharing networks using HARQ in terms of their throughput and outage probability.
	Y. Yang *et. al* [218]	developed a cross-layer frame work, in which adaptive modulation and coding was used at their physical layer and truncated ARQ was employed at the data link layer for minimizing the CU's packet loss ratio and for increasing the spectrum efficiency.
2013	J. Hu *et. al* [197]	proposed a HARQ assisted CR system, which amalgamates the interweave and underlay approaches for the sake of increasing the probability of transmission opportunities and for reducing the overall average delay.
	J. Wang *et. al* [219]	investigated the parameters having an impact on the QoS of the CR systems and based on these parameters, a protocol framework was proposed by considering both the lower and upper communication layers.

Continuation of Table 2.4		
	W. C. Ao and K. C. Chen [220]	focused on the impact of error-control techniques such as simple ARQ retransmissions, Chase combining and incremental redundancy on the performance of local broadcasting in heterogeneous *ad-hoc* networks.
	R. Andreotti *et. al* [221]	proposed a link adaptation technique relying on specific adaptive modulation and coding as well as ARQ mechanisms for improving the goodput and for reducing the complexity.
2014	Y. Wang *et. al* [222]	introduced a pair of optimal transmission for the underlay and overlay modes in order to improve the QoS and network throughput.
2014	G. Ozcan *et. al* [223]	studied the error rate performance of CR transmission in sensing-based spectrum sharing and opportunistic spectrum access.
	J. S. Harsini and M. Zorzi [224]	proposed a cross-layer operation aided scheme in which both the CU and the PU transmitters employ DSA at the physical layer and ARQ at the data link layer in order to improve the throughput subject to specific packet loss ratio constrain of both the PU and CU.
	Y. C. Chen *et. al* [225]	struck a trade-off between the reliability and latency employing the end-to-end transmission in CR aided *ad-hoc* networks.
2015	J. Li *et. al* [226]	introduced a cross-layer aided technique having the capability of link maintenance in order to mitigate the problem of link establishment and reliable transmission.
	Y. Zou *et. al* [227]	reviewed various physical-layer security issues and attacks that affect the communication of the CUs. An opportunistic relay scheme was also proposed to attain reliable transmission between the CR source and destination.
	B. Makki *et. al* [189, 228]	studied the throughput using finite-length codewords in spectrum sharing networks.
2016	A. A. Khan *et. al* [85]	surveyed the architecture, the networking techniques, applications and CR communication protocols employed in smart grids.
	L. Zhang *et. al* [70]	introduced energy-efficient DSA protocols for improving the overall channel utilization without affecting the performance of the PU.
	D. W. K. Ng *et. al* [229]	studied resource allocation, transmit power minimization and energy harvesting in order to maximize the efficiency and information security of CR systems.

In Fig. 2.11, we summarized the factors that are affecting the data transmission in CR systems as well as affecting the throughput and delay performance. These factors make the analytical modelling highly challenging whereas, in the literature, very limited research have been dedicated for exact theoretical modelling of CR assisted HARQ techniques. Therefore, against this background,

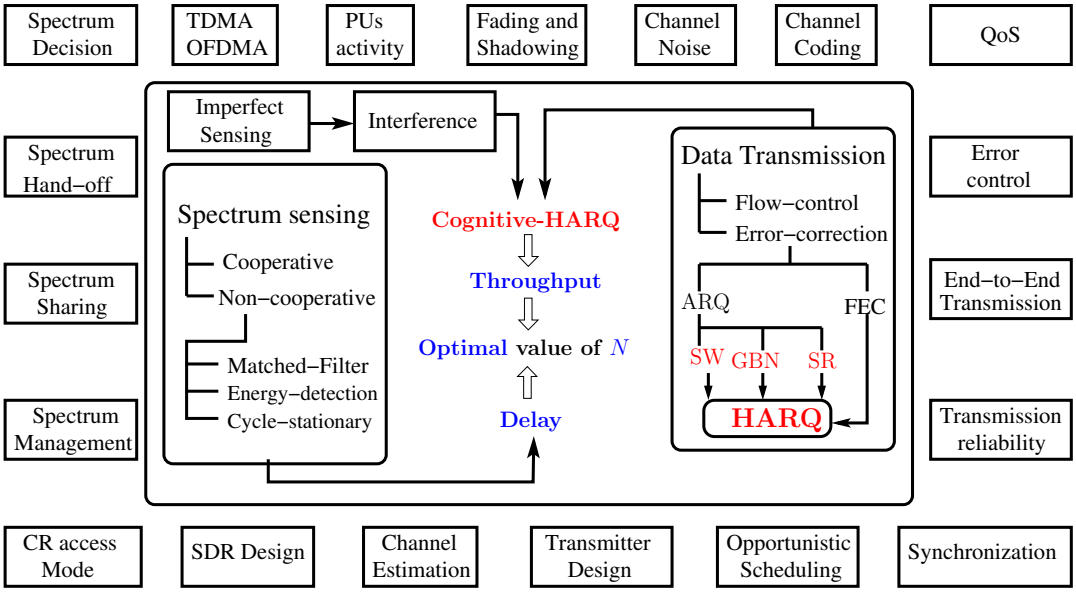

Figure 2.11: Overview of factors affecting the data transmission ins CR systems.

in this thesis, we analytically modelled the family of HARQ techniques incorporated in CR systems for the sake of achieving reliable communication. The operations of the classic transmitters and receivers based on HARQ techniques were redesigned in order to operate in dynamically fluctuating CR environments. Specifically, we proposed a pair of distinctive analytical approaches, namely the probability based and the DTMC based approach, which consider the stochastic nature of the PUs. Based on these approaches, novel closed-form expressions were derived for the throughput, for the average packet delay and for the end-to-end packet delay, which includes both the probability distribution and the average end-to-end packet delay. The analytical approaches have been lavishly validated by simulations.

2.4 Summary and Conclusions

In this chapter, we highlighted the importance of CR systems in mitigating the spectrum scarcity problem. In Subsection 2.1.1, we discussed the concept of DSA and its various models. Then, the concept of CR systems and its functions were discussed in Subsection 2.1.2. Explicitly, the performance of various non-cooperative sensing algorithm versus their complexity was compared. Then in Section 2.2, the classic ARQ protocols including the SW-ARQ, GBN-ARQ and SR-ARQ as well as HARQ techniques applied in conventional wireless systems were reviewed. In Section 2.3, we then proceeded with a literature review and challenges of intrinsically amalgamating HARQ protocols with CR systems in order to achieve reliable transmission. In the following chapters, we will provide the theoretical analysis and simulation based performance studies of the aforementioned HARQ protocols in the context of CR systems.

Chapter 3

Performance of Cognitive Stop-and-Wait Hybrid Automatic Repeat reQuest in the Face of Imperfect Sensing [1]

In Chapter 2, we have reviewed the consequences of spectrum shortfall and discussed the proposed solutions. Among many alternatives for circumventing the spectrum scarcity issues, our point of interest is the popular Cognitive Radio (CR) paradigm. Therefore, we briefly elaborate on the concept of CR in terms of its design, architecture, functions and upto-date advances. Then classic wireless communications and their challenges in achieving reliable communication were discussed in Section 2.2. A detailed introduction to the ARQ protocols and classic HARQ techniques has been presented in Chapter 2. In Section 2.3, we studied reliable transmission in CR system and performed state-of-the-art literature survey with an emphasis on the implementation of HARQ protocols. Indeed, we conclude that the concept of CR system has been a hot research topic for over a decade, but only limited attention has been dedicated to reliable communication. Therefore, in this chapter, we proposed a Stop-and-Wait (SW)-HARQ-aided CR system, for reliable data transmission in the context of CR systems. Furthermore, we provide detailed analytical modelling of the proposed transmission scheme, which is validated by simulations.

3.1 Introduction

Since, the germination of the CR concept, a substantial amount of research has been dedicated to the CR architecture, to its operating principle, spectrum sensing, reconfiguration, spectrum sharing,

[1] A part of this chapter has been published in IEEE Vehicular Technology Conference, Glasgow, May 2015 [230] and in IEEE Access, Voume 4, July 2016 [231].

mobility etc., are studied in Chapter 2 [11, 232]. For instance, the throughput of CR networks has been widely studied in the context of perfectly detecting the activity of the PUs [80], relying on the assumption of the optimal sensing time [61, 83], on cooperative sensing [233] and using the optimal frame length [82]. More particularly, in [61,82], Liang *et al.* and Tang *et al.* have proposed various approaches of maximizing the throughput of the CUs by finding both the optimal sensing duration and the time-slot (TS) duration both in perfect and realistic imperfect sensing scenarios. By contrast, the trade-off between the sensing duration and throughput has been optimized by proposing a hybrid spectrum sensing and data transmission technique in [234].

Following the spectrum sensing operation, the CUs access the channel for data transmission. As discussed in Chapter 2, data transmission in CR systems is faced with the usual hostile wireless communication channels, hence powerful error-correction and detection are techniques have been proposed for achieving reliable communication [18, 19]. In this regard, the SW-ARQ has been studied as an error-control scheme when operating in a time-invariant parallel multi-channel environment [235]. As further development, the throughput of the generalized network coding nodes based on SW-ARQ has been investigated in [236]. Moreover, HARQ-aided superposition coding has been proposed for improving the cell-edge coverage, while improving the energy efficiency [134]. Following that, De *et al.* [138] proposed channel-adaptive stop-and-wait retransmission schemes in the environment of short-range wireless links for reducing the energy consumption as compared to the classic SW retransmission schemes. Qin and Yang [237] studied the steady-state throughput of network coding using SW-ARQ protocol for data transmission. Kao [238] proposed decode-and-cooperate protocol and confirmed that it achieves better throughput and delay than the classic SW-HARQ protocol. Moreover, HARQ has also been invoked in various IEEE standards [77, 139–141].

There is a paucity of studies on the analysis of ARQ protocols in the context of CR. Based on our observations, the dynamic nature of PUs makes the analytical modelling of the ARQ protocols in the context of CR more challenging. The studies performed in this direction include [64, 183–189, 191–198]. However, these studies do not provide the complete theoretical throughput and delay analysis of the CR system employing ARQ protocols. Specifically, in [191–193], the CUs sense the presence of the PUs by listening to their ARQ feedback. However, the authors did not investigate the performance of CUs using ARQ techniques. Ao and Chen [194] as well as Touati *et al.* [195] performed seminal analysis of ARQ-aided relay-assisted CR systems. Moreover, Roy and Kundu [239] considered the underlay spectrum sharing paradigm for authorizing the CUs to perform its packets transmission operation in the presence of PUs, where packets transmission are assumed to be performed using SW-HARQ protocol. Makki *et al.* [188, 189] analyzed the performance of spectrum sharing networks using HARQ feedback in terms of throughput and outage probability, where as, in [189], the efficiency of data transmission is studied for finite-length codewords in spectrum sharing networks. Yue *et al.* [185, 186] introduced an improved HARQ scheme employing an anti-jamming coding approach for achieving reliable communication in CR systems.

As a further development, a network coding assisted ARQ scheme has been proposed in [187], which aims for improving the efficiency of the conventional ARQ schemes. A hybrid of the spectrum interweave and underlay sharing paradigms has been proposed in [196,197] for improving the performance of the CU. The authors of [197] have also invoked the ARQ technique for improving the attainable reliability. Moreover, in [70] energy-efficient dynamic spectrum access protocols are proposed for CR nodes in order enhance the overall channel utilization without effecting the performance of the PU. On the other hand, the authors of [64,183,184] comprehensively surveyed the various techniques employed in the context of CR systems. In summary, the existed contributions in the direction of achieving reliable data transmission failed in providing exact theoretical analysis for the CR system employing ARQ protocols for data transmission. Hence, in this chapter, we theoretically modelled the CR-aided stop-and-wait HARQ regime.

In this chapter, we focus our attention on the spectrum interweave access mode [9,10] discussed in Section 2.1.3.1, which enables the CU to sense and exploit the PR's channel for its own transmission, provided that the PR's channel is not occupied at the instant of the demand [61,67,207]. Specifically, the activity of the PU is modelled using a two-state Markov chain, having the 'ON' and 'OFF' states [83,207,240]. The channel is considered to be occupied by the PUs in the 'ON' state and to be free in the 'OFF' state. However, when the sensing is unreliable, the Markov chain has four states [1], including the false-alarm and mis-detection events. In this scenario, a TS of duration T is divided into two portions: a sensing epoch (T_s) and a transmission epoch (T_d) [61,234]. The sensing epoch T_s is used for detecting spectrum holes, while the transmission epoch $T_d = T - T_s$ is used for data transmission. In our CR system, the data transmission relies on the principles of classic stop-and-wait hybrid automatic repeat request (SW-HARQ) [18,21,22].

Our proposed cognitive stop-and-wait (CSW-HARQ) scheme intrinsically amalgamates CR system with the classic SW-HARQ regime in both perfect and imperfect sensing environments. We opted for the SW-HARQ protocol as a benefit of its low complexity at both the transmitter and receiver. However, it wastes time between the end of transmitting a packet and reception of its feedback acknowledgement [18,21]. Again, in the CSW-HARQ, the CR transmitter first senses a PR's channel and only transmits data if the channel is deemed to be free. Otherwise, it waits until the next TS. After the transmission of a data packet, the transmitter waits for the feedback. At the receiver side, when the CR receiver receives the packet, it starts its decoding and generates a feedback flag [194,241]. A positive feedback (ACK) is generated and sent to the transmitter, if an error-free packet is received. Otherwise, a negative feedback (NACK) is generated and sent to the transmitter. Then, the CR transmitter sends a new packet after the reception of an ACK. Otherwise, the previous packet is retransmitted in the next free TS, if it receives a NACK. Note that the ACK/NACK feedback signals are assumed to be always error-free, which is justified by the fact that the feedback signals are usually well protected [242,243]. Moreover, the information content is usually low, since a single bit is enough for the CSW-HARQ. Therefore, the reception of feedback can be readily protected from errors and it does not adversely affect the sensing and

transmission processes. Based on the above arrangements, we investigate the throughput and delay of the CSW-HARQ scheme both by analysis and by simulation, when assuming either perfect or imperfect sensing.

3.1.1 Contributions and Chapter Structure

Against the above background, the contributions of this chapter can be summarized as follows:

1. The proposed CSW-HARQ scheme intrinsically amalgamates the CR capability with the conventional SW-HARQ protocol in order to achieve reliable data transmission in realistic imperfect sensing. Our protocol enables the CR transmitter to sense the channel before using it and to receive feedback at all times, regardless of the PUs activity.
2. Firstly, the CSW-HARQ scheme is modelled and theoretically analysed using a probability-based approach considering both perfect and imperfect reusing. Using this approach, closed-form expressions are derived for the a) average packet delay, b) for the throughput of the CU system and c) for the end-to-end packet delay. Both the probability distribution and the average of the end-to-end packet delay are formulated.
3. Secondly, based on Discrete Time Markov Chain (DTMC) approach, closed-form expressions are derived for the a) throughput of the CU system b) for the average packet delay and c) for the end-to-end packet delay, including its probability distribution and average end-to-end packet delay.
4. Finally, we validate theoretical results by simulations.

3.2 System Model

In this section, we describe both the primary radio (PR) and the CR systems, as well as the assumptions invoked in our analysis and for obtaining the results of Section 3.6.

3.2.1 Modelling the Primary User

As in [1], we assume that there is a PR's channel, which is sensed and used by the CR system considered. We assume that the PUs become active during each TS of duration T independently with the same probability. Specifically, the activation of the PR's channel by the PUs is modelled as a two-state Markov chain having the state transitions shown in Fig. 3.2. The state 'OFF' represents that the channel is free for the CU to use, whereas the state 'ON' indicates that the channel is occupied by the PUs; α and β represent the transition probabilities from the 'OFF' and 'ON' to the 'ON' and 'OFF' state, respectively. Let the probabilities of the PUs channel being in the 'ON' and

Figure 3.1: The structure of this chapter.

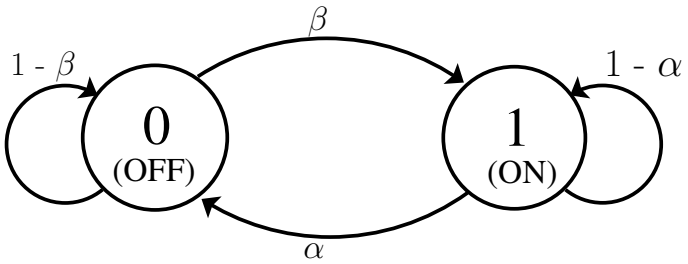

Figure 3.2: Two-state discrete-time Markov chain model of the PU system.

'OFF' states be P_{on} and P_{off}, respectively. Then, it can be readily shown that if the Markov chain is in its steady state, we have [21]

$$P_{on}\alpha = P_{off}\beta, \tag{3.1}$$

and from $P_{off} = 1 - P_{on}$ we have:

$$P_{on} = \frac{\beta}{\alpha+\beta}, \;\; P_{off} = \frac{\alpha}{\alpha+\beta}. \tag{3.2}$$

Furthermore, as shown in Fig. 3.3(a), we assume that if the PR's channel is found in the 'ON' state at the start of a TS, it remains in the 'ON' state until the end of that TS, and using this TS should be avoided by the CU. On the other hand, if a TS is deemed to be free from the PUs, then the CU may use it [83].

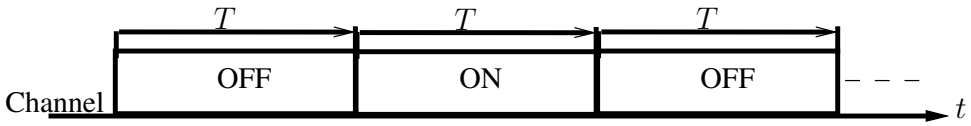

(a) Pattern of channel usage by PU

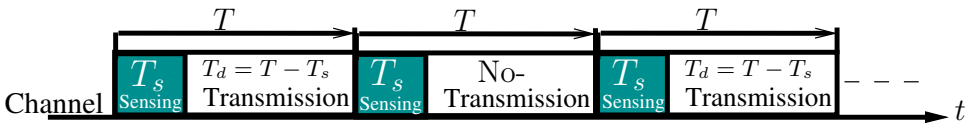

(b) Pattern of channel usage by CU

Figure 3.3: Time-slot structure of PU and CU, where a CU TS consists of a sensing duration of T_s and a transmission duration of $T_d = T - T_s$, when given the total duration T of a time-slot.

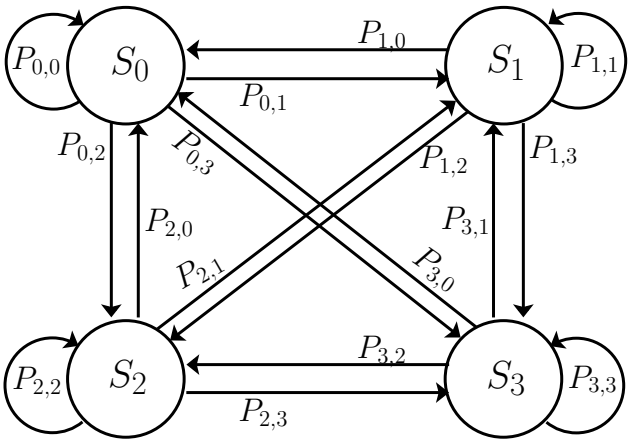

Figure 3.4: Discrete-time Markov chain modeling of the CR system. In state $S_0 = 00$, the channel is sensed free when given that it is free; $S_1 = 01$, the channel is sensed busy when given that it is free. Similarly, the states $S_2 = 10$ and $S_3 = 11$ are defined.

3.2.2 Modelling the Cognitive User

In the CR system, each TS of duration T is divided into two phases: the sensing duration of T_s seconds and the data transmission duration of $T_d = T - T_s$ seconds, as shown in Fig. 3.3(b). When the PR's channel is deemed to be 'OFF' within the sensing period T_s, the CR system can use the time T_d for its data transmission based on the principles of CSW-HARQ. However, the sensing decision of the PR's channel may be imperfect, hence resulting in false-alarm, when the channel is 'OFF', but detected to be 'ON'. Alternatively, mis-detection is encountered when the PR's channel is 'ON', but detected to be 'OFF'. In summary, the transitions are shown in Fig. 3.4. Correspondingly,

$$\boldsymbol{P} = \begin{bmatrix} P_{0,0} & P_{0,1} & P_{0,2} & P_{0,3} \\ P_{1,0} & P_{1,1} & P_{1,2} & P_{1,3} \\ P_{2,0} & P_{2,1} & P_{2,2} & P_{2,3} \\ P_{3,0} & P_{3,1} & P_{3,2} & P_{3,3} \end{bmatrix}. \tag{3.3}$$

Let the false-alarm and mis-detection probabilities be expressed as P_{fa} and P_{md}, respectively. Then from Fig. 3.4, we obtain

$$\begin{aligned}
P_{0,0} &= P_{1,0} = (1-\beta)(1-P_{fa}) \\
P_{0,1} &= P_{1,1} = (1-\beta)P_{fa} \\
P_{0,2} &= P_{1,2} = \beta P_{md} \\
P_{0,3} &= P_{1,3} = \beta(1-P_{md}) \\
P_{2,0} &= P_{3,0} = \alpha(1-P_{fa}) \\
P_{2,1} &= P_{3,1} = \alpha(1-P_{fa}) \\
P_{2,2} &= P_{3,2} = (1-\alpha)P_{md} \\
P_{2,3} &= P_{3,3} = (1-\alpha)(1-P_{md}).
\end{aligned} \tag{3.4}$$

Furthermore, let the steady state probabilities of the Markov chain be expressed as $\mathbf{\Phi} = [\Phi_0, \Phi_1, \Phi_2, \Phi_3]^T$. Then, we have [21, 244]

$$\mathbf{\Phi} = \boldsymbol{P}^T\mathbf{\Phi}. \tag{3.5}$$

Explicitly, $\mathbf{\Phi}$ is the right eigenvector of $\mathbf{P}^T$ associated with an eigenvalue of 1. Therefore, when substituting the items in (3.4) into (3.3) and solving Equation (3.5), we obtain

$$\begin{aligned}
\mathbf{\Phi} &= [\Phi_0 \;\; \Phi_1 \;\; \Phi_2 \;\; \Phi_3]^T \\
&= \lambda \times \left[\frac{\alpha(1-P_{fa})}{\beta(1-P_{md})} \;\; \frac{\alpha(P_{fa})}{\beta(1-P_{md})} \;\; \frac{(P_{md})}{(1-P_{md})} \;\; 1\right]^T,
\end{aligned} \tag{3.6}$$

where $\lambda \in \mathbb{R}$. Upon exploiting the property of

$$\sum_{i=0}^{3} \Phi_i = 1, \tag{3.7}$$

gives

$$\lambda = \frac{\beta(1-P_{md})}{\alpha+\beta}. \tag{3.8}$$

Consequently, the steady state probabilities of the CR system in the state S_0, S_1, S_2 and S_3 are

$$\begin{aligned}
\Phi_0 &= \frac{\alpha(1-P_{fa})}{\alpha+\beta}, & \Phi_1 &= \frac{\alpha P_{fa}}{\alpha+\beta}, \\
\Phi_2 &= \frac{\beta P_{md}}{\alpha+\beta}, & \Phi_3 &= \frac{\beta(1-P_{md})}{\alpha+\beta}.
\end{aligned} \tag{3.9}$$

3.3 Cognitive Stop-and-Wait Hybrid Automatic Repeat Request

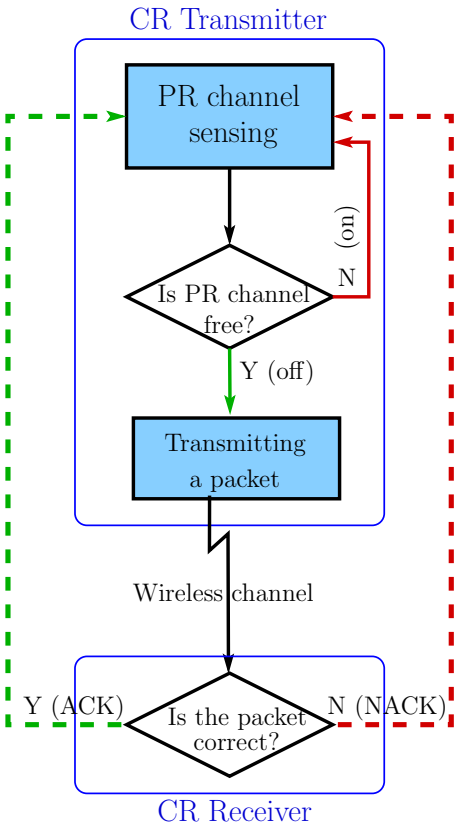

Figure 3.5: Flow chart showing the operations of the proposed CSW-HARQ scheme.

In our CSW-HARQ system, data are encoded using a Reed-Solomon (RS) code RS(N_d, K_d) [18], defined over the Galois Field of GF(q)=GF(2^m), where K_d and N_d represent the number of information and coded symbols, respectively, and m is the number of bits per symbol. We assume that every packet consists of a RS codeword, which is transmitted within T_p seconds. Let $N = T_d/T_p$. Then, within a free TS, the CR transmitter can transmit a packet using the T_p seconds and then waits for the feedback. We assume that the RS code is capable of correcting upto t random symbol errors and can ideally detect the uncorrectable errors, which is time for sufficiently long codes.

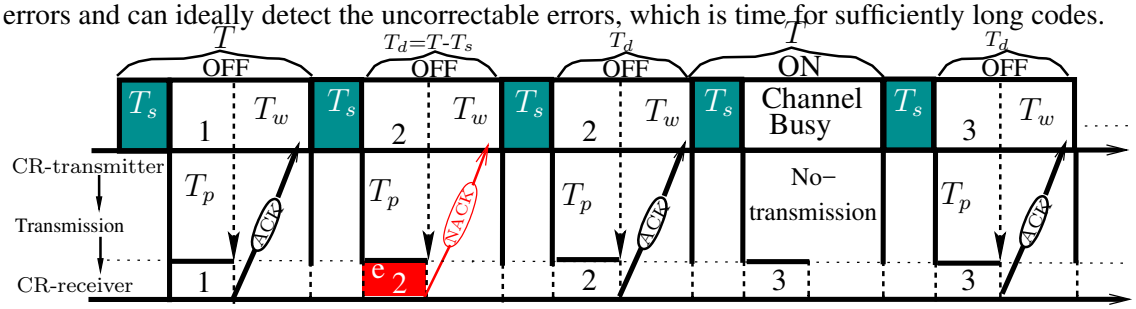

Figure 3.6: The transmission flow of the proposed CSW-HARQ scheme. The total duration of each time-slot is $T = T_s + T_d$, where T_d consists of a packet's transmission duration and its waiting epoch T_w.

Given the above assumptions, data are transmitted between a pair of CUs over the PR channel based on the principles of our CSW-HARQ scheme, which is characterized in Fig. 3.5 and formally

stated in Algorithm 1, as detailed below. For clear insight, the Algorithm 1 is divided into two parts, the transmitter part and the receiver part. The transmitter always senses the PR channel and (re)transmit a packet when channel is free from PUs. On the other hand, at receiver side, RS decoding and error correction is performed, based on which feedback signal is generated for the received packet. We assume that the receiver can perfectly understand about the status of the decoding and update its buffer accordingly.

Algorithm 1 : CSW-HARQ Algorithm

Initialization: M_c = number of packets, $T_d = NT_p$, $T_s = kT_p$, $i = 1$, TS$= 1$, $T_p = 1$.
Input: T_d, T_s, packets.
while $i \leq M_c$ **do**
    CR transmitter senses a time-slot (TS).
    if TS is free and no false-alarm **OR** TS is busy but mis-detected **then**
        transmits the ith packet and, then,
        waits for T_w duration to receive feedback.
        if the ith packet is received error-free **then**
            receiver sends ACK signal.
            $i = i + 1$.
        else
            receiver sends NACK. It could be because of
            mis-detection or channel noise.
        end if
    else
        The TS may be found busy due to correct detection or false-alarm,
        hence, the transmitter waits until the next TS.
    end if
    TS=TS+1.
end while

3.3.1 Operation of the CR Transmitter

In the classic SW-HARQ, the transmitter sends a single packet in a TS and then waits for its feedback, which is expected to be received after a specified round-trip time (RTT). By contrast, in the CSW-HARQ, the CR transmitter first has to sense the PR's channel before the transmission or retransmission of a packet. If the PR channel is correctly detected to be 'OFF', or when the PR channel is mis-detected as being 'OFF' state when it is actually 'ON', the CR transmitter transmits a packet. Otherwise, if the PR channel is correctly sensed to be 'ON' or when it is falsely detected to be 'ON', while it is actually 'OFF', then the transmitter has to wait until the next TS and has to sense the channel again. The CSW-HARQ operations are summarized both in the Algorithm 1 and in Fig. 3.5. Similar to the classic SW-HARQ scheme, the CR transmitter in CSW-HARQ has a buffer of size one, which is updated based on the feedback flag of each transmitted packet.

We assume that all the packets are of the same length and that the CR transmitter is always ready to transmit these packets, provided that there are free TSs. As shown in Fig. 3.6, each CU packet consists of a RS coded codeword, which is transmitted within the duration of T_p seconds. After transmitting a packet, the CR transmitter waits for a duration of T_w seconds in order to receive its feedback. We assume that the RTT is T_d, which is the time interval between the transmission of

a packet, and the instant when its feedback acknowledgement is received. Therefore, in our CSW-HARQ scheme, the feedback flag of each packet should be received within the RTT duration of T_d, as shown in Fig. 3.6. Specifically, if a positive feedback (i.e., ACK) of a packet is received by the CR transmitter within the RTT, this packet is then deleted from the transmitter's buffer and a new packet is transmitted in the next free TS which is also stored in the transmitter buffer. However, if a NACK is received, then the transmitter retransmits the erroneous packet in the next free TS. It is worth mentioning that, when there is a mis-detection of the PR channel, the packet transmitted will become erroneous with a high probability, due to collision with the PU's transmitted signals. On the other hand, when there is a false-alarm, the CU will not transmit, even though the PR channel is free, which results in a reduced throughput.

3.3.2 Operation of the CR Receiver

When the CR receiver receives a packet from the CR transmitter, it invokes RS error-correction/detection and then generates a feedback flag accordingly. Specifically, if a packet is correctly recovered by the RS decoder, an ACK signal is fed back to the CR transmitter. Otherwise, a NACK signal is sent to the CR transmitter in order to request a retransmission. In this chapter, we assume that the feedback channel is perfect and that the receiver has a buffer size of one packet, which is updated only when a packet is correctly received [18, 21, 22].

3.4 Probability-based Analysis Approach

In this and the next sections, we analyze the performance of the proposed CSW-HARQ scheme. We consider three performance metrics, namely, 1) the Average packet delay; 2) the End-to-end packet delay; and 3) the Throughput. They are defined as follows. **Average packet delay**: the average number of TSs (or T_p's) required for the successful transmission of a packet. **End-to-end packet delay**: the average time duration from the first transmission of a packet to the instant when it is finally successfully received. **Throughput**: the error-free transmission rate of the CR system [18, 237].

In this chapter, we introduce two approaches in our analysis, which are the probability-based approach employed in this section, and the DTMC-based approach employed in Section 3.5. Our analytical approaches will be validated in Section 3.6 by comparing the results obtained from the numerical evaluation of the derived formulas with those obtained from simulations. Let us first use the probability-based analysis to analyze the average packet delay.

3.4.1 Average Packet Delay

In the traditional SW-HARQ scheme, the delay is generated by the data transmitted over unreliable channels, which results in erroneous transmission and thereby requires retransmission, in addition to the basic transmission delay. In our proposed CSW-HARQ scheme, the unreliable channels also introduce delay similarly to the traditional SW-HARQ. Furthermore, in the CSW-HARQ, there is an extra delay both owing to the unavailability and due to the false detection of the PR's channel. In order to analyze the packet delay of the CSW-HARQ scheme, let us denote the average delay due to the busy PR's channels as T_{DP}. It can be shown that the PR's channel is found busy in the following two scenarios:

1. The PR channel is 'ON' state and the state is correctly detected.
2. The PR channel is 'OFF', but false-alarm occurs, resulting in the CU not using the channel.

Therefore, according to the definitions in Section 3.2.2, the probability that the CU finds that a TS is busy can be expressed as

$$\begin{aligned} P_{bs} &= P_{on} \cdot (1 - P_{md}) + P_{off} \cdot P_{fa}, && (3.10) \\ &= \frac{\beta(1 - P_{md})}{\alpha + \beta} + \frac{\alpha P_{fa}}{\alpha + \beta}, \\ &= \frac{1}{\alpha + \beta}\big[\beta(1 - P_{md}) + \alpha P_{fa}\big]. && (3.11) \end{aligned}$$

On the other hand, there are only two scenarios for the CU to access the PR's channel for its own transmission:

1. The PR's channel is in the 'OFF' state, which is correctly detected by the CU.
2. The PR's channel is in the 'ON' state, but it is mis-detected by the CU.

Correspondingly, the probability of the above events can be expressed as

$$\begin{aligned} P_{fr} &= P_{off} \cdot (1 - P_{fa}) + P_{on} \cdot P_{md}, && (3.12) \\ &= \frac{1}{\alpha + \beta}\big[\alpha(1 - P_{fa}) + \beta P_{md}\big]. && (3.13) \end{aligned}$$

Explicitly, we have $P_{fr} = 1 - P_{bs}$. Moreover, let $T_{DP}(i)$ be defined as the delay imposed by $(i-1)$ busy TSs prior to a free TS, yielding

$$T_{DP}(i) = (i-1)T. \tag{3.14}$$

Then, the average delay T_{DP} required by the CU to find a free TS may be formulated as

$$\begin{aligned} T_{DP} =& E\left[T_{DP}(i)\right] \\ =& E\left[(i-1)T\right] \\ =& \sum_{i=1}^{\infty}(i-1)TP_{bs}^{i-1}P_{fr} \\ =& \frac{(P_{bs}\cdot P_{fr})T}{(1-P_{bs})^2} = \frac{P_{bs}T}{(1-P_{bs})}, \\ =& \frac{\alpha P_{fa}+\beta(1-P_{md})}{\alpha(1-P_{fa})+\beta P_{md}}\cdot T. \end{aligned} \tag{3.15}$$

Let us assume that a packet is transmitted over a TS that is supposed to be free, but a delay is introduced by transmission over an unreliable channel. If a packet is successfully delivered in the first attempt, it induces a delay of a T/T_p seconds. By contrast, each retransmission will impose a delay of T seconds. As the analysis of Section 3.4.1 shows, erroneous transmissions may take place in the actually free TSs, or in busy TSs misclassified by the from CR transmitter. Let $T_D(i)$ denote the delay given by the event that the CR transmitter uses a total of i transmissions for successfully delivering a packet to the CR receiver. Here, $T_D(i)$ includes both the delay imposed by finding free TSs and the delay due to the packet's transmission. Furthermore, some of the TSs are free and correctly sensed by the CU system, while others are actually busy TSs but they may be mis-detected by the CU. Therefore, given that a free TS is identified by the CU, the probability that the TS is actually free can be expressed as

$$P_A = \frac{P_{off}(1-P_{fa})}{P_{fr}}. \tag{3.16}$$

By contrast, given that a free TS is discovered by the CU, the probability that it is resulted from a mis-detection is

$$P_B = \frac{P_{on}P_{md}}{P_{fr}}. \tag{3.17}$$

Remembering that each transmission attempt requires an average time of T_{DP} seconds for finding a free TS, plus a subsequent delay of T seconds for the actual round trip transmission, we hence have,

$$T_D(i) = i(T+T_{DP}), \tag{3.18}$$

when i transmissions are used for the successfully delivery of a single packet. According to the principles of the CSW-HARQ, the transmitter sends a packet in each free TS. Hence, the average

packet delay T_D can be evaluated by

$$\begin{aligned} T_D =& \frac{1}{N} E\left[T_D(i)\right] \\ =& \frac{1}{N} E\left[i(T + T_{DP})\right], \end{aligned} \tag{3.19}$$

where the multiplier $1/N$ is because each packet is transmitted within N packet durations. Let us denote the packet error probability (PEP) for the packets sent in the free TSs by P_e, after RS decoding. We assume that the PEP of those packets that were transmitted because of mis-detection in the busy TSs is as high as one. Then, it can be shown that we have

$$T_D = \left(\frac{k+N}{N}\right)\left(\frac{P_A(1-P_e)(1+N_{DP})}{(P_B + P_A P_e - 1)^2}\right) T_p's, \tag{3.20}$$

where k represents the sensing duration and $T = (k+N)T_p$ is applied.

3.4.2 End-to-End Packet Delay

In this section, we derive the probability mass function (PMF) of the end-to-end packet delay, as well as the average end-to-end packet delay. Here the end-to-end delay of a packet represents the time duration spanning from the first transmission of the packet to the time that the packet is successfully received.

3.4.2.1 Probability Mass Function

First, it is worth restating that the delay between the first transmission and the final error-free reception of a packet depends on two factors: 1) the delay for retransmissions, and 2) the delay imposed by the occurrence of busy TSs. Below we first derive the PMF of the end-to-end packet delay incurred purely due to retransmissions, when there are no sensed busy TSs. Then, the delay of the general cases including both sensed busy and free TSs between the first transmission and the final successful reception of a packet is considered.

Firstly, when the sensing results at CU is such that there exist no busy TSs between the first transmission and the final reception of a packet, the probability that n TSs are used for successfully delivering a packet can be expressed as

$$P_{MF}(n) = \sum_{j=0}^{n-1} \left(\binom{n-1}{j} (P_{on}P_{md})^j (P_{off}(1-P_{fa})P_e)^{n-j-1}(1-P_e)P_A \right), \; n = 1, 2, \ldots \tag{3.21}$$

For clarity, the above equation can be explained as:

- $(P_{on}P_{md})^j$ defines the probability that j out of $(n-1)$ TSs are detected free by CU due to

mis-detection and thus the transmission on these TSs are always in error.

- $(P_{off}(1-P_{fa})\cdot P_e)^{n-j-1}$ implies the probability that the remaining $(n-j-1)$ TSs are free and are detected free by CU and transmission takes place in these TSs. However, due to channel noise, the packets transmitted in these $(n-j-1)$ TSs are received in error, which cause retransmission.
- Finally, $(1-P_e)P_A$ is the probability that the final TS is free as well as it is correctly sensed, and hence, the packet is successfully delivered.

Secondly, in the general cases that there might be busy TSs between the first transmission and the final reception of a packet, the probability that n TSs are used can be expressed as

$$P_{MF}(n) = \sum_{i=0}^{n-2}\sum_{j=0}^{n-i-1}\binom{n-2}{i}\binom{n-i-1}{j}(P_{bs})^i(P_{on}P_{md})^j(P_{off}(1-P_{fa})P_e)^{n-i-j-1}\cdot \\ \cdot(1-P_e)P_A,\ \ n=1,2,\ldots \quad (3.22)$$

where, in addition to the terms that are similar to those in (3.21), $\binom{n-2}{i}P_{bs}^i$ represents the probability that there are i sensed busy TSs between the first transmission and the final reception of a packet. Note that the largest value for i is $n-2$, as the first and the last TSs are sensed to be free.

3.4.2.2 Average End-to-End Packet Delay

Having obtained the PMF of the end-to-end packet delay, which is given by Eq. (3.22), the average end-to-end packet delay quantified in terms of TSs can be expressed as

$$\begin{aligned}\tau &= \sum_{n=1}^{\infty} n\cdot P_{MF}(n) \\ &\approx \sum_{n=1}^{M_T} n\cdot P_{MF}(n),\ \ (\text{TSs})\end{aligned} \quad (3.23)$$

where M_T is set as the maximum delay to be considered. Note that M_T can be rendered of ensuring that the unconsidered components becomes negligible. For example, we may choose M_T to satisfy $\sum_{m=1}^{M_T} P_{MF}(m) = 1-10^{-8}$.

3.4.3 Throughput

Given the average packet delay expression of (**??**), we can readily obtain the throughput of the CU system operated under the CSW-HARQ, which can be expressed as

$$
\begin{aligned}
R_T =& \frac{1}{T_D} \\
=& \frac{N}{T}\Big(\frac{(P_B + P_A P_e - 1)^2}{P_A(1-P_e)(1+N_{DP})}\Big) \text{ (PPS)} && (3.24)\\
=& N\Big(\frac{(P_B + P_A P_e - 1)^2}{P_A(1-P_e)(1+N_{DP})}\Big) \text{ (PPTS)} && (3.25)\\
=& \frac{N}{k+N}\Big(\frac{(P_B + P_A P_e - 1)^2}{P_A(1-P_e)(1+N_{DP})}\Big) \text{ (PP}T_p\text{)}, && (3.26)
\end{aligned}
$$

where PPS, PPTS and PPT_p denote packet per second, packet per TS and packet per T_p, respectively. Furthermore, let us assume that a (N_d, K_d) RS code is employed denote by B, the number of bits per code symbol. Then, the throughput can also be expressed in terms of bits per second (bps) as

$$R_T = \frac{1}{T_D} \cdot K_d \cdot B \text{ (bps)}. \tag{3.27}$$

In the above, we have analyzed the performance of the proposed CSW-HARQ scheme using the probability-based approach. In the following section, we also provide a Markov-chain based approach for analysing the CSW-HARQ scheme.

3.5 Markov Chain-based Analysis

In this section, we first model the CSW-HARQ scheme relying on realistic imperfect sensing using the DTMC. Then, we analyze the stationary throughput of the CSW-HARQ. Finally, we analyse the end-to-end packet delay by conceiving both its PMF and the average end-to-end packet delay.

Let us first define the states of the CSW-HARQ, where a state can be jointly defined by 1) the real status of the PR's channel (μ), 2) the status of the PR's channel sensed by the CU (ν), and 3) the status of a specific packet (ξ), which is either a new or an old packet stored in the transmitter's buffer. The state is observed and updated at the end of each TS. Let us express the eight legitimate states as

$$\mathbb{S} = \{S_0, S_1, S_2, \ldots, S_7\}, \tag{3.28}$$

where each state is a binary number of length 3, expressed as

$$S_i = \{\mu, \nu, \xi\}, \tag{3.29}$$

where the index i represents the decimal value given by $\{\mu\nu\xi\}$. In (3.29), μ, ν and ξ are defined as

$$\mu = \begin{cases} 0, & \text{the PR's channel is free,} \\ 1, & \text{the PR's channel is busy;} \end{cases} \tag{3.30}$$

$$\nu = \begin{cases} 0, & \text{the PR's channel is sensed to be free,} \\ 1, & \text{the PR's channel is sensed to be busy;} \end{cases} \tag{3.31}$$

and

$$\xi = \begin{cases} 0, & \text{if the packet stored in the transmitter buffer is a new packet,} \\ 1, & \text{if the packet stored in the transmitter buffer is an old packet.} \end{cases} \tag{3.32}$$

The index of the state S_i is the combination of 0 and 1 values of μ, ν and ξ, where the first digit represents the real status of the TS, while the second digit represents the sensed status of the TS and third digit represents the status of the packet in the transmitter buffer, as illustrated in Table 3.1.

State	(μ,ν,ξ)	State	(μ,ν,ξ)
S_0	(0,0,0)	S_4	(1,0,0)
S_1	(0,0,1)	S_5	(1,0,1)
S_2	(0,1,0)	S_6	(1,1,0)
S_3	(0,1,1)	S_7	(1,1,1)

Table 3.1: Possible number of states for the CSW-HARQ.

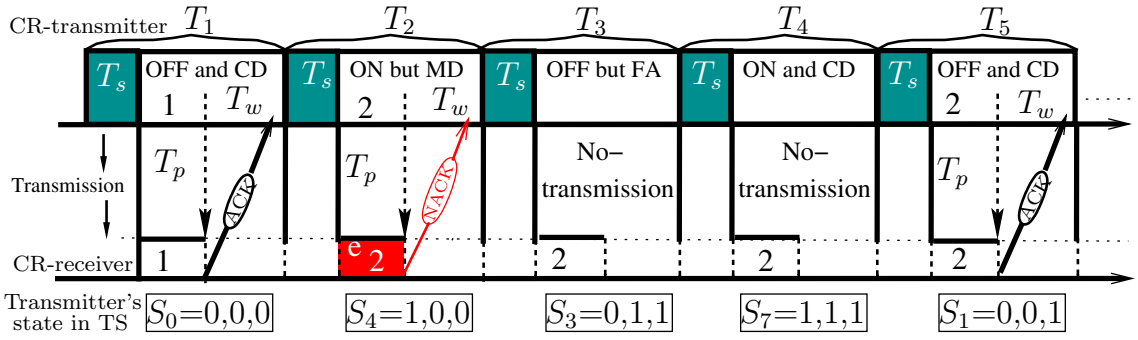

Figure 3.7: Transmission flow of CSW-HARQ, where CD, MD and FA are for correct-detection, mis-detection and false-alarm, respectively. The state is observed by the transmitter at the end of TS.

As an example, Fig. 3.7 illustrates the transitions between states in the context of five TSs. The number in the boxes of the CR transmitter and the receiver represents the packet that is transmitted and received, respectively. In more detail, Fig. 3.7 is interpreted as follows.

1. Assume that during TS T_1, the PR's channel is free and it is correctly sensed to be free corresponding to $\mu = 0, \nu = 0$. Assume furthermore that a new packet which gives $\xi = 0$ is transmitted. Hence, the state observed by transmitter in this TS is $S_0 = \{0,0,0\}$. As shown in the figure, we assume that the packet is correctly received and hence an ACK flag is sent by the receiver to the transmitter as seen in Fig. 3.7.

2. As a benefit of the error-free transmission in the TS T_1, the transmitter buffer is updated to a new packet. In TS T_2, the PR's channel is busy, but it is mis-detected by the CR transmitter. Therefore, a new packet waiting in the buffer is transmitted in TS T_2. Hence, the state during TS T_2 is $S_4 = \{1, 0, 0\}$. Furthermore, it can be shown that the transition from S_0 to S_4 takes place with a probability of $P_{0,4} = (1 - P_e)P_{on}P_{md}$. Note that, due to the mis-detection of the busy PR's channel, the packet sent in TS T_2 is received in error and hence, a NACK flag is fed back.

3. Still referencing to Fig. 3.7 in TS T_3, the PR channel is free but it is found busy due to false-alarm. Since the transmission in TS T_2 is erroneous and the packet requires retransmission, hence the state of the transmitter in TS T_3 is $S_3 = \{0, 1, 1\}$ with the transition probability $P_{4,3} = P_{off}P_{fa}$.

4. Similarly, we can find that the state during TS T_4 is $S_7 = \{1, 1, 1\}$. The transition from S_3 to S_7 takes place with a probability of $P_{3,7} = P_{on}(1 - P_{md})$.

5. Finally, in TS T_5, the PR's channel is correctly detected to be free and therefore the old packet stored in the transmitter buffer is transmitted, which results in the transition from state S_7 to S_1 in Fig. 3.7, with the transition probability of $P_{7,1} = P_{off}(1 - P_{fa})$.

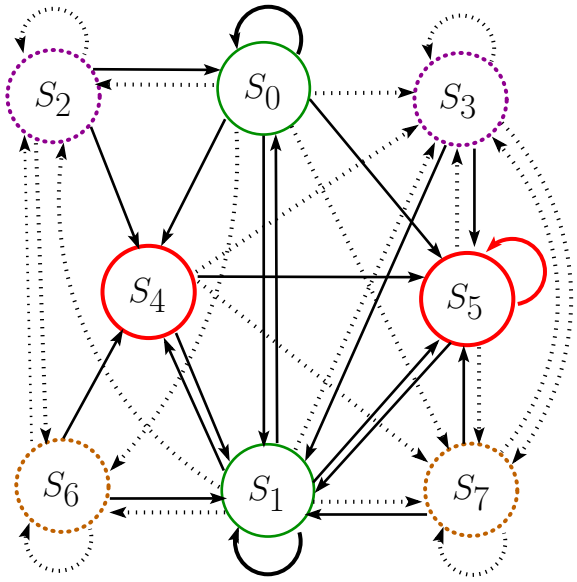

Figure 3.8: The state transition diagram for the DTMC modelling the proposed CSW-HARQ scheme, where *dashed* lines correspond to the transitions towards busy states, while *solid* lines illustrate the transitions towards free states. The *solid green* and *red* circles represent the states in which the PR's channel is free due to correct detection and mis-detection, respectively, while *dashed brown* and *magenta* color circles represent the state in which the PR's channel is found busy due to correct detection and false-alarm, respectively.

Following the above analysis, we can see that the legitimate state to state transitions can be summarized, as shown in Fig. 3.8. Let the state-transition matrix be expressed as **P**, where the (i, j)th element of has the transition probability $P_{i,j}$, which can be found as shown in the above

example. Furthermore, according to the properties of the DTMC [21, 244], we have

$$0 \leq P_{i,j} \leq 1.$$
$$\sum_{j=0}^{7} P_{i,j} = 1, \ \forall \ S_i \ \in \mathbb{S}, \tag{3.33}$$

The probabilities of the transitions between states shown in Fig. 3.8 are stored in $\mathbf{P}$,

$$\boldsymbol{P} = \begin{bmatrix} P_{0,0} & P_{0,1} & \dots & P_{0,7} \\ P_{1,0} & P_{1,1} & \dots & P_{1,7} \\ \vdots & \vdots & \dots & \vdots \\ P_{7,0} & P_{7,1} & \dots & P_{7,7} \end{bmatrix}, \tag{3.34}$$

where the respective state to state transition probabilities are shown in Table 3.2. Note that if a state S_j is not accessible from state S_i in a single step, then the probability of transition from S_i to S_j is set to zero.

State S_i	S_j with probability	S_j with probability	S_j with probability	S_j with probability
$P_{i,j}$, $i = 0, 1$ and $j = 0, 1 \dots 7$	$P_{i,0}$=P_{off}(1-P_{fa})(1-P_e)	$P_{i,1}$=P_{off}(1-P_{fa})P_e	$P_{i,2}$=$P_{off}P_{fa}$(1-P_e)	$P_{i,3}$=$P_{off}P_{fa}P_e$
	$P_{i,4}$=$P_{on}P_{md}$(1-P_e)	$P_{i,5}$=$P_{on}P_{md}P_e$	$P_{i,6}$=P_{on}(1-P_{md})(1-P_e)	$P_{i,7}$=P_{on}(1-P_{md})P_e
$P_{i,j}$, $i = 2, 6$ and $j = 0, 1 \dots 7$	$P_{i,0}$=P_{off}(1-P_{fa})	$P_{i,1} = 0$	$P_{i,2}$=$P_{off}P_{fa}$	$P_{i,3} = 0$
	$P_{i,4}$=$P_{on}P_{md}$	$P_{i,5} = 0$	$P_{i,6}$=P_{on}(1-P_{md})	$P_{i,7} = 0$
$P_{i,j}$, $i = 3, 4, 5, 7$ and $j = 0, 1 \dots 7$	$P_{i,0} = 0$	$P_{i,1}$=P_{off}(1-P_{fa})	$P_{i,2} = 0$	$P_{i,3}$=$P_{off}P_{fa}$
	$P_{i,4} = 0$	$P_{i,5}$=$P_{on}P_{md}$	$P_{i,6} = 0$	$P_{i,7}$=P_{on}(1-P_{md})

Table 3.2: State to state transition probabilities with respect to TS.

In TS (n), the transmitter is in one of the eight legitimate states with the probability of $\boldsymbol{p}(n) = [P_0(n), P_1(n), \dots, P_7(n)]^T$. Then, in TS $(n+1)$, the probabilities of the eight possible states can be found from [21, 245]

$$\boldsymbol{p}(n+1) = \mathbf{P}^T \boldsymbol{p}(n). \tag{3.35}$$

According to [245], when $n \to \infty$, the Markov chain reaches its steady-state condition [21], and in this case we have

$$\boldsymbol{p}(n+1) = \boldsymbol{p}(n). \tag{3.36}$$

Let the steady-state probabilities be expressed as $\boldsymbol{\pi} = \lim_{n\to\infty} \boldsymbol{p}(n)$, where we have $\boldsymbol{\pi} = [\pi_0, \pi_2 \dots, \pi_i \dots]^T$, and π_i represents the steady state probability that the transmitter is in state S_i. Then, from (3.35) and (3.36) we have

$$\boldsymbol{\pi} = \mathbf{P}^T \boldsymbol{\pi}, \tag{3.37}$$

which shows that the steady state probabilities of the different states which can be obtained by computing the right eigenvector of $\mathbf{P}^T$ corresponding to the eigenvalue of 1 [21, 244, 245]. Note that the steady state probabilities satisfy the relationship of

$$\sum_{j \in \mathbb{S}} \pi_j = 1 \quad \text{or} \quad \boldsymbol{\pi}^T \times \mathbf{1} = 1, \tag{3.38}$$

where $\mathbf{1}$ represents a unit of column vector.

3.5.1 Throughput of CSW-HARQ

As defined in Section 3.4, the throughput of the CSW-HARQ scheme is the rate of successful transmission per TS. Carrying out a successful transmission depends on two factors: 1) a free TS is successfully sensed, and 2) error-free transmission is a achieved. Hence, as shown in (3.37), when the DTMC reaches its steady state, the throughput of the CSW-HARQ scheme can be obtained from specific state transitions yielding a successful transmission. According to the definition of states in (3.29) and Fig. 3.8, the transmission of new packet is only possible when the CR transmitter is in state S_0 or S_4. Therefore, the achievable throughput of the CSW-HARQ is given by

$$R_T = \pi_0 + \pi_4 \quad (\text{packets / TS}). \tag{3.39}$$

Additionally, using $T = (T_d + T_s)T_p$, the throughput quantified in terms of the number of packets per T_p can be expressed as

$$R'_T = \frac{1}{T} \cdot R_T \quad (\text{packets / } T_p). \tag{3.40}$$

Let us now analyze the delay of the CSW-HARQ scheme under the DTMC framework.

3.5.2 Delay Analysis of CSW-HARQ

In this subsection, we analyse both the average packet delay and the end-to-end packet delay with the aid of the DTMC model of the CSW-HARQ. For the end-to-end packet delay, we derive both its probability distribution and the average end-to-end packet delay.

3.5.2.1 Average Packet Delay

The average packet delay is defined as the average number of TSs or T_p's needed for the successful transmission of a packet. After obtaining the achievable throughput of Eqs. (3.39) or (3.40), the

average packet delay can be readily obtained, which can be expressed as

$$T_D = \frac{1}{R_s} \text{ (TS per packet)} \tag{3.41}$$

$$= \frac{k+N}{R_T} \text{ (T_p's per packet).} \tag{3.42}$$

3.5.2.2 End-To-End Packet Delay

We first analyze the probability distribution of the end-to-end packet delay. Let $\mathbb{S}_N$ be the specific subset of $\mathbb{S}$, which contains the subsets of states $\mathbb{S}_i$. Here, $\mathbb{S}_i$ is a subset that a new packet transmitted from state S_i is correctly received in state S_j, with the delay of m TSs, i.e.,

$$\mathbb{S}_i = \{S_j | \text{a new packet transmitted from } S_i \text{ is correctly received in state } S_j \text{ after a delay of } m \text{ TSs}\}, \tag{3.43}$$

where we have $\mathbb{S}_i \subset \mathbb{S}_N$. Following the above definitions, the probability mass function of the end-to-end packet delay can be formulated as

$$P(m) = \frac{1}{(\pi_0 + \pi_4)} \sum_{S_i \in \mathbb{S}_N} \sum_{S_j \in \mathbb{S}} \pi_i \cdot P_{i,j}^{(m)}, m = 1, 2 \ldots \tag{3.44}$$

$$= \frac{\pi_0}{\pi_0 + \pi_4} \sum_{S_j \in \mathbb{S}_0} P_{0,j}^{(m)} + \frac{\pi_4}{\pi_0 + \pi_4} \sum_{S_j \in \mathbb{S}_4} P_{4,j}^{(m)}, \tag{3.45}$$

where $P_{i,j}^{(m)}$ denotes the transition probability from state S_i to state S_j after a delay of m TSs.

Let us express the PMF of the end-to-end packet delay as

$$\boldsymbol{P}_{MF} = [P(1), P(2), \ldots, P(M_T)]^T, \tag{3.46}$$

where M_T is the largest delay considered, beyond which the probability of occurrence becomes negligible. From the properties of the DTMC, we know that given a state S_i, after q transitions, we have

$$\boldsymbol{p}^{(q)} = (\mathbf{P}^T)^q \boldsymbol{e}_i, \; q = 1, 2, \ldots \tag{3.47}$$

where $\boldsymbol{e}_i$ is the ith column of the identity matrix. From (3.47) we can see that whenever we multiply $\mathbf{P}^T$ on a current $\boldsymbol{p}^q$, we can obtain the following information:

a) The end-to-end packet delay is q TSs, if the packet is firstly transmitted in state S_i is correctly received in some states after q TSs.

b) The transition probabilities from state S_i to any of the states in $\mathbb{S}$, which contains the states

generating the end-to-end delay of q TSs.

c) The transition probabilities from state S_i to any other states without resulting in correct reception of the packet firstly sent in state S_i.

Using the above information, we can update $\boldsymbol{P}_{MF}$ by the following formula.

$$P(m) \leftarrow P(m) + \pi_i \cdot P_{i,j}^{(m)}, \text{ where } m = 1,2\ldots,M_T, S_j \in \mathbb{S} \text{ and } S_i \in \mathbb{S}_N. \quad (3.48)$$

Finally, when $\boldsymbol{P}_{MF}$ does not change, we can compute the average end-to-end packet delay, which can be formulated as

$$\tau = \sum_{i=1}^{M_T} i \cdot P(i) \quad (\text{TSs}) \quad (3.49)$$

$$= \sum_{i=1}^{M} i(k+N)P(i) \;\; T_p's. \quad (3.50)$$

After completion of our theoretical analysis of the proposed CSW-HARQ scheme, we proceed to validate the accuracy of both the approaches discussed in Sections 3.4 and 3.5 by comparing the analytical results to those obtained through simulations.

3.6 Performance Results

In this section, we demonstrate the performance of the CSW-HARQ system in terms of three performance metrics, namely, 1) throughput 2) average packet delay and 3) end-to-end packet delay, when both idealized perfect sensing and practical imperfect sensing environments are considered. We will characterize the impact of the false-alarm probability (P_{fa}), of the mis-detection probability (P_{md}), the channel's busy probability (P_{on}) and of the packet error probability (P_e) on the performance. Note that, in the case of perfect sensing, P_{fa} and P_{md} are always zero. In our studies, Matlab-based simulations are used, and fifty thousand packets are transmitted for every specific conditions. The observation period commences from the first TS, which continues until all packets are successfully received by the CR receiver.

Fig. 3.9 shows the correct detection probability Φ_0 of a free channel, the false-alarm probability Φ_1, the mis-detection probability Φ_2 and the correct detection probability Φ_3 of a busy channel, as seen in (3.9) of Section 3.2.2, with respect to the parameter α. It can be seen from Fig. 3.9 that when the transmission chances for a CU over those of a PR channel increase, i.e., when α increases, $P_{off} = \Phi_0$ also significantly increases, while $P_{fa} = \Phi_1$ increases only slightly. The slight increase in P_{fa} is the consequence of imperfect sensing. On the other hand, when α increases, P_{on} is dramatically reduced, while P_{md} exhibits only a moderate reduction. As shown in Fig. 3.9, the analytical results evaluated from Eq. (3.9) closely agree with the simulation results.

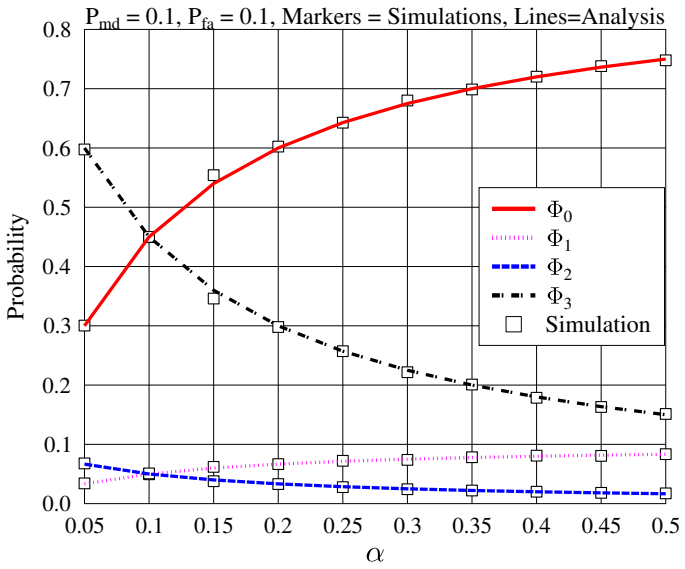

Figure 3.9: Steady-state probabilities of $[\Phi_0, \Phi_1, \Phi_2, \Phi_3]$ seen in (3.9) with respect to α.

Fig. 3.10 depicts the throughput achieved by the CSW-HARQ scheme both for perfect and imperfect sensing versus the packet error probability P_e and with respect to the probability P_{on} of the channel being busy. In our simulations, the throughput is calculated as

$$R'_S = \frac{N_s}{N_t} \cdot \frac{T_p}{T_s + T_d} \quad \text{(packets per } T_p\text{)}, \tag{3.51}$$

where N_t represents the total number of TSs used for the successful transmission of N_s packets by the CU.

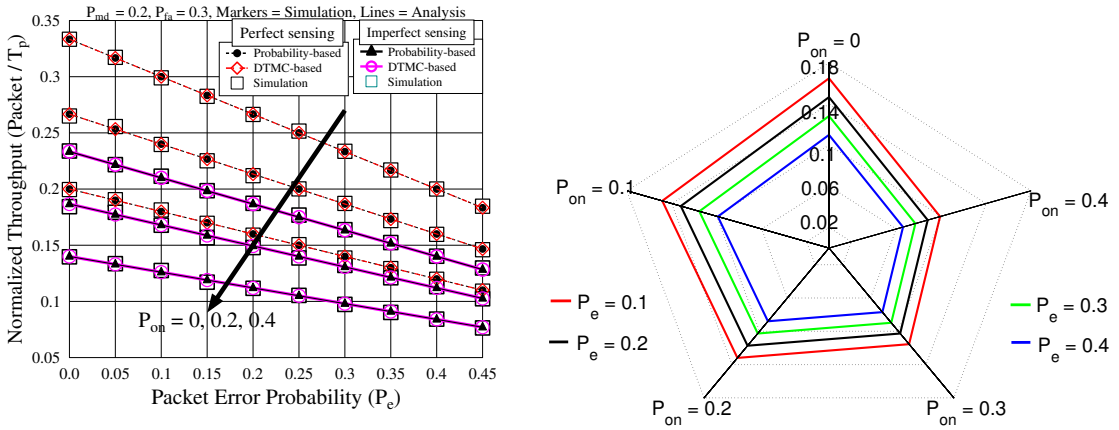

(a) (b)

Figure 3.10: Normalized Throughput in terms of T_p versus packet error probability P_e for the CSW-HARQ scheme associated with various channel busy probabilities P_{on}, when assuming $T_s = 1T_p$ and $T_d = 2T_p$. a) Throughput is investigated in both perfect and imperfect cases, where in the case of imperfect sensing $P_{md} = 0.3$ and $P_{fa} = 0.2$. b) Throughput is again analyzed in realistic imperfect sensing, when $P_{md} = 0.45$ and $P_{fa} = 0.45$ for different values of P_e and P_{on}.

As shown in Fig. 3.10(a) and 3.10(b), the throughput is at its maximum, when the channel is perfectly reliable, i.e. when $P_e = 0$ for both the perfect and imperfect sensing scenarios. As P_e

increases, implying that the channel becomes less reliable, the achievable throughput reduces nearly linearly with P_e, which is a direct consequence of retransmissions. At a given P_e, the throughput attains its maximum, when the channel is always free to use, i.e. when $P_{on} = 0$. However, as P_{on} increases, the attainable throughput significantly reducing, since the CU has to wait longer for finding free channels for its data transmission. Furthermore, Fig. 3.10 shows that realistic imperfect sensing may result in a significant throughout drop, implying that indeed it is important to achieve reliable sensing in cognitive radios.

Additionally, Fig. 3.10(a) shows that the analytical results evaluated from Eqs. (3.26) and (3.40) agree well with the simulation results.

Having characterized the throughput, let us now elaborate on the delay of the CSW-HARQ scheme. Firstly, we consider the average packet delay, as shown in Fig. 3.11. Note that for the results obtained by simulations, the average packet delay is given by the total number of TSs N_t used for the successful transmission of N_s packets, divided by N_s, which is expressed as

$$T_{DS} = \frac{N_t \cdot (T_s + T_d)}{N_s} \quad \text{(seconds)}. \tag{3.52}$$

The results depicted in Fig. 3.11 are normalized by T_p, yielding:

$$T'_{DS} = \frac{T_{DS}}{T_p} \quad (T_p s). \tag{3.53}$$

where $\delta(.)$ represents delta function. In Fig. 3.11, the average packet delay of the CSW-HARQ

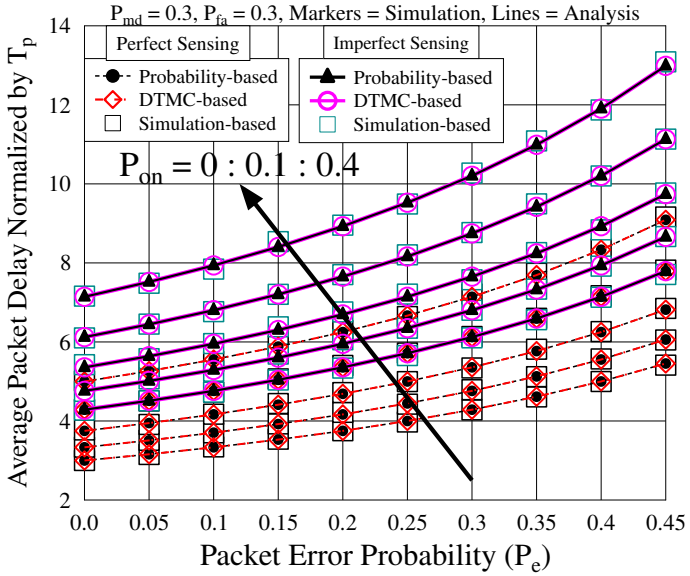

Figure 3.11: Average packet delay of the CSW-HARQ system versus P_e for various channel busy probabilities when either perfect sensing ($P_{fa} = P_{md} = 0$) or imperfect sensing ($P_{fa} = P_{md} = 0.3$) are considered.

system is studied, both for perfect and imperfect sensing. For a given P_{on}, the average packet delay is at its minimum, when P_e is zero and it increases, when P_e or/and P_{on} increases. As discussed

above, the increase of P_e triggers more retransmissions, while the increase of P_{on} reduces the transmission opportunities for the CU's, which hence result in the increase of the average packet delay. Additionally, imperfect sensing results in the mis-use of the channel, which increases the average delay. Finally, as shown in Fig. 3.11, the results obtained both from our probability-based and from the DTMC-based approaches are accurate, closely agreeing with on simulation results.

In Fig. 3.12, we depict the probability of the end-to-end packet delay of the CSW-HARQ scheme in terms of both perfect and imperfect sensing. In the simulations, the end-to-end delay is evaluated as the total time duration from each individual packet's first transmission until its successful reception, divided by the total number of packets, N_s. In detail, let a vector $\boldsymbol{d}$ of length N_s be used to store the end-to-end delay experienced by each of the N_s transmitted packets. Specifically, $\boldsymbol{d}(j)$ represents the end-to-end delay of the jth packet. Then, the PMF of the end-to-end packet delay illustrated in Fig. 3.12 is given by

$$\boldsymbol{P}_d(i) = \frac{\sum_{j=1}^{N_s} \delta(d(j)-i)}{N_s}, \quad 1 \leq i \leq \max(\boldsymbol{d}). \tag{3.54}$$

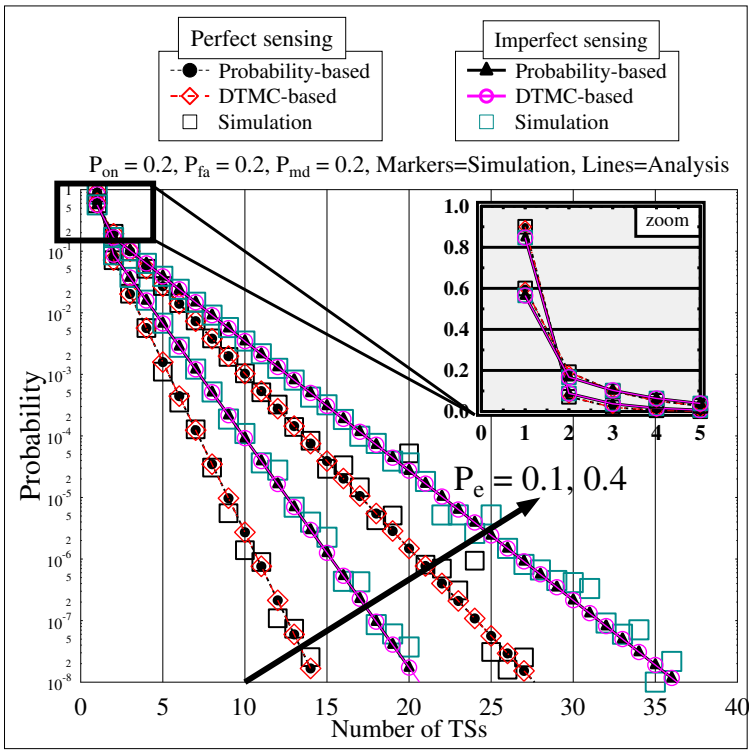

Figure 3.12: Probability of the end-to-end packet delay in the perfect ($P_{fa} = P_{md} = 0$) and imperfect ($P_{fa} = P_{md} = 0.2$) sensing scenarios for $P_{on} = 0.2$ and $P_e = \{0.1, 0.4\}$.

Observe from Fig. 3.12 that in the case of perfect sensing, 90% of the packets are successfully received with an end-to-end delay of one TS, when $P_e = 0.1$, as accurately shown in the zoomed-in portion of the figure. To elaborate further, Following is 7.2% of packets are correctly received with an end-to-end delay of 2 TSs, and 2% of the packets are correctly received with an end-to-end delay of 3 TSs, as shown in Fig. 3.12. On the other hand, in the case of imperfect sensing, at $P_e = 0.1$, the number of packets having an end-to-end delay of one TS is reduced to 84%, and the number

packets having an end-to-end delay of 2 and 3 TSs is increased to 8.8% and 3.7%, respectively. By contrast, when P_e is increased to 0.4, the ratio of the packets having an end-to-end delay of one TS is reduced to 60% and 54% in the perfect and imperfect sensing scenarios, respectively. In a similar manner, the ratio of the packets having an end-to-end delay of two or more TSs also reduces correspondingly. Hence, the tail of the PMF curves increases as P_e increases, implying an increase of the end-to-end packet delay.

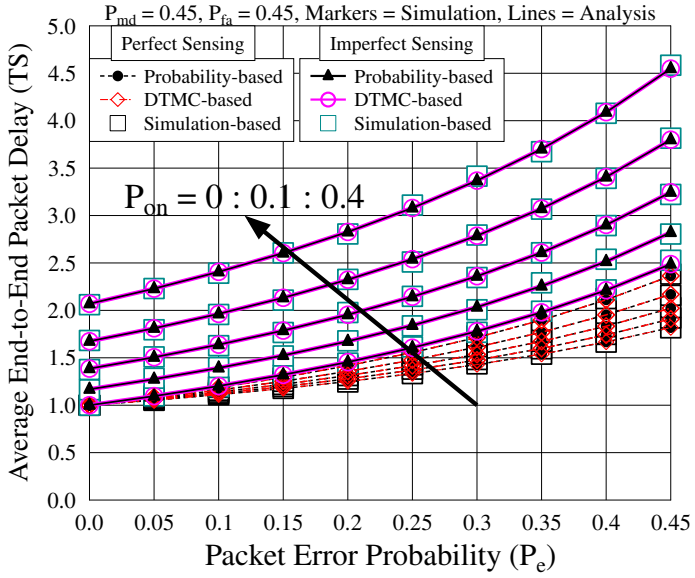

Figure 3.13: Average end-to-end packet delay versus packet error probability (P_e) for the CSW-HARQ with respect to different channel busy probabilities P_{on} and in the case of imperfect sensing.

The average end-to-end packet delay is shown in Fig. 3.13, where the results gleaned from our simulations are evaluated from the formula

$$\tau_s = \sum_{i=1}^{\max(\boldsymbol{d})} \boldsymbol{P}_d(i) \times i(T) \ \ (\text{seconds}). \tag{3.55}$$

It can be observed from Fig. 3.13 that the average end-to-end packet delay increases, as P_e and/or P_{on} increases. More importantly, it can be seen that in the case of perfect sensing, the average end-to-end packet delay has a minimum of one TS when $P_e = 0$, regardless of the value of P_{on}. This is because, when the channel is highly reliable and when the probability of mis-detection is zero, correct delivery of a transmitted packet is ensured in the first attempt. By contrast, when P_e and/or P_{on} increases, the delay increases significantly, although it remains still lower than the corresponding delay in the case of imperfect sensing. In the case of imperfect sensing, there is a delay caused by the false-alarm and mis-detection of the PR's channel.

Finally, we compare the average packet delay to the average end-to-end packet delay in Fig. 3.14. Explicitly, for a given scenario, the average packet is always higher than the average end-to-end delay. Furthermore, the average packet delay increases faster than the end-to-end packet delay, when P_e or/and P_{on} increases. This is because, the average packet delay considers all the time spanning

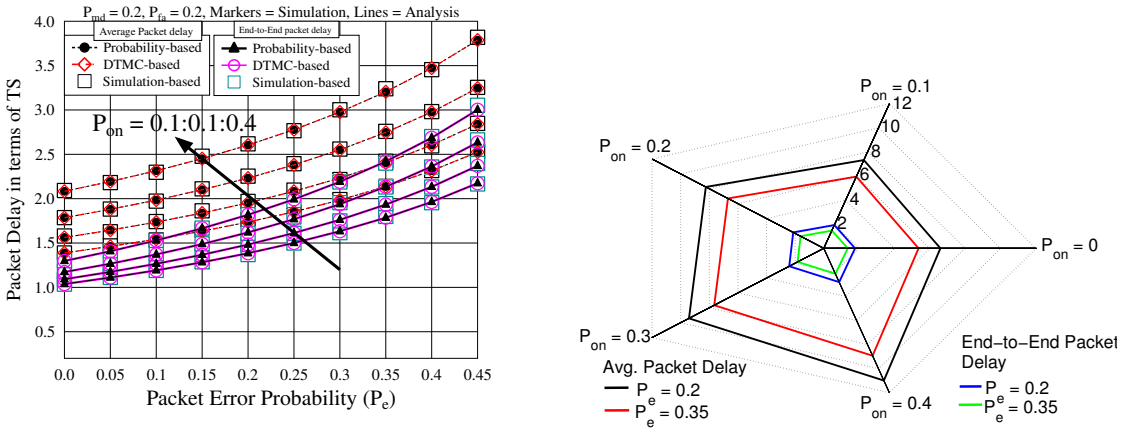

(a) (b)

Figure 3.14: Comparison of average packet delay and end-to-end packet delay measured in terms of TS, when operating with realistic imperfect sensing. a) Delay versus packet error probability for different values of P_{on}, when $P_{md} = 0.2$ and $P_{fa} = 0.2$. b) Again, both the average packet delay and the end-to-end packet delay are analysed, when $P_{md} = 0.3$ and $P_{fa} = 0.3$.

from the start of transmitting the first packet until the successful reception of the last packet. By contrast, the end-to-end delay only considers the delay of each individual packet from the instant of its transmission to its correct reception, but it does not consider the time between two successful packets.

3.7 Chapter Conclusions

In this chapter, we have investigated the performance of the CSW-HARQ transmission scheme both in the perfect and imperfect sensing scenarios. Both the throughput and delay of the CSW-HARQ scheme have been investigated both by analytical and simulation techniques. Furthermore, two analytical approaches, namely the probability-based approach and the DTMC-based approach have been involved for deriving the closed-form formulas of the throughput and delay. Both analytical approaches have been validated by our simulation results. Based on our studies and performance results, we can conclude that the achievable throughput and delay performance of the CSW-HARQ are substantially affected by the activity of the PUs, by the reliability of the CU channels and by the reliability of sensing. When the PR channel becomes busier, the CSW-HARQ's throughput becomes lower and the average packet delay increases, even when the CU sensing and transmission are reliable. When the sensing is reliable, the CSW-HARQ system achieves a higher throughput and a lower delay compared to the cases of imperfect sensing. Given that in CR the opportunity for data transmission is limited, it is therefore, highly important to employ highly reliable sensing approaches for improving the CU throughput and delay, in addition to minimizing the interference imposed on the PU system.

Chapter 4

Performance Analysis of Cognitive Go-Back-N Hybrid Automatic Repeat reQuest with Perfect Sensing [1]

In Chapter 3, we have investigated the achievable throughput and delay of the proposed Cognitive Stop-and-Wait HARQ (CSW-HARQ) transmission in the presence of both idealistic perfect and realistic imperfect sensing. The CSW-HARQ advocated has been analytically modelled using a pair of different approaches, namely, 1) the probability-based technique of Section 3.4 and 2) the Discrete Time Markov chain (DTMC)-based regime of Section 3.5. Based on these, closed-form expressions were derived for both the throughput and the delay, which were validated by simulations. Similar to the classic SW-HARQ, the proposed CSW-HARQ scheme was convenient for implementation, but this implementational convenience was achieved at a reduced throughput and increased transmission delay. This is because the CSW-HARQ scheme transmits a single packet and then waits for its acknowledgement, as illustrated in Fig. 3.6. During this waiting time the transmitter is not allowed to (re)transmit a packet. In other words, the transmitter wastes its resources by waiting for the acknowledgement flag, even if the channel is relatively reliable.

Therefore, to circumvent the problem of longer waiting time, in this chapter, we propose a CR-aided Go-Back-N HARQ scheme, which enables the CR transmitter to continuously transmit N packets one after another without waiting for their acknowledgements until the reception of a negative feedback or until the detection of a busy time-slot (TS), as shown in Fig 4.1. Hence, a buffer of size N packets is used at the transmitter, which however increases the complexity, but significantly enhances the performance of the system in terms of increased throughput and reduced delay.

[1] A part of this chapter has been accepted in IEEE Access, November 2016 [246].

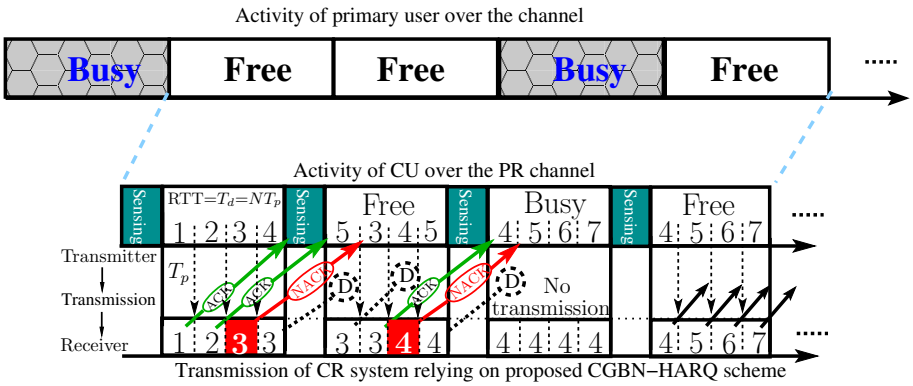

Figure 4.1: Transmission flow of the proposed CGBN-HARQ in the presence of both free and busy TSs. Each TS has the duration of $T = T_s + T_d$ seconds and in each free TS, $N = 4$ packets are transmitted where T_p is the duration required for the transmission of a packet.

4.1 Introduction

The concept of CR systems has attracted substantial attention and it has been systematically studied, for example in [9–11, 14, 16, 17]. In Chapter 2, we have studied the fundamental principles of CR systems in terms of its operational modes, capabilities, spectrum sensing, spectrum decisions, spectrum sharing, etc. Data transmission in CR systems faces usual shadowing, multi-path fading, path-loss, noise and interference effects. In order to mitigate these problems and to design efficient CR-aided transmission schemes for achieving reliable communications only limited research has been carried out. The studies [64, 183–187, 191–197], performed in this context have not provided any detailed theoretical analysis of the throughput and delay of CR systems employing HARQ protocols. Specifically, in [191–193], it is assumed that the CUs sense the activity of the PUs via observing their feedbacks (ACK and NACK). However, the performance of the CR systems using ARQ protocols have not been investigated. In [194] Ao and Chen as well as Touati *et al.* in [195], performed a seminal analysis of the performance for the ARQ relay-assisted CR systems. Moreover, Yue and Wang [185, 186], proposed an improved HARQ scheme for the CR systems invoking anti-jamming coding approach for achieving reliable communication. Following that, a network coding assisted ARQ scheme has been proposed in [187], which aims at improving the efficiency of the conventional ARQ schemes. Fujii *et al.* [203] introduced space-time-block-coding aided distributed ARQ in an *ad hoc* CR network relying on retransmitting the erroneous packets using ARQ. As a further advancement, cross-layer operation of the physical layer and MAC layer has been proposed [210]. By contrast, a hybrid of the spectrum interweave and underlay sharing paradigms have been proposed in [196, 197] for improving the performance of CUs. Specifically, Hu *et al.* [197] proposed the ARQ approach for improving the transmission reliability. Patel *et al.* [77, 247] focused their attention on maximizing the achievable rates of both underlay-based and interweave-based CR systems, when assuming realistic imperfect sensing. Various communication techniques have been surveyed in the context of CR systems [64, 85, 183, 184, 227].

To the best of the author's knowledge, no published work has theoretically analyzed the HARQ protocols in context of CR systems. However, the dynamic nature of PUs activity and unreliable sensing render the modelling and analysis of the HARQ protocols in CR systems quite challenging. Therefore, in this chapter, we design a novel communication protocol, namely the cognitive Go-Back-N HARQ (CGBN-HARQ), which relies on cognition and maintains reliable communications. Firstly, for the sake of improving the spectrum exploitation, similar to Chapter 3, we model the presence and absence of the PU in the channel by a two-state Markov chain [207, 240, 248] having the 'ON' and 'OFF' states [249]. Specifically, in the 'ON' state, the channel is considered to be occupied by the PUs, whereas in the 'OFF' state, the channel is free and hence it is available for the CU's transmission. Furthermore, similar to [61, 234, 250], we also assume that the channel is partitioned into time-slots (TS) of duration T, where each TS is further divided into two segments, namely the sensing time of duration T_s and the data transmission time of duration $T_d = T - T_s$. The sensing epoch is used for detecting the activity of the PUs in the channel, and the remaining time duration is used for data transmission relying on the traditional Go-Back-N HARQ protocol [18, 21, 22].

Secondly, to achieve reliable data transmission, our proposed CGBN-HARQ scheme incorporates the traditional GBN-HARQ protocol into our CR system. We favour the GBN-HARQ protocol over the SW-HARQ and SR-HARQ schemes, because, it has a higher throughput and lower delay than the classic SW-HARQ, whilst imposing a lower complexity than the SR-HARQ [18, 21, 22]. As mentioned above, when the CR transmitter deems the channel to be free, it transmits N packets in a chronological order based on GBN-HARQ protocol. On the other hand, the CR receives packets one after the other and generates feedback accordingly, which is then conveyed back to the transmitter accordingly. The transmitter always transmits a new packet when an ACK is received whereas, after the reception of a NACK, both the erroneous and the subsequent packets are retransmitted in the next free TSs

The operating principle of the classic GBN-ARQ protocol has been extensively studied in [18, 21, 22]. The performance of the conventional Go-Back-N HARQ has been investigated in [251–256]. In more detail, Turin [253] and Cabric as well as Brodersen [256] have modelled the GBN ARQ using hidden Markov chains and investigated the effect of both reliable and unreliable feedback on the throughput. Chakraborty and Liinaharja [254] proposed an adaptive GBN-ARQ protocol in which the transmitter changes its operational mode based on the feedback received. Additionally, Zorzi [255] proposed an error-control scheme in order to improve the performance of the GBN retransmission scheme under the delay constraints. The distribution of packet delay has been studied in [257, 258].

4.1.1 Chapter Contributions

The main contributions of this paper may be summarised as follows:

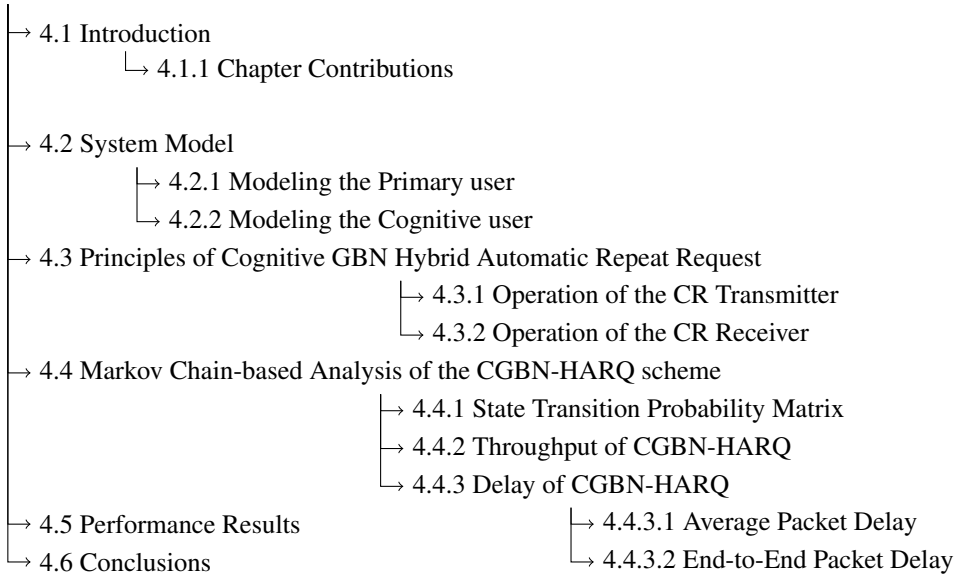

Figure 4.2: The structure of this paper.

1. A novel cognitive protocol CGBN-HARQ is proposed for CR systems in order to achieve reliable communication. Naturally, the proposed CGBN-HARQ scheme is inspired by the classic GBN-HARQ scheme, but we have to reformulate its transmission regime in order to meet the demanding requirements of CR systems. In our CGBN-HARQ arrangement, the transmitter first has to sense the channel prior to using it. Furthermore, the transmitter may receive feedback information both during the sensing period and the data transmission period.

2. By modelling this novel CGBN-HARQ arrangement using a discrete time Markov chain, we study both the attainable throughput and the average delay. We derive closed form expressions both for the throughput and the average delay of the CR systems operated under our CGBN-HARQ scheme.

3. Equations have been derived for quantifying the end-to-end packet delay performance in terms of its probability distribution and the average end-to-end packet delay.

4. Finally, a range of simulation results are provided for the verification of our theoretical analysis and for characterizing the achievable performance of our CGBN-HARQ scheme.

The structure of this chapter is shown in Fig. 4.2.

4.2 System Model

We continue by formulating both the PR and CR system models used in our analysis.

4.2.1 Modelling the Primary User

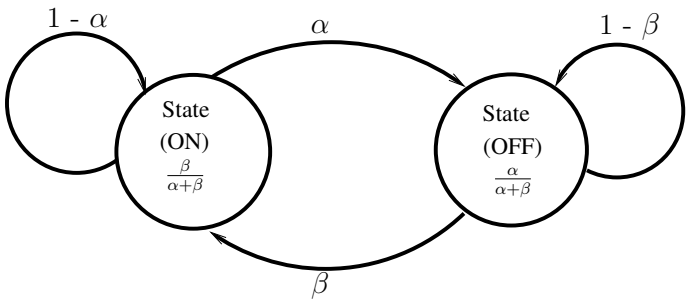

Figure 4.3: Discrete-time two-state Markov chain modelling the process of PR system [207, 240, 248].

As in stated in Subsection 3.2.1, we consider a PU transmitting in time-slots (TSs) of duration T at an independent and identical probability. This process is modelled as a two-state Markov chain obeying the transition probabilities of Fig. 4.3, where the 'ON' state represents that the channel is activated by the PUs. By contrast, the state 'OFF' indicates that the channel is free for the CU to use it. In Fig. 4.3, α and β denote the probabilities of traversing from the states 'ON' and 'OFF' to the opposite states. Let us denote the probabilities of the PU being 'ON' and 'OFF' by P_{on} and $P_{off} = 1 - P_{on}$. Then, in the steady state of Markov model, we have [21]

$$P_{on}\alpha = P_{off}\beta\,, \tag{4.1}$$

yielding:

$$P_{on} = \frac{\beta}{\alpha+\beta}\,,\;\; P_{off} = \frac{\alpha}{\alpha+\beta}\,. \tag{4.2}$$

Furthermore, as observe in Fig. 4.4(a) that if PU is in the 'ON' state at the beginning of a TS, it remains active until the end of that TS, hence, it cannot be used by the CU. Naturally, if a TS is not used by the PUs, then it is free for the CU [83, 207, 240]. Note that the state probabilities in Markov chain decides the 'ON' and 'OFF' duration of the PU.

4.2.2 Modelling the Cognitive User

The CU obeys the overlay paradigm of [10,259], where the CU is only at liberty to use the channel, if it is free from the PUs. We assume perfect activity sensing, yielding no mis-detection and no false-alarm. Similar to [61,234,250], each TS is partitioned into the channel sensing duration of T_s and the data transmission duration of $T_d = T - T_s$, as seen in Fig. 4.4(b). Hence, when the PU is deemed to be in the 'OFF' state within T_s, the CU exploits the time duration T_d for its transmission by involving the GBN-HARQ protocol. Additionally, the CU's buffer is always assumed to have data in it.

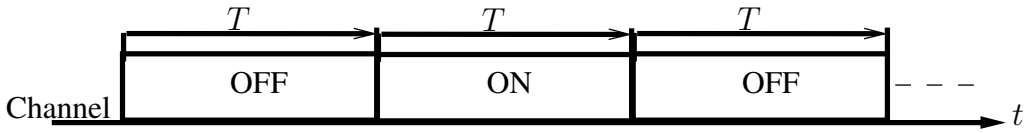

(a) Pattern of channel usage by PR

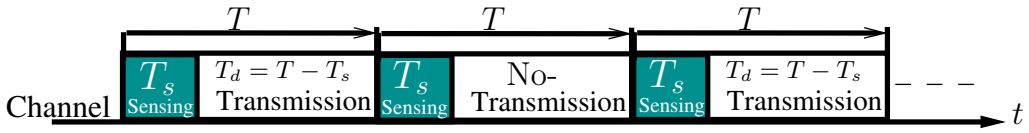

(b) Pattern of channel usage by CR.

Figure 4.4: Time-slot structure of the PR and CR systems, where a CR TS consists of a sensing duration of T_s and a transmission duration of $T_d = T - T_s$ seconds, given the total duration T of a time-slot [61, 234, 250].

4.3 Principles of Cognitive GBN Hybrid Automatic Repeat Request

Recall that the CGBN-HARQ regime relies on two main functions, namely channel sensing and data transmission. Specifically, at the commencement of a TS, channel sensing is used for ascertaining whether the TS is busy or free. Provided that the TS is deemed to be free, transmission ensures using a Reed-Solomon (RS) code RS(N_d, K_d) [18] defined over the Galois-field GF(q), where K_d and N_d denote the number of original information symbols and coded symbols, respectively. Each RS codeword encodes a packet, which is transmitted within T_p seconds. Upon arranging for $N = T_d/T_p$, the CR transmitter conveys N packets per TS. The RS code is capable of correcting number of $t = (N_d - K_d)/2$ symbol errors that reliable cyclic redundancy check (CRC) codes are used for detecting, if there are uncorrectable errors in a received packet.

This CGBN-HARQ protocol sequentially transmits N packets, while waiting for the corresponding feedback. Explicitly, N represents the maximum number of packets transmitted during the round-trip time (RTT), which is assumed to be T_d. Note that the RTT is defined as the time interval between the transmission of a packet and the reception of a feedback for the same packet. The operation of the CGBN-HARQ protocol of Fig. 4.5 is described by Algorithm 2, which is mainly organized in two steps.

- In the first step, the transmitter transmits packets in the sensed free TS. Following that, if the ACK flags are received after the elaps of the sensing time, then the transmitter keeps on transmitting new packets until the end of the TS (i.e., $(N - k)$ seconds), as stated on Line 16, where k represents the sensing duration. On the other hand, if the ACK flags are received within the sensing time or in a busy TS, then the transmitter remains silent, as stated on Line 21. Moreover, if a NACK flag is received, the algorithm returns to Line 6 and provided that the TS is free, the ith erroneous and $(N - c + i - 1)$ subsequent packets are retransmitted, where c is the counter keeping track of packets that have already been transmitted in the current TS.

- Secondly, the receiver generates feedback flags based on the error-free or erroneous recep-

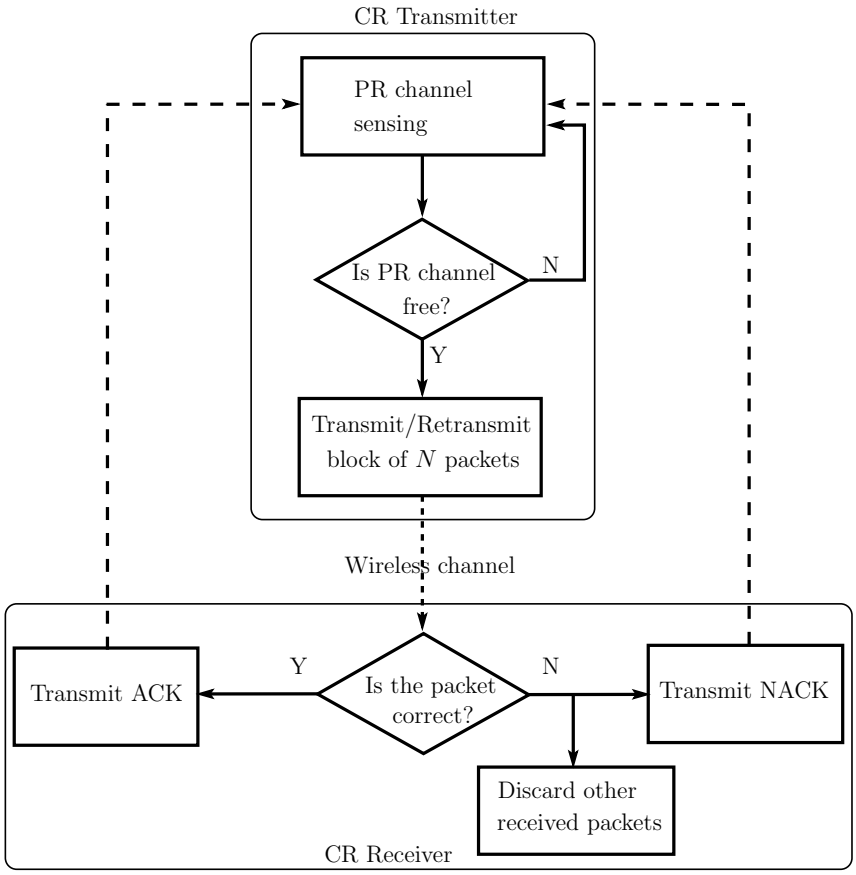

Figure 4.5: Flow chart showing the operations of the proposed CGBN-HARQ scheme.

tion of packet, as stated on lines 11 and 25, respectively, and sends them to the transmitter accordingly.

4.3.1 Operation of the CR Transmitter

The transmitter of conventional GBN-HARQ, continuously transmits packets, until a NACK signal is received. In presence of decoding errors both the error-infested packet as well as the other packets transmitted after the corrupted packet are retransmitted. By contrast, observing both Algorithm 2 and Fig. 4.5, in our proposed CGBN-HARQ scheme, the CU is only allowed to transmit packets in the TSs free from the PUs. Hence, the CU has to sense PU's presence/absence before the transmission or retransmission of packets. If the PU is in its 'OFF' state, the CR transmitter transmits N packets, which may include both new packets and the corrupted packets requiring retransmission. Otherwise, the transmitter waits for the next TS and senses the channel again. In our scheme, we assume that all packets are of the same length and the CR transmitter is always ready to transmit these packets in free TSs. Furthermore, each CU packet consists of a RS coded codeword, which is transmitted within the duration of T_p seconds, as shown in Fig. 4.6. The feedback of each packet is received after the RTT of $T_d = NT_p$ seconds, where again $T_s = 1T_p$ is assumed.

It is worth mentioning that for implementing the CGBN-HARQ, the CU is assumed to have a buffer of size N, which follows the FIFO principle [18, 21, 22]. The CU stores the transmitted

Algorithm 2 : CGBN-HARQ Algorithm

1: **Initialization**: M_c = number of packets, $T_d = NT_p$, $T_s = kT_p$, $i = 1$, $c = 0$, $P_t = 0$, TS$= 1$.
2: **Input:** N, k, packets.
3: **while** $i \leq M_c$ **do**
4: CR transmitter senses a TS.
5: **if** TS is free **then**
6: Transmit packets from i to $N - c + i - 1$.
7: TS $=$ TS $+1$, $j = i$.
8: Transmitter starts sensing next TS immediately.
9: **while** $j \leq N - c + i - 1$ **do** ▷ Check each received packet.
10: **if** the jth packet is received error-free **then**
11: receiver transmits ACK for the jth packet.
12: $j = j + 1$.
13: **if** TS is free && ACK is received in T_d period **then**
14: Transmit a new packet i.e. $P_t = (N - k) + (j - 1)$.
15: $c = c + 1$; ▷ Counter of packets transmitted
16: **if** $c == N - k$ **then**
17: Transmit packets from $(P_t + 1)$ to $N + j - 1$.
18: **Set** $c = 0$, TS $=$ TS $+1$, $i = j$ and **Goto** line 8.
19: **end if**
20: **else**
21: TS is busy $||$ ACK is received in T_s
22: No transmission and wait.
23: **end if**
24: **else**
25: reciever transmits NACK for the jth packet and discard the following packets.
26: **if** TS is free $||$ NACK is received during T_s or T_d **then**
27: **Set** $i = j$, **Goto** Line 6
28: **else**
29: TS is busy && NACK is received.
30: No transmission and wait.
31: **Set** $c \leftarrow 0$, $i = j$ and **Break**.
32: **end if**
33: **end if**
34: **end while**
35: **else**
36: Waits until the next TS.
37: **end if**
38: TS=TS+1.
39: **end while**

packets in its buffer until they are positively acknowledged (ACK). The buffer is updated according to the feedbacks gleaned from the CR receiver. Therefore, if the CR transmitter receives a positive ACK for a packet, its copy is deleted from the buffer and a new packet is appended at the end. Otherwise, no new packet is appended and both the erroneous packet as well as the subsequent packets are retransmitted in the next free TS.

We also assume that the CR transmitter is capable of receiving feedback for the transmitted packets both during the sensing period and the data transmission period, regardless of whether the channel is free or not. The ACK/NACK feedback signals are assumed to be always error-free, which is justified by the fact that the feedback signals are usually well protected [242, 243]. Moreover, the information content is usually low, since a single bit is enough for the CGBN-HARQ. Therefore, the reception of feedback can be readily protected from errors and it does not adversely affect the sensing and transmission processes.

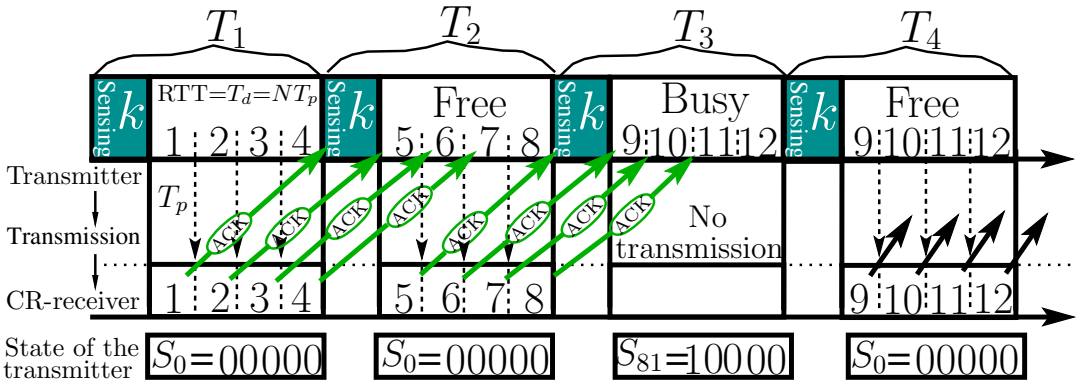

Figure 4.6: Transmission flow of the CGBN-HARQ scheme with the parameters of $k = 1$ and $N = 4$, when assuming the ideal scenario that all packets are correctly received.

Owing to the above assumptions, the CGBN-HARQ protocol has two scenarios for the reception of feedback: 1) reception of feedback within the sensing periods; and 2) reception of feedback outside the sensing periods, as shown in Figs. 4.6, 4.7 and 4.8.

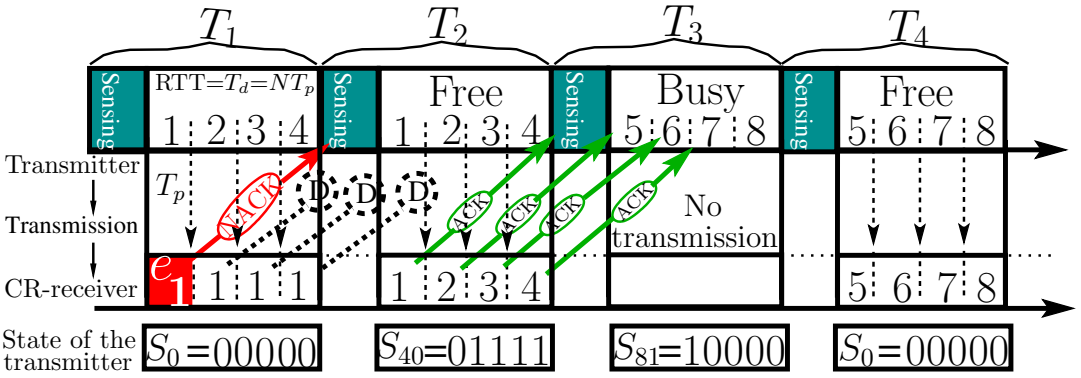

Figure 4.7: The transmission flow of CGBN-HARQ using $k = 1$ and $N = 4$ when an erroneous packet is received during a sensing period. The *green* and *red* solid lines represent error-free and erroneous transmission, whereas the dotted lines depict the discarded packets. The box with letter '*e*' shows the position of the erroneous packet in the TS.

In the first case, when a feedback is received within a sensing period, as stated on line 21 of Algorithm 2, if the ACK of a transmitted packet is received, then the CR transmitter deletes the copy of the corresponding packet from its buffer and continues to transmit new packets in the next free TS, as shown in Fig. 4.6. On the other hand, when a NACK of a transmitted packet is received during a sensing period, then the CR transmitter prepares to retransmit the erroneous packet as well as its $(N - 1)$ subsequent packets in the next free TS, as depicted in Fig. 4.7.

In the context of the second case, as shown in Fig. 4.8, a feedback received for a transmitted packet is in the next TS, after a sensing period, which is presented on line 13 of Algorithm 2. If the next TS is sensed to be free and an ACK signal is received, a new packet waiting in the buffer is then transmitted immediately. By contrast, if a NACK signal is received, the corresponding erroneous packet as well as its subsequent discarded packets have to be retransmitted, and the erroneous packet is retransmitted immediately. However, if a NACK signal is received during a 'busy' TS, then the erroneous packet and its $(N - 1)$ subsequent packets are transmitted during the next free

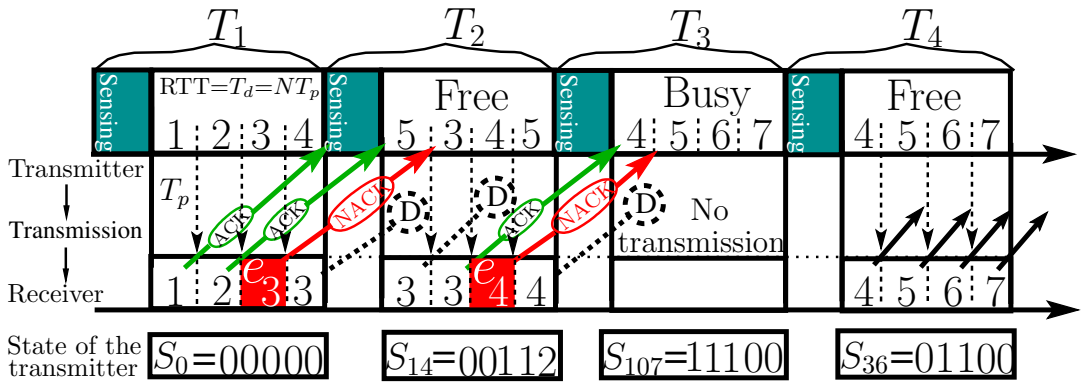

Figure 4.8: Transmission flow of CGBN-HARQ scheme using $k = 1$ and $N = 4$, when a NACK is received after a sensing period followed by a free TS and a NACK is received within a busy TS.

TS, as shown in Fig. 4.8.

4.3.2 Operation of the CR Receiver

The CR receiver operates similarly to the conventional GBN-HARQ. In the CGBN-HARQ, the CR receiver is assumed to have a buffer for storing the index of the received packets [21, 22], which increases by one only when an error-free packet is received, as presented in Algorithm 2. In detail, the operations of the CR receiver can be explained in terms of its *normal state* and *erroneous state*, as follows.

4.3.2.1 Normal State

The CR receiver is considered to be operated in the normal state, when the index of a received packet matches the sequence number stored in the receiver buffer. If this is the case, the CR receiver first carries out RS decoding, then, it generates the corresponding ACK or NACK signal, to be sent to the CR transmitter. Furthermore, if the packet becomes error-free after RS decoding, the CR receiver increases the index by one, as stated on lines 11 and 12 of Algorithm 2. Then, the CR receiver waits for the reception of the next packet.

4.3.2.2 Erroneous State

When the CR receiver is in the normal state but an erroneous packet is received after RS decoding, the CR receiver changes to the erroneous state. During this state, the CU discards the erroneous packet and transmits a NACK flag to the CR transmitter. Furthermore, the index in the CR receiver's buffer remains unchanged. Additionally, the CU discards the subsequent packets received within the period $(N-1)T_p$ following the erroneous packet, regardless of whether they are correct or not, as stated on line 25 of Algorithm 2. Following the above actions, the CR receiver enters into the normal state and waits for receiving the retransmission of the erroneous packet.

As the example of Fig. 4.8 shows, when the CR receiver finds that *packet* 3 is in error, it discards the erroneous *packet* 3 as well as the pair of subsequent packets, i.e. *packets* 4 and 5, since the CR receiver has to first correctly receive *packet* 3. Furthermore, as shown in Fig. 4.8, after the reception of a NACK for *packet* 3, the CR transmitter stops transmitting new packets and immediately retransmits *packet* 3 as well as the other packets already transmitted, provided that there are free TSs for transmission. The above process continues until all packets have been successfully received by the CR receiver.

4.4 Markov Chain-based Analysis of the CGBN-HARQ scheme

Similar to the classic GBN-HARQ, the operations of our CGBN-HARQ can also be modelled with the aid of a discrete-time markov chain (DTMC). However, as the CR system can only access the PR channel, when the channel is set free by the PUs, the modelling and analysis of the CGBN-HARQ become challenging. In this section, we propose a technique of circumventing the challenges of modelling the CGBN-HARQ as an DTMC. Based on our modelling technique, both the attainable throughput and the delay performance of the CGBN-HARQ will be analyzed in Sections 4.4.2 and 4.4.3.

We assume that states are defined with respect to the TSs, i.e. the state transition rate is synchronized with the TSs. The state of a TS is jointly determined by the 'ON' or 'OFF' state of the PU and the 'new packet', 'retransmitted packet', and 'packet repeated in one TS' states of the contents stored in the CR transmitter's buffer, when the buffer is observed at the end of a TS. In more detail, let us express the list of states as

$$\mathbb{S} = \{S_0, S_1, \ldots, S_i, \ldots, S_T\}. \tag{4.3}$$

The total number of states is denoted by S_T, where we have $S_T = |\mathbb{S}|$, and S_i is the ith legitimate state, which is a $(N+1)$-length base-3 digit expressed as

$$S_i = S_{i0}S_{i1}\cdots S_{iN},\ i = 0, 1, \cdots, S_T \tag{4.4}$$

where S_i is also referred to as the ith state sequence. In (4.4), the definition of S_{i0} is

$$S_{i0} = \begin{cases} 0, & \text{if the considered TS is free} \\ 1, & \text{if the considered TS is busy,} \end{cases} \tag{4.5}$$

while the definition of $S_{ij},\ j = 1, \ldots, N$, is

$$S_{ij} = \begin{cases} 0, & \text{if the } j\text{th packet is a new one;} \\ 1, & \text{if the } j\text{th packet is a retransmitted one when the TS is free, or one to be} \\ & \text{retransmitted when the TS is busy;} \\ 2, & \text{if the } j\text{th packet is a repeated one of a previous packet in the same TS.} \end{cases} \tag{4.6}$$

Based on the definitions of (4.5) and (4.6), we can find a one-to-one mapping for i of S_i as

$$i = \sum_{j=0}^{N} S_{ij} 3^{N-j} \tag{4.7}$$

Below we use a pair of examples to briefly introduce the principles of modelling and the state transitions. First, let us consider a simple CGBN-HARQ scheme, which has the parameters of $k = 1$ and $N = 1$, implying that the CR transmitter uses a single T_p interval for channel sensing and the transmitter buffer stores a single packet transmitted/retransmitted or to be transmitted/retransmitted in a TS. In this case, we should note that the third case in (4.6) will never occur, implying that no packet will be repeated within a specific TS and the digit 2 of (4.6) will never appear. Then, according to the above definitions, the corresponding DTMC has 4 states, which are $S_0 = 00$, $S_1 = 01$, $S_3 = 10$ and $S_4 = 11$. The state $S_2 = 02$ never appears.

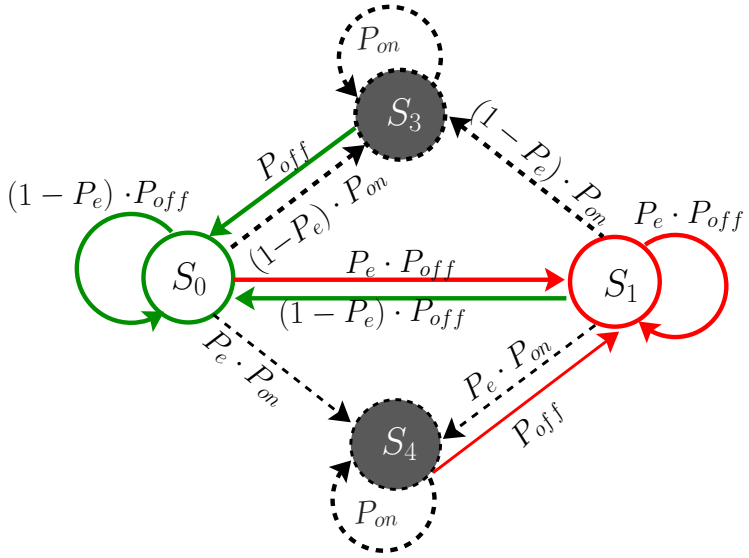

Figure 4.9: State diagram of the CGBN-HARQ scheme with $N = 1$ and $k = 1$, *dashed* lines correspond to the transitions towards the busy states $S_3 = 10$ and $S_4 = 11$, *solid* lines illustrate the transitions towards free state $S_0 = 00$ and $S_1 = 01$, while *red* and *green* lines correspond to that the packet is received error free and received in error, respectively.

The state diagram associated with the transitions is shown in Fig. 4.9. In this simple CGBN-HARQ scheme, the transition probabilities can be readily found. For example, assuming that the CGBN-HARQ is currently in state $S_0 = 00$, which means that the current TS is free and a new packet transmitted, when the packet is correctly received by the CR receiver and the next TS is also sensed to be free, the next state will also be $S_0 = 00$. Correspondingly, the transition probability is $P_{0,0} = P_{off}(1 - P_e)$, as shown in the Fig. 4.9, where P_{off} is the probability that the TS is free and P_e is the error probability of receiving a corrupted packet. By contrast, when the packet is received in error and the next TS is free, the next state will be $S_1 = 01$. Correspondingly, the state-transition probability is $P_{0,1} = P_{off}P_e$. Furthermore, when the packet is received error-free and the next TS is sensed to be busy, the next state will become $S_3 = 10$ associated with a transition probability of $P_{0,2} = P_{on}(1 - P_e)$, where $P_{on} = 1 - P_{off}$, as shown in Section 4.2.1. Similarly, we can analyze

the other state-transitions and transition probabilities, which are all shown in Fig. 4.9.

In the second example, we assume the parameters of $k = 1$ and $N = 4$. Then, let us return to Fig. 4.8 for considering the special cases that are not shown in the Fig 4.9. As shown in Fig. 4.8, the first TS is free and 4 new packets are transmitted. Hence, the state of the CGBN-HARQ is $S_0 = 00000$. The second TS is also sensed to be free. However, the third packet sent in the first TS is received in error. In this case, as shown in Fig. 4.8, the packets transmitted in the second TS are packets 5, 3, 4 and 5. Correspondingly, the state is $S_{14} = 00112$, and the probability of transition from S_0 to S_{14} is $P_{0,14} = P_{off}(1 - P_e)^2 P_e$. Following the second TS, the third TS is found to be busy. Furthermore, among the packets transmitted in the second TS, packet 3 is successfully delivered, while packet 4 is received in error. Hence, during the third TS, the packets stored in the transmitter buffer and to be transmitted in the next free TS are packets 4, 5, 6 and 7. Correspondingly, the state is $S_{107} = 11100$, and the state-transition probability from S_{14} to S_{107} is $P_{14,107} = P_{on}(1 - P_e)P_e$. Then, as shown in Fig. 4.8, the fourth TS is free to use and packets 4, 5, 6 and 7 are transmitted, which yields a state of $S_{36} = 01100$ associated with a transition probability of $P_{107,36} = P_{off}$ from S_{107}. Similarly, we can analyze the transitions in the other cases, as and when the various situations are considered.

According to the principles of the CGBN-HARQ and to the above examples, we may infer that the DMTC exhibits the following characteristics.

- When a TS is in 'ON' state, i.e. when we have $S_{i0} = 1$, digit 2 does not appear in the corresponding state sequence.
- When a transition changes from an 'ON' state to an 'OFF' state, $S_{i0} = 1$ in the current state sequence is changed to $S_{i0} = 0$ in the new state sequence, while all the other digits in the state sequence retain the same. Hence, owing to the above observations, the new state sequence does not contain the digit 2 of (4.6).
- The first digit, i.e., S_{i1}, never takes the value of 2 seen in (4.6).

Although we can remove a lot of states from consideration based on the above-mentioned characteristics, it still remains extremely hard to mathematically derive a formula for calculating the total number of states as well as to represent the state sequences in some general expressions. However, once we know the states and their relationship, we can readily determine the corresponding transition probabilities. In this paper, we propose the Algorithm, of Fig. 4.10 for finding the states or state sequences. The algorithm is detailed as follows.

In our algorithm, we assume that the CR transmitter starts transmitting N new packets using a free TS, which gives a state $S_0 = 0, 0, \ldots, 0$ of $(N + 1)$ zeros. Therefore, the set of states S initially contains S_0. In order to generate new states from the current state of $S_{cur} = S_0$, we allow errors occur at all the possible positions of the state S_{cur}, and also consider both free and busy TSs. For example, as shown in Fig. 4.7, if the first packet is received in error and the next TS is found to

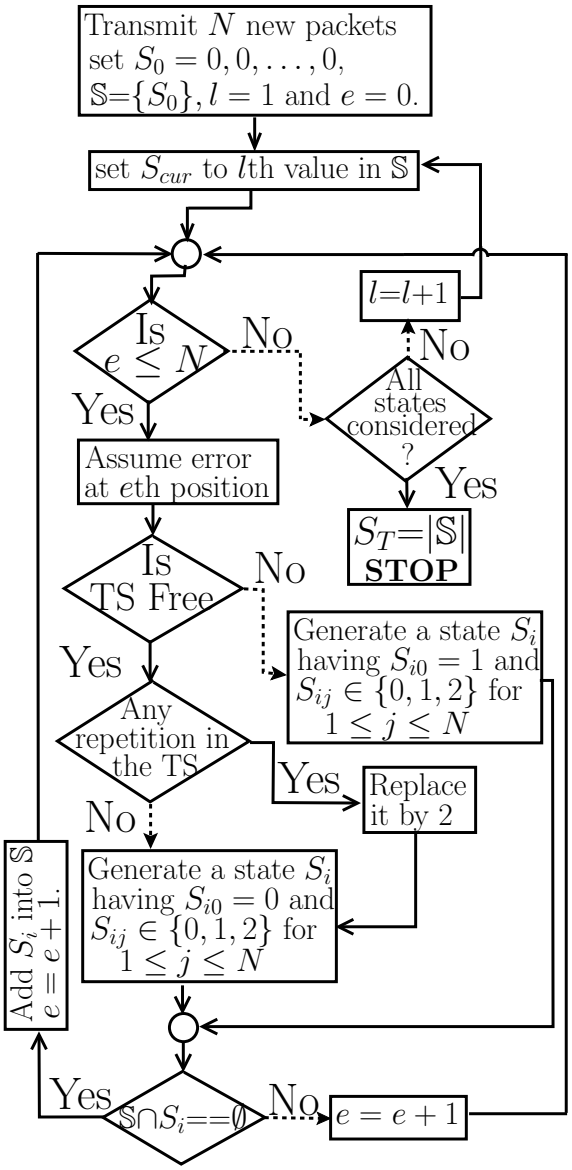

Figure 4.10: The flow chart illustrates the process of generating states represented by $(N + 1)$-length base-3 digits. In each state, the TS is either free (0) or busy (1) as well as it has new (0) and/or old (1) and/or repeated (2) packets. e represents the position of the erroneous packet in the TS, while $e = 0$ is a special case when all the received packets are error-free.

be free, then the transmitter retransmits both the erroneous packet and the discarded packets. Our algorithm assists in generating a new state $S_{40} = 01111$, where the first digit 0 indicates that the TS is free, while the remaining digits represent that four old packets are retransmitted. After the generation of a new state, for example S_{40}, it is then compared to all the existing states in $\mathbb{S}$. If it is not contained in $\mathbb{S}$, the state is then concatenated to the end of $\mathbb{S}$. Otherwise, it is deleted.

After generating all the possible new states from state S_0, the algorithm moves to the next state S_l in $\mathbb{S}$, which is S_{40} for the example of Fig. 4.7. The state S_l is then set as the current state and the above procedure is repeated in order to derive other possible states. Since the Markov chain is irreducible and aperiodic, the algorithm is finally terminated, when all the states in $\mathbb{S}$ have been

considered as the current states, but without generating new states. At the end of the algorithm, the cardinality of set $\mathbb{S}$ is given by the total number of states S_T, i.e., $S_T = |\mathbb{S}|$.

4.4.1 State Transition Probability Matrix

The probability of transition from one state to another is recorded in the state-transition probability matrix $\mathbf{P}$. Let the state of the ith TS be represented by $S(i)$. Then, in the example shown in Fig. 4.7 and discussed in Section 4.3.1, we have $S(1) = S_0$, $S(2) = S_{40}$, $S(3) = S_{81}$ and $S(4) = S_0$. Given the state S_i during TS t, the probability $P_{i,j}$ that the next state is S_j during the $(t+1)$st TS is [21, 244].

$$\begin{aligned} P_{i,j} &= P\left\{S(t+1) = S_j \mid S(t) = S_i, \ldots S(1) = S_0\right\} \\ &= P\{S(t+1) = S_j | S(t) = S_i\}, \text{ where } S_i, S_j \in \mathbb{S}. \end{aligned} \tag{4.8}$$

According to the properties of the DTMC, we have

$$\begin{aligned} &0 \leq P_{i,j} \leq 1 \\ &\sum_{S_j \in \mathbb{S}} P_{i,j} = 1, \ \forall S_i \in \mathbb{S}. \end{aligned} \tag{4.9}$$

As an example, let us consider the simple example of $N = 1$ and $k = 1$, having the state-transitions shown in Fig. 4.9. We have demonstrated in Section 4.4 that the DTMC has the state space of

$$\mathbb{S} = \{S_0, S_1, S_3, S_4\}. \tag{4.10}$$

We can now readily show that the state-transition matrix is

$$\begin{aligned} \mathbf{P} &= \begin{bmatrix} P_{0,0} & P_{0,1} & P_{0,3} & P_{0,4} \\ P_{1,0} & P_{1,1} & P_{1,3} & P_{1,4} \\ P_{3,0} & P_{3,1} & P_{3,3} & P_{3,4} \\ P_{4,0} & P_{4,1} & P_{4,3} & P_{4,4} \end{bmatrix} \\ &= \begin{bmatrix} (1-P_e)P_{off} & P_e P_{off} & (1-P_e)P_{on} & P_e P_{on} \\ (1-P_e)P_{off} & P_e P_{off} & (1-P_e)P_{on} & P_e P_{on} \\ P_{off} & 0 & P_{on} & 0 \\ 0 & P_{off} & 0 & P_{on} \end{bmatrix}. \end{aligned}$$

Let the probability that the transmitter is in state S_i during TS n be expressed as $P_i(n)$. Then, we have $\sum_{i \in \mathbb{S}} P_i(n) = 1$. Let $\boldsymbol{p}(n) = [P_0(n), P_1(n), \ldots, P_{S_T}(n)]^T$ collect all the S_T probabilities in TS n. Furthermore, let us assume that the transmitter starts transmitting, when it is in state $S(1) = S_0$, meaning that

$$\boldsymbol{p}(1) = [1, 0, \ldots, 0]^T. \tag{4.11}$$

Then, by the law of total probability [21, 245], the probability that the DTMC traverses to state j at TS $(n+1)$ can be written as

$$P_j(n+1) = \sum_{\forall S_i \in \mathbb{S}} P_i(n) P_{i,j} \; \forall \; S_j \in \mathbb{S} \text{ and } n \geq 1. \tag{4.12}$$

Upon considering all the S_T possible states in $\mathbb{S}$, we have arrive at recursive equation of

$$\boldsymbol{p}(n+1) = \mathbf{P}^T \boldsymbol{p}(n), \; n = 1, 2, \ldots \tag{4.13}$$

From this equation, we can readily infer that

$$\boldsymbol{p}(n+1) = (\mathbf{P}^T)^n \boldsymbol{p}(1). \tag{4.14}$$

As shown in Equation (4.9), the sum of each column of $\mathbf{P}^T$ is 1. Hence, the transition matrix $\mathbf{P}^T$ is a left stochastic matrix. Then, according to the *Perron-Frobenius theorem*, the limit of $\lim_{n\to\infty}(\mathbf{P}^T)^n$ exists [245]. Consequently, when $n \to \infty$, the Markov chain reaches its steady state [21] and hence we have

$$\boldsymbol{p}(n+1) = \boldsymbol{p}(n). \tag{4.15}$$

Let the steady-state probabilities be expressed by $\boldsymbol{\pi}$, i.e. we have $\boldsymbol{\pi} = \lim_{n\to\infty} \boldsymbol{p}(n)$. Then, from (4.15) we have [21, 244],

$$\boldsymbol{\pi} = \mathbf{P}^T \boldsymbol{\pi}, \tag{4.16}$$

which shows that the steady state probability vector $\boldsymbol{\pi}$ is the right eigenvector of $\mathbf{P}^T$, corresponding to the eigenvalue of one. Therefore, $\boldsymbol{\pi}$ can be obtained via calculating the eigenvector of $\mathbf{P}^T$ [21, 244, 245]. Note that the steady state probabilities satisfy the following constraint of

$$\sum_{S_j \in \mathbb{S}} \pi_j = 1 \quad \text{or} \quad \boldsymbol{\pi}^T \times \mathbf{1} = 1, \tag{4.17}$$

where $\mathbf{1}$ represents an all-one column vector.

4.4.2 Throughput of CGBN-HARQ

The throughput of the CGBN-HARQ is defined as the average number of successfully transmitted packets per TS [18, 237]. As mentioned previously, in CGBN-HARQ, successful transmission of a packet in a TS is achieved, when 1) the TS is free; and 2) error-free transmission of the packet using the free TS is achieved. Given the steady-state probabilities of (4.16) and the state transitions, the throughput (R_T) of the CGBN-HARQ can be analyzed as follows.

When the DTMC reaches its steady-state, its throughput is only dependent on the following two events a) The PR channel is free, implying that the first digit of the state sequence is zero. Hence, considering that the length of state sequences is $(N+1)$ and the digits are base-3 digits, the states

contributing to the throughput should have an index lower than 3^N; b) the number of new packets transmitted with in the state, when then PR channel is free.

Let $n_p(S_i)$ be the number of new packets associated with the state S_i with $i < 3^N$, which equals to the number of zeros in the state sequence of S_i minus one, since the first zero is only an indicator that the PR channel is free. Then, given the steady state probabilities $\boldsymbol{\pi}$, the throughput of the CGBN-HARQ scheme can be expressed as

$$R_T = \sum_{S_i \in \mathbb{S}, i<3^N} \pi_i \times n_p(S_i), (\text{packets / TS}). \tag{4.18}$$

Furthermore, if we express the attainable throughput in terms of the number of packets per T_p (packet duration), we have,

$$R'_T = \frac{T_p}{T} \times R_T = \frac{1}{k+N} \times R_T \quad (\text{packets / } T_p). \tag{4.19}$$

Let us now continue by analyzing the delay performance of the CGBN-HARQ.

4.4.3 Delay of CGBN-HARQ

In the classic GBN-HARQ, the packet delay includes both the duration of the first transmission as well as that of for any retransmission of the packets. By contrast, in our CGBN-HARQ, the packet delay includes not only the traditional GBN-HARQ, but also the duration of waiting for free channels. Hence, in the traditional GBN-HARQ, the delay performance can be simply characterized by the average packet-delay. By contrast, in our CGBN-HARQ, there are two types of delays, both of which provide unique insights into the performance of the CGBN-HARQ systems. The first type is the average packet-delay while the second one is the end-to-end packet-delay. Here, the average packet-delay is given by the total time spent by a CR transmitter between the start of sensing a TS until the successful delivery of all packets, divided by the number of packets transmitted. By contrast, the average end-to-end delay is the average duration from the start of transmitting of a packet until it is confirmed to be successfully received. Below we consider both of these delays.

4.4.3.1 Average Packet Delay

The average packet delay T_D can be quantified in terms of the average number of TSs (or T_p's) required for the successful transmission of a packet. Hence, given the throughput formulated in (4.18) or (4.19), we can readily express the average packet-delay as

$$T_D = \frac{N_t}{N_s} = \frac{1}{R_s} \quad (\text{TS per packet}) \tag{4.20}$$

$$= \frac{k+N}{R_T} \quad (T_p \text{ per packet}), \tag{4.21}$$

where k represents the delay due to sensing process.

4.4.3.2 End-to-End Packet Delay

In this subsection, we investigate the end-to-end packet-delay. First, we study the probability distribution of the end-to-end packet-delay. Then, the average end-to-end packet-delay of CGBN-HARQ is evaluated.

Let $\mathbb{S}_N \subset \mathbb{S}$ be a subset of $\mathbb{S}$, which contains all the states associated with new packets transmitted. Given $S_i \in \mathbb{S}_N$, we define a set $\mathbb{S}_i^{(m)}$, which contains all the states S_j emerging from state S_i to state S_j, in which there are $l_{i,j} \geq 1$ correctly received new packets with exactly mT_p of delay, i.e. we have

$$\mathbb{S}_i^{(m)} = \{S_j | \text{ emerging from } S_i \text{ to } S_j, \text{ there are } l_{i,j} \geq 1 \text{ new packets transmitted in state } S_i \text{ that are correctly received in state } S_j \text{ with the exactly } mT_p \text{ of delay.}\} \tag{4.22}$$

Furthermore, let the number of new packets transmitted while in state S_i be expressed as L_i. Then, the probability mass function (PMF) of the end-to-end packet-delay can be expressed as:

$$P(m) = \frac{1}{c} \sum_{S_i \in \mathbb{S}_N} \sum_{S_j \in \mathbb{S}_i^{(m)}} \frac{\pi_i \times l_{i,j} \times P_{i,j}^{(m)}}{L_i}, \quad \text{for } m = 1, 2, \ldots, \tag{4.23}$$

where we have $c = \sum_{S_i \in \mathbb{S}_N} \pi_i$ and $P_{i,j}^{(m)}$ denotes the probability of traversing from state S_i to state S_j after the delay of mT_p.

Now, given $\boldsymbol{\pi}, \boldsymbol{P}$ and $\mathbb{S}$, the PMF of end-to-end packet-delay can be derived as follows. Let us define:

$$\boldsymbol{P}_{MF} = [P(1), P(2), \ldots, P(M_T)]^T, \tag{4.24}$$

where M_T is the highest delay considered, which can be set to a high value so that the probability of having such a delay becomes very small such as, 10^{-8}. We first initialize $\boldsymbol{p}$ to a vector whose element corresponding to $S_i \in \mathbb{S}_N$ equals one, while all the other elements are equal to zero. In other words, $\boldsymbol{p} = \boldsymbol{I}_i$ represents a single column of the identity matrix $\boldsymbol{I}_{S_T}$. Then, according to the properties of DTMC, the state-transition are described by the following recursive equation

$$\boldsymbol{p}^{(j)} = \mathbf{P}^T . \boldsymbol{p}^{(j-1)} = \cdots = (\mathbf{P}^T)^j \boldsymbol{I}_i, \; j = 1, 2, \ldots \tag{4.25}$$

From (4.25) we can see that whenever we multiply $\mathbf{P}^T$ on the current $\boldsymbol{p}^i$, we obtain the following information:

a) The end-to-end packet-delay, such as mT_p of the new packets whose transmission was started during state S_i.

b) The probability of transmission $P_{i,j}^{(m)}$ from $\boldsymbol{I}_i$ (i.e., $S_i \in \mathbb{S}_N$) to the different termination states in $\mathbb{S}$

c) The number of packets $l_{i,j}$ whose transmission was started in state S_i and was correctly re-

ceived in state S_j.

With the aid of the above information, we update $\boldsymbol{P}_{MF}$ as follows:

$$P(m) \leftarrow P(m-1) + \frac{\pi_i \times l_{i,j} \times P_{i,j}^{(m)}}{L_i} m = 1, 2 \ldots, M_T, S_i \in S_i^{(m)}, S_i \in \mathrm{S}_N. \tag{4.26}$$

Having obtained the PMF of the end-to-end packet-delay, the average end-to-end packet-delay can be formulated as

$$\tau = \sum_{i=1}^{M_T} iT_P \times P(i). \tag{4.27}$$

Let us now characterize the attainable throughput and the delay performance of the CGBN-HARQ system.

4.5 Performance Results

In this section, we characterize the performance of the CGBN-HARQ. Both analytical and simulation results are provided for confirming each other. The proposed CGBN-HARQ scheme is configured in Matlab, where the CR transmitter is enabled to sense the channel and continuously transmit transmit N packets in the sensed free time-slot. On the other hand, the CR receiver receives a packet and performs RS decoding. Fifty thousand Monte Carlo simulations are performed for various values of P_{on}, P_{off}, P_e and N. Moreover, the observation period starts from the first TS and continues until all packets are successfully received by the CR receiver.

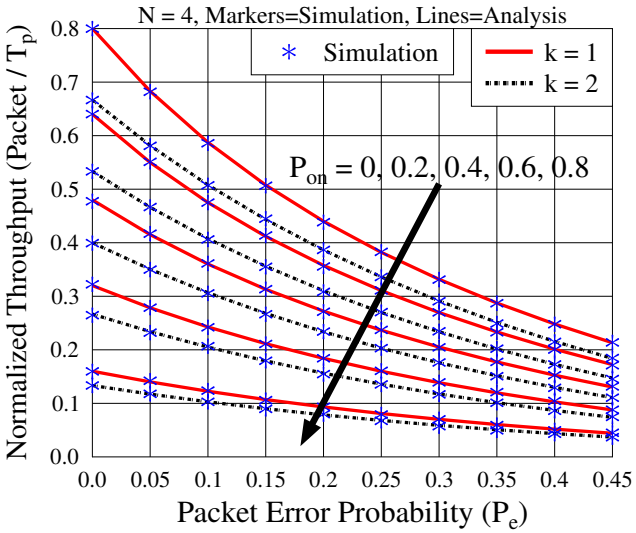

Figure 4.11: Throughput performance of the CGBN-HARQ versus packet error probability in terms of various channel busy probabilities, when $k = 1$ or 2, and $N = 4$.

From our studies in the previous sections, we can see that both the throughput and delay performance are dependent on the following system parameters: the PU's channel utilization probability

(P_{on}), CU error reliability (P_e), the number of packets (N) transmitted in a TS and the time kT_p required for reliable sensing. Thus, we will characterize the performance as a function of these parameters. Note that in our simulations the observation period of N_t TSs spans from the first TS until the instant when all N_s packets have been successfully received. From this, the throughput is obtained as

$$R_S = \frac{N_s}{N_t(k+N)} \text{ (packets per } T_p\text{)}. \tag{4.28}$$

Note that, N_t includes both the free and the busy TSs encountered during the observation period. Correspondingly, the average packet-delay is given by:

$$T_{DS} = \frac{N_t(k+N)}{N_s} \times T_p \text{ (seconds)} \tag{4.29}$$

or simply by $T_{DS} = \frac{N_t(k+N)}{N_s}$ in terms of number of T_p's intervals which represent the normalized average packet-delay T_{DS} in units of T_p.

Fig. 4.11 shows the effect of packet error probability on the achievable throughput of CGBN-HARQ for various combinations of P_{on} and k. Observe the high degree of agreement between the analytical and simulation results. Explicitly, the throughput decreases as P_e increases due to the increase in the number of packet retransmissions, as P_e increases. For a given P_e, the throughput decreases as P_{on} increases, because the CR system is granted less time for its information transmission. Finally, it can also be seen that the throughput is affected by the time used for reliable channel sensing. The throughput is reduced, as the sensing duration increases.

Fig. 4.12 and 4.13 show the throughput attained by CGBN-HARQ, when various values of N and P_e are assumed. These figures also show the optimum values of N for each P_e and for the other fixed parameters. It may be concluded from the plots of Fig. 4.12 and 4.13 that the optimum

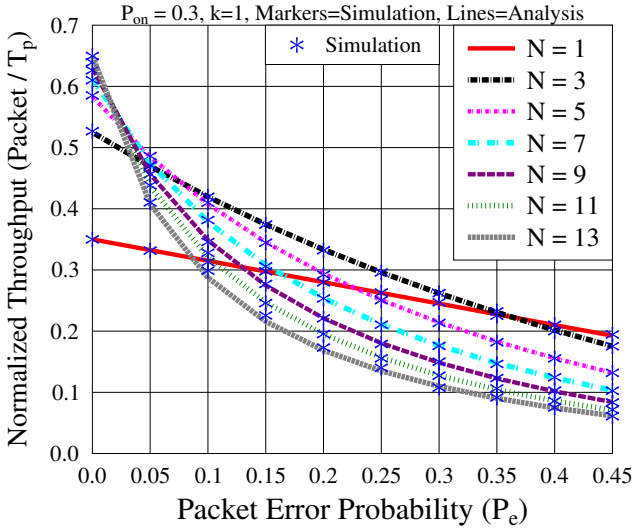

Figure 4.12: Throughput performance of the CGBN-HARQ versus packet error probability and for various values of N, when $k = 1$ and $P_{on} = 0.3$.

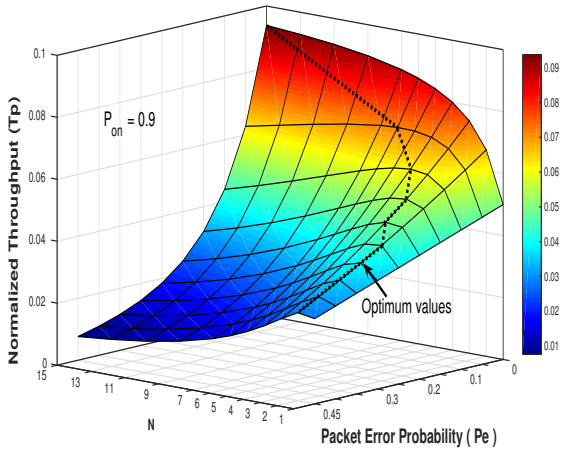

Figure 4.13: Throughput performance of the CGBN-HARQ versus packet error probability and various values of N, when $k = 1$ and $P_{on} = 0.9$. The optimum values of N which maximize the throughput are shown using *solid* black line.

values of N maximizing the throughput increases, when the channel becomes more reliable. When comparing Fig. 4.12 to 4.13, we observe once again observe that the throughput decreases, when P_{on} increases.

Having characterized the attainable throughput, we now continue by quantifying the delay in terns of both the average packet-delay and the end-to-end packet-delay. Let us first consider the average packet-delay.

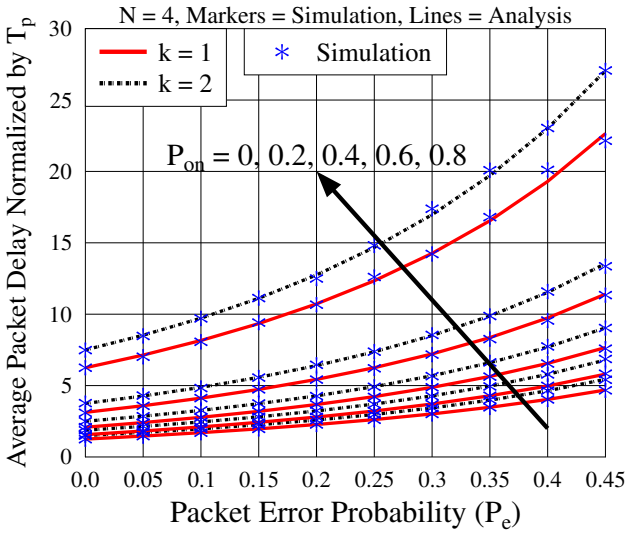

Figure 4.14: Average packet-delay of the CGBN-HARQ system versus packet error probability, when $k = 1$ or 2, and $N = 4$.

Fig. 4.14 illustrates the effect of P_e on the average packet-delay. It can be observed from Fig. 4.14 that the average packet-delay increases, when P_e or/and P_{on} increase, when the other system parameters. Explicitly, the average packet-delay increases due to the increased number of retransmissions, when P_e increases. When P_{on} increases, there is a lower probability of finding free TS for transmission by the CR system, hence the average packet-delay increases. As shown

in Fig. 4.14, increasing the sensing duration also increases the average packet-delay owing to the reduced time in each TS used for packet transmission. When comparing Fig. 4.11 to 4.14, we can observe the inverse relationship between the attainable throughput and the average packet-delay, as formulated in Equation (4.18) and (4.21). Additionally, the simulation results of Fig. 4.14 agree well with the analytical results.

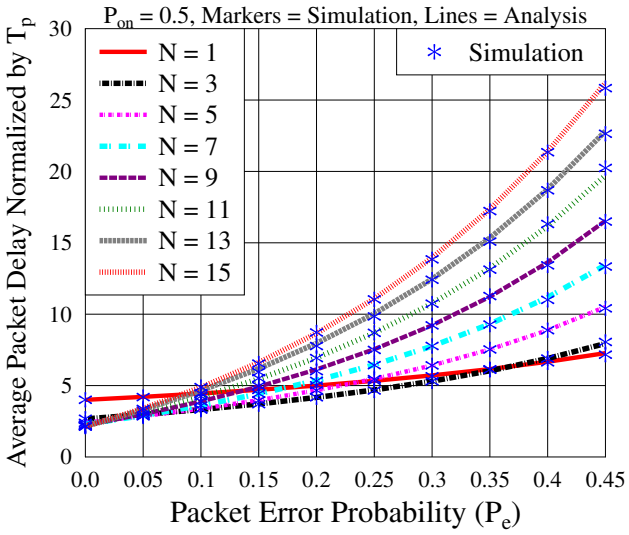

Figure 4.15: Average packet-delay of the CGBN-HARQ system versus packet error probability, when $P_{on} = 0.5$ and $k = 1T_p$.

First, Fig. 4.15 shows the effect of the number of packets N per TS on the average packet-delay. An interesting trend in the results shown of Fig. 4.15 is the cross-over between the curves for the different values of N. This may be explained as follows. There are two factors contributing to the average packet-delay, namely the sensing time and the retransmission duration imposed by the corrupted transmissions. Increasing the value of N reduces the contribution of the delay due to sensing. For example, for $N = 1$, a single packet is transmitted with a single T_p duration of sensing delay. By contrast, when $N = 15$, as many as 15 packets are transmitted within the same single T_p duration of sensing delay. On the other hand, as N increases, a higher delay is imposed, when a packet has to be retransmitted. Thus, increasing the value of N decreases the relative sensing delay per packet but increases the relative retransmission delay. Naturally, the delay due to the sensing operation only becomes explicit, when the communication channel is very reliable. When the channel becomes less reliable, the delay imposed by retransmissions will dominate the overall packet-delay. Therefore, the average packet-delay decreases with N for low values of P_e, while it increases for higher values of P_e, hence the curves intersect each other.

Having considered the average packet-delay, we now turn our attention to the end-to-end delay. As discussed earlier in Section 4.4.3.2, the end-to-end delay is defined as the time duration between the transmission of a packet and its ultimate successful reception. In simulations, the end-to-end packet-delay can be calculated for each packet of say N_s packets that the transmitter is required to transmit. Let us define a vector $\boldsymbol{d}$ of length N_s, in which the jth element $\boldsymbol{d}(j)$ is the end-to-end

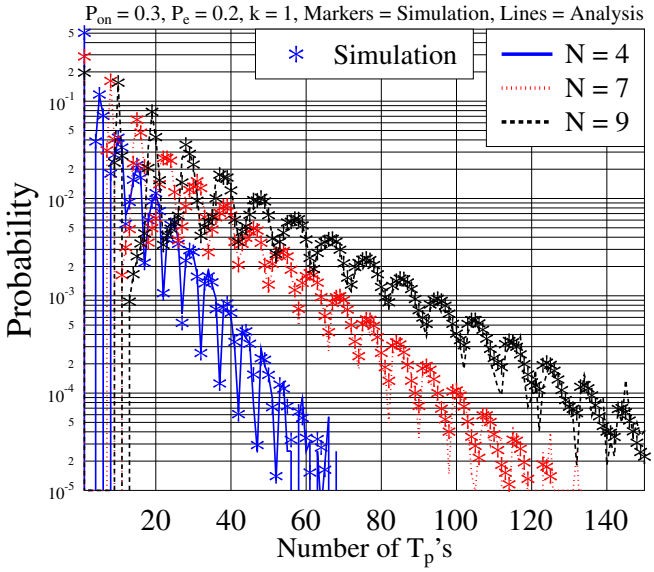

Figure 4.16: Probability of end-to-end packet-delay in the CGBN-HARQ systems, when $P_{on} = 0.3$, $P_e = 0.2$, $k = 1$ and $N = 4, 7$ and 9.

delay of the jth packet. Then, the PMF of the end-to-end packet-delay may be formulated as:

$$P(i) = \frac{\sum_{j=1}^{N_s} \delta(d(j)-i)}{N_s}, \quad 1 \leq i \leq \max(\boldsymbol{d}). \tag{4.30}$$

where $\max(\boldsymbol{d})$ denotes the maximum delay of the N_s packets.

Fig. 4.16 shows the probability distribution of the end-to-end packet-delay of the proposed CGBN-HARQ scheme. It can be observed from Fig. 4.16 that for the case of $N = 4$, 50.59% of packets are received successfully in the first instance of transmission (i.e. within an end-to-end delay of a single T_p), 3.86% packet are received successfully with an end-to-end delay of $4T_p$, and 1.56% packets are received successfully with an end-to-end delay of $14T_p$.

Similarly, the probability distributions can be evaluated for the scenarios of $N = 7$ and $N = 9$ by either simulations or based on the analytical results of Section 4.4.3.2. It can be seen from Fig. 4.16 that the simulation results agree well with the analytical ones. Furthermore, the length of the tail increases, as the value of N increases, implying that the maximum possible delay increases, when N increases.

Fig. 4.17 shows the average end-to-end packet-delay versus P_e with respect to different values of P_{on}. In the figure, the values obtained from simulations are calculated according to:

$$\tau_s = \sum_{i=1}^{\max(\boldsymbol{d})} \boldsymbol{P}_{ds}(i) \times i \ \ (T_p\text{'s}). \tag{4.31}$$

It can be seen from Fig. 4.17 that the average end-to-end packet-delay explicitly increases, as P_e increases because of the increase in the number of retransmission. The average end-to-end packet-delay also increases, when P_{on} increases, because the CU has to wait for longer to acquire a free

TS.

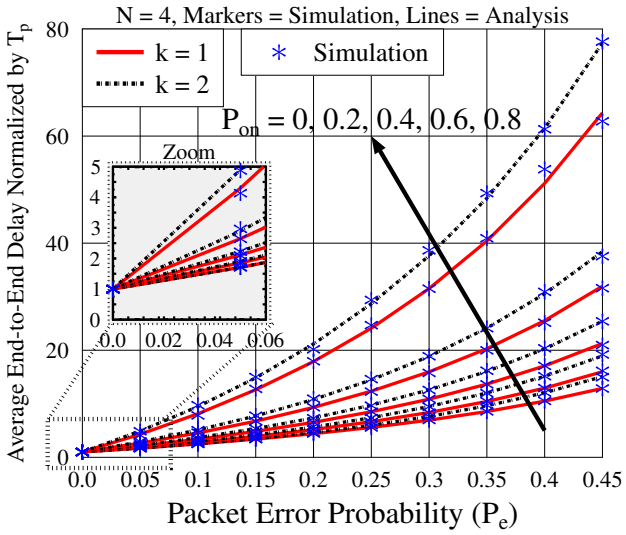

Figure 4.17: Average end-to-end packet-delay of the CGBN-HARQ versus packet error probability for various values of P_{on}, when $N = 4$ and $k = 1$ or 2.

When comparing Fig. 4.14 and 4.17, there are two striking differences. The first difference concerns the minimum values of both the delays, while the second difference concerns the increasing rates of the delays, as P_e or/and P_{on} increases. In more detail, firstly, as depicted in Fig. 4.17, the minimum end-to-end packet-delay equals to one for $P_e = 0$, regardless of the value of P_{on}. However, in the case of the average packet-delay, as shown Fig. 4.14, the minimum value becomes higher than one and increases as P_{on} increases. This is because, unlike the average packet-delay, which is calculated by averaging the observations over N_t TSs, the end-to-end packet-delay is individually calculated for each packet from the start of their transmission. In other words, when $P_e = 0$, the average packet-delay includes the sensing delay, the delay due to the PR channel being busy, as well as owing to the transmission delay of one T_p. On the other hand, when $P_e = 0$, the average *end-to-end* packet-delay always equals one T_p, because the error-free channel ensures the correct delivery of a transmitted packet during the first attempt. Secondly, when comparing Fig. 4.17 to Fig. 4.14, we can find that the average end-to-end packet-delay increases significantly faster than the average packet delay, when P_e or/and P_{on} increases. This is because in the CGBN-HARQ every packet transmitted is dependent on the $(N-1)$ packets transmitted in the front of it. Explicitly, if any of these packets is received in error, the packet considered has to be retransmitted, regardless whether it has or has not been correctly received, thereby resulting in a longer end-to-end packet-delay.

Finally, in Fig. 4.18, we show the effect of increasing N on the average end-to-end packet-delay, where for the reason mentioned above, the average end-to-end delay has a minimum value of one at $P_e = 0$, regardless of the value of N. Explicitly, at a given P_e, the average end-to-end delay increases, as the value of N becomes higher.

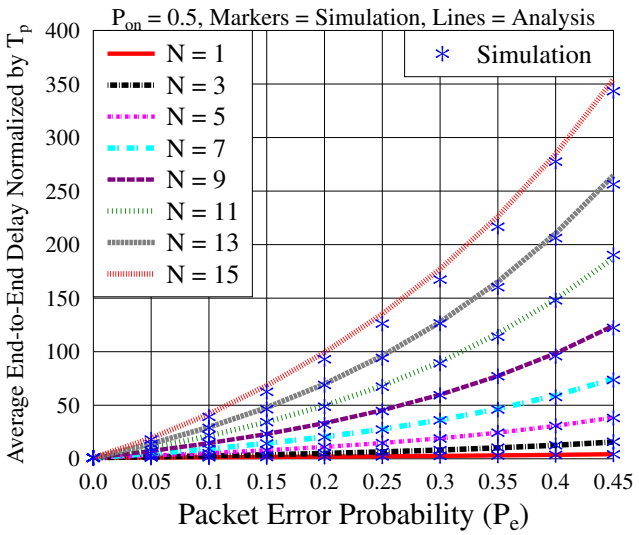

Figure 4.18: Average end-to-end packet-delay of the CGBN-HARQ versus packet error probability for various values of N, when $P_{on} = 0.5$ and $k = 1$.

4.6 Chapter Conclusions

We proposed a CGBN-HARQ transmission scheme for a CR system with the objective of improving the attainable bandwidth efficiency, while maintaining reliable data transmission. Our investigations have included both its mathematical analysis and simulations. The analytical study of the proposed scheme has relied on the CR system being modelled using a discrete-time Markov chain. The results obtained for this system model include an algorithm conceived for generating all possible states of the CR transmitter. We have also derived closed-form expressions for the throughput and delay of the CGBN-HARQ scheme. The analytical results have also been confirmed by simulations. Specifically, the performance results demonstrated that both the throughput and the delay of the proposed system is significantly affected by the PU's activities and by the PU's channel quality. The results shows a significant increase in the transmission delay owing to less reliable communication and/or due to the increase in the channel occupancy by the PUs. Moreover, we also investigated the impact of transmitting various number of packets on both the achievable throughput and on the transmission delay. It was demonstrated that in order to achieve the maximum attainable throughput and minimum delay, the number of packet transmission in a TS should be carefully adopted according to the communication environment. Our future research will focus on extending this work for finding the optimal transmission frame length.

Chapter 5

Performance of Cognitive Hybrid Automatic Repeat reQuest: Go-Back-N with Imperfect Sensing [1]

In Chapter 4, CR-aided Go-Back-N-HARQ (CGBN-HARQ) was proposed for mitigating the problem of transmission latency, when idealized perfect sensing is assumed. However, in practice the sensing cannot be perfectly reliable, hence resulting in false-alarm and mis-detection. Hence, the CR system may wrongly detect the presence/absence of PUs in the PR channel, where the false-alarm represents the scenario in which the PU is inactive but the CR system deems it to be active. On the other hand, mis-detection represents the scenario, where the PU is active, yet CR system deems the channel to be free. Hence, in order to take into account all these scenarios, the two-state Markov chain used in Chapter 4 is extended to a four state Markov chain by explicitly considering both the sensed state and the true state of the PR channel. Additionally, in contrast to the analytical model of Section 4.4, in this chapter, the analytical model is redesigned in Section 5.4 along with the new state definition and state generation algorithm for the sake of capturing the consequences of the unreliable sensing decisions. Note that in order to reduce the redundancy, in this chapter, we will focus our attention on characterizing the specific parts different from those of the previous chapters. Finally, we will compare the performance results of the CGBN-HARQ transmission scheme for both perfect and imperfect sensing.

5.1 Introduction

Similar to Chapter 3 and 4, the activity of the PUs is modelled using a two-state Markov chain with the states of 'ON' and 'OFF' [83]. The PR channel is considered to be busy, when it is in the 'ON' state and free from PUs, when it is in the 'OFF' state. In order to find the status of the PR channel, the CR system first senses the PR channel and utilizes it only on condition, when it is found in the

[1] A part of this chapter has been published in IEEE Vehicular Technology Conference, Nanjing China, May 2016 [1].

'OFF' state. However, when the sensing is unreliable, the CR system may erroneously identify the PR channel's state, hence generating either a false-alarm or a mis-detection event. In this case, the channel perceived by the CR system may described as a four state Markov chain by considering both the actual state of the PR channel and the sensed state of the CR system. Again, we assume that the PR channel is partitioned into time-slots (TSs) of duration T. Correspondingly, in the CR system, each TS is divided into two segments, namely the sensing time of duration T_s seconds and the data transmission time of duration $T_d = T - T_s$ seconds [61, 234]. The first T_s seconds of a TS are used for sensing the channel, while the remaining T_d seconds are used for data transmission relying on the Go-Back-N hybrid automatic repeat request (GBN-HARQ) principles [1, 18, 21], if the PR channel is found to be in its 'OFF' state.

Additionally, in [1], we have addressed the throughput and delay characteristics of the CGBN-HARQ, where we assumed that the feedback flags are always received after the sensing duration of a TS, which results in a simplified model for the CR transmitter. By contrast, in this chapter, we relinquished the above constraint and assumed that the transmitter is capable of receiving feedback flags any time during a TS, including both the sensing period and the data transmission period. Since the feedback flags are strongly protected and typically require only a single bit of information [242, 243], this overhead does not hamper the sensing process or the PU's transmission. By eliminating the above simplifying assumptions, the analytical modelling of the CGBN-HARQ scheme with imperfect sensing became challenging, due to the facts: 1) the reception of the ACK and NACK flags both during the sensing period and data transmission period; 2) owing to the imperfect sensing decisions. However, it helps the transmitter in avoiding the unnecessary retransmission of packets, whose ACK flags are received during the sensing time, which improves the overall throughput and reduces the delay of the system. Moreover, in this chapter, we extend the solution presented in [1] by deriving a new analytical framework, which allows us to derive closed-form expressions both for the throughput as well as for the average packet delay and for the end-to-end packet delay. Our studies show that both the activity of the PR system and the transmission reliability of the CR system imposes a substantial impact on the achievable performance of the CGBN-HARQ. Hence, the parameters may have to be adapted according to the near-instantaneous communication environment in order to maximize the attainable performance. Recall that we have detailed the related literature in Section 4.1.

5.1.1 Chapter Contributions

The novel contributions of this chapter can be summarized as follows,

1. The cognitive protocol proposed in Chapter 4 is extended by enabling the transmitter to simultaneously sense and receive the feedback flag of the packet transmitted in the previous free TS in a realistic imperfect sensing environment. To do so, the CR transmitter requires significant improvements for reformulating the transmission principles of the classic GBN-

HARQ, when incorporating it in CR systems.

2. The CGBN-HARQ regime is theoretically modelled and analysed by a DTMC-based approach in an imperfect sensing environment. Based on this modelling, closed form expressions are derived for the throughput, for the average packet delay and for the end-to-end packet delay. As for the end-to-end packet delay, both its probability distribution and its average end-to-end packet delay are analysed.

3. We demonstrated that the CGBN-HARQ proposed in this chapter provides a better throughput and delay than [1].

4. Finally, a range of simulation results are provided for the verification of the theoretical analysis.

The rest of this chapter is organized as follows. The models of the PR and CR systems are described in Section 5.2. The principles of CGBN-HARQ are stated in Section 5.3. Sections 5.3.1 and 5.3.2 consider the operations of the CR transmitter and receiver. Our performance results are provided in Section 5.5, whilst our conclusions are offered in Section 5.6.

5.2 System Model

The main assumptions used in our analysis and for the performance results are described below.

5.2.1 Modelling the Primary User

In the system model considered in this chapter, the PR system is identical to of Section 4.2.1, where the PU activities are modelled using a two-state Markov chain having 'ON' and 'OFF' states.

5.2.2 Modelling the Cognitive User

As in Chapter 3 and in Fig. 4.4(b), in our CR systems each TS is divided into two phases: sensing using a time duration of T_s seconds and data transmission in the remaining $T_d = T - T_s$ seconds. During the sensing phase, the CU senses the 'ON' and 'OFF' activity of the PUs on the PR channel. If the PR channel is deemed to be in the 'OFF' state, the CU can use the time T_d for its data transmission based on the principles of the GBN-HARQ, as it will be detailed below. Otherwise, it waits until the next TS, during which the above procedure is repeated.

In practice, the CU may not always be capable of perfectly detecting the activity of the PUs due to the channel-induced shadowing and fading, aggravated by the background noise. In this case, the sensing of CU may generate false-alarms and mis-detection, in addition to the correct detection of the 'ON' and 'OFF' state of the PR system. In summary, the states of this realistic CR

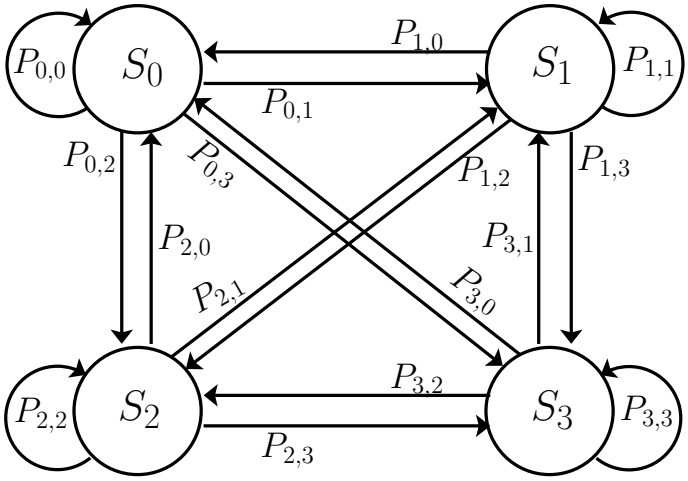

Figure 5.1: Discrete-time Markov chain for modelling the CR system, where $S_0 = 00$ illustrates that the respective TS is free and also the CU detected it free, $S_1 = 01$ represents that the channel is free but the CU finds it busy. Likewise $S_2 = 10$ and $S_3 = 11$.

system are shown in Fig. 5.1, where the transition probabilities between the states are also shown. Furthermore, the transition probabilities can be expressed in matrix form as

$$\boldsymbol{P} = \begin{bmatrix} P_{0,0} & P_{0,1} & P_{0,2} & P_{0,3} \\ P_{1,0} & P_{1,1} & P_{1,2} & P_{1,3} \\ P_{2,0} & P_{2,1} & P_{2,2} & P_{2,3} \\ P_{3,0} & P_{3,1} & P_{3,2} & P_{3,3} \end{bmatrix}.$$

Let us represent the false-alarm and mis-detection probabilities by P_{fa} and P_{md}. Then with the aid of Eq. (4.2), and Fig. 5.1, we obtain

$$\begin{aligned} P_{0,0} &= P_{1,0} = (1-\beta)(1-P_{fa}) \\ P_{0,1} &= P_{1,1} = (1-\beta)P_{fa} \\ P_{0,2} &= P_{1,2} = \beta P_{md} \\ P_{0,3} &= P_{1,3} = \beta(1-P_{md}) \\ P_{2,0} &= P_{3,0} = \alpha(1-P_{fa}) \\ P_{2,1} &= P_{3,1} = \alpha(1-P_{fa}) \\ P_{2,2} &= P_{3,2} = (1-\alpha)(P_{md}) \\ P_{2,3} &= P_{3,3} = (1-\alpha)(1-P_{md}). \end{aligned} \tag{5.1}$$

Let the steady-state probabilities of the Markov chain be expressed as $\boldsymbol{\Phi} = [\Phi_0, \Phi_1, \Phi_2, \Phi_3]^T$. Then, we have

$$\boldsymbol{\Phi} = \boldsymbol{P}^T \boldsymbol{\Phi}, \tag{5.2}$$

which shows that $\boldsymbol{\Phi}$ is the right eigenvector of $\mathbf{P}^T$ corresponding to an eigenvalue of one. Therefore,

after solving Equation (5.2), we obtain

$$\begin{aligned}\mathbf{\Phi} &= [\Phi_0 \;\; \Phi_1 \;\; \Phi_2 \;\; \Phi_3]^T \\ &= \lambda \times \left[\frac{\alpha(1-P_{fa})}{\beta(1-P_{md})} \;\; \frac{\alpha(P_{fa})}{\beta(1-P_{md})} \;\; \frac{(P_{md})}{(1-P_{md})} \;\; 1\right]^T,\end{aligned} \tag{5.3}$$

where $\lambda \in \mathbb{R}$ is applied to satisfy

$$\sum_{i=0}^{3} \Phi_i = 1, \tag{5.4}$$

giving

$$\lambda = \frac{\beta(1-P_{md})}{\alpha+\beta}. \tag{5.5}$$

Upon substituting (5.5) into (5.3), the steady-state probabilities of the CR system at states S_0, S_1, S_2 and S_3 are given by

$$\Phi_0 = \frac{\alpha(1-P_{fa})}{\alpha+\beta}, \;\; \Phi_1 = \frac{\alpha(P_{fa})}{\alpha+\beta} \tag{5.6}$$

$$\Phi_2 = \frac{\beta(P_{md})}{\alpha+\beta}, \quad \Phi_3 = \frac{\beta(1-P_{md})}{\alpha+\beta}. \tag{5.7}$$

5.3 Principles of Cognitive Go-Back-N Hybrid Automatic Repeat Request

The principles of CGBN-HARQ are described in Section 4.3. Particularly, the operation of the CGBN-HARQ protocol presented in Fig. 4.5 was described by Algorithm 2 in Chapter 4, where the CR transmitter continuously (re)transmits N packets in a free TS, without waiting for their feedback flags. The consequences of imperfect sensing in the CGBN-HARQ are discussed below.

5.3.1 Operation of the CR Transmitter

In our proposed CGBN-HARQ scheme, as demonstrated in Algorithm 2 and Fig. 4.5, the transmitter first senses the PR channel using T_s seconds and then either transmits packets if the TS is free or waits for the next TS, if the current TS is found busy. Specifically, the transmission of packets takes place when the PR channel is correctly detected to be in the 'OFF' state, or when it is deemed to be in the 'OFF' state but it is actually 'ON'. Otherwise, the transmitter waits for the next TS, when the PR channel is correctly detected to be in the 'ON' state or when falsely detected to be in the 'ON' state, while it is actually 'OFF'. As mentioned above, once a 'free' TS is detected, the CU can transmit N packets, which may include new packets and/or the packets requiring retransmission.

In contrast to Figs. 4.6, 4.7 and 4.8, it is worth noting that in Fig. 5.2, TS T_2 is mis-detected, which implies that the TS is actually occupied by the PU but, due to the wrong sensing decision, it

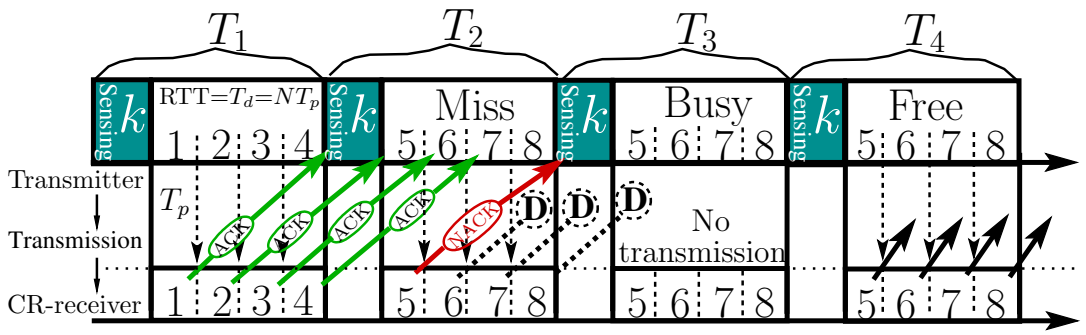

Figure 5.2: Transmission flow of the CGBN-HARQ scheme with the parameters of $k = 1$ and $N = 4$, when considering the affect of mis-detection and false-alarm. The *green* and *red* solid lines represent error-free and erroneous transmission, whereas the dotted lines depict the discarded packets.

is declared to be free. As a result, new packets, i.e., packets $5, 6, 7$ and 8 of Fig. 5.2 are transmitted. However, due to their collisions with the PU transmissions, these packets are corrupted and hence, all N packets are received in error. Moreover, in the case of false-alarm, the free TS is sensed to be busy, hence no transmission takes place.

5.3.2 Operation of the CR Receiver

In this chapter, the CR receiver operates in a similar way to that described in Section 4.3.2. This is because, the receiver can only receive packets and generate feedback flags. Hence, in the case of mis-detection, the CR receiver considers the packet to be erroneous and transmits a NACK flag to the transmitter's control channel receiver for the respective packet. The detailed operational principles of the CR receiver can be found in Section 4.3.2.

5.4 Markov Chain based Analysis

In contrast to the classic GBN-HARQ scheme, the modelling of the proposed CGBN-HARQ scheme in imperfect sensing environments hinges on the dynamic activity of the PU and on the potentially incorrect sensing of the PR channel. In this section, we model the operations of the CGBN-HARQ scheme using DTMC in a realistic imperfect sensing environment. Based on the DTMC modelling, we then evaluate the steady-state throughput of the system, the distribution of the end-to-end packet delay and of the average end-to-end packet delay.

To commence the analysis, let us define the states of the CGBN-HARQ system, which can be jointly determined by the following factors:

1. The real status of the PR channel.

2. The status of the PR channel sensed by the CR system.

3. The status of the N packets stored in the transmitter buffer, (which may be the 'new packet', 'retransmitted packet' and 'packet repeated in the same TS').

We assume that the states are defined on the basis of the TSs, i.e. the state transition rate is the same as the rate of TSs, and the transmitter buffer is observed at the end of each TS. In detail, let us formulate the list of states as

$$\mathbb{S} = \{S_0, S_1, \ldots, S_i, \ldots S_T\}, \tag{5.8}$$

where S_T is the total number of states, i.e we had $S_T = |\mathbb{S}|$, and S_i is the ith legitimate state, which is a $(N+2)$-length base-3 digit expressed as

$$S_i = \{S_{i0}S_{i1}S_{i2}\cdots S_{i(N+1)}\},\ i = 0, 1, \cdots, S_T \tag{5.9}$$

For convenience, S_i is also referred to as the ith state sequence. Specifically, in the state sequence of Eq (5.9), the first digit S_{i0} represents the status of the PR channel,

$$S_{i0} = \begin{cases} 0, & \text{if the PR channel is free,} \\ 1, & \text{if the PR channel is busy.} \end{cases} \tag{5.10}$$

The second digit S_{i1} represents the status of the PR channel sensed by the CR system, which is given by

$$S_{i1} = \begin{cases} 0, & \text{if the PR channel is sensed free;} \\ 1, & \text{if the PR channel is sensed busy.} \end{cases} \tag{5.11}$$

Finally, the digit S_{ij} for $j = 2, \ldots, N+1$, is determined as

$$S_{ij} = \begin{cases} 0, & \text{if the } j\text{th packet is a new one;} \\ 1, & \text{if the } j\text{th packet is a retransmitted one, when the TS is free; or the one to be} \\ & \text{retransmitted, when the TS is busy;} \\ 2, & \text{if the } j\text{th packet is a repeated replica of a previous packet in the same TS.} \end{cases} \tag{5.12}$$

Having determined S_{ij} according to (5.10), (5.11) and (5.12), we can find one-to-one mapping between i and S_i as

$$i = \sum_{j=0}^{N+1} S_{ij} 3^{N-j+1}, \tag{5.13}$$

which gives the subscript of S_i, representing the ith state of the DTMC.

Below we use a pair of examples to explain the principles of modelling and transitions.

5.4.1 Example 1

First, let us consider a simple example of the CGBN-HARQ scheme with the parameters $k = 1$ and $N = 1$, assuming that the CR transmitter uses one T_p for PR channel sensing and that the transmitter buffer stores only a single packet. In this case, we should note that the third case in (5.12) will never occur, implying that no packet will be repeated within a specific TS and therefore digit 2 will never appear. According to the above definitions, we can show that the DTMC of this system has $S_T = 8$ states, which are explicitly shown in Table 5.1.

State	$(S_{i0}\ S_{i1}\ S_{i2})$	State	$(S_{i0}\ S_{i1}\ S_{i2})$
S_0	(0 0 0)	S_9	(1 0 0)
S_1	(0 0 1)	S_{10}	(1 0 1)
S_3	(0 1 0)	S_{12}	(1 1 0)
S_4	(0 1 1)	S_{13}	(1 1 1)

Table 5.1: Possible states of the CGBN-HARQ, with $N = 1$ and $k = 1$.

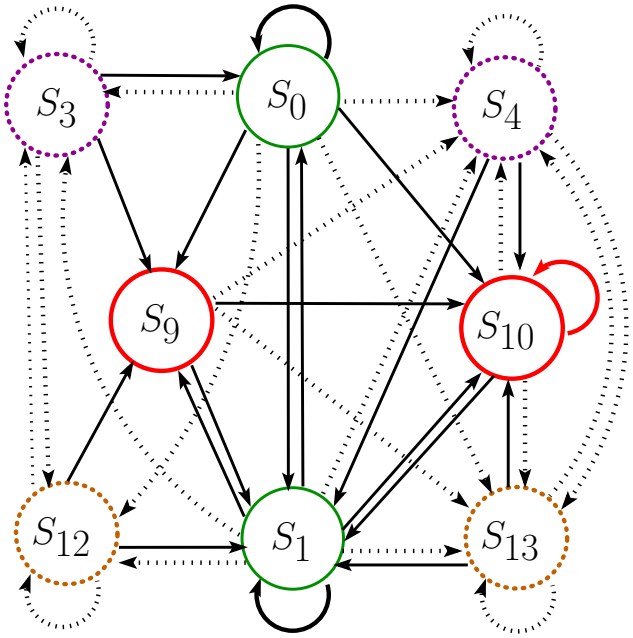

Figure 5.3: The DTMC-based state diagram for modelling the CGBN-HARQ scheme with $N = 1$ and $k = 1$. The *dashed* lines correspond to the transitions towards busy states, because the next TS is found to be busy TSs; *solid* lines illustrate the transitions towards free states due to the detection of free TSs. The *solid green* and *red* circles represent the free states due to no false-alarm and mis-detection, respectively, and *dashed magenta* and *brown* color circles represent busy states due to false-alarm and no mis-detection.

Correspondingly, the state diagram showing the state transitions given in Fig. 5.3, where the transitions and their transition probabilities are detailed below. Let us assume that the transmitter is first in state $S_0 = 000$. This state is defined by the events that the TS is correctly detected to be free (the TS is free in reality $(S_{i0} = 0)$ and it is also correctly sensed to be free $(S_{i1} = 0)$. Therefore, a new packet is transmitted $(S_{i2} = 0)$. When the transmitter receives an ACK related to the transmitted packet and the next TS is found free, the transmitter remains in the same state S_0.

This gives the transition probability of $P_{0,0} = P_{off}(1 - P_{fa}) \times (1 - P_e)$, where P_e is the packet's error probability. On the other hand, if a NACK is received and the next TS is found free, the state transits to S_1. Correspondingly, the transition probability is $P_{0,1} = P_{off}(1 - P_{fa}) \times P_e$. In a similar manner, if the next TS is correctly detected to be busy and an ACK (or a NACK) is received for a transmitted packet, then the transmitter changes its state from S_0 to S_{12} (or S_{13}), with a transition probability of $P_{0,12} = P_{on}(1 - P_{md}) \times (1 - P_e)$ (or $P_{0,13} = P_{on}(1 - P_{md}) \times P_e$). Likewise, if the next busy TS is mis-detected and ACK (or NACK) is received, then the transmitter traverses from S_0 to S_9 (or S_{10}), with a transition probability of $P_{0,9} = P_{on}P_{md} \times (1 - P_e)$ (or $P_{0,10} = P_{on}P_{md} \times P_e$).

When the transmitter is in state S_9 or S_{10}, in the next TS the transmitter can only make a transition to one of the states of S_1, S_4, S_{10} and S_{13}. This is because the transmissions associated S_9 and S_{10} are always assumed to be incorrect due to mis-detection. If the next TS yields false-alarm or it is correctly detected to be busy, then the transmitter moves to state S_4 or S_{13}, associated with the transition probability of $P_{9,4} = P_{off}P_{fa}$ or $P_{9,13} = P_{on}(1 - P_{md})$. Similarly, based on Fig. 5.3, we can analyze the remaining state transitions. The corresponding state transition probabilities are presented in Table. 5.2.

5.4.2 Example 2

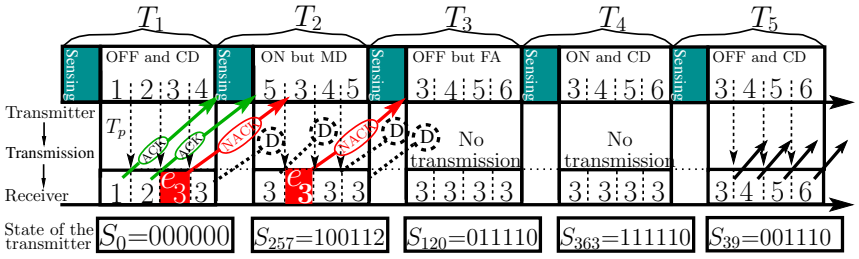

Figure 5.4: Transmission flow of CGBN-HARQ, where CD, MD and FA are for correct-detection, mis-detection and false-alarm, respectively. The state of the transmitter is observed at the end of TS.

In the second example, we assume that the CGBN-HARQ uses the parameters of $k = 1$ and $N = 4$. For clarity, we consider the scenario shown in Fig. 5.4, which illustrates that the transitions takes place across five TSs, with the following justification.

1. Assume that during TS T_1, the PR channel is free and it is also correctly sensed. Hence, we have $S_{i0} = 0$ and $S_{i1} = 0$. In this case, we assume that $N = 4$ new packets are transmitted, which give $S_{ij} = 0$ for $j = 2, 3, 4, 5$. Therefore, the state observed by the transmitter at the end of TS T_1 is $S_0 = \{0, 0, 0, 0, 0, 0\}$. As shown in the figure, the first two packets are correctly received and hence ACK flags are transmitted. By contrast, packet 3 is received in error, hence a NACK flag is transmitted.

2. Due to the mis-detection, the TS T_2 is deemed to be free, although it is actually busy. There-

fore, the transmitter receives an ACK after the sensing duration and it transmits the new packet 5. However, after the reception of a NACK at the end of the first T_p in T_2, the transmitter retransmits both the erroneous as well as the discarded packets, where the indices of the 4 packets transmitted during T_2 are $5, 3, 4, 5$. In this case, as shown in Fig. 5.4, packet 5 is transmitted twice in the same TS. Furthermore, both packets 3 and 4 are old packets requiring retransmission. All the above-mentioned events result in the following state of the transmitter in TS T_2: $S_{257} = 100112$. Correspondingly, the transition probability from state S_0 to S_{257} is $P_{0,257} = P_{on}P_{md} \times (1 - P_e)^2 P_e$. Note that due to the mis-detection of the busy PR channel, the packets transmitted in TS T_2 are all received in error. Hence, the receiver feeds back a NACK, while packets 4 and 5 are discarded, regardless whether they are received correctly or incorrectly.

3. During TS T_3, the channel is free but it is sensed to be busy due to a false-alarm. Since all packets transmitted during the TS T_2 are erroneous, they require retransmission. Hence, the transmitter changes its state from S_{257} to $S_{120} = 011110$ with a probability of $P_{257,120} = P_{on} \times P_{md}$.

4. Similarly, we can find that the state associated with TS T_4 is S_{363} and the corresponding transition probability from state S_{120} to S_{363} is $P_{257,363} = P_{on} \times (1 - P_{md})$.

5. Finally, during TS T_5, the PR channel is correctly detected to be free. Therefore, all the N packets waiting in the buffer are transmitted, which results in a transition from state S_{363} to the state S_{39} with a transition probability of $P_{363,39} = P_{off} \times (1 - P_{fa})$.

According to the principles of our CGBN-HARQ, we can infer that the DMTC derived for the CGBN-HARQ relying on realistic imperfect sensing exhibits the following characteristics.

- When a TS is found busy due to correct sensing of an occupied PR channel, or owing to the false-alarm encountered in a free PR channel, digit 2 does not appear in the corresponding state sequence. This is because, in this case a packet will never be retransmitted within a specific TS.

- When a transition from a busy state to a free state occurs, only the first two digits of the current state sequence $S_{i,0}$ and $S_{i,1}$ may change in the new state sequence, while all the other digits in the state sequence remain the same. This is explicitly shown in TS T_5 of Fig. 5.4. Hence the new state sequence does not contain any digit associated with the value of 2.

- The first two digits of a state sequence, i.e. S_{i0} and S_{i1}, never assume a value of 2.

With the aid of these properties, we can remove a large fractions of the states from consideration. However, there are still a large number of states. In this context, it remains an open challenge to mathematically derive a formula for calculating the total number of states as well as to represent

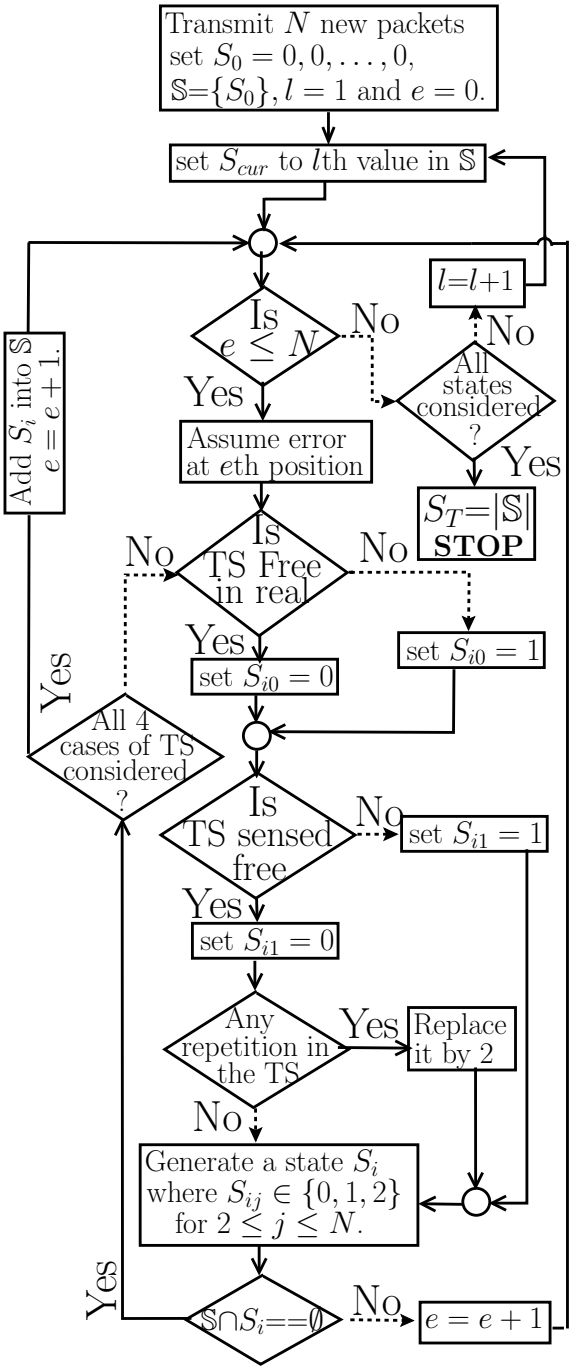

Figure 5.5: The flow chart illustrates the process of generating states represented by $(N + 2)$-length base-3 digits. For each value of e, the 4 cases: 1) correct detection of a free PR channel 2) correct detection of a busy PR channel 3) mis-detection; and 4) false-alarm are considered. Here, e represents the position of the erroneous packet in the TS, while $e = 0$ is a special case when all the received packets are error-free.

the state sequences with the aid of general expressions. However, for any pair of state, we can readily derive the corresponding transition probability. Hence, we propose the Algorithm shown in Fig. 5.5 for finding the number of states and the state sequences. The algorithm is conceived as follows.

Fundamentally, this algorithm uses a search technique for finding the legitimate states. Initially,

the transmitter is set to the state $S_0 = 000000$. Let the legitimate states from set $\mathbb{S}$, which initially contains only S_0. In order to generate new states from the current state S_0, we arrange for an erroneous transmission to occur at each possible position of the packets sent in the TS. Let us simultaneously assume that the next TS is either free or busy, which is correctly sensed, mis-detected or sensed subject to a false-alarm.

For example, during the TS T_1 of Fig. 5.2, only new packets are transmitted, which are correctly received. Hence ACK flags are fed back. In the algorithm, this case is represented by $e = 0$. Continuing this example, when the next TS is busy, but it is sensed to be free, 4 new packets are transmitted in TS T_2. Consequently, the state is changed to $S_{243} = 100000$. Moreover, in the same case of $e = 0$, it is possible that TS T_2 may be sensed to be busy due to false detection of a free PR channel or owing the correct detection of a busy PR channel. If this is the case, the current state changes to $S_{81} = 010000$ for the false-alarm or to $S_{324} = 110000$ for the correct detection, respectively. After the generation of a new state, for example S_{324}, it is compared to all the existing states in $\mathbb{S}$. Provided that S_{324} is already in $\mathbb{S}$, it is ignored. Otherwise, S_{324} is added to the set $\mathbb{S}$. Similarly, by considering the cases of $e = 1$ to $e = N$, the algorithm will generate all legitimate states that the transmitter may encounter upon emerging from state S_0. After generating all the possible new states upon emerging from state S_0, the algorithm moves to the next state S_l in in set $\mathbb{S}$, which is S_{243} for the example of Fig. 5.2. Then, the state S_l becomes the current state, and the above procedure is repeated in order to derive other legitimate new states for the set $\mathbb{S}$. Since the Markov chain is irreducible and aperiodic, the algorithm finally terminates, when all the states in the set $\mathbb{S}$ have been considered as the current states, but without generating new states. At the conclusion of the algorithm, the cardinality of the set $\mathbb{S}$ gives the total number of states S_T, i.e. we have $S_T = |\mathbb{S}|$.

5.4.3 State Transition Probability Matrix

Let the state transition probability matrix be expressed as $\mathbf{P}$, and the state at the ith TS be represented by $S(i)$. Then, for the example of Fig. 5.4, we have $S(1) = S_0$, $S(2) = S_{257}$, $S(3) = S_{120}$ $S(4) = S_{363}$ and $S(5) = S_{39}$. Given the state S_i in TS n, we have $S(n) = S_i$. Then the probability $P_{i,j}$ of transition to the next state is S_j, i.e. $S(n+1) = S_j$ can be expressed [21, 244] as;

$$\begin{aligned} P_{i,j} &= P\left\{S(n+1) = S_j \mid S(n) = S_i, \ldots, S(1) = S_0\right\} \\ &= P\{S(n+1) = S_j | S(n) = S_i\}, \end{aligned} \tag{5.14}$$

which is the $(j,i)th$ element of $\mathbf{P}$. According to the properties of the DTMC, we have

$$\begin{aligned} &0 \leq P_{i,j} \leq 1 \\ &\sum_{S_j \in \mathbb{S}} P_{i,j} = 1, \ \ \forall\, S_i \in \mathbb{S}. \end{aligned} \tag{5.15}$$

Current State S_i	State S_j probability	State S_j probability	State S_j probability	State S_j probability
$P_{i,j}$=$i = 0,1$ &	$P_{i,0}$=P_{off}(1-P_{fa})(1-P_e)	$P_{i,1}$=P_{off}(1-P_{fa})P_e	$P_{i,3}$=$P_{off}P_{fa}$(1-P_e)	$P_{i,4}$=$P_{off}P_{fa}P_e$
$j = 0,1,3,\ldots 13$	$P_{i,9}$=$P_{on}P_{md}$(1-P_e)	$P_{i,10}$=$P_{on}P_{md}P_e$	$P_{i,12}$=P_{on}(1-P_{md})(1-P_e)	$P_{i,13}$=P_{on}(1-P_{md})P_e
$P_{i,j}$=$i = 3,12$ &	$P_{i,0}$=P_{off}(1-P_{fa})	$P_{i,1} = 0$	$P_{i,3}$=$P_{off}P_{fa}$	$P_{i,4} = 0$
$j = 0,1,3\ldots 13$	$P_{i,9}$=$P_{on}P_{md}$	$P_{i,10} = 0$	$P_{i,12}$=P_{on}(1-P_{md})	$P_{i,13} = 0$
$P_{i,j}$=$i = 4,8,9,13$	$P_{i,0} = 0$	$P_{i,1}$=P_{off}(1-P_{fa})	$P_{i,3} = 0$	$P_{i,4}$=$P_{off}P_{fa}$
& $j = 0,1\ldots 7$	$P_{i,9} = 0$	$P_{i,10}$=$P_{on}P_{md}$	$P_{i,12} = 0$	$P_{i,13}$=P_{on}(1-P_{md})

Table 5.2: State to state transition probabilities with respect to TS for $N = 1$ and $k = 1$ case.

It is worth noting that the transition probability $P_{i,j}$ is set to zero, if the transmitter cannot make a transition from S_i to S_j in one step (i.e. in the next TS). To continue our modelling, let the probability $P_i(n)$ represent the state of the transmitter in TS n. Then, we have $\sum_{i\in\mathbb{S}} P_i(n) = 1$. Let $\boldsymbol{p}(n) = [P_0(n), P_1(n), \ldots, P_{S_T}(n)]^T$ collect the S_T probabilities in TS n. Furthermore, let us assume that the transmitter starts its transmission from state $S(1) = S_0$ with the probabilities of

$$\boldsymbol{p}(1) = [1, 0, \ldots, 0]^T. \tag{5.16}$$

Then, by the law of total probability [21,245], the specific probability that the DTMC traverses into state j at TS $(n+1)$ can be expressed as

$$P_j(n+1) = \sum_{\forall S_i\in\mathbb{S}} P_i(n)P_{i,j},\ \forall\ S_j \in \mathbb{S} \text{ and } n > 1. \tag{5.17}$$

By considering all the states in $\mathbb{S}$, we arrive at a recursive equation of

$$\boldsymbol{p}(n+1) = \mathbf{P}^T\boldsymbol{p}(n),\ n = 1,2,3,4,\ldots \tag{5.18}$$

From this equation, we can readily infer that

$$\boldsymbol{p}(n+1) = (\mathbf{P}^T)^n\boldsymbol{p}(1) \tag{5.19}$$

As shown in Eq (5.15), the sum of each column of $\mathbf{P}^T$ is 1. Therefore, the state transition probability matrix $\mathbf{P}^T$ is a left stochastic matrix [245], because the sum of each column is equal to one. Consequently, according to the *Perron-Frobenius theorem*, the limit of $\lim_{n\to\infty}(\mathbf{P}^T)^n$ exists [245], and when we have $n \to \infty$, the Markov chain reaches its steady state [21], implying that

$$\boldsymbol{p}(n+1) = \boldsymbol{p}(n). \tag{5.20}$$

Let the steady-state probabilities be expressed by $\boldsymbol{\pi}$, i.e. $\boldsymbol{\pi} = \lim_{n\to\infty}\boldsymbol{p}(n)$. Then, from (5.18) and (5.20) we have [21,244],

$$\boldsymbol{\pi} = \mathbf{P}^T\boldsymbol{\pi}, \tag{5.21}$$

which shows that steady state probability vector $\boldsymbol{\pi}$ is the right eigenvector of $\mathbf{P}^T$, corresponding to an eigenvalue of one. Therefore, $\boldsymbol{\pi}$ can be obtained via calculating the eigenvector of $\mathbf{P}^T$ [21,244, 245].

5.4.4 Throughput of CGBN-HARQ

The throughput of the CGBN-HARQ scheme is quantified in terms of the average number of packets successfully transmitted per TS. The successful transmission of a packet in a TS depends on two factors: 1) a free PR TS is correctly sensed by the CR system, and 2) the packet is delivered error-freely. As shown in (5.21), when the DTMC reaches its steady state, the throughput is determined by those states which have one or more new packets successfully transmitted. Let us analyze the throughput in detail as follows.

As mentioned above, when the DTMC reaches its steady state, the additional throughput generated during the TS considered depends on the following two events: 1) the PR channel is sensed free, corresponding to the scenario, when the first and second digits in the state sequence are either 00 or 10; and 2) the number of new packets transmitted associated with the state, when the PR channel is sensed to be free. Let $n_p(S_i)$ be the number of new packets transmitted in association with state $S_i \in \mathbb{S}_N$. Explicitly, $n_p(S_i)$ equals the number of zeros in the state sequence of S_i minus two, when the first two digits are 00 or minus one, if the first two digits are 10. Considering the first event, let us collect the states with the first two digits being 00 or 10 into a set denoted as $\mathbb{S}_N$. Then, when we obtained the steady state probabilities $\boldsymbol{\pi}$, the throughput of the CGBN-HARQ scheme can be evaluated as

$$R_T = \sum_{S_i \in \mathbb{S}_N} \pi_i \times n_p(S_i), (\text{packets / TS}). \tag{5.22}$$

Furthermore, if we express the throughput in terms of the number of packets per T_p (packet duration), we have

$$R'_T = \frac{T_p}{T} \times R_T = \frac{1}{k+N} \times R_T \quad (\text{packets / } T_p). \tag{5.23}$$

Let us now analyze the delay attained by our CGBN-HARQ scheme.

5.4.5 Delay of CGBN-HARQ

In the traditional GBN-HARQ, the transmission delay of a packet is contributed by the time required for its first transmission as well as the time associated with its retransmission. By contrast, in the proposed CGBN-HARQ, in addition to the above delay, extra delay may be imposed by the unavailability of the PR channel, which may either be due to the correct sensing of the busy PR channel or owing to the false sensing of the free PR channel. Therefore, in our CGBN-HARQ scheme, it is desirable to consider two types of delays. The first type of delay is the average packet delay, while the second one is the end-to-end packet delay. Specifically, the average packet delay is given by the total time required by a CR transmitter, measured from the start of sensing a TS until the successful transmission of all packets, divided by the total number of packets transmitted during this period. By contrast, the average end-to-end delay is the average delay of a packet from

its first transmission until the instant that it is confirmed to be successfully received. Below we consider both types of delays.

5.4.5.1 Average Packet Delay

In the previous section, we have obtained the throughput quantified in terms of the average number of the packets per TS (or T_p). Hence, given the throughput as expressed in (5.22) or (5.23), we can readily infer that the average packet delay can be evaluated as

$$T_D = \frac{1}{R_T} \ \text{(TS per packet)} \tag{5.24}$$

$$= \frac{k+N}{R_T} \ (T_p \text{ per packet}). \tag{5.25}$$

5.4.5.2 End-To-End Packet Delay

In this subsection, we investigate the average end-to-end packet delay. We commence by studying the probability distribution of the end-to-end packet delay.

Let $\mathbb{S}_N \subset \mathbb{S}$ be a subset of $\mathbb{S}$, which contains all the states having new packets transmitted. Given a state $S_i \in \mathbb{S}_N$, we define a set $\mathbb{S}_i^{(m)}$, which contains the states $\{S_j\}$ in which $l_{i,j} \geq 1$ new packets have been transmitted from state S_i that are correctly received in state S_j with exactly a delay of mT_p, i.e.,

$$\mathbb{S}_i^{(m)} = \{S_j |\ l_{i,j} \geq 1 \text{ new packets transmitted at state } S_i \text{ are correctly received at state } S_j \text{ with exactly the delay of } mT_p.\} \tag{5.26}$$

Furthermore, let the total number of new packets transmitted from S_i be expressed as L_i. Then, the probability mass function (PMF) of the end-to-end packet delay can be evaluated by the formula

$$P(m) = \frac{1}{c} \sum_{S_i \in \mathbb{S}_N} \sum_{S_j \in \mathbb{S}_i^{(m)}} \frac{\pi_i \times l_{i,j} \times P_{i,j}^{(m)}}{L_i}, \ m = 1, 2, \ldots. \tag{5.27}$$

where $c = \sum_{S_i \in \mathbb{S}_N} \pi_i$ and $P_{i,j}^{(m)}$ denotes the probability of transition from state S_i to state S_j with the delay of mT_p.

Given $\boldsymbol{\pi}, \boldsymbol{P}$ and $\mathbb{S}$, the PMF of end-to-end packet delay can be obtained as follows. Let

$$\boldsymbol{P}_{MF} = [P(1), P(2), \ldots, P(M_T)]^T, \tag{5.28}$$

where M_T is the highest delay considered, which can be set to a sufficiently high value so that the probability of having such a delay can be ignored, such as, say 10^{-8}. Let us first initialize $\boldsymbol{p}^{(0)} = \boldsymbol{I}_i$, where $\boldsymbol{I}_i$ is the ith column of the identity matrix $\boldsymbol{I}_{S_T}$. Then, according to the properties

of the DTMC, we have

$$\boldsymbol{p}^{(j)} = \mathbf{P}^T.\boldsymbol{p}^{(j-1)} = (\mathbf{P}^T)^j \boldsymbol{I}_i,\ j = 1, 2, \ldots \tag{5.29}$$

From (5.29) we can obtain the following information:

a) If a packet first transmitted in state S_i is successfully received in state S_j, the effective end-to-end delay is jT_ps;

b) The probabilities of transition from state S_i to any other states in $\mathbb{S}$, which are given in $\boldsymbol{p}$(j);

Therefore, with the aid of the above information, we can update $\boldsymbol{P}_{MF}$ using the following formula:

$$P(m) \leftarrow P(m-1) + \frac{\pi_i \times l_{i,j} \times P_{i,j}^{(m)}}{L_i}, \tag{5.30}$$

for $m = 1, 2 \ldots, M_T, S_j \in \mathbb{S}_i^{(m)}, S_i \in \mathbb{S}_N$. Having obtained the PMF of the end-to-end packet delay, the average end-to-end packet delay can be formulated as

$$\tau = \sum_{i=1}^{M_T} iT_p \times P(i). \tag{5.31}$$

Below we proceed to provide our performance results and validate our theoretical analysis by comparing the analytical results to that obtained from our simulations.

5.5 Performance Results

In this section, the performance of the CGBN-HARQ scheme is characterized, when both perfect and imperfect sensing are explicitly assumed. We quantify the throughput, average packet delay and average end-to-end packet delay. More specifically, we quantify the impact of false-alarm probability (P_{fa}), mis-detection probability (P_{md}), channel busy probability (P_{on}), packet error probability (P_e), as well as the number of packets N transmitted per TS. Note that in the perfect sensing environment of Chapter 4, P_{fa} and P_{md} are zero.

In our simulations, the observation period starts from the first TS, which the CR system starts sensing the PR channel, which continues until all the packets considered are successfully received by the CR receiver. Correspondingly, the throughput is evaluated as

$$R_S' = \frac{N_s}{N_t \times (k+N)} \ \text{(packets per } T_p\text{)}, \tag{5.32}$$

where N_t represents the total number of TSs used for the successful transmission of N_s packets.

Fig 5.6 shows that for a given probability of P_{on}, the achievable throughput of the CGBN-HARQ is at its maximum in both perfect and imperfect sensing scenarios, when the channel used by the CU is perfectly reliable, yielding $P_e = 0$. However, when the channel becomes less reliable, i.e. when P_e increases, the throughput reduces with P_e due to the increased number of packet

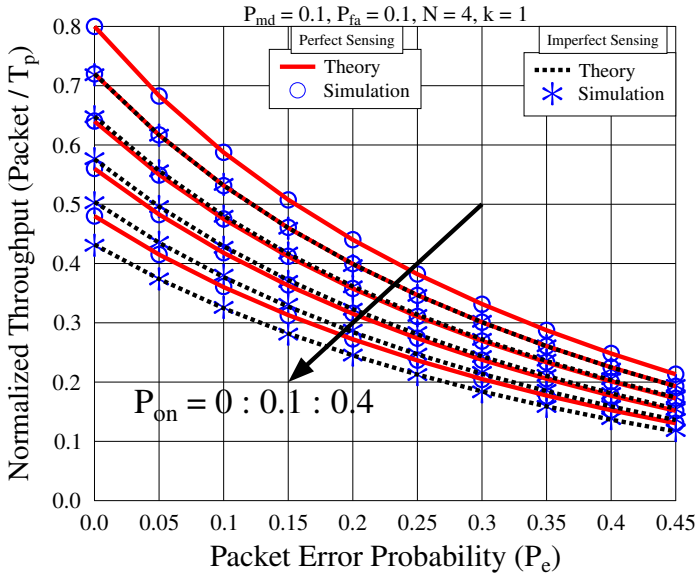

Figure 5.6: Throughput of the CGBN-HARQ versus packet error probability in terms of various channel occupancy probabilities, when $k = 1$ and $N = 4$. The theoretical results were calculated from (5.23) and the simulation results were obtained from (5.32).

retransmissions. As shown in Fig 5.6, at a given P_e, the highest throughput is attained, when the PR channel is always free to use, corresponding to $P_{on} = 0$. By contrast, when P_{on} increases, the throughput of the CGBN-HARQ system decreases, since less time is available for the CU to transmits its data. Moreover, Fig 5.6 demonstrates the effect of unreliable sensing on the throughput, exhibiting a substantial drop due to the inaccurate sensing for a given P_e and/or P_{on}. Finally, as demonstrated in Fig 5.6, the results obtained from our analysis agree well with the simulation results, which hence validates our analytical results.

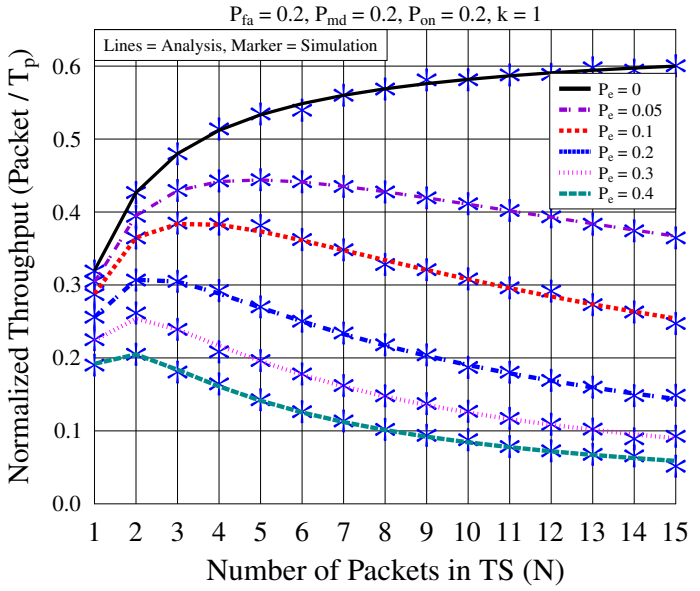

Figure 5.7: Investigating the optimal throughput of the CGBN-HARQ scheme based on the number of packet transmission (N) per TS, for various values of P_e in a perfect sensing environment.

Continuing with the throughput performance, the optimal value of N is investigated in Fig. 5.7

versus P_e, P_{fa}, P_{md} and P_{on}. It can be seen that the throughput always increases upon increasing the value of N provided that the channel is perfectly reliable, i.e. we have $P_e = 0$. This is due to the fact that the packet transmission is always error-free hence, the higher number of packets transmission, the higher is the throughput. When P_e increases, an increased value of N may results in a reduced throughput. This is because for a large value of N the number of retransmissions increases, once there is a packet in error. Furthermore, as seen in Fig. 5.7, for a given packet error probability $P_e \geq 0$, there exists an optimum value for N, which results in the highest throughput. The optimum value of N reduces, as the packet error probability P_e increases.

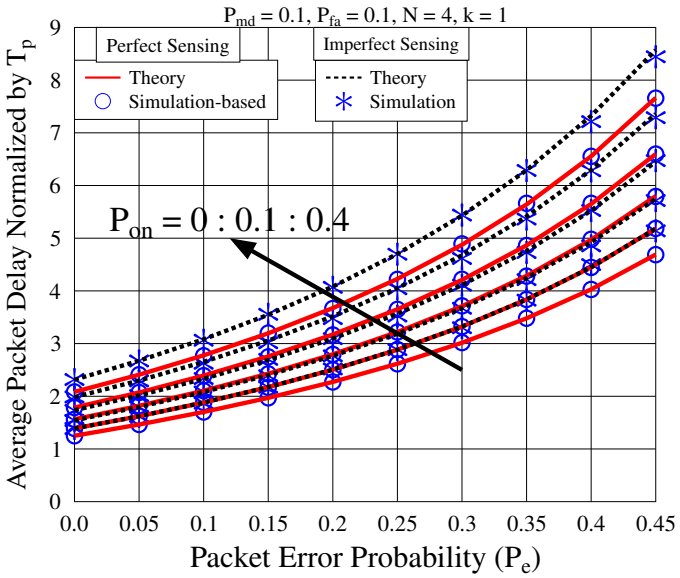

Figure 5.8: Average packet delay of the CGBN-HARQ system versus packet error probability for various channel busy probabilities, when perfect and imperfect sensing are respectively considered. The theoretical results were calculated from (5.25) and the simulation results were obtained from (5.33).

Having characterized the attainable throughput, we now continue to quantify the delay imposed. In our simulations, the average packet delay is computed as the total time used for the successful transmission of N_s packets, divided by N_s, which is formulated as

$$T'_{DS} = \frac{N_t(k+N)}{N_s} \times T_p \ \text{(seconds)}. \tag{5.33}$$

The results presented in Figs. 5.8 and 5.9 are normalized by T_p.

Specifically, Fig. 5.8 shows the average packet delay versus the packet error probability P_e, in terms of the channel busy probability P_{on}. As shown Fig. 5.8, the minimum delay is observed, when the channel is ideal, i.e. when $P_e = 0$ and/or when the channel is always free for the CU to use, corresponding to $P_{on} = 0$. The average packet delay increases upon increasing P_e and/or of P_{on}, as a result of the increased number of retransmissions and/or the reduced transmission opportunities for the CU. Furthermore, similar to the above discussions, due to unreliable sensing, a free TS may be falsely deemed to be busy, which increases the average packet delay. On the other hand, the increase of the average packet delay may also be the result of transmitting packets during busy TSs,

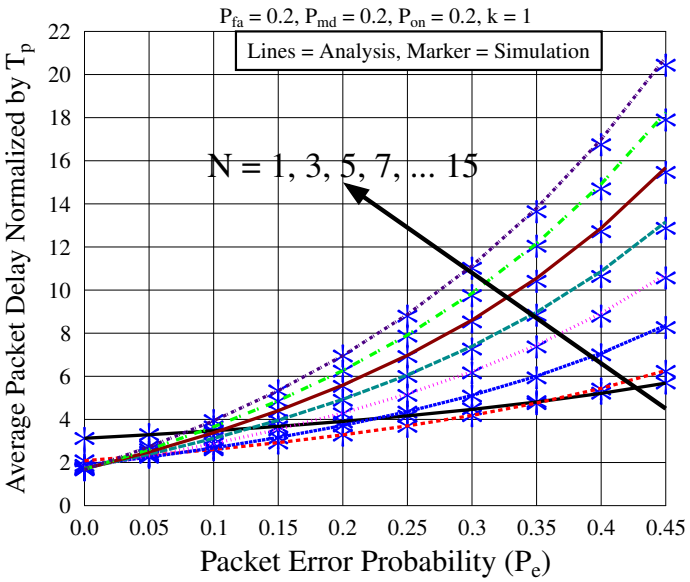

Figure 5.9: Investigating the optimal average packet delay of the CGBN-HARQ system based on the number of packets (N) per TS versus P_e in a realistic imperfect sensing environment, when $P_{on} = 0.2$ and $T_s = T_p$.

which increases the erroneous reception and retransmission probability. Additionally, as shown in Fig. 5.8 and also in Fig. 5.9, the results evaluated from the analytical approach agree with the simulation results.

In Fig. 5.9, the average packet delay versus P_e relationship is characterized in terms of the number of packets transmitted in a single TS, given P_e, P_{fa}, P_{md} and P_{on}. As shown in the figure, at $P_e = 0$, a higher value of N gives a lower delay. However, when P_e is sufficiently large, a higher value of N results in a higher delay. For a given value of N, the average packet delay increases, as the channel becomes less reliable, i.e. when P_e increases. Again, as shown in Fig. 5.9, the simulation results validate our analytical results.

In Fig. 5.10, the probability mass function (PMF) of the *end-to-end packet delay* is characterized in the context of $N = 4, 7$ and 9, when unreliable sensing is considered. In our simulations, the end-to-end delay of a packet is evaluated in terms of the time duration spanning from its first transmission to the instant, when it is successfully received. Specifically, let the vector $\boldsymbol{d}$ of length N_s store the end-to-end delay in terms of T_p of the N_s packets, where N_s is a large number and $\boldsymbol{d}(j)$ represents the end-to-end delay of the jth packet. Then, the PMF of the end-to-end packet delay presented in Fig. 5.10 is evaluated as

$$\boldsymbol{P}_d(i) = \frac{\sum_{j=1}^{N_s} \delta\left(d(j) - i\right)}{N_s}, \quad 1 \leq i \leq \max(\boldsymbol{d}), \tag{5.34}$$

where $\max(\boldsymbol{d})$ denotes the maximum delay of the N_s packets. Note that, in Fig. 5.10, the PMF associated with a delay beyond $120T_p's$ is not shown, since the values are all close to zero.

From Fig. 5.10 we observe that for the given parameter values and $N = 4$, 47.7% of the packets are successfully received after their first transmission. For the packets that are successfully

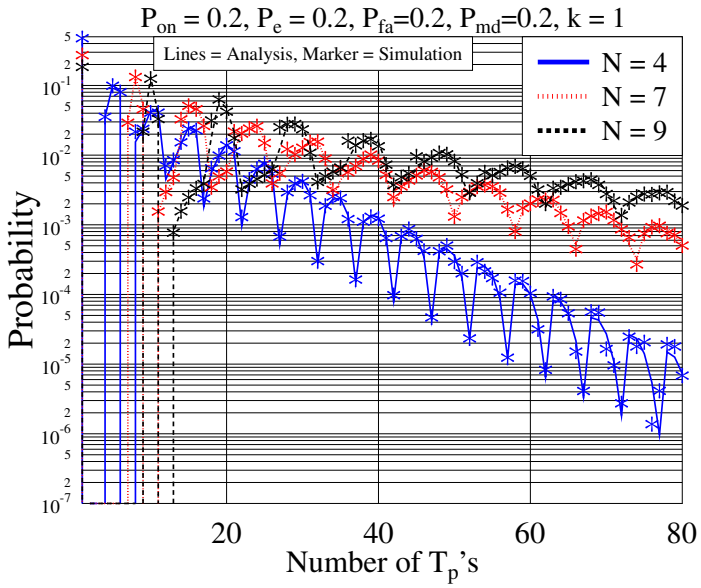

Figure 5.10: Probability of end-to-end packet delay in the CGBN-HARQ systems in the case of imperfect sensing, when $P_{on} = 0.2$, $P_F = 0.2$, and $N = 4, 7$ and 9. The theoretical results were calculated from (5.30) and the simulation results were obtained from (5.34)

received after their second transmissions, there are two cases. In the first case, if the TS following the first transmission is free, on average 3.5%, 10% and 8.3% of the packets are successfully received with the delays of $4T_p, 5T_p$ and $6T_p$, respectively. In the second case, if the TS during the first transmission is busy, then approximately 1.5%, 2.3%, 4.3% and 4.2% of the packets are successfully received with the delay of $8T_p, 9T_p, 10T_p$ and $11T_p$, respectively. Similarly, we can find the probabilities for the cases, when $N = 7$ and 9 are considered.

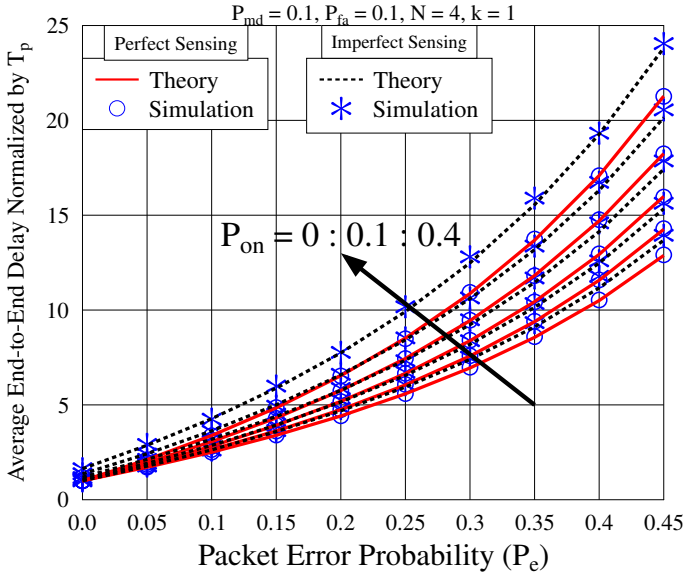

Figure 5.11: Average end-to-end packet delay versus packet error probability with respect to different channel busy probabilities P_{on}, when both perfect and imperfect sensing are considered. The theoretical results were calculated from (5.31) and the simulation results were obtained from (5.35)

Having characterized the PMF of the end-to-end packet delay, we now turn our attention to the average-end-to-end packet delay of the CGBN-HARQ scheme. Here, the average end-to-end packet delay is evaluated by the formula,

$$\tau = \sum_{i=1}^{max(\boldsymbol{d})} \boldsymbol{P}_d(i) \times i(T_p). \tag{5.35}$$

Fig. 5.11 depicts the average end-to-end packet delay for $N = 4$ versus P_e with respect to different values of P_{on}, when both perfect and imperfect sensing are considered. Similar to the trends observed for the average packet delay, the average end-to-end packet delay increases with P_e and/or P_{on}. However, when comparing Fig. 5.8 and 5.11, there are two striking differences associated with the minimum delays and the increasing rates of the delays. Specifically, in terms of the minimum delays, observe in Fig. 5.11, at $P_e = 0$ that the minimum end-to-end packet delay is one T_p in the case of perfect sensing, regardless of the channel busy probability of P_{on}. In the case of imperfect sensing, the minimum delay increases to an average of 1.6 T_p, when $P_{on} = 0.4$. By contrast, in the context of the average packet delay, observe in Fig. 5.8 that the minimum delay is higher than one T_p, and increases as P_{on} increases, regardless of using perfect or imperfect sensing. The reason for this observation is that the end-to-end packet delay is individually calculated for each of packets, from the start of their transmission until their successful reception. By contrast, the average packet delay includes the busy time before a packet's transmission. As for the increased rate of the delay, when comparing Fig. 5.11 to Fig. 5.8, we find that the average end-to-end packet delay increases much faster than the average packet delay, when P_e or/and P_{on} increases. This is because, in the CGBN-HARQ scheme, every transmitted packet is dependent on the $(N-1)$ packets transmitted in the front of it. If any of these packets is received in error, the packet considered has to be retransmitted, regardless whether it is correctly received, thereby resulting in a longer end-to-end packet delay.

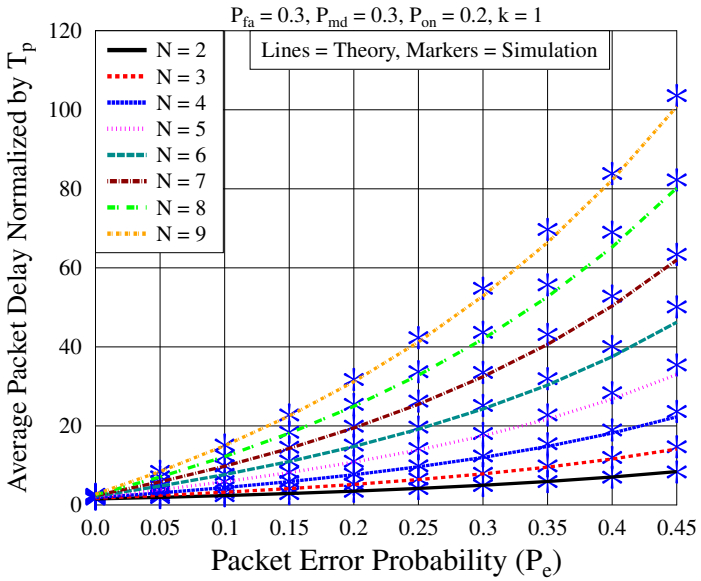

Figure 5.12: The optimal average end-to-end packet delay of the CGBN-HARQ system based on the number of packets (N) versus P_e in the scenario of imperfect sensing.

In Fig. 5.12, we show the effect of increasing N on the average end-to-end packet delay. Explicitly, for a given value of P_e, the average end-to-end packet delay increases, as the value of N increases. Furthermore, at a given P_e, the increasing rate of the average end-to-end delay increases, as the value of N becomes higher.

5.5.1 Comparison with the model proposed in [1]

When comparing the model proposed in this chapter to that in our previous work [1], it is shown in Figs. 5.13 and 5.14, that the proposed system achieves abetter throughput and a lower average packet delay. The improvement is mainly due to two factors:

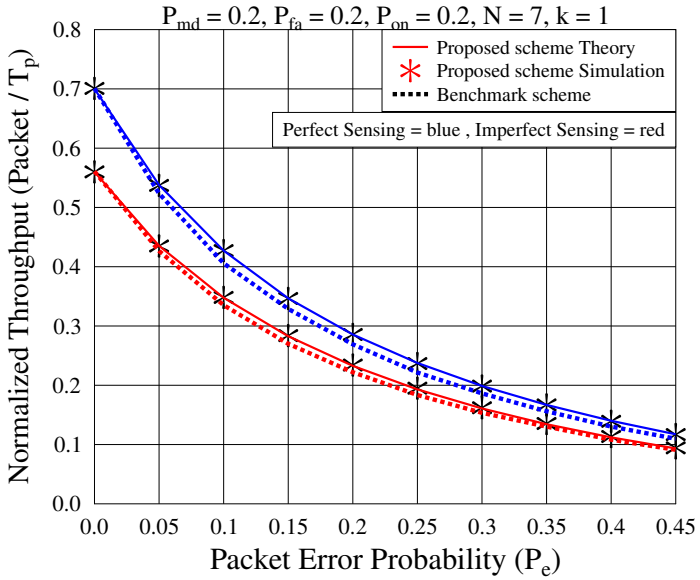

Figure 5.13: Throughput comparison of CGBN-HARQ scheme proposed in this chapter with the benchmark scheme proposed in [1], for different packet error probabilities in perfect and imperfect sensing. In this chapter, the theoretical and simulation results are calculated from (5.23) and (5.32), whereas, in [1], the simulation results were calculated from (10).

1. When the transmitter receives feedback in a sensing period, it adjusts the buffer based on the feedback and transmit either a new or an old packet, when a feedback is received after the sensing duration. This way, k packets avoid being discarded, when a NACK is received during or after the sensing period.

2. The proposed system also allows the retransmission of the discarded packets in the same free TS based on the packet's position in the transmitter buffer, which is only possible, when the transmitter receives feedback during sensing period. As a result, the delay of the discarded packets, which are retransmitted in the same TS reduces from $(N+k)T_p$'s to $(N-k)T_p$'s, if the following TS is free.

By contrast, in [1], when ever an ACK is received in the free TS, a new packet is transmitted which is retransmitted if a NACK is received after it. All discarded packets are retransmitted after the

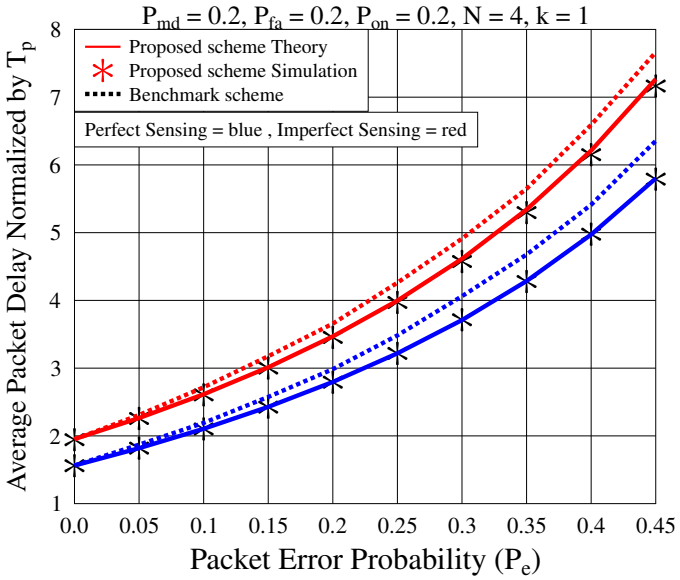

Figure 5.14: Average packet delay comparison of CGBN-HARQ scheme proposed in this chapter with the benchmark scheme proposed in [1], for different packet error probabilities in both perfect and imperfect sensing. In this chapter, the theoretical and simulation results are calculated from (5.25) and (5.33), whereas, in [1], the simulation results were calculated from (11).

RTT of $((N+k)T_p)$, provided that the next TS is free.

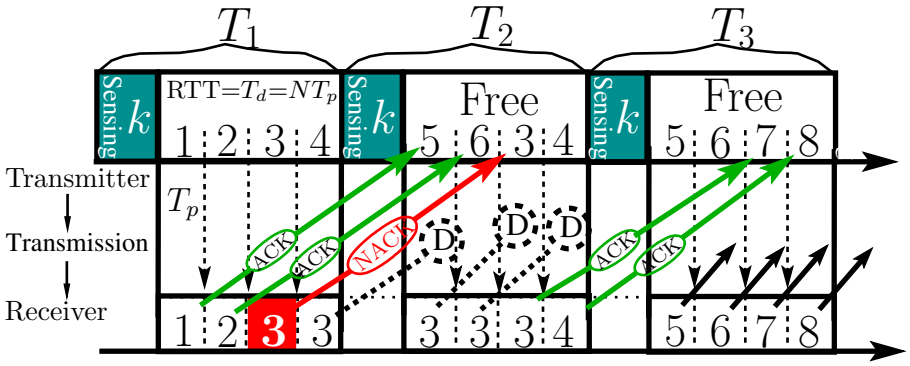

Figure 5.15: Transmission flow of CGBN-HARQ scheme, when $N = 4T_p$ and $k = T_p$, proposed in [1].

For example, as shown in Figs. 5.2 and 5.4, the feedback flag of packet 1 is received during the sensing interval, whereas that of packets 2 and 3 is received after the sensing interval. As a result, the transmitter transmits the new packet 5 only when the sensed TS is found to be free and an ACK is received during the transmission period, as shown in TS T_2 of Fig. 5.4. However, packet 5 is retransmitted after the reception of NACK for packet 3. When considering the same example in the context of [1] as shown in Fig. 5.15, the ACKs for packet 1 and 2 are received, therefore the new packets 5 and 6 are transmitted, which have to retransmitted after the NACK reception for packet 3. Hence, the CGBN-HARQ scheme proposed in this chapter reduces the number of retransmissions which in turn improves both the throughput and the average packet delay.

5.6 Chapter Conclusions

In this chapter, we have proposed and investigated a CGBN-HARQ transmission scheme conceived for CR systems, when both reliable and unreliable sensing are considered. Both the throughput and delay of the CGBN-HARQ has been investigated both by analysis and simulation. The CGBN-HARQ system was modelled using the DTMC-based approach, based on which closed-form expressions have been derived both for the throughput and for the delay. Both the average packet delay and the average end-to-end packet delay have been studied. Finally, our analytical results have been validated by our simulations results. Our results demonstrate that the channel exploitation of the PUs as well as the reliability of both the CR transmission and the spectrum sensing have a substantial impact on the throughput and delay of the CGBN-HARQ. When the wireless links becomes less reliable or when the PU has a high probability of occupying the channel, the CR system's throughput drops significantly, which ultimately results in an increased transmission delay. Furthermore, our results suggest that when the propagation environment is time-variant, the number of packets transmitted within a time-slot should be appropriately adapted, in order to attain the highest possible throughput and the shortest average transmission delay.

Chapter 6

Performance of Cognitive Selective-Repeat Hybrid Automatic Repeat Request[1]

The Cognitive Stop-and-Wait HARQ (CSW-HARQ) transmission scheme was proposed in Chapter 3, where the performance results revealed that despite its low-complexity implementation, both the throughput and the delay of the CSW-HARQ scheme is poorer even in reliable channels. Therefore, in Chapter 4 and 5, we proposed Cognitive Go-Back-N HARQ (CGBN-HARQ) scheme, which was investigated in perfect and in realistic imperfect sensing environments, respectively. This arrangement significantly enhanced the performance in terms of both a higher throughput and a lower delay than the CSW-HARQ scheme. However, the complexity increases with the buffer of size N, which enabled the CR transmitter to seamlessly, transmit N packets one after another to the CR receiver, without waiting for their feedback flags, as presented in Section 4.3.1. After the reception of each packet, the CR receiver performs error correction/decoding and then generates its feedback to be sent back to the transmitter. If an ACK flag is received, the transmitter transmits a new packet, provided that the next TS is found to be free. Otherwise, if a NACK flag is received, the transmitter retransmits both the erroneous packet as well as all the subsequent packets (transmitted after the erroneous packet), regardless whether they are error-free or not. The unnecessary retransmission of the subsequent packets imposes further delay, since the packets have to wait for the correct reception of the previous packets. Additionally, the number of retransmissions increases, when the channel is unreliable, hence further degrading the performance. Therefore, to avoid unnecessary transmissions, in this chapter, a buffer of size N is provided at the receiver, which results in a more complex CR receiver. This is the price paid for substantially improving both the throughput and the delay, as transpires from Fig. 6.1.

[1] A part of this chapter has been accepted in IEEE Access, November 2016 [260]

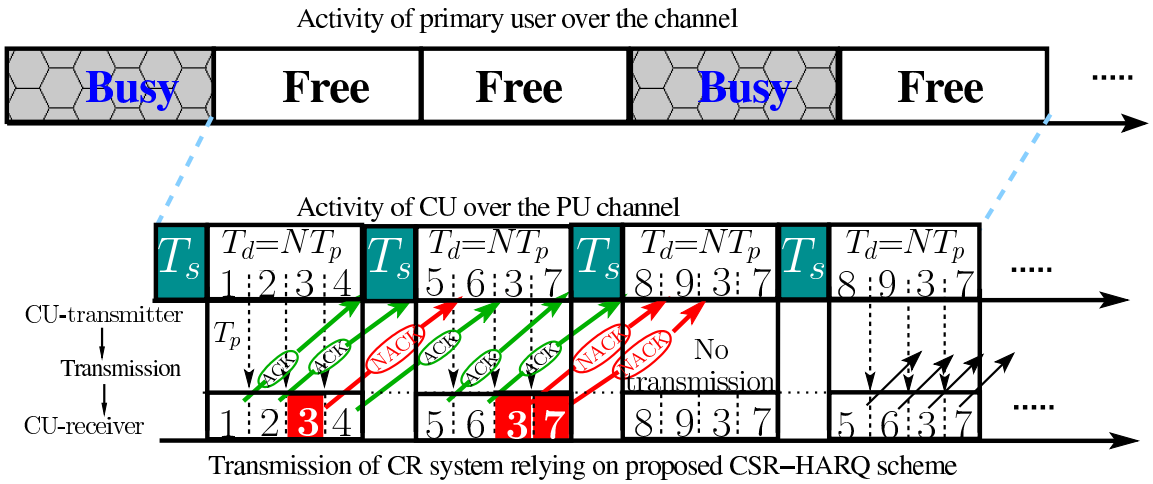

Figure 6.1: Transmission flow of the proposed CSR-HARQ in the presence of both free and busy TSs. Each TS has the duration of $T = T_s + T_d$ seconds and in each free TS, $N = 4$ packets are transmitted where T_p is the duration required for the transmission of a packet.

6.1 Introduction

Naturally, CR systems suffer from the ubiquitous interference, noise, fading and other impairments [64, 183, 184]. Therefore, to achieve both a high integrity and a high throughput, robust error correction techniques have been proposed for both the physical and data link layer [18, 19].

For example, powerful anti-jamming coding was conceived by Yue *et al.* in [185, 186] for CR systems. Liu *et al.* [187] proposed a network-coding technique for classic ARQ protocols. Zhong and Hanzo [134] introduced HARQ-based superposition coding for improving both the cell-edge coverage and the energy efficiency. The end-to-end delay is minimized by reducing the number of retransmissions using HARQ [175]. Furthermore, Makki *et al.* [188] used HARQ protocols and investigated both the throughput and outage probability, while in [189] Makki *et al.* invoked block coding for improving the throughput. Ngo and Hanzo [129] studied the state-of-the-art of HARQ scheme in cooperative wireless scenarios. As a further development, Liang *et al.* [190] conceived an adaptive dynamic network coding technique for cooperative communication between the PUs and CUs, whilst relying on powerful turbo trellis coded modulation (TTCM).

In this context, we propose the Cognitive Selective-Repeat HARQ (CSR-HARQ) scheme for a spectrum overlay environment [9–11, 88], which relies on the CU's ability to sense the activity of PUs over the channel and to access it for its own transmission, when the channel is deemed to be free at the time of the CU's request to transmit, as shown in Fig. 6.1. Similar to Chapter 3 and 4, the activity of PU is modelled using a two-state Discrete Time Markov chain (DTMC), having 'ON' and 'OFF' states [83, 261]. The CU is only allowed to communicate, when the PU is in the 'OFF' state, which implies that the PU is silent. Otherwise, the CU continues sensing the channel until it is found to be in the 'OFF' state. Furthermore, the temporal partitioning of the channel into T seconds long TS is relied upon, where the PUs employ time division multiplexing. Furthermore,

for the CR system, each free TS is further partitioned into sensing epochs of T_s seconds followed by a transmission epoch of T_d seconds as shown in Fig. 6.1 [234, 261]. Specifically, the sensing duration is T_s, while the remaining $T_d = T - T_s$ duration is invoked for data transmission during the 'OFF' state. Spectrum sensing has been widely studied. In [16] Akyildiz *et al.* provided a survey related to spectrum management and CR architectures. Yucek and Arslan [80] proposed a multi-dimensional sensing technique for detecting the PU's transmission. The state-of-the-art of spectrum sensing and recent advances were reviewed by Axell *et al.* [262]. Moreover, an optimal sensing and TS duration have been determined by Liang *et al.* in [61] and Tang *et al.* [82] for the sake of maximizing throughput of the CUs. As further development, Stotas and Nallanathan [234] provided the trade-off between the sensing duration and throughput, which has been optimized by proposing a hybrid spectrum sensing and data transmission technique. Liang *et al.* [196] proposed a cooperative CR system in which the PUs trade with CUs and allocate the free TSs on the basis of reducing the transmission power and maximizing the transmission rate.

Given the stochastic nature of the PUs ON/OFF pattern, its theoretical analysis in an ARQ-aided CR environment is a challenge. Hence, there is a paucity of contributions on this subject [64, 183, 184, 194, 195, 198, 263], because, these have left the theoretical throughput and delay analysis of the ARQ protocols open. Specifically, Ao and Chen [194] as well as Touati *et al.* [195] analysed the performance of their relay-aided ARQ protocol in CR environments. By contrast, the throughput of a SR-ARQ protocol aided CR-based multi-hop relaying system was studied by Jeon and Cho [198]. Park *et al.* [263] quantified the throughput gain attained in the absence of inference imposed on the PUs transmission. Then Roshid *et al.* [212] reviewed various cooperative sensing and transmission techniques between the CUs and PUs for the sake of improving the throughput, while avoiding collisions between the PUs and CUs. Finally, [64,183,184] offered a detailed survey of the sophisticated CR systems.

Our proposed CSR-HARQ transmission scheme intrinsically incorporates the SR-HARQ protocol into the CR system. We advocate the SR-HARQ scheme over other ARQ schemes, as benefit of its improved throughput and delay. This is achieved at the cost of resequencing buffer for queuing the out-of-order error-free packets. Explicitly, it is depicted in Fig. 6.1 that the channel is initially sensed by the CR transmitter and provided that it is deemed to be free from PUs, then the CU transmits its packets relying on SR-HARQ protocol. The CR receiver receives packets in a chronological order and transmits an acknowledgement to the CR transmitter after each packet. A new packet is transmitted by the CR transmitter after receiving a positive feedback (ACK). By contrast, for a negative feedback (NACK), the related packet is retransmitted, provided that the channel is deemed to be free.

The performance of the classical Selective-Repeat-HARQ (SR-HARQ) protocol has been lavishly published in [264–267]. In particular, Kim and Krunz [264] as well as Ausavapattanakun and Nosratinia [265] investigated the throughput as well as the delay of the SR-HARQ technique using a Markov chain. Moreover, Badia *et al.* [266] analysed the delay as well as throughput of the SR

technique using the moment-generating function and quantified the detrimental effects of practical imperfect feedbacks modelled by a hidden Markov model. The total delay of transmission, queuing and resequencing was also quantified for the classical SR-ARQ regime by Badia [267]. Chen *et al.* [150] discussed the challenges of amalgamating HARQ with turbo codes for reducing the complexity. As a further advance, a distributed multiple component turbo code (MCTC) was also designed [178] for cooperative HARQ, for the sake of reducing the decoding complexity compared to the classic twin-component turbo parallel code. Moreover, in [268], the so-called absorbing Markov chain theory was conceived by Chiti *et al.* for modelling the SR-ARQ for investigating its resequencing delay. By contrast, the probability distribution of the packet delay was analysed by Dong *et al.* [257, 258].

6.1.1 Contributions and Chapter Structure

Against the above background, the contributions of this chapter may be summarised as follows:

1. We propose a novel CR protocol, namely CSR-HARQ, for attaining reliable communication. The proposed scheme is based on the classic SR-HARQ scheme. The CR transmitter in our protocol senses the channel before using it and it can always receive feedback, regardless of its specific activity (waiting, sensing or transmitting). However, fulfilling this requirement demanded a significant reformulation of the SR-HARQ transmission principles.

2. Firstly, a probability-based technique has been used to model and to theoretically analyse the proposed scheme. We derived closed-form expressions for the CR system's average packet delay, throughput as well as end-to-end packet delay. Expressions for the probability distribution of the end-to-end packet delay as well as for the average end-to-end packet delay have also been derived.

3. Secondly, the proposed scheme has been also modelled and to theoretically analysed by using a DTMC approach. Relying on this approach we derived closed-form expressions for generating DTMC state index, the total number of states, the throughput of the CR system, the average packet delay as well as the end-to-end packet delay. Expressions for the probability distribution of the end-to-end packet delay as well as for the average end-to-end packet delay have also been derived.

4. Ultimately, we provide a simulation-based validation of both the theoretical probability-based methodology and of the Markov chain based methodology.

Figure 6.2: The structure of this chapter.

6.2 Chapter 6 System Model

6.2.1 Modelling the Primary User

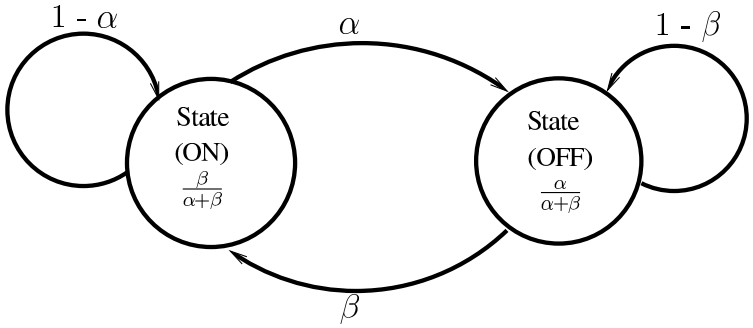

Figure 6.3: Discrete-time two-state Markov chain modelling the 'ON' 'OFF' process of PU system

Similar to Subsection 3.2.1, let us assume that the wireless channel is exclusively allocated to the PUs, using the classic TDMA technique, where each TS has a duration of T seconds. Each TS has the same probability of activation, which is also independent from the other TSs. The utilization of the channel by the PUs may be modelled using the DTMC presented in Fig. 6.3, which has the 'ON' and 'OFF' states. We assume that the probability of the channel making a transition from 'ON' to 'OFF' is α, while the probability of the reverse transition is β. Moreover, we assume that the channel obeys the probabilities P_{on} and P_{off} of being in the 'ON' and 'OFF' states, respectively,

where we have $P_{off} = 1 - P_{on}$. By definition, the Markov chain is said to be steady, when we have [21],

$$P_{on}\alpha = P_{off}\beta, \tag{6.1}$$

yielding:

$$P_{on} = \frac{\beta}{\alpha + \beta}, \quad P_{off} = \frac{\alpha}{\alpha + \beta}. \tag{6.2}$$

The employment of TDMA ensures that PU's transmission duration is always quantized to an integer multiple of the TS duration T, as shown in Fig. 6.4(a). For example, the duration of the PU transmission may be equal $2T$ or $3T$ seconds but never to $2.5T$ seconds. Additionally, time synchronization of the TDMA system ensures that the start and end of the PU transmission corresponds to the start and end of the TSs, respectively. It becomes clear from the above discussion that, in the PU's 'OFF' state, the CU may acquire the channel for its own transmission without interfering with the transmissions of the PUs. Having modelled the activity pattern of the PUs, we now model that of the CU in the next section.

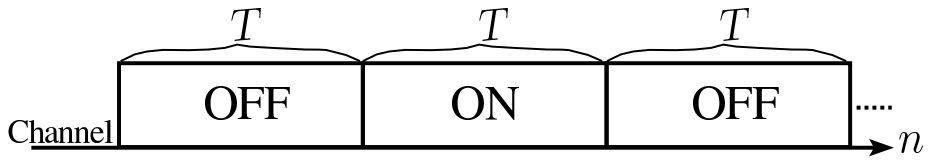

(a) Pattern of channel usage by PR

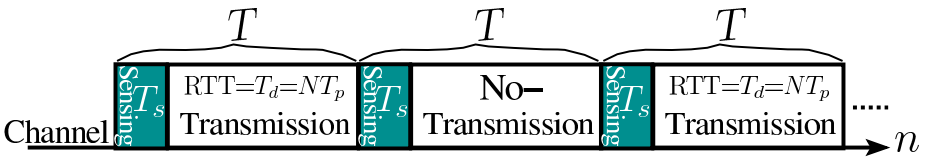

(b) Pattern of channel usage by CR

Figure 6.4: Time-slot structure of PU and CU systems, where a CU TS consists of a sensing duration of T_s and a transmission duration of $T_d = T - T_s$, when given the total duration T of a time-slot.

6.2.2 Modelling the Cognitive User

As discussed in the previous section, we assumed that the CU may acquire the channel for its own transmission by following the spectrum overlay technique [9–11], which constrains it to use the channel only when it is free from PU's transmissions. Just like the PU, the CU too acquires the channel for a duration, which equals an integer multiple of the TSs. However, unlike the PU, the CU does not utilize the entire TS duration for data transmission. Instead, it divides each TS into two phases, namely, the sensing phase of duration T_s seconds and the transmission phase of duration $T_d = T - T_s$ seconds as shown in Fig. 6.4(b). We assume that CU transmits N packets in the transmission duration of T_d. Thus, if T_p seconds are needed for the transmission of a single packet, we can state that $T_d = NT_p$. For ease of analysis, we assume that the sensing duration too equals an integer multiple of T_p, i.e. $T_s = kT_p$ seconds. An underlying assumption of our

analysis is that the CU is capable of ideally sensing the activity of the PUs without miss-detection or false-alarm. Here, miss-detection refers to the CU falsely concluding that the channel is free, while false-alarm refers to the CU falsely detecting the channel to be busy. In the next section, we discuss the proposed CSR-HARQ scheme employed by the CU for transmitting its data during the free TSs.

6.3 Principles of Cognitive Selective Repeat Hybrid Automatic Repeat Request

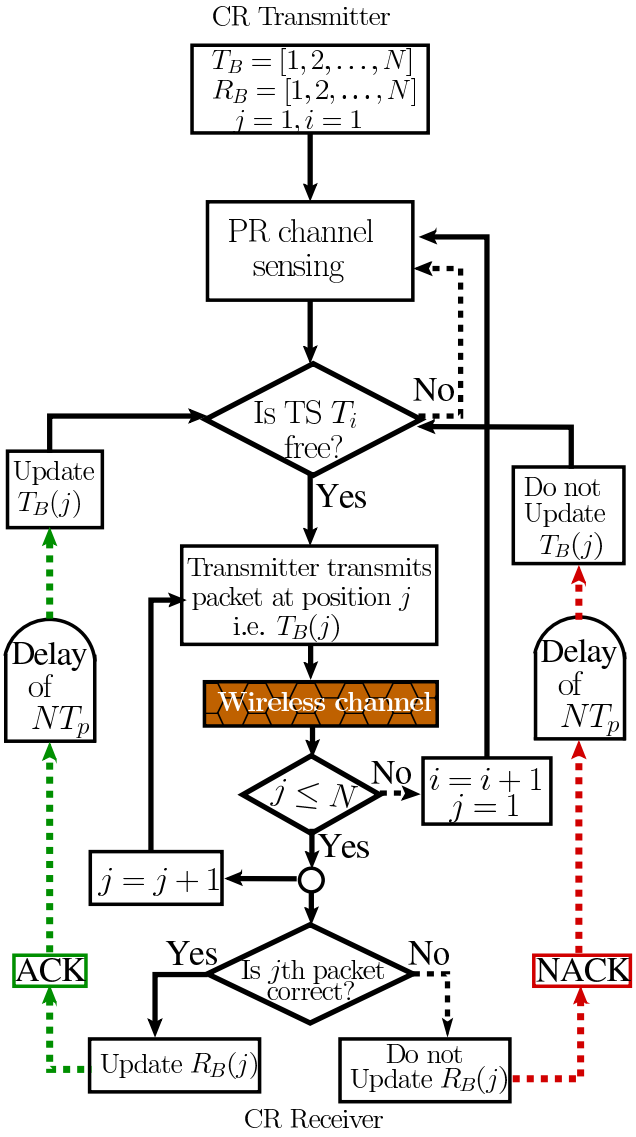

Figure 6.5: Flow chart showing the operations of the proposed CSR-HARQ scheme, where T_B and R_B represent the transmitter and receiver buffer, respectively. The transmitter receives the feedback of each packet after NT_p seconds of its transmission.

The proposed CSR-HARQ scheme relies on Reed-Solomon (RS) decoder at the receiver for detecting as well as correcting the errors imposed by the channel, which is denoted as RS(N_d, K_d) [18], where K_d and N_d denote the number of original information and coded symbols, respectively. We

assume that each N_d − symbol packet is protected by a single RS codeword. The error detection capability of the RS code is assumed to be ideal, while it is capable of correcting upto $t = \frac{N_d - K_d}{2}$ erroneous symbols. The packet is said to be erroneous when the channel inflicts more than t errors.

The round-trip-time (RTT) of a packet is equal to T_d seconds, which is the time between its transmission and the reception of its feedback flag. Hence, during the RTT, the CU can also transmit upto $(N-1)$ subsequent packets before receiving its feedback.

Given these assumptions, the operation of our CSR-HARQ scheme is shown in Fig. 6.5. Specifically, when a free TS is found, the CR transmitter sends a sequence of N packets to the receiver, where a feedback signal is generated for each of the packets for notifying the transmitter whether the packet is received error-free or in error. The operation of CSR-HARQ is formally stated in Algorithm 3 as detailed in sections 6.3.1 and 6.3.2.

Algorithm 3 : CSR-HARQ

Initialization: M_c = number of packets, $T_d = N$, $T_s = k$, $i = 1$, TS= 1, $T_B = [1, 2, \ldots, N]$, $R_B = [1, 2, \ldots, N]$.
Input: N, k, packets.
while $i \leq M_c$ **do**
  CR transmitter senses a TS.
  if TS is free **then**
    Transmitter transmits N packets from the buffer T_B.
    $j = 1,\ a = 0,\ b = 0$, TS=TS+1.
    while $j \leq N$ **do** ▷ Check each received packet.
      if Packet at position $R_B(j)$ is correctly received **then**
        Transmit ACK signal for the respective packet and update receiver's buffer R_B.
        $R_B(j) = R_B(j) + N - a$.
      else
        Receiver transmits NACK for the packet at position $R_B(j)$ and $R_B(j)$ remains unchanged.
        $a = a + 1$.
      end if
      if ACK is received for a packet at position $T_B(j)$ **then**
        Transmitter updates buffer at position $T_B(j)$.
        $T_B(j) = T_B(j) + N - b$.
      else NACK is received for a packet at position $T_B(j)$, then
        Transmitter's buffer $T_B(j)$ is not updated.
        $b = b + 1$.
      end if
      if TS is free & feedback is received during T_d period **then**
        A new or old packet at position $T_B(j)$ is transmitted.
      else TS is busy $\|$ feedback is received during T_s period
        No transmission and wait.
      end if
      $j = j + 1$.
    end while
    $i = \max(R_B)$ ▷ how many packets are correctly received
  else
    transmitter waits for the next TS.
    TS=TS+1.
  end if
end while

6.3.1 Operation of the CR Transmitter

In the classic SR-HARQ scheme, the transmitter only has to retransmit those specific packets for which we receive NACK signals. Hence, upon receiving a positive ACK flag for a previous packet, a new packet is transmitted. By contrast, observe our proposed CSR-HARQ scheme both in Fig. 6.5 and in Algorithm 3 that the CR transmitter first senses the channel for T_s seconds and then transmits

or retransmits its packets during the ensuing T_d seconds, if the PU's channel is deemed to be free, as presented on line 6 and 24 of Algorithm 3. However, if the PU's channel is found to be busy in a TS, then the CU has to wait until the next TS, as illustrated on line 32 and 26 of Algorithm 3. In the proposed CSR-HARQ scheme, we have assumed that the CU always has packets in its buffer to transmit, that all packets are of the same length, and each of the packet is transmitted in T_p seconds. As mentioned in Section 6.3, the ACK/NACK feedback of each transmitted packet is assumed to be received after the RTT of T_d seconds without error. Furthermore, as in the classical SR-ARQ, we assume that the CR transmitter has a buffer of size N [18, 21], where packets are entered and transmitted in a first-in-first-out (FIFO) fashion, with their copies being kept in the transmitter's buffer until they are positively acknowledged. If this is the case, then the buffer is updated, as shown on line 18 of Algorithm 3. Moreover, we also assumed that the CR transmitter may receive feedback both during free and busy TSs. This assumption may be justified, since the feedback flag is a single-bit message [242, 243]. Hence, the CR transmitter does not have to wait for a free TS to receive feedback concerning the packets transmitted in the previous free TS.

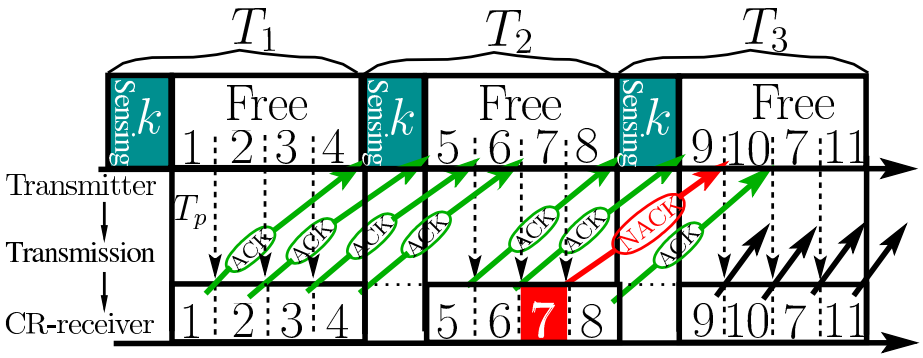

Figure 6.6: Transmission flow of error-free and erroneous packets based on the principle of CSR-HARQ scheme for $N = 4T_p$ and $T_s = k = 1T_p$.

For instance, consider the ideal scenario of Fig. 6.6, where the CU transmits N packets from the transmitter's buffer within the free TS T_1. In Fig. 6.6, all packets transmitted in TS T_1 are correctly received and, correspondingly, positive ACKs are sent back by the CR receiver. Upon receiving an ACK, the transmitter removes the corresponding copy of the packet from the buffer and fills the vacant space with a new packet. This process repeats, provided that the following TS is sensed free and that the transmitted packets are positively acknowledged. However, if a NACK is received for a packet, say at the jth position, as shown in Fig. 6.6, then the transmitter's buffer is not updated and the corresponding packet is retransmitted without influencing the other packets.

In the case that there are busy TSs, as shown in Fig. 6.7, where a free TS is followed by a busy TS, the CSR-HARQ acts as follows. During the free TS T_1, the transmitter transmits $N = 4$ packets. It can be seen that packets $1, 2$ and 4 are successfully delivered, while packet 3 is in error. Consequently, the transmitter's buffers $T_B(j)$ are updated at positions $j = 1, 2$ and 4 by new packets, while $T_B(3)$ remains unchanged. Furthermore, as shown in Fig. 6.7, T_2 and T_3 are busy, hence the CU is not allowed to transmit. Therefore, it waits until the next TS of T_4. In the TS T_4, the four packets having indices $5, 6, 3$ and 7 are transmitted.

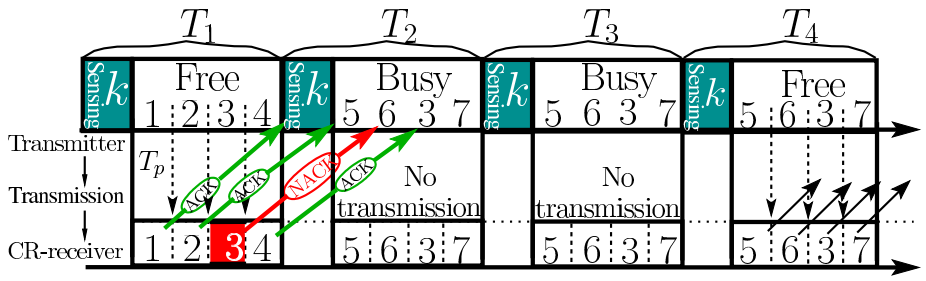

Figure 6.7: Transmission flow of error-free and erroneous packets in the presence of busy TS for $N = 4T_p$ and $T_s = k = 1T_p$.

6.3.2 The Operation of the CR Receiver

Similar to the classic SR-HARQ scheme [18, 21, 22], the CSR-HARQ receiver has a buffer of size N for storing the indices of the packets that the receiver is expecting to receive. Upon receiving a packet, the CR receiver checks whether the index of this packet matches the index in the receiver's buffer. If so, then the CR receiver invokes the RS decoding and generates the corresponding ACK or NACK depending on whether the received packet is error-free or in error. Furthermore, the CU's receiver buffer is updated, if the packet is error-free. In Algorithm 3, these operations are presented on lines 9 to 15. Additionally, the operations of the CR receiver may be interpreted using the examples depicted in Figs. 6.6 and 6.7, where we can see that the CR receiver only accepts those packets having the same index as those expected by the CR receiver. Note that although the receiver may receive the packets, out of ordered it delivers the packets to the higher ISO layers in the correct order [18, 21, 242, 243].

6.4 Probability-based Analysis

We employ three metrics for studying the performance of the proposed CSR-HARQ scheme, namely the average packet delay, throughput and end-to-end packet delay. Again, we discuss the probability-based methodology and the (DTMC-based methodology in this section and in Section 6.5, respectively. Before we present our analysis, we first define the above-mentioned performance metrics.

Firstly, the average number of TSs (or T_ps) employed until a packet is successfully transmitted is referred to as the average packet delay T_D. All the free as well as busy TSs commencing from the time the CR system is activated are included in the average packet delay quantified in terms of the number of TSs per packet [230, 231].

Secondly, the time delay between the initial attempt to transmit a packet and the final successful attempt is referred to as the packet's end-to-end packet delay [231]. We derive expressions for both the end-to-end packet delay's probability mass function as well as for the average end-to-end packet delay.

Finally, the CSR-HARQ scheme's throughput is the error-free transmission rate of the CR

transmitter. Specifically, it is the total number of successfully transmitted packets per TS.

We now employ the probability-based methodology to derive the above-mentioned performance metrics.

6.4.1 Average Packet Delay

Encountering the corrupted packets results in retransmissions, which is the source of delay in the classical SR-HARQ scheme. However, in our proposed CSR-HARQ scheme, delay is not only due to unreliable transmissions, but also due to the unavailability of CR channels for transmission. Therefore, to analyze the packet delay of our proposed CSR-HARQ scheme, we denote the delay imposed by busy PR channels as T_{DP}. In other words, after a free TS, there is an average delay of T_{DP} while obtaining the next free TS, where $T_{DP}(i)$ is the delay, when transmissions occur in TS i after encountering $(i-1)$ busy TSs, i.e. we have $T_{DP}(i) = (i-1)T$. Following an approach similar to our previous study in [230, 231], the average delay T_{DP} required for finding a free TS is mathematically expressed as

$$\begin{aligned} T_{DP} =& E\left[T_{DP}(i)\right] = E\left[(i-1)T\right] \\ =& \sum_{i=1}^{\infty}(i-1)TP_{on}^{i-1}(1-P_{on}) \\ =& \frac{P_{on}T}{1-P_{on}}, \end{aligned} \tag{6.3}$$

where P_{on} is the probability that the PU has occupied the channel, which is given in (6.2). When substituting $P_{on} = \beta/(\alpha+\beta)$ of (6.2) in equation (6.3), we get

$$T_{DP} = \frac{\beta T}{\alpha}. \tag{6.4}$$

In the free TSs, additional delays can only be imposed by the unreliable transmissions, where every retransmission imposes a delay of T seconds. Let $T_D(i)$ represent the delay of the scenario in which the CR transmitter activates i transmissions for ensuring the successful delivery of a packet. Here, $T_D(i)$ is the sum of delays in obtaining free TSs plus the delay imposed by the successful in transmission of the packets. On average total of T_{DP} seconds are needed for finding a free TS and T seconds are required for the actual round trip transmission in a free TS. Thus, we can state that

$$T_D(i) = i(T_{DP} + T). \tag{6.5}$$

Similar to the typical CSR-HARQ scheme, N packets are transmitted in every TS that is free. Hence, the average delay T_D of the packets is computed using

$$T_D = \frac{1}{N}E\left[T_D(i)\right] = \frac{1}{N}E\left[i(T_{DP}+T)\right]. \tag{6.6}$$

If P_e denotes the packet error probability (PEP) after RS decoding, then we have

$$\begin{aligned} T_D =& \frac{1}{N}\sum_{i=1}^{\infty} i(T_{DP}+T)P_e^{i-1}(1-P_e) \\ =& \frac{T}{N}\left(1+\frac{\beta}{\alpha}\right)\sum_{i=1}^{\infty} iP_e^{i-1}(1-P_e) \\ =& \frac{T}{N}\left(1+\frac{\beta}{\alpha}\right)\frac{1}{1-P_e} \text{ [seconds]} \\ =& \left(\frac{k+N}{N}\right)T_p\left(1+\frac{\beta}{\alpha}\right)\frac{1}{1-P_e} \text{ [seconds]}. \end{aligned} \tag{6.7}$$

After normalization of the average packet delay T_D using the packet duration T_p, T_D is given by

$$T_D = \left(\frac{k+N}{N}\right)\left(1+\frac{\beta}{\alpha}\right)\frac{1}{1-P_e} \quad [T_p\text{'s}]. \tag{6.8}$$

Explicitly, Eq. (6.7) quantifies the average packet delay increases, due to increasing β/α, P_e and/or k.

6.4.2 End-to-End Packet Delay

The time delay between the initial attempt to transmit a packet and the final successful attempt is referred to as the packet's end-to-end packet delay [231]. In this section, we derive expressions for both the end-to-end packet delay's probability mass function (PMF) as well as for the average end-to-end packet delay.

6.4.2.1 Probability Mass Function

The end-to-end delay of a packet depends on two factors: 1) the delay imposed by retransmissions, and 2) the delay incurred because of busy TSs. Let us represent the number of retransmissions of a packet by G, while the total number of busy TSs between the first transmission and the final successful reception of the packet by B. According to the principles of SR-HARQ, a retransmission does not result in the subsequently transmitted packets being discarded by the receiver, which is in contrast to the CGBN-HARQ [246]. Hence, in CSR-HARQ every retransmission results in a delay of only one T_p duration. Thus, the total end-to-end delay m suffered by a packet in units of T_p may be expressed as follows,

$$m = (G + (k+N)B + 1) \quad [T_p\text{'s}], \tag{6.9}$$

where the final T_p interval denotes the time taken by the final successful transmission. In order to derive the end-to-end packet delay's PMF, we consider the following two scenarios.

Scenario 1: In this scenario, we assume that successful transmission is achieved in the first attempt, i.e. we have $G = 0$ and $B = 0$, which results in an end-to-end delay of $m = 1T_p$. It can

be readily shown that this event has the probability of

$$P(1) = 1 - P_e. \tag{6.10}$$

Scenario 2: In this scenario, we assume that a successful transmission is achieved after retransmissions associated with $G \geq 1$ and $B \geq 0$ busy TSs. Below we formulate $P(m)$ for this scenario in detail.

1. Firstly, the probability of the event that a packet is successfully transmitted after G retransmissions and B busy TS can be expressed as

$$P(G,B) = \binom{B+G-1}{B} P_{on}^{B} P_{off}^{G} P_e^{G} (1 - P_e). \tag{6.11}$$

   More explicitly, Eq. (6.11) is valid, since for the above-mentioned event the packet considered is transmitted a total of $(G+1)$ times, where the first transmission is always a failed attempt, while the final transmission is always a successful one. The B busy TSs can be any of the TSs spanning from the second to the last but one.

   For example, let us assume having $B = 2$ and $G = 3$. Let us assume furthermore that f, b and s denote an erroneous transmission, a busy TS and a successful transmission, respectively. Then, we have the combinations of $\{(f,f,f,b,b,s),(f,f,b,b,f,s),(f,b,b,f,f,s),(f,b,f,f,b,s),(f,b,f,b,f,s),(f,f,b,f,b,s)\}$. In other words, there are $\binom{B+G-1}{B} = \binom{4}{2} = 6$ possible ways of encountering this scenario. Hence we have:

$$P(3,2) = 6 P_{on}^{2} P_{off}^{3} P_e^{3} (1 - P_e). \tag{6.12}$$

2. Secondly, when we observe Eq. (6.9), the same delay m may be generated by multiple combinations of B and G. In this case, an exhaustive search for all possible combinations of B and G can be invoked. However, given $G \geq 1$, it can be shown that $0 \leq B \leq \lfloor \frac{m-2}{N+k} \rfloor$. Furthermore, for a given value of B, we infer from Eq. (6.9) that $G = m - (k+N)B - 1$. Consequently, the probability of an end-tSo-end delay of m T_ps for $m > 1$ may be formulated as

$$P_{MF}(m) = \sum_{B=0}^{\lfloor \frac{m-2}{N+k} \rfloor} \binom{B+G-1}{B} P_{on}^{B} P_{off}^{(m-(k+N)B-1)} P_e^{(m-(k+N)B-1)} (1 - P_e),\ m = 2,3,\ldots \tag{6.13}$$

6.4.2.2 Average end-to-end packet delay

The average end-to-end packet delay formula can be derived using the PMF of the end-to-end packet delay, which is given in Eqs. (6.10) and (6.13), yielding:

$$\tau = \sum_{m=1}^{M_T} m \times P_{MF}(m), \ \ [T_p\text{'s}] \tag{6.14}$$

where M_T is the maximum delay considered, which can be made sufficiently high to render the un-considered components negligible. As an example, an M_T value that satisfies $\sum_{m=1}^{M_T} P_{MF}(m) = 1 - 10^{-8}$ may be chosen.

6.4.3 Throughput

The throughput of the CR system relying on the CSR-HARQ protocol may be derived using the average delay of (6.7), yielding:

$$R_s = \frac{1}{T_D} \tag{6.15}$$

$$= \frac{N}{T}\left(\frac{\alpha}{\alpha+\beta}\right)(1-P_e) \ \ [\text{PPS}] \tag{6.16}$$

$$= \left(\frac{\alpha}{\alpha+\beta}\right)(1-P_e) \ \ [\text{PPTS}] \tag{6.17}$$

$$= \frac{N}{k+N}\left(\frac{\alpha}{\alpha+\beta}\right)(1-P_e) \ \ [\text{PP}T_p]. \tag{6.18}$$

where PPS, PPTS and PPT_p denote packet per second, packet per TS and packet per T_p, respectively. Furthermore, since we assume that an TS (N_D, K_d) code is employed, if b is the number of bits in each code word, then the throughput in units of bits per second is as follows

$$R_s = \frac{1}{T_D} \times K_d \times b \ \ \text{(bits per seconds)}. \tag{6.19}$$

Having studied the proposed CSR-HARQ scheme's performance using a probability-based methodology, in the forth coming section we will analyze the CSR-HARQ scheme using a Markov-chain-based approach.

6.5 Markov Chain-based Analysis

As in CGBN-HARQ scheme studied in [246], the performance of the CSR-HARQ can also be analysed with the aid of DTMC modelling of the state transitions. The states in the CSR-HARQ can be defined jointly by considering whether the PR channel is 'ON' or 'OFF', and by taking into account whether the packets stored in the transmitter's buffer are new packets or old packets requiring re-transmission. Note that the buffer is observed, when each TS ends. The list of states

can be expressed as

$$\mathbb{S} = \{S_0, S_1, \dots S_i, \dots, S_{S_T}\} \tag{6.20}$$

where $S_T = 2^{N+1} - 1$ denotes the total number of states, while S_i represents the ith state, which is a $(N+1)$-length base-2 digit, expressed as

$$S_i = S_{i0}, S_{i1}, \dots, S_{iN}, \;\; i = 0, 1, \dots S_T. \tag{6.21}$$

In Eq. (6.21), S_{i0} is defined as

$$S_{i0} = \begin{cases} 0, & \text{if the PR channel is free in the considered TS,} \\ 1, & \text{if the PR channel is busy in the considered TS.} \end{cases} \tag{6.22}$$

while $S_{ij},\ j = 1, \dots, N$, is defined as

$$S_{ij} = \begin{cases} 0, & \text{if the } j\text{th packet in state } S_i \text{ is new,} \\ 1, & \text{if the } j\text{th packet in state } S_i \text{ is a retransmitted one.} \end{cases} \tag{6.23}$$

Based on Eqs. (6.22) and (6.23), the index of state S_i can be obtained as

$$i = \sum_{j=0}^{N} S_{ij} 2^{N-j}. \tag{6.24}$$

According to the above definitions, we can see that a state represents a unique combination of new or/and old packets in a free or busy TS. For showing this, below we highlight the principles of modelling with the aid of two examples. Firstly, let us consider a CSR-HARQ transmitter that transmits/retransmits a single packet in a free TS having the sensing duration of one T_p, i.e. $N = 1$ and $k = 1$. In this system, according to our definitions, the states are

$$\mathbb{S} = \{S_0, S_1, S_2, S_3\}, \tag{6.25}$$

where $S_0 = 00$, $S_1 = 01$, $S_2 = 10$ and $S_3 = 11$. Specifically, the first digit in a state denotes the status of the TS, while the second digit denotes the status of the packet in the transmitter buffer, as illustrated in Table 6.1. Given the states as shown in Eq. (6.25), we now proceed to find

Status of the TS	Status of packet	State
0 (free)	0 (new)	S_0
0 (free)	1 (old)	S_1
1 (busy)	0 (new)	S_2
1 (busy	1 (old)	S_3

Table 6.1: Possible number of states for the CSR-HARQ with $N = 1$ and $k = 1$.

state transitions, which are demonstrated in Fig. 6.8. In detail, the transitions can be illustrated in Table 6.2. It is worth mentioning that the transition rate of states is the same as the rate of TSs.

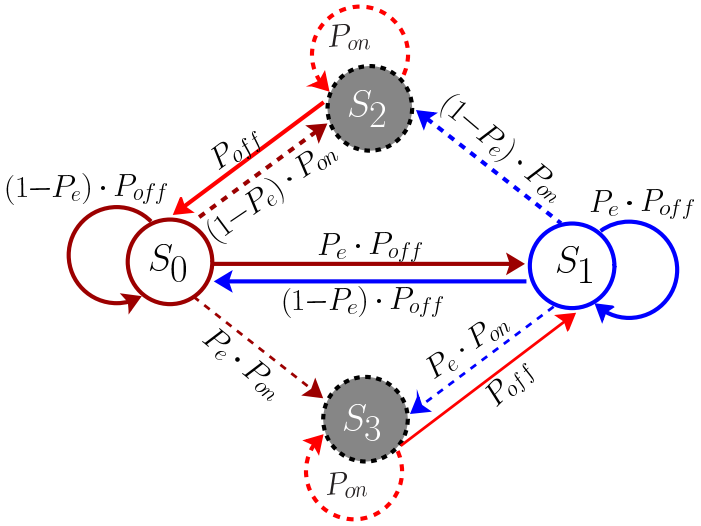

Figure 6.8: The state transition diagram for the DTMC, modelling the proposed CSR-HARQ scheme where $N = 1$ and $k = 1$. The *dashed* lines correspond to the transition towards a busy state, because the next TS is found to be a busy TS; the *solid* lines illustrate transition towards a free state due to the detection of a free TS.

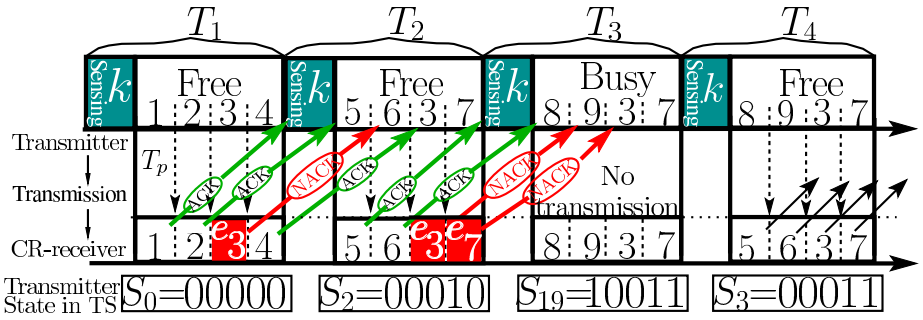

Figure 6.9: Transmission flow of CSR-HARQ in the presence of both free and busy TSs for $N = 4T_p$ and $T_s = k = 1T_p$, where the state of the transmitter is observed at the end of TSs.

Let us now consider the second example of modelling the CSR-HARQ scheme with the aid of the parameters $k = 1$ and $N = 4$, for the observations of 4 TSs, as shown in Fig. 6.9. Observe from Fig. 6.9 that the first TS is found to be free and 4 new packets are transmitted. Hence, the state of the transmitter in this TS is $S_0 = 00000$. However, the packet at position $e = 3$ transmitted in TS T_1 is received in error, while the following TS T_2 is found to be free. Therefore, in TS T_2, the transmitter transmits packets $5, 6, 3$ and 7, which includes the new packets $5, 6, 7$ and the old packet 3, yielding a state $S_2 = 00010$. As a result, the probability of traversing from S_0 to S_2 is $P_{0,2} = P_{off}(1 - P_e)^3 P_e$. As shown in Fig. 6.9, TS T_3 is busy. Furthermore, it is observed that the two packets at positions $e = 3$ and 4, i.e., packets 3 and 7, are received in error. Hence, we have the state $S_{19} = 10011$ for TS T_3 and the probability of traversing from S_2 to S_{19} is $P_{2,19} = P_{on}(1 - P_e)^2 P_e^2$. Note that in the cases when two or more subsequent TSs are found busy, the transmitter's state remains the same in conjunction with the transition probability of P_{on} until a free TS is detected. Once a free TS is detected, the packets stored in the transmitter buffer are transmitted and the transmitter moves to the corresponding free state, as shown in Fig. 6.10. In this

State transition	Conditions for the event	Transition probability
$S_0 \rightarrow S_0$	Two or more error-free transmission in free TSs	$P_{00} = (1-P_e)P_{off}$
$S_0 \rightarrow S_1$	Erroneous transmission and next TS is free	$P_{01} = P_e P_{off}$
$S_0 \rightarrow S_2$	Error-free transmission but next TS is busy	$P_{02} = (1-P_e)P_{on}$
$S_0 \rightarrow S_3$	Erroneous transmission but next TS is busy	$P_{03} = P_e P_{on}$
$S_1 \rightarrow S_1$	Two or more erroneous transmission in free TSs	$P_{11} = P_e P_{off}$
$\vdots$	$\vdots$	$\vdots$
$S_2 \rightarrow S_0$	If CUrrent TS is busy followed by a free TS given that previous transmission was error-free	$P_{20} = P_{off}$
$S_2 \rightarrow S_2$	If two or more busy TSs given that previous transmission was error-free.	$P_{22} = P_{on}$
$\vdots$	$\vdots$	$\vdots$

Table 6.2: Illustrates the state to state transition with respect to the event that take place.

example, we can readily see that the state of T_4 is $S_3 = 00011$, and the probability of traversing from S_{19} to S_3 is $P_{19,3} = P_{off}$. The state transition probabilities can be found in a similar manner.

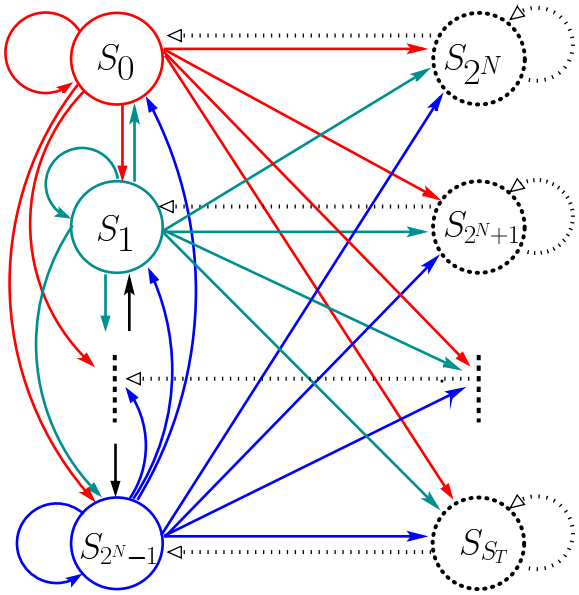

Figure 6.10: A state transition diagram for the operations of the CSR-HARQ scheme. The *solid* and *dashed* lines represent the transitions from free and busy states, respectively.

Following the above definition of states, we proceed to derive the transition probability matrix **P**, where, the state transition probabilities are recorded. Assuming that at TS n, the CR transmitter is in state S_i, while at TS $n+1$, it is in state S_j, the transition probability is denoted by $P_{i,j}$. Then, according to the properties of the DTMC, this probability is independent of how the transmitter arrived at the state S_i [21, 244], which may be formulated as

$$\begin{aligned} P_{i,j} &= P\left\{S(n+1)=S_j \mid S(n)=S_i, \ldots S(1)=S_0\right\}, \\ &= P\{S(n+1)=S_j | S(n)=S_i\}, \quad \text{where} \\ &0 \leq i \leq S_T \; 0 \leq j \leq S_T \text{ and } n = 1,2,\ldots \end{aligned} \tag{6.26}$$

Furthermore, we have the properties of [21, 244]

$$0 \leq P_{i,j} \leq 1.$$
$$\sum_{j=0}^{S_T} P_{i,j} = 1, \ \forall \ S_i \ \in \mathbb{S}. \tag{6.27}$$

For the example shown in Fig. 6.8, which has the states of $\mathbb{S} = S_0, S_1, S_2, S_3$, the state transition matrix $\mathbf{P}$ can be readily expressed as:

$$\mathbf{P} = \begin{array}{c} \\ S_0 \\ S_1 \\ S_2 \\ S_3 \end{array} \begin{array}{c} \begin{array}{cccc} S_0 & S_1 & S_2 & S_3 \end{array} \\ \begin{bmatrix} (1-P_e)P_{off} & P_eP_{off} & (1-P_e)P_{on} & P_eP_{on} \\ (1-P_e)P_{off} & P_eP_{off} & (1-P_e)P_{on} & P_eP_{on} \\ P_{off} & 0 & P_{on} & 0 \\ 0 & P_{off} & 0 & P_{on} \end{bmatrix} \end{array}.$$

The probabilities of the transmitter being in its legitimate states in TS n is

$$\boldsymbol{p}(n)=[P_0(n), P_1(n), \ldots, P_{S_T}(n)]^T. \tag{6.28}$$

Furthermore, let us assume that the transmitter commences its transmission in state $S(1) = S_0$ with the probability of $\boldsymbol{p}(1) = [1, 0, \ldots, 0, \ldots]^T$. Then, it can be shown that [21, 245]

$$\boldsymbol{p}(n+1) = \mathbf{P}^T\boldsymbol{p}(n), \tag{6.29}$$
$$= (\mathbf{P}^T)^n\boldsymbol{p}(1). \tag{6.30}$$

For our CSR-HARQ, the state transition probability matrix $\mathbf{P}^T$ is a left stochastic matrix, because the sum of each column is 1, which is shown in Eq. (6.27). Moreover, according to the *Perron-Frobenius theorem*, the limit of the transition matrix i.e, $\lim_{n\to\infty} (\mathbf{P}^T)^n$ exists, [245]. Hence, the Markov chain reaches its steady, when $n \to \infty$, [21], which yields

$$\boldsymbol{p}(n+1) = \boldsymbol{p}(n). \tag{6.31}$$

The steady-state probabilities are denoted by $\boldsymbol{\pi}$, where we have $\boldsymbol{\pi} = [\pi_0, \pi_2 \ldots, \pi_i \ldots]^T$, and the steady state probability of the transmitter being in state S_i is π_i. Then, from Eq. (6.31) we have

$$\boldsymbol{\pi} = \mathbf{P}^T\boldsymbol{\pi}. \tag{6.32}$$

Thus, the right eigenvector of $\mathbf{P}^T$ for an eigenvalue of 1 gives the steady state probabilities of all the states [21, 244, 245]. It is worth stating that the steady state probabilities fulfill the following condition

$$\sum_{j\in\mathbb{S}} \pi_j = 1 \quad \text{or} \quad \boldsymbol{\pi}^T \times \mathbf{1} = 1, \tag{6.33}$$

where $\mathbf{1}$ is a unit column vector.

6.5.1 Throughput Analysis of CSR-HARQ Scheme

When the DTMC reaches its steady state, the throughput of the CSR-HARQ scheme can be evaluated from the states having new packets to transmit. Hence, let $n_p(S_i)$ be the number of new packets transmitted in state S_i for $i < 2^N$, where $n_p(S_i)$ equals the number of zeros in the state sequence of S_i, excluding the first zero indicating that the TS is free. Then, the achievable throughput of the CSR-HARQ scheme can be evaluated from:

$$R_s = \sum_{i=0}^{2^N-1} \pi_i \cdot n_p(S_i), \text{ where } S_i \in \mathbb{S} \text{ [packets / TS]}. \tag{6.34}$$

Additionally, when expressing the throughput in terms of the number of packets per T_p, upon using $T = (N+k)T_p$, we arrive at:

$$R'_s = \frac{1}{k+N} \times R_s \quad \text{[packets / } T_p\text{]}. \tag{6.35}$$

Let us now study the delay performance of the CSR-HARQ scheme using the DTMC framework.

6.5.2 Delay Analysis of CSR-HARQ

In this subsection, the average packet delay as well as the end-to-end packet delay are studied by evaluating both its probability distribution as well as the average end-to-end packet delay.

6.5.2.1 Average Packet Delay

The average number of TSs or T_ps required for successfully delivering a packet to the receiver is the average packet delay which can be computed from the achievable throughput in Eqs. (6.34) and (6.35) as follows

$$T_D = \frac{1}{R_s} \quad \text{[TS per packet]} \tag{6.36}$$

$$= \frac{k+N}{R_s} \quad [T_p \text{ per packet}]. \tag{6.37}$$

6.5.2.2 End-To-End Packet Delay

We continue by studying the PMF of the end-to-end packet delay. Let $\mathbb{S}_N$ be the subset of $\mathbb{S}$ defined as,

$$\mathbb{S}_N = \{S_i \mid L_i \geq 1 \text{ new packets are transmitted in } S_i\}. \tag{6.38}$$

In other words, $\mathbb{S}_N$ is the set of states S_i, each of which transmits one or more new packets. For each $S_i \in \mathbb{S}_N$, we define a set $\mathbb{S}_i^{(m)}$, which contains all the states S_j, where $l_{i,j} \geq 1$ new packets

transmitted for the first time in state S_i are correctly received in state S_j, with exactly the delay of mT_p. This is expressed as

$$\mathbb{S}_i^{(m)} = \{S_j | l_{i,j} \geq 1 \text{ new packets transmitted in } S_i \text{ are correctly received in } S_j \text{ with a delay of } mT_p\}. \tag{6.39}$$

Using these definitions, the PMF of the end-to-end packet delay may be expressed as

$$P(m) = \frac{1}{c} \sum_{S_i \in \mathbb{S}_N} \sum_{S_j \in \mathbb{S}_i^{(m)}} \frac{\pi_i \times l_{i,j} \times P_{i,j}^{(m)}}{L_i}, \tag{6.40}$$

where $c = \sum_{S_i \in \mathbb{S}_N} \pi_i$, $P_{i,j}^{(m)}$ refers to the probability of transition from state S_i to state S_j after a delay of mT_p and $m = 1, 2, \ldots$.

The PMF of end-to-end packet delay is

$$\boldsymbol{P}_{MF} = [P(1), P(2), \ldots, P(M_T)]^T, \tag{6.41}$$

where M_T is the longest delay that is considered in the analysis, because the probabilities of longer delays are negligible. From the properties of the DTMC, we know that from a given state S_i, after q transitions, we have

$$\boldsymbol{p}^{(q)} = \mathbf{P}^T . \boldsymbol{p}^{(q-1)} = \cdots = (\mathbf{P}^T)^q \boldsymbol{e}_i, \; q = 1, 2, \ldots \tag{6.42}$$

where $\boldsymbol{e}_i$ is the ith column of the identity matrix. From (6.42) it is observed that if we multiply $\mathbf{P}^T$ by the CUrrent $\boldsymbol{p}^q$, we get the following information:

a) The end-to-end delays of the packets that were transmitted for the first time in state S_i;

b) The probabilities of traversing from state S_i to any of the states in $\mathbb{S}$;

c) The number of packets $l_{i,j}$ that were transmitted for the first time in state S_i and correctly received in state S_j.

Based on the above, the state transition probability matrix $\boldsymbol{P}_{MF}$ can be updated using the following relationship

$$P(m) \leftarrow P(m) + \frac{\pi_i \times l_{i,j} \times P_{i,j}^{(m)}}{L_i}, \text{ where } m = 1, 2 \ldots, M_T, S_j \in S_i^{(m)}, S_i \in \mathbb{S}_N. \tag{6.43}$$

Finally, when $\boldsymbol{P}_{MF}$ does not change, we arrive at the average end-to-end packet delay, which can be formulated as

$$\tau = \sum_{i=1}^{M_T} i \times P(i) \;\; \text{in units of } [T_p\text{'s}]. \tag{6.44}$$

We now validate the accuracy of the analytical results obtained through both methodologies

presented in Sections 6.4 and 6.5 using the results of our simulation-based study.

6.6 Performance Results

In this section, we present the performance results of the proposed CSR-HARQ systems. The three previously stated performance metrics, namely 1) throughput 2) average packet delay, and 3) end-to-end packet delay are investigated. These metrics are evaluated in terms of the packet error probability (P_e), channel busy probability (P_{on}), the number of packets transmitted in a TS (N) and the duration k of sensing time.

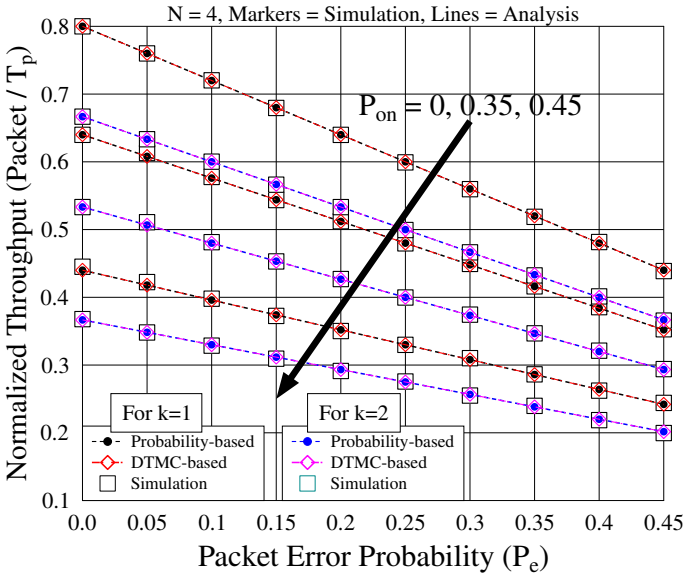

Figure 6.11: Throughput performance of the CSR-HARQ scheme versus packet error probability in terms of various channel busy probabilities, when $k = 1$ or 2, and $N = 4$.

In our simulations, we considered N_t TSs, which are observed and used by the CR transmitter for the successful transmission of N_s packets to the CR receiver. Note that the N_t TSs include both busy and free TSs. Hence, the throughput obtained in our simulations is evaluated as,

$$R'_S = \frac{N_s}{N_t} \times \frac{1}{k+N} \quad [\text{packets per } T_p], \tag{6.45}$$

where $N_t(k+N)$ is the total number of T_ps used for transmitting N_s packets.

The throughput of the proposed CSR-HARQ is presented in Fig. 6.11 and 6.12, versus the pair-wise (PEP) both for different P_{on} probability (Fig. 6.11) and for different values of N (Fig. 6.12). As seen in Fig. 6.11, for a given P_{on}, the throughput of the CSR-HARQ reaches its maximum when $P_e = 0$. As P_e increases, the number of retransmissions increases, hence, resulting in a reduced throughput. Furthermore, for a given P_e, Fig. 6.11 shows that the throughput of the CSR-HARQ is maximum, when the channel is always free from PU, i.e. when we have $P_{on} = 0$. However, when P_{on} increases, the achievable throughput of the CSR-HARQ drops significantly, since that the CU has to wait for longer to acquire free channels to send its information. In Fig. 6.11, we also investigate the impact of the sensing time $T_s = kT_p$ on the throughput of the CSR-HARQ. It is

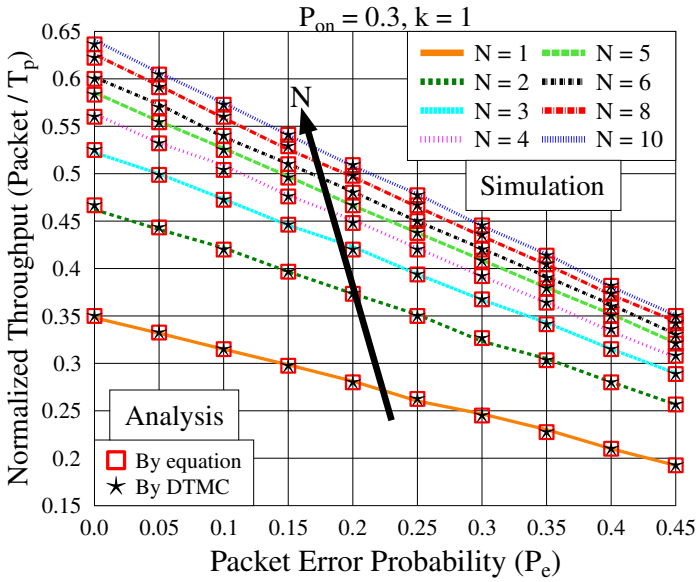

Figure 6.12: Throughput performance of the CSR-HARQ scheme versus packet error probability for various values of N, when $k = 1$ and $P_{on} = 0.3$.

observed that for the cases considered when the sensing duration increases from $k = 1$ to 2, the throughput of the system reduces. Note that in Fig. 6.11, the throughput at $P_e = 0$ is given by

$$P_{off} \times \frac{T_d}{T} = P_{off}\left(\frac{N}{N+k}\right) = P_{off}\left(1 - \frac{k}{N+k}\right) \quad [T_p's]. \tag{6.46}$$

Based on (6.46) we can find in Fig. 6.11 that for $P_e = 0$, $P_{on} = 0$ and $N = 4T_p$, the throughput is reduced from 80% to 66.67%, when the sensing duration increases from $1T_p$ to $2T_p$.

Fig. 6.12 shows the effect of the P_e, and the number of packets transmitted per TS on the performance of CSR-HARQ systems. It can be observed from Fig. 6.12 that the throughput of CSR-HARQ increases, as the value of N increases. However, when N is relatively large, such $N \geq 6$, any further increase of N only results in a marginal additional improvement of the throughput. More explicitly, this improvement remains marginal because the percentage of transmission duration, i.e. $\frac{T_d}{T} \times 100$, changes very slow, when N is relatively large. In other words, the sensing overhead per packet decreases as N increases. Furthermore, we can observe from Fig. 6.11 and 6.12 similar trends for the results obtained from the two types of analytical approaches and the simulation results, which validate the theoretical analysis.

Having characterized the throughput, let us now quantify the delay of the CSR-HARQ. Firstly, we consider the average packet delay. Again, the total time spanning from the start of PR channel sensing to the successful transmission of all the packets is taken into account. Specifically, let us assume that N_s packets are successfully transmitted within N_t TSs. Then, in our simulations, the average packet delay is characterized by

$$T_{DS} = \frac{N_t(k+N)}{N_s} \quad [T_p\text{'s}]. \tag{6.47}$$

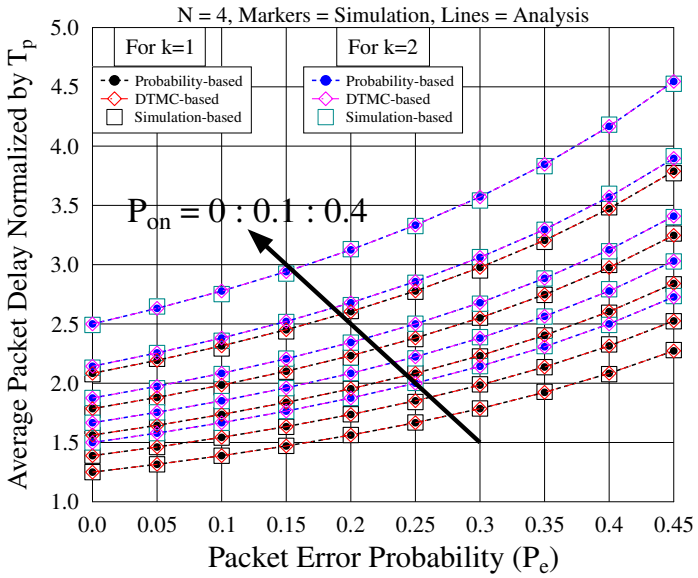

Figure 6.13: Average packet delay of the CSR-HARQ scheme versus the packet error probability (P_e) with respect to different channel busy probabilities (P_{on}), when $N = 4$ and $k = 1$ or 2.

Fig. 6.13 portrays the effect of P_e and P_{on} on the average packet delay. It can be observed from Fig. 6.13 that the average packet delay achieves its minimum, when P_e and P_{on} are zero. It increases with the increase of P_e and/or P_{on}. The reason behind this phenomenon may be explained as follows. When P_e increases, the channel becomes less reliable, which increases the number of retransmission, hence resulting in an increased delay. On the other hand, when P_{on} increases, implying that the CR system becomes busier and there are fewer opportunities for the CR system to transmit, and hence resulting in an increase of the average packet delay. Furthermore, as seen in Fig. 6.13, the average packet delay increases with the sensing time.

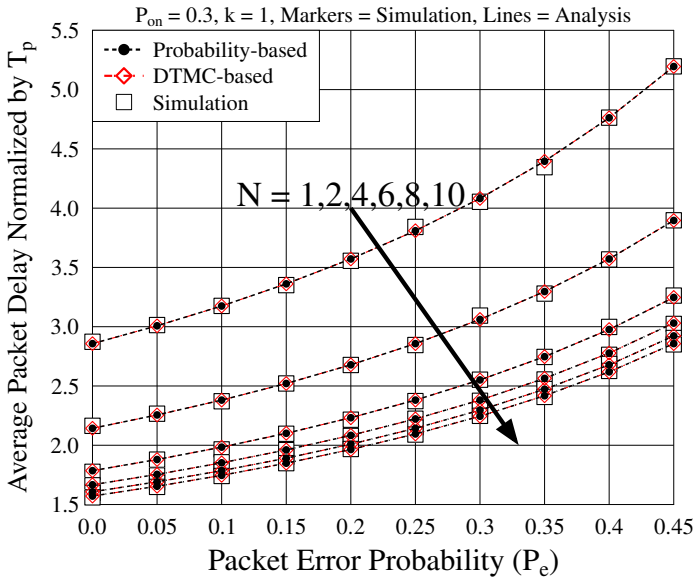

Figure 6.14: Average packet delay of the CSR-HARQ scheme with respect to different values of N, when $P_{on} = 0.3$ and $k = 1$.

In Fig. 6.14, we continue to illustrate the impact of N on the average packet delay of CSR-HARQ. Explicitly, as the value of N increases, the average packet delay decreases. However, once N has reached a certain value, further increasing N does not result in any significant reduction of the average packet delay. Additionally, our theoretical results agree well with the simulation results.

Finally, we consider the end-to-end delay of the CSR-HARQ, which is evaluated in our simulations as follows. Let a vector $\boldsymbol{d}$ of length N_s be used to store the delays experienced by each of the N_s packets, where $\boldsymbol{d}(j)$ is the end-to-end delay of the jth packet. Then, the PMF of the end-to-end packet delay is evaluated as [231, 246]

$$\boldsymbol{P}_d(i) = \frac{\sum_{j=1}^{N_s} \delta\left(d(j) - i\right)}{N_s}, \; 1 \leq i \leq \max(\boldsymbol{d}), \tag{6.48}$$

where $\max(\boldsymbol{d})$ denotes the maximum delay of the N_s packets.

Fig. 6.15 portrays the probability distribution obtained from our analytical approaches and simulations, when $N = 4$ and $N = 9$. It can be observed from Fig. 6.15 that for both cases, 50% of the packets can be correctly received in their first transmission attempt corresponding to a delay of one T_p, 12.5% of the packets are successfully received with an end-to-end delay of $2T_p$s, 3.13% packets are successfully received with an end-to-end delay of $3T_p$s, and so on. For clarity, in Fig. 6.15, we have used logarithmic vertical axis for plotting the PMF values.

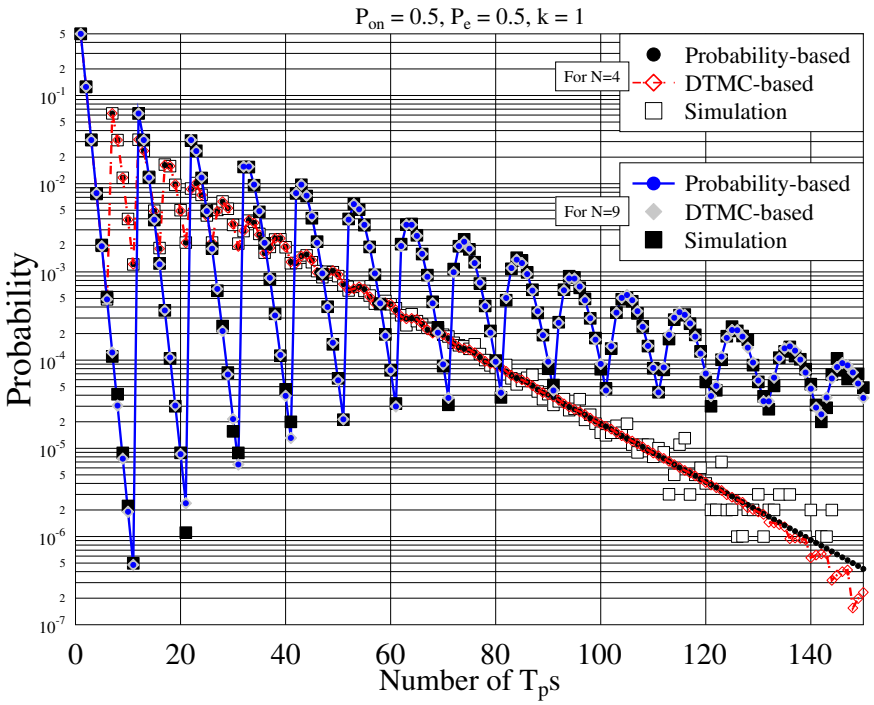

Figure 6.15: Probability of end-to-end packet delay of the CSR-HARQ systems, when $P_{on} = 0.5$, $P_e = 0.5$, $k = 1$ and $N = 4$, and 9.

The variations in Fig. 6.15 illustrate the effect of busy TSs on the end-to-end delay. For the case of $N = 4$, we can see that 6.2% of the packets are successfully received with a delay of $7T_p$,

which includes the scenario of 7 transmissions of a packet without encountering busy TSs, and the scenario of 2 transmissions imposed by a busy TS. By contrast, for the case of $N = 9$, 6.2% of the packets are successfully received with a delay of $12T_p$, which includes the delay due to 12 transmissions when there is no busy TSs, as well as the delay due to one busy TS associated with 2 transmissions. Specifically, the 2 transmissions include an erroneous transmission and a successful transmission.

In Figs. 6.16 and 6.17, we demonstrate the average end-to-end packet delay, which is evaluated by the formula of

$$\tau_s = \sum_{i=1}^{\max(\boldsymbol{d})} \boldsymbol{P}_d(i) \times i \quad [T_p\text{'s}], \tag{6.49}$$

in our simulations. As in Fig. 6.13, the average end-to-end packet delay of the CSR-HARQ is investigated for various values of P_e and P_{on}, while assuming constant values of k and N. It is found in Fig. 6.16 that when $P_e = 0$, the average end-to-end delay is minimum, regardless of the values of P_{on}. However, when $P_e > 0$, the average end-to-end packet delay increases with P_{on}. Furthermore, for a given value of P_{on}, the average end-to-end packet delay increases, as P_e increases.

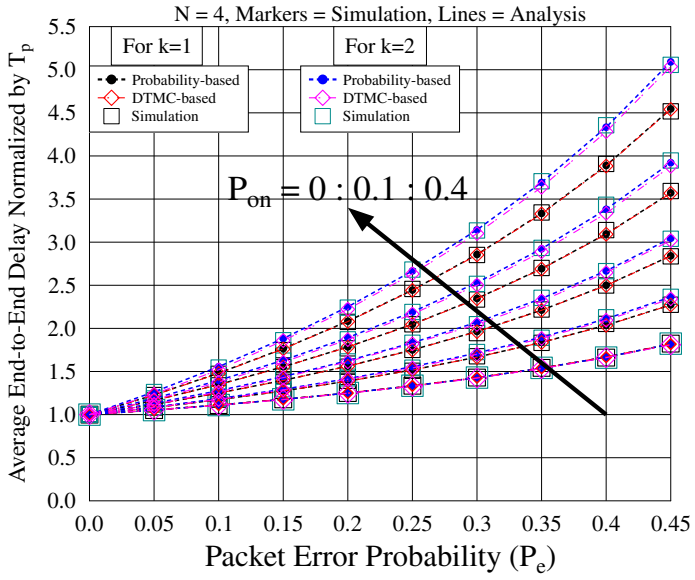

Figure 6.16: Average end-to-end packet delay of the CSR-HARQ scheme for different values of channel busy probability (P_{on}), when $N = 4$ and $k = 1$ or 2.

When comparing the results of Fig. 6.13 and Fig. 6.16, we can observe the difference between the average end-to-end packet delay and the average packet delay. Firstly, it can be observed that for a given set of parameters the average end-to-end packet delay is lower than the average packet delay at $P_e = 0$. The reason behind this is that the average packet delay includes the sensing time, the transmission time as well as the busy TSs both before and after the transmission of a packet. By contrast, the average end-to-end delay only considers the delay after the transmission of a packet. Secondly, we can find from Fig. 6.13 and 6.16 that for higher values of P_e and/or P_{on}, the

average end-to-end packet delay becomes higher than the average packet delay. This is because, the average packet delay is the average transmission time of many packets, whereas, the end-to-end packet delay is the average delay per individual packet. Thirdly, when the sensing duration is increased from $k = 1$ to $k = 2$, the average end-to-end packet delay observed for a given P_e and a given P_{on} increases.

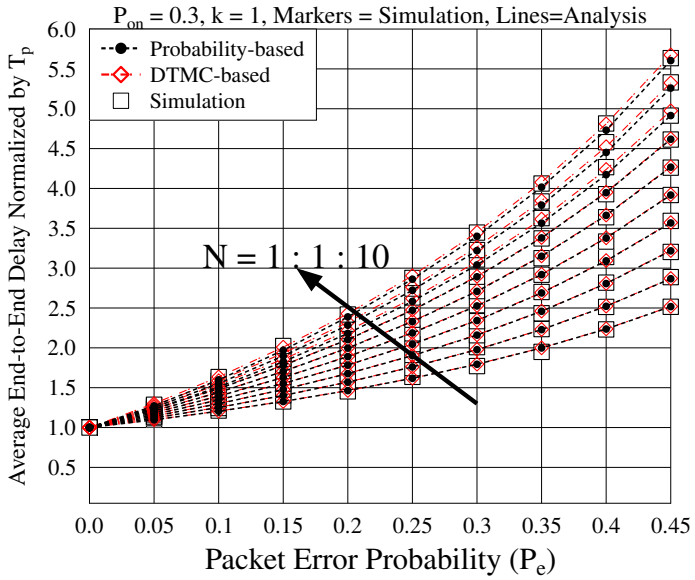

Figure 6.17: Average end-to-end packet delay of the CSR-HARQ scheme as function of packet error probability (P_e) for various values of N, when $P_{on} = 0.3$ and $k = 1$.

Finally, Fig. 6.17 shows the effect of N on the average end-to-end packet delay. Explicitly, at a given P_e, the average end-to-end packet delay increases as N increases. This is the result of the contribution made by the busy TSs to the end-to-end packet delay. Hence, for a given P_{on}, a higher N results in a longer end-to-end packet delay due to having longer busy TSs. This is in contrast to the trend depicted in Fig 6.14 for the average packet delay. Since, a longer TS can transmit more packets, once a free TS is acquired, the average packet delay decreases, when N increases.

6.7 Chapter Conclusions

A novel CSR-HARQ transmission scheme has been proposed for a CR system to improve the exploitation of free PR channels. The proposed scheme allows a CR transmitter to sense and exploit a PU channel for its own data transmission using a modified SR-HARQ protocol. Specifically, during a TS, the CU first senses the PR channel. Once a free TS is sensed, N data packets are transmitted over the free TS. In this chapter we analyzed both the throughput and delay using two analytical approaches: 1) the probability-based approach and 2) the DTMC-based approach. The performance of the proposed CSR-HARQ scheme was investigated in terms of its throughput, average packet delay and end-to-end packet delay with aid of the both closed form expressions and simulations. It can be shown that our simulation results verify the results obtained from the evaluation of our analytical formulas. Furthermore, the performance results demonstrate that both

the throughput and delay of the CSR-HARQ scheme is significantly affected both by the activity of the PU and by the channel's reliability. The throughput drops significantly, when the PR channel has a higher probability of being busy and/or when the channel's reliability becomes lower. The effect of the number of packets (N) per TS was also investigated, which shows that for higher N, the average packet delay is lower, while the end-to-end packet delay is higher. In our future studies, we aim for evaluating the impact of the buffer resequencing technique employed at the receiver. Moreover, we intend to incorporate the effect of unreliable feedback into our future studies.

Chapter 7

Thesis Conclusions and Future Research

The cognitive radio concept is considered to be one of the favourable paradigms for improving the attainable spectrum exploitation. Therefore, it has attracted substantial research attention since its invention and has been widely studied in recent years in the context of its operational principles, functions, architecture, etc. However, in context of reliable data transmission, the CR concept is still in its infancy. Therefore, in this thesis we specifically focused our attention on designing CR aided HARQ schemes and on characterizing them both by analysis and simulations. The motivation of invoking HARQ in the context of CR systems has been discussed in Chapter 1. In this chapter, the overall summary and conclusions of this treatise will be provided in Section 7.1, followed by the comparison of the proposed transmission schemes in Section 7.2. Finally, in Section 7.3, we will suggest a range of promising future research directions.

7.1 Summary and Conclusions

7.1.1 Chapter 2

In Chapter 2, we have briefly reviewed the concept of CR systems in terms of their design, architectures, functions and applications. In Subsection 2.1.4, the well-known spectrum sensing algorithms are discussed and compared in terms of their complexity and accuracy in terms of identifying the unoccupied spectrum holes. Following that we have also discussed spectrum management functions for the sake of choosing a suitable spectrum slot for data transmission. Data transmission in CR system shares the same problems conventional wireless systems. In Section 2.2, we have discussed the challenges of protecting data transmissions in conventional wireless systems relying on various HARQ schemes for achieving reliable data transmission. In Section 2.3, we have extensively discussed the contributions focused on designing communication models for the CR systems and the family of HARQ techniques employed in the context of CR systems for achieving error-free communications. However, there is a paucity of studies on the theoretical analysis of HARQ techniques employed in CR system. Therefore, to fill this research gap, we have carried out the

exact theoretical modelling and analysis of CR-aided HARQ techniques in the ensuing chapters of this thesis.

7.1.2 Chapter 3

As stated in Chapter 2, the CR paradigm has the potential of improving the exploitation of the electromagnetic spectrum by near-instantaneously detecting unoccupied spectrum slots allocated to PUs. In order to support the process of spectrum reuse, in this chapter we proposed a scheme, which senses and opportunistically accesses a PR's spectrum for communication between a pair of nodes relying on the SW-HARQ protocol known as CSW-HARQ. Specifically, in Section 3.2, the availability/unavailability of the PR's channel was modelled as a two-state Markov chain having 'OFF' and 'ON' states, respectively. Once the CU finds that the PR's channel is available (i.e. in 'OFF' state), the CU transmits its data over the PU's spectrum, whilst relying on the principles of SW-HARQ. Moreover, due to unreliable sensing, the CU may not correctly detect the 'ON/OFF' activity of the PR's channel. Therefore, in Section 3.2.2, the two-state Markov chain model is extended into a four-state model for quantifying the impact of unreliable sensing.

Section	**Contributions**
Section 3.1	Introduced the concept of CR and reviewed the existing literature for achieving reliable communication both in conventional wireless systems and in the context of CR systems. The contributions of this chapter are also provided.
Section 3.2	The presence and absence of PU in the PR channel and the CR system are modelled in this section.
Section 3.3	The basic principles of the proposed CSW-HARQ transmission scheme and the transmitter and receiver operations are discussed in section.
Section 3.4 and 3.5	The probability-based as well as the Markov chain-based analytical approaches are provided.
Section 3.6	Presented our simulation and corresponding analytical results.

Table 7.1: The contributions of Chapter 3.

In Section 3.3, the operation of the transmitter and receiver was redesigned in order to satisfy the demanding requirements of data transmission using the SW-HARQ aided CR system. A pair of analytical approaches, namely, 1) the probability-based technique of Section 3.4; and 2) the Discrete Time Markov chain (DTMC)-based regime of Section 3.5 have been proposed. Based on these techniques, closed-form expressions were derived for both the throughput and the delay both under idealized perfect and realistic imperfect sensing environments, which were also validated by simulation. Based on the performance results presented in Table 7.2, we conclude that both the achievable throughput and the delay of the CSW-HARQ are substantially affected both by the activity of the PUs, as well as by the reliability of the CU channels and by the reliability of sensing. When the PR's channel becomes busier, the CSW-HARQ's throughput becomes lower and the average packet delay increases, even when the CU's sensing and transmission are reliable. Moreover, when the sensing is reliable, the CSW-HARQ system achieves a higher throughput and a lower delay than that of realistic imperfect sensing. Given that in CR systems the opportunities for

Packet error Probability	P_{on}	Throughput	Average Packet Delay	End-to-end Packet Delay
$P_e = 0$	0	0.233	4.3	1
	0.1	0.210	4.76	1.07
	0.2	0.187	5.35	1.17
	0.3	0.163	6.12	1.31
$P_e = 0.2$	0	0.187	5.35	1.35
	0.1	0.168	5.95	1.47
	0.2	0.149	6.7	1.62
	0.3	0.131	7.65	1.83
$P_e = 0.4$	0	0.14	7.8	1.95
	0.1	0.126	7.94	2.13
	0.2	0.112	8.93	2.36
	0.3	0.098	10.2	2.68

Table 7.2: Performance results summary of the CSW-HARQ scheme in the case of realistic imperfect sensing, when $P_{md} = 0.3$ and $P_{fa} = 0.3$. The results shown are normalized to the TS duration.

data transmission are limited, it is of paramount importance to employ reliable sensing techniques for improving the CU's throughput and delay, in addition to minimizing the interference imposed on the PU system.

7.1.3 Chapter 4

Section	**Contributions**
Section 4.1	Discussed the background of the HARQ and GBN-ARQ techniques and stated the motivation and novel contributions .
Section 4.2	The activities of PU in the PR channel was by two-state DTMC followed by the CR system modelling.
Section 4.3	The transmitter and receiver operations based on the principles of the CGBN-HARQ scheme are discussed.
Section 4.4	The CGBN-HARQ was analytically modelled by DTMC-based approaches.
Section 4.5	Presented our simulation and corresponding analytical results.

Table 7.3: The contributions of Chapter 4.

To further extended our studies and to circumvent the problem of the low throughput and high delay exhibited by the CSW-HARQ scheme, in this chapter we proposed a CGBN-HARQ scheme operated in a perfect sensing environment, which improves both the throughput and delay. The proposed CGBN-HARQ scheme allowed the CR transmitter to (re)transmit the data packets over an under-utilized PR channel. Therefore, similar to Chapter 3, in Section 4.2 of this chapter, the PR channel was modelled by a two-state Markov chain having 'ON' and 'OFF' states. Hence, when the CR transmitter deems the channel to be in 'OFF' state, it transmits its data packets based on the principles of GBN-HARQ. Otherwise, the transmitter waits until the next TS. Using the GBN-HARQ, the CR transmitter seamlessly transmits N packets, one after another, without waiting for their acknowledgements until the reception of a negative feedback or until the detection of a busy TS, as illustrated in Figs. 4.1, 4.6, 4.7 and 4.8. To support this operation, in Section 4.3, a buffer of size of N was provided at the transmitter side, which significantly improved both the throughput and the delay of the system, but slightly increased the complexity.

Moreover, the proposed CGBN-HARQ scheme was analytically modelled by a DTMC in Sec-

tion 4.4. To elaborate a little further, a state generating algorithm was proposed in order to eliminate the unnecessary states for the sake of reducing the dimension of the state transition probability matrix. Based on the DTMC, closed-form expressions were derived both for the throughput and for the delay of CGBN-HARQ scheme, which were then validated by simulations in Section 4.5. The performance results presented in Table 7.4 show that the channel exploitation of the PUs and

(a) For $P_{on} = 0$

P_e	N	R_T	T_D	τ
0	1	0.5	2	1
	2	0.66	1.5	1
	3	0.75	1.33	1
	4	0.8	1.25	1
	5	0.83	1.2	1
	6	0.86	1.16	1
	7	0.87	1.14	1
0.2	1	0.4	2.5	1.5
	2	0.48	2.1	2.05
	3	0.47	2.13	3
	4	0.44	2.25	4.4
	5	0.41	2.45	6.4
	6	0.37	2.7	8.8
	7	0.34	3	11.8
0.4	1	0.3	3.3	2.33
	2	0.32	3.12	4
	3	0.28	3.5	6.62
	4	0.26	3.9	10.5
	5	0.23	4.4	15.75
	6	0.2	5.23	22.5
	7	0.17	5.9	30.8

(b) For $P_{on} = 0.2$

P_e	N	R_T	T_D	τ
0	1	0.4	2.5	1
	2	0.533	1.87	1
	3	0.6	1.66	1
	4	0.64	1.56	1
	5	0.66	1.5	1
	6	0.68	1.45	1
	7	0.7	1.42	1
0.2	1	0.32	3.12	1.6
	2	0.38	2.6	2.3
	3	0.37	2.63	3.5
	4	0.36	2.77	5.2
	5	0.33	3.01	7.5
	6	0.3	3.25	10.3
	7	0.28	3.5	13.8
0.4	1	0.24	4.16	2.66
	2	0.25	3.9	4.81
	3	0.23	4.35	8.1
	4	0.21	4.86	12.9
	5	0.17	5.66	19.3
	6	0.15	6.39	27.5
	7	0.14	7.13	37.5

(c) For $P_{on} = 0.4$

P_{on}	N	R_T	T_D	τ
0	1	0.3	3.33	1
	2	0.4	2.5	1
	3	0.45	2.2	1
	4	0.48	2.1	1
	5	0.5	1	1
	6	0.51	1.94	1
	7	0.52	1.9	1
0.2	1	0.24	4.17	1.83
	2	0.29	3.47	2.83
	3	0.28	3.5	4.33
	4	0.27	3.66	6.5
	5	0.25	3.9	9.44
	6	0.24	4.2	13.1
	7	0.22	4.5	17.4
0.4	1	0.18	5.5	3.21
	2	0.19	5.21	6.15
	3	0.17	5.76	10.62
	4	0.15	6.4	17.1
	5	0.13	7.44	25.6
	6	0.12	8.38	36.4
	7	0.106	9.4	49.4

Table 7.4: Summary of the variables used for generating both the analytical and simulation results for CGBN-HARQ scheme, where the results shown are normalized to T_p and to the sensing duration of T_p. The variables R_T, T_D and τ represent the throughput, average packet delay and average end-to-end packet delay.

the reliability of CR communications have a substantial impact on the throughput and delay of CGBN-HARQ. When the propagation environment becomes more hostile or when the PU has a high probability of occupying the channel, the CR system's throughput may drop significantly, which also implies having a longer transmission delay. Furthermore, our studies show that when the propagation environment is time variant, the number of packets transmitted within a TS should be accordingly adapted, in order to attain the highest throughput and the shortest average transmission delay.

7.1.4 Chapter 5

Section	Contributions
Section 5.1	Stated the motivation and novel contributions.
Section 5.2	Modelled the CR system in imperfect sensing scenario.
Section 5.3	Presented the CR transmitter operation in the case of imperfect sensing.
Section 5.4	The CGBN-HARQ was modelled by DTMC-based approach in imperfect sensing.
Section 5.5	Presented our simulation and corresponding analytical results.

Table 7.5: Contributions of Chapter 5.

It is well recognized that there is no perfect spectrum sensing algorithm for detecting the presence and absence of the PUs in the channel due to numerous reasons, such as the lack of line of sight, shadowing, fading, etc. Therefore, in this chapter, we extend the CGBN-HARQ scheme proposed in Chapter 4 to more practical scenarios of realistic imperfect sensing resulting in false-alarm and mis-detection. To incorporate the effects of imperfect of sensing, the two-state modelling considered in Chapter 4 was extended to a four-state Markov chain as in Chapter 3. The four-state Markov chain has additional states for taking into account the sensing decisions and the true state of the PR channel. Then, in Section 5.4 the DTMC-based analytical approach was extended, as characterized by the new state definition of $(N+2)$-length Eq. (5.8). Moreover, as illustrated in Fig. 5.5, the state generation algorithm was also redesigned to capture the above-mentioned affects and to remove the unnecessary states. Based on the above-mentioned DTMC modelling, closed-form expressions were derived for the throughput, average packet delay and the end-to-end packet delay, including both the probability distributions and of the average end-to-end packet delay, which were then verified by our simulations results presented in Section 5.5.

(a) For $P_{on} = 0$

P_e	N	R_T	T_D	τ
0	1	0.4	2.5	1
	2	0.53	1.87	1
	3	0.6	1.67	1
	4	0.64	1.56	1
	5	0.67	1.5	1
	6	0.69	1.45	1
	7	0.7	1.42	1
0.2	1	0.32	3.1	1.6
	2	0.38	2.6	2.35
	3	0.37	2.63	3.4
	4	0.35	2.7	5.1
	5	0.33	3	7.3
	6	0.31	3.2	10.13
	7	0.28	3.5	13.5
0.4	1	0.24	4.15	2.66
	2	0.25	3.91	4.8
	3	0.23	4.35	7.8
	4	0.2	5	12.2
	5	0.17	5.6	18.1
	6	0.15	6.4	25.5
	7	0.14	7.12	34.6

(b) For $P_{on} = 0.2$

P_e	N	R_T	T_D	τ
0	1	0.32	3.13	1.18
	2	0.43	2.34	1.3
	3	0.48	2.1	1.4
	4	0.51	1.95	1.5
	5	0.53	1.87	1.6
	6	0.55	1.82	1.64
	7	0.56	1.78	1.7
0.2	1	0.26	3.9	1.9
	2	0.31	3.25	2.3
	3	0.30	3.28	4.4
	4	0.28	3.46	6.5
	5	0.27	3.7	9.3
	6	0.25	4	12.8
	7	0.23	4.3	17
0.4	1	0.19	5.2	3.3
	2	0.2	4.9	6.1
	3	0.18	5.44	10.1
	4	0.16	6.2	15.8
	5	0.14	7.1	23.4
	6	0.125	8	33
	7	0.11	9	44.4

(c) For $P_{on} = 0.4$

P_{on}	N	R_T	T_D	τ
0	1	0.24	4.14	1.5
	2	0.26	3.12	2
	3	0.36	2.8	2.2
	4	0.38	2.6	2.5
	5	0.4	2.5	2.8
	6	0.41	2.4	3.1
	7	0.42	2.3	3.4
0.2	1	0.17	5.23	2.6
	2	0.18	4.34	4.2
	3	0.23	4.36	6.3
	4	0.22	4.6	9.3
	5	0.2	4.9	13.12
	6	0.19	5.25	17.8
	7	0.18	5.6	23.3
0.4	1	0.14	7	4.4
	2	0.13	6.5	8.4
	3	0.14	7.25	14.1
	4	0.12	8.3	22.13
	5	0.1	9.4	32.6
	6	0.09	10.6	45.7
	7	0.08	12	61.4

Table 7.6: Summary of the variables used for generating both the analytical and simulation results for CGBN-HARQ scheme, where the results shown are normalized to T_p and to the sensing duration of T_p. We used $P_{md} = 0.2$ and $P_{fa} = 0.2$. The variables R_T, T_D and τ represent the throughput, average packet delay and average end-to-end packet delay.

The performance results of CGBN-HARQ in both perfect and imperfect sensing were compared in this chapter. The results presented in Tables 7.4 and 7.6 reveal that the reliability of spectrum sensing, the activity of the PUs and the reliability of the CR communications have a substantial impact on the throughput and delay of CGBN-HARQ. When the CR communication becomes less reliable or when the PU has a high probability of occupying the channel, the CR system's throughput may drop significantly, which also implies having a longer transmission delay. Furthermore, our results show that when the propagation environment becomes time-variant, the number of pack-

ets transmitted within a TS should be appropriately adapted, in order to attain the highest possible throughput and the shortest average transmission delay.

7.1.5 Chapter 6

Section	Contributions
Section 6.1	Reviewed the related contributions on the proposed CSR-HARQ scheme and then stated the novel contributions.
Section 6.2	Modelled both the PU's and the CR's system in this section.
Section 6.3	The transmission principles of CR transmitter and receiver relying on the CSR-HARQ scheme are discussed.
Section 6.4 and 6.5	The probability-based as well as the DTMC-based analytical approaches are provided.
Section 6.6	Demonstrated our simulation and the corresponding analytical results.

Table 7.7: The contributions of Chapter 6.

The transmission scheme proposed in Chapter 3, namely CSW-HARQ was simple to model. However, its performance was poor even for transmission over reliable channels. This is because the transmitter has to wait for a certain amount of time in order to (re)transmit a single packet. The transmitter's idle time was mitigated by the CGBN-HARQ transmission scheme proposed in Chapter 4 and 5, which enabled the transmitter to continuously transmit packets rather than waiting for their feedback flags. Hence, the CGBN-HARQ scheme significantly enhanced both the throughput and delay of the system at the cost of slightly increased complexity. Moreover, when the channel is unreliable, the performance of the CGBN-HARQ scheme became inadequate, since each packet's reception probability is dependent on the successful reception of the previous packet, which results in an increased number of packet retransmissions.

To reduce the number of retransmissions and hence enhance both the throughput and delay of the system, in this chapter, we proposed a CR aided transmission scheme, which incorporates the classic Selective-Repeat HARQ known as the CSR-HARQ scheme. We assumed that the PU's transmits its information based on TSs. Hence, this system was modelled by a two-state Markov chain in Section 5.2.1. Specifically, during a TS, the CR transmitter first senses the PR channel and then transmits a number of packets to the CR receiver based on the principles of the SR-HARQ, provided that the TS was found to be free. After the reception of packets, the CR receiver generates feedback flags based on error-free or erroneous nature of the packets. In contrast to the receiver's operation in the CSW-HARQ and CGBN-HARQ scheme, in CSR-HARQ a buffer of size N was provided at the receiver for storing the indices of the packets that the receiver expects to receive. Hence, after the reception of a packet, the CR receiver first checks whether the index of this packet matches with the index stored in the buffer. If it matches, then the receiver performs RS decoding and generates as well as transmits the corresponding feedback flags. Moreover, the buffer content is only updated, when an error-free packet is received. The transmitter transmits a new packet, when an ACK flag is received, whereas, a packet is retransmitted when a NACK flag is received.

(a) For $P_e = 0$

P_{on}	N	R_T	T_D	τ
0	1	0.5	2	1
	3	0.75	1.33	1
	5	0.83	1.2	1
	7	0.88	1.14	1
	9	0.9	1.11	1
	10	0.91	1.1	1
0.2	1	0.4	2.5	1
	3	0.6	1	1
	5	0.67	1.5	1
	7	0.7	1.43	1
	9	0.72	1.39	1
	10	0.73	1.38	1
0.4	1	0.3	3.3	1
	3	0.45	2.22	1
	5	0.5	2	1
	7	0.53	1.9	1
	9	0.54	1.86	1
	10	0.55	1.83	1

(b) For $P_e = 0.2$

P_{on}	N	R_T	T_D	τ
0	1	0.4	2.5	1.25
	3	0.6	1.67	1.25
	5	0.67	1.5	1.25
	7	0.7	1.43	1.25
	9	0.72	1.39	1.25
	10	0.73	1.38	1.25
0.2	1	0.32	3.13	1.35
	3	0.48	2.1	1.5
	5	0.149	1.9	1.52
	7	0.56	1.8	1.8
	9	0.57	1.74	1.9
	10	0.58	1.72	1.94
0.4	1	0.24	4.2	1.6
	3	0.36	2.8	1.9
	5	0.4	2.5	2.3
	7	0.42	2.4	2.6
	9	0.43	2.31	3
	10	0.44	2.3	3.1

(c) For $P_e = 0.4$

P_{on}	N	R_T	T_D	τ
0	1	0.3	3.3	1.67
	3	0.45	2.2	1.67
	5	0.5	2	1.67
	7	0.53	1.9	1.67
	9	0.54	1.85	1.67
	10	0.55	1.83	1.67
0.2	1	0.24	4.16	2
	3	0.36	2.8	2.3
	5	0.4	2.5	2.7
	7	0.42	2.4	3
	9	0.43	2.31	3.3
	10	0.44	2.3	3.5
0.4	1	0.18	5.6	2.6
	3	0.27	3.7	3.4
	5	0.3	3.3	4.3
	7	0.31	3.2	5.2
	9	0.32	3.1	6.1
	10	0.33	3	6.6

Table 7.8: Performance summary of the CSR-HARQ scheme, where the results are normalized to T_p. The variables R_T, T_D and τ represent the throughput, average packet delay and average end-to-end packet delay.

In this chapter, we analyzed the throughput, average packet delay and end-to-end packet delay of CSR-HARQ. We proposed a pair of analytical approaches. The first one is probability based, while the second one relies on the classic DTMC principles. The simulation-based studies agree well with the analytical results. The performance results demonstrated that both the throughput and the delay of the CSR-HARQ scheme is significantly affected both by the activity of the PU and by the channel's reliability. The throughput drops significantly, when the PR's channel has a higher probability of being busy and/or when the channel's reliability becomes lower. As shown in Table 7.8, the throughput increases and the delay decreases upon increasing the number of packets transmitted within a TS, given that the channel is absolutely reliable and free from the PU's transmission. However, when channel's reliability decreases and the probability of PU's transmission increases, the throughput is reduced and the delay is increased, as shown in Table 7.7(b) and 7.7(c). Moreover, we may also conclude that when N becomes high, the increase in throughput and the decrease in delay becomes marginal.

7.2 Comparison of the Proposed CR-aided HARQ Schemes

In this section, we compare the throughput and delay of the CR aided HARQ schemes studied in the previous chapters. Explicitly, in Figs. 7.1 and 7.2, we compare the throughput of the CSW-HARQ, CGBN-HARQ and the CSR-HARQ schemes. Note that in the CSW-HARQ scheme, the transmitter requires an epoch of T_p for sensing the PR channel during a TS and then T_p for transmitting a packet when the channel is free. Then the rest of a TS is used to wait for the feedback of the packet. On the other hand, in the CGBN-HARQ and CSR-HARQ schemes, the transmitter does not have to wait for the reception of the feedback, it rather continues transmitting packets after the sensing

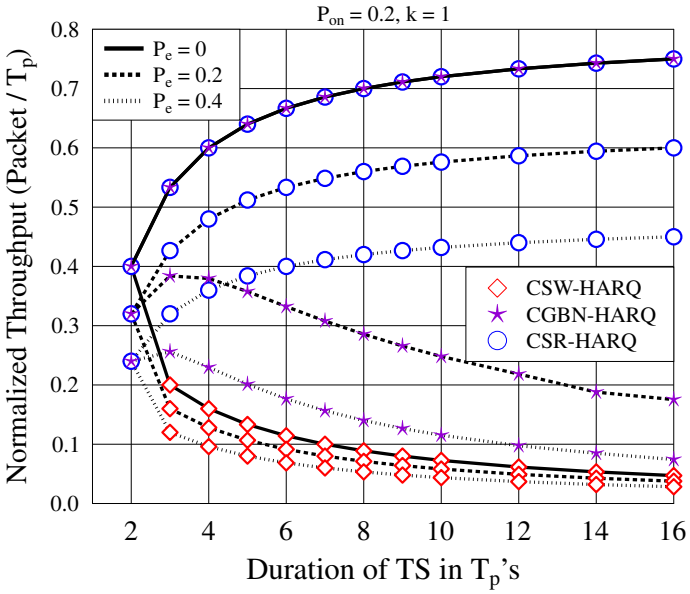

Figure 7.1: Throughput comparison of CSW-HARQ, CGBN-HARQ and CSR-HARQ.

duration, if the PR channel is free. The results of Figs. 7.1 and 7.2 reveal that regardless of the channel reliability and of the probability P_{on} of the channel being occupied by the PUs, the CSR-HARQ scheme is capable of achieving a higher throughput than the other schemes, provided that $N \geq 2$. Specifically, in contrast to the CSW-HARQ scheme, the throughput of CSR-HARQ is in

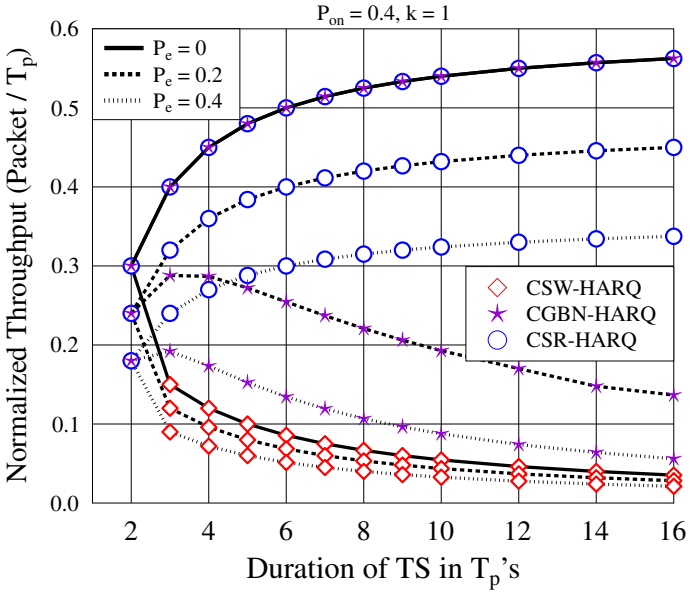

Figure 7.2: Throughput comparison of CSW-HARQ, CGBN-HARQ and CSR-HARQ.

general significantly higher, because the CSR-HARQ scheme is capable continuously transmitting N packets without waiting for their feedbacks flags, and only the erroneous packets have to be retransmitted. As seen in Figs. 7.1 and 7.2, in the cases of $P_e > 0$ the CSR-HARQ scheme is also capable of achieving a significantly higher throughput than CGBN-HARQ. This is due to the fact that in the CSR-HARQ scheme, only the erroneous packets are retransmitted, while, in CGBN-HARQ, the erroneous packets as well as all the subsequent packets have to be retransmitted. In other words, the CSR-HARQ scheme reduces the number of retransmissions of the predominantly error-free packets.

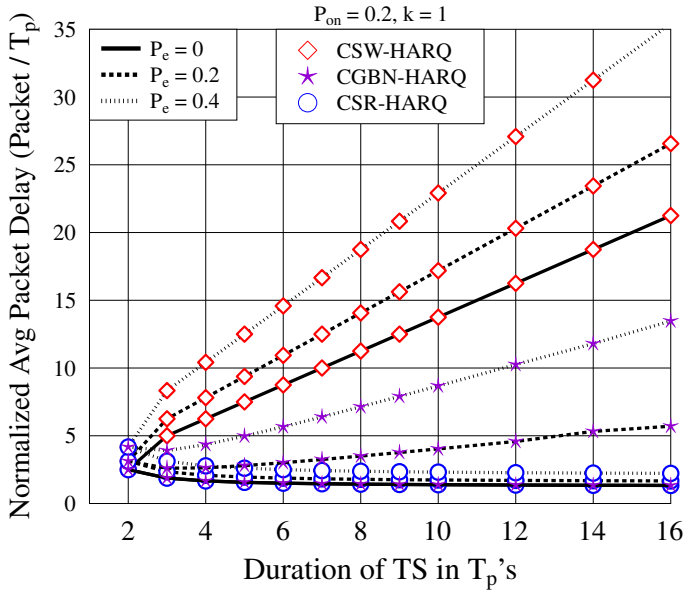

Figure 7.3: Average packet delay comparison of CSW-HARQ, CGBN-HARQ and CSR-HARQ.

It is important to mention that in the case of highly reliable channels, the CGBN-HARQ arrangement is favourable compared to the CSR-HARQ scheme, because both schemes support a similar throughput, but the complexity of the CGBN-HARQ scheme is lower than that of the CSR-HARQ scheme. Furthermore, as shown in Figs. 7.1 and 7.2, when the channel becomes highly unreliable, the throughput of the CGBN-HARQ associated with a high value of N becomes similar as that of CSW-HARQ [18, 128, 164].

Figs. 7.3 and 7.4 compare the average packet delay of the CSW-HARQ, CGBN-HARQ and the CSR-HARQ schemes. For the reasons mentioned above in the context of Figs. 7.1 and 7.2, CSR-HARQ provides a significantly lower average delay than the CSW-HARQ and CGBN-HARQ schemes, when the channel is unreliable. By contrast, the CGBN-HARQ and CSR-HARQ have a similar delay performance, when the channel is highly reliable.

Finally, we may conclude that when the channel is highly reliable, i.e. $P_e = 0$, the CGBN-HARQ scheme is favourable than the CSR-HARQ scheme, because the implementation of CGBN-HARQ is easier due to less complex receiver operations but provides similar performance like CSR-HARQ scheme. On the other hand, when the channel is highly unreliable, i.e. $P_e > 0.4$, then CSR-HARQ is favourable in contrast to both CGBN-HARQ and CSW-HARQ. However, in the scenario of less complex systems, the CSW-HARQ is preferred. This is because, the CGBN-HARQ performance converge to the CSW-HARQ performance when operating over highly unreliable channel.

7.3 Future Research

In this section, we provide some suggestions for extending the research performed in this thesis.

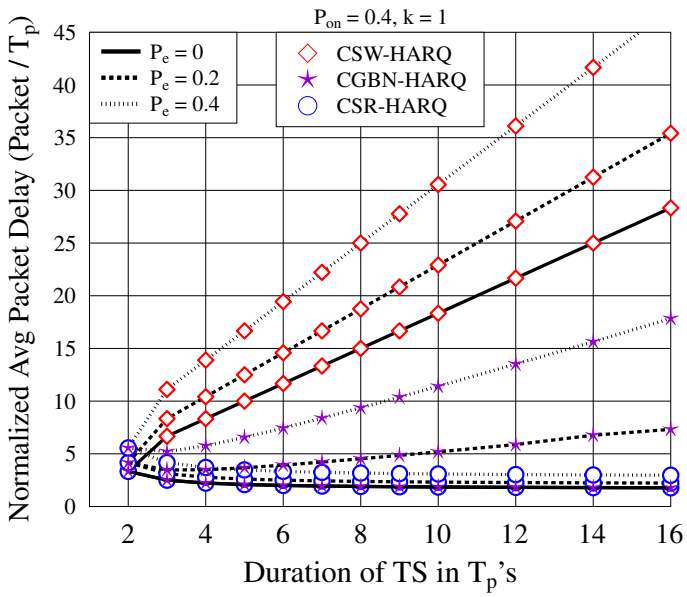

Figure 7.4: Average packet delay comparison of CSW-HARQ, CGBN-HARQ and CSR-HARQ.

1. The Reed-Solomon (RS) code used has been assumed to have a perfect error-detection capability. Hence, it is capable of detecting with probability one all the uncorrectable errors. However, in practice, reliable cyclic redundancy checking (CRC) has to be used.

2. In the current models, we have assumed that spectrum sensing is performed by the CR transmitter. In some cases, it might be desirable that the sensing is performed at the CR receiver, which is capable of reducing the potential collisions with the PUs at the CR receiver.

3. In this thesis, we have assumed that the PUs start their transmission at the beginning of a TS and use the channel until its end. However, in practice, the PUs are free to access and leave the channel any time. If this is the case, there is an optimal TS duration, which allows the CUs to maximize the exploitation of the spectrum. For example, the channel utilization by PUs can be modelled using a Gaussian-Markov process expressed as [269]:

$$X_n = \rho X_{n-1} + w_n, \tag{7.1}$$

where X_n represents a random process, w_n is a zero mean Gaussian random variable and ρ denotes the degree of correlation between the previous and current variables. Based on (7.1), if the probability of the channel being occupied is known, then we can readily obtain a threshold ($\mathcal{T}_h$)

$$P_{on} = Pr(X_k > \mathcal{T}_h) = Q(\frac{\mathcal{T}_h}{\sigma})$$
$$\mathcal{T}_h = \sigma Q^{-1}(P_{on}). \tag{7.2}$$

By doing so, one can predict the probability of the channel being free or busy in the next T_p. This may also ease the burden on spectrum sensing process, since the CUs do not have to sense the channel so often and helps predict the activities of the PUs in the next T_ps.

Moreover, using this approach the transmitter may also vary the number of packets per TS based on the activities of the PUs.

4. The analytical modelling performed in Chapters 4, 5 and 6 using the DTMC-based approach is versatile and may be used to model any systems, once the states have been appropriately defined. However, as the number of states increases, the situation may become excessively complicated to handle. For example, as shown in Fig. 6.10, when $N = 10$, the total number of states becomes $2^{N+1} = 2048$. In this case, despite eliminating a large fraction of states by our proposed state generation algorithm, the process still requires a very large amount of computational resources for processing and generating the results, due to the excessive size of the state transition matrices involved. In this regard, we have proposed the probabilistic approach of Chapter 3 and 6, which is capable of reducing the computational complexity. Hence, in order to model and analyze sophisticated cognitive HARQ schemes, it is worth investigating the less resource-hungry approaches. Specifically, it is worth modelling the CGBN-HARQ scheme proposed in Chapters 4 and 5 by technique imposing a lower computation complexity than the DTMC based modelling.

5. It is equally challenging and interesting to characterize the performance of ARQ schemes combined with various diversity combining schemes. In these ARQ schemes, if a packet is erroneously received, the receiver would ask for retransmission. However, instead of throwing away the erroneous packet, it can be combined with the retransmitted copies in order to improve both the reliability and the throughput. In these regimes, different ARQ schemes and different diversity combining schemes may be employed.

6. In Chapter 6, the CSR-HARQ scheme was studied under the assumption of perfect spectrum sensing. However, in practice spectrum sensing can never be perfect, hence mis-detection and false-alarm may occur. Therefore, as carried out in Chapter 5 for the CGBN-HARQ, it is important to analyze the throughput and delay of the CSR-HARQ scheme of Chapter 6 for non-ideal spectrum sensing.

7. Throughout this thesis, we have only considered single PR channel scenarios, and also assumed that there is a single pair of CR users, namely a CR transmitter and a CR receiver. Explicitly, the CSW-HARQ, CGBN-HARQ and CSR-HARQ schemes may be extended to the multi-user and multi-channel scenarios, where multiple pairs of CUs sense and share multiple PR channels. Naturally, in these scenarios the situation becomes more complicated, because the CUs may cooperate with each other in order to share important information, including sensing information, channel quality, hand-off, etc.

Glossary

A

ACK Positive Acknowledgement.

ARQ Automatic Repeat reQuest.

AWS Advanced Wireless Services.

B

BS Base Station.

C

CGBN Cognitive Go-Back-N.

CR Cognitive Radio.

CRC cyclic redundancy check.

CSR Cognitive Selective-Repeat.

CSW Cognitive Stop-and-Wait.

CU Cognitive Radio User.

D

DSA Dynamic Spectrum Access.

DTMC Discrete Time Markov Chain.

E

ED Energy Detection.

ETSI European Telecommunication Standard Institute.

F

FCC Federal Communication Commission.

FEC Forward Error Correction.

G

GBN Go-Back-N.

GHz Gigahertz.

H

HARQ Hybrid Automatic Repeat reQuest.

HSDPA High Speed Downlink Packet Access.

I

ISM Industrial, Scientific and Medical.

ITU International Telecommunication Union.

M

MAC Medium Access Control.

MCTC Multi-Component Turbo Coded.

MF Matched Filter.

N

NACK Negative Acknowledgement.

NTIA National Telecommunication and Information Administration.

O

OFDMA Orthogonal Frequency-Division Multiple Access.

OFF DTMC in OFF state, where channel is free from PUs.

ON DTMC in ON state, where channel is occupied by PUs.

P

PEP Packet Error Probability.

PMF Probability Mass Function.

PR Primary Radio.

PU Primary Radio User.

Q

QoS Quality-of-Service.

R

RCPC Rate Compatible Punctured Convolutional.

RS Reed-Solomon.

RTT Round-Trip-Time.

S

SDR Software Defined Radio.

SNR Signal-to-Noise Ratio.

SR Selective-Repeat.

SU Secondary User.

SW Stop-and-Wait.

T

TDMA Time-Division Multiple Access.

TS Time-Slot.

TTCM Turbo Trellis Coded Modulation.

TV Television.

U

UHF Ultra-High Frequency.

UNII Unlicensed National Information Infrastructure.

US United States.

V

VHF Very-High Frequency.

Bibliography

[1] A. U. Rehman, L. L. Yang, and L. Hanzo, "Performance of cognitive hybrid automatic repeat request: Go-back-n," in *IEEE 83rd Vehicular Technology Conference (VTC Spring)*, pp. 1–5, May 2016.

[2] J. Mitola, *Cognitive radio*. PhD thesis, Royal Institute of Technology, 2000.

[3] J. Mitola and G. Q. Maguire, "Cognitive radio: Making software radios more personal," *IEEE Personal Communications*, vol. 6, pp. 13–18, Aug 1999.

[4] A. Goldsmith, S. A. Jafar, I. Maric, and S. Srinivasa, "Breaking spectrum gridlock with cognitive radios: An information theoretic perspective," *Proceedings of the IEEE*, vol. 97, pp. 894–914, May 2009.

[5] FCC, "Et docket No. 02-155 spectrum policy task force report technical report," Nov 2002.

[6] G. Staple and K. Werbach, "The end of spectrum scarcity [spectrum allocation and utilization]," *IEEE Spectrum*, vol. 41, pp. 48–52, March 2004.

[7] J. Yang, "Spatial channel characterization for cognitive radios," Tech. Rep. UCB/ERL M05/8, Master's Thesis, EECS Department, University of California, Berkeley, Jan 2005.

[8] M. A. McHenry, P. A. Tenhula, D. McCloskey, D. A. Roberson, and C. S. Hood, "Chicago spectrum occupancy measurements & analysis and a long-term studies proposal," in *Proceedings of the First International Workshop on Technology and Policy for Accessing Spectrum (TAPAS)*, 2006.

[9] Q. Zhao and B. M. Sadler, "A survey of dynamic spectrum access," *IEEE Signal Processing Magazine*, vol. 24, pp. 79–89, May 2007.

[10] E. Hossain, D. Niyato, and Z. Han, *Dynamic Spectrum Access and Management in Cognitive Radio Networks*. Cambridge University Press, 2009.

[11] I. F. Akyildiz, W.-Y. Lee, M. C. Vuran, and S. Mohanty, "Next generation/dynamic spectrum access/cognitive radio wireless networks: A survey," *in Computer Networks Journal (Elsevier)*, vol. 50, pp. 2127–2159, Sept 2006.

[12] FCC, "Second report and order, washington, dc, (et docket no. 08-260)," Nov 2008.

[13] E. Hossain, D. Niyato, and Z. Han, *Dynamic spectrum access and Management in Cognitive Radio Networks*. Cambridge University Press, 2009.

[14] S. Haykin, "Cognitive radio: Brain-empowered wireless communications," *IEEE Journal on Selected Areas in Communications*, vol. 23, pp. 201–220, Feb 2005.

[15] FCC, "Notice of proposed rulemaking, in the matter of unlicensed operation in the tv broadcast bands and order (et docket no 04-186) and additional spectrum for unlicensed devices below 900 mhz and in the 3 ghz band (et docket no. 02-380), fcc 04-113," May 2004.

[16] I. F. Akyildiz, W.-Y. Lee, M. C. Vuran, and S. Mohanty, "A survey on spectrum management in cognitive radio networks," *in IEEE,Communications Magazine*, vol. 46, pp. 40–48, April 2008.

[17] E. Z. Tragos, S. Zeadally, A. G. Fragkiadakis, and V. A. Siris, "Spectrum assignment in cognitive radio networks: A comprehensive survey," *IEEE Communications Surveys Tutorials*, vol. 15, pp. 1108–1135, Third 2013.

[18] S. Lin and D. J. Costello, *Error Control Coding: Fundamentals and Applications*. Upper Saddle River, NJ: Prentice-Hall, 2nd ed., 1999.

[19] L. Hanzo, T. Liew, B. Yeap, R. Tee, and S. X. Ng, *Turbo coding, turbo equalisation and space-time coding: EXIT-chart-aided near-capacity designs for wireless channels, second edition*. John Wiley & Sons, 2011.

[20] S. Chang, "Theory of information feedback systems," *IRE Transactions on Information Theory*, vol. 2, pp. 29–40, September 1956.

[21] D. Bertsekas and R. Gallagher, *Data Networks*. Englewood Cliffs, NJ: Prentice Hall, 2nd ed., 1991.

[22] A. Leon-Garcia and I. Widjaja, *Communication Networks*. McGraw-Hill Education, 2004.

[23] J. M. Wozencraft and M. Horstein, "Digitalised communication over two-way channels," in *Fourth London Symp. Inform. Theory, London, UK*, Sept 1960.

[24] J. M. Wozencraft and M. Horstein, "Coding for two-way channels," 1961.

[25] "IEEE standard for local and metropolitan area networks part 16: Physical and medium access control layers for combined fixed and mobile operation in licensed bands and corrigendum 1," *IEEE Std 802.16e-2005 and IEEE Std 802.16-2004/Cor 1-2005 (Amendment and Corrigendum to IEEE Std 802.16-2004)*, pp. 1–822, Feb 2006.

[26] 3GPP TR 25.848 V4.0.0, "3rd generation partnership project; technical specification group radio access network; physical layer aspects of UTRA high speed downlink packet access (release 4)," March 2001.

[27] J. A. Stine and D. L. Portigal, "Spectrum 101: An introduction to spectrum management," tech. rep., DTIC Document, 2004.

[28] A. M. Foster, M. Cave, and R. W. Jones, "Radio spectrum management, module 5 ict regulation toolkit exective summary," tech. rep., DTIC Document, Jan 2007.

[29] C. T. C. III, *Dynamic spectrum access in cognitive radio networks*. PhD thesis, University of Maryland, College Park, 2006.

[30] Q. Zhao and B. M. Sadler, "A survey of dynamic spectrum access," *IEEE, Signal Processing Magazine*, vol. 24, no. 3, pp. 79–89, 2007.

[31] ITU Radio Regulations, "Chapter 11-frequencies, article 5 frequency allocations, section 4-table of frequency allocations," tech. rep., ITU, 2012.

[32] Cisco Visual networking index, "Global mobile data traffic forecast update, 2015-2020, white paper," Feb 2016.

[33] GSM Association, "The mobile economy," Nov 2016.

[34] S. Ravi and D. M. West, "Spectrum policy in india," 2015.

[35] D. Cabric, "Phd thesis on cognitive radios: System design perspective, University of California at Berkeley," 2007.

[36] FCC, "Et docket no 03-222 notice of proposed rule making and order," December 2003.

[37] M. H. Islam, C. L. Koh, S. W. Oh, X. Qing, Y. Y. Lai, C. Wang, Y. C. Liang, B. E. Toh, F. Chin, G. L. Tan, and W. Toh, "Spectrum survey in singapore: Occupancy measurements and analyses," in *3rd International Conference on Cognitive Radio Oriented Wireless Networks and Communications (CrownCom)*, pp. 1–7, May 2008.

[38] D. P. Satapathy and J. M. Peha, "Spectrum sharing without licenses: Opportunities and dangers," in *Telecommunications Policy Research Conference*, pp. 15–29, 1996.

[39] H. Salgado-Galicia, M. Sirbu, and J. M. Peha, "A narrowband approach to efficient pcs spectrum sharing through decentralized dca access policies," *IEEE Personal Communications*, vol. 4, pp. 24–35, Feb 1997.

[40] D. P. Satapathy and J. M. Peha, "Performance of unlicensed devices with a spectrum etiquette," in *IEEE Global Telecommunications Conference, GLOBECOM '97*, vol. 1, pp. 414–418, Nov 1997.

[41] D. P. Satapathy and J. M. Peha, "Etiquette modification for unlicensed spectrum: approach and impact," in *48th IEEE Vehicular Technology Conference*, vol. 1, May 1998.

[42] J. M. Peha, "Spectrum management policy options," *IEEE Communications Surveys*, vol. 1, pp. 2–8, First 1998.

[43] J. Zander, "Radio resource management in future wireless networks: requirements and limitations," *IEEE Communications Magazine*, vol. 35, pp. 30–36, Aug 1997.

[44] T. K. Fong, P. S. Henry, K. K. Leung, X. Qiu, and N. K. Shankaranarayanan, "Radio resource allocation in fixed broadband wireless networks," *IEEE Transactions on Communications*, vol. 46, pp. 806–818, Jun 1998.

[45] J. C. I. Chuang and N. R. Sollenberger, "Spectrum resource allocation for wireless packet access with application to advanced cellular internet service," *IEEE Journal on Selected Areas in Communications*, vol. 16, pp. 820–829, Aug 1998.

[46] I. F. Akyildiz, Y. Altunbasak, F. Fekri, and R. Sivakumar, "Adaptnet: An adaptive protocol suite for the next-generation wireless internet," *IEEE Communications Magazine*, vol. 42, no. 3, pp. 128–136, 2004.

[47] Y. Benkler, "Overcoming agoraphobia: Building the commons of the digitally networked environment," *Harv. JL & Tech.*, vol. 11, p. 287, 1997.

[48] W. Lehr and J. Crowcroft, "Managing shared access to a spectrum commons," in *First IEEE International Symposium on New Frontiers in Dynamic Spectrum Access Networks, DySPAN*, pp. 420–444, 2005.

[49] W. Kim, S. Y. Oh, M. Gerla, and J.-S. Park, "Cocast: multicast mobile ad hoc networks using cognitive radio," in *IEEE Military Communications Conference(MILCOM)*, pp. 1–7, IEEE, 2009.

[50] W. Kim, M. Gerla, S. Y. Oh, K. Lee, and A. Kassler, "Coroute: a new cognitive anypath vehicular routing protocol," *Wireless Communications and Mobile Computing*, vol. 11, no. 12, pp. 1588–1602, 2011.

[51] Z. Ji and K. J. R. Liu, "Cognitive radios for dynamic spectrum access-dynamic spectrum sharing: A game theoretical overview," *IEEE Communications Magazine*, vol. 45, no. 5, pp. 88–94, 2007.

[52] R. H. Coase, "The federal communications commission," *Journal of law and economics*, vol. 56, no. 4, pp. 879–915, 2013.

[53] D. N. Hatfield and P. J. Weiser, "Property rights in spectrum: Taking the next step," in *First IEEE International Symposium on New Frontiers in Dynamic Spectrum Access Networks DySPAN*, pp. 43–55, 2005.

[54] L. Xu, R. Tonjes, T. Paila, W. Hansmann, M. Frank, and M. Albrecht, "Drive-ing to the internet: Dynamic radio for ip services in vehicular environments," in *25th Annual IEEE Conference on Local Computer Networks, (LCN)*, pp. 281–289, 2000.

[55] K.-L. A. Yau, P. Komisarczuk, and P. D. Teal, "Cognitive radio-based wireless sensor networks: Conceptual design and open issues," in *IEEE 34th Conference on Local Computer Networks, LCN*, pp. 955–962, IEEE, 2009.

[56] E. Buracchini, "The software radio concept," *IEEE Communications Magazine*, vol. 38, pp. 138–143, Sep 2000.

[57] J. Neel, R. M. Buehrer, B. H. Reed, and R. P. Gilles, "Game theoretic analysis of a network of cognitive radios," in *The 45th Midwest Symposium on Circuits and Systems, MWSCAS*, vol. 3, pp. 409–412, Aug 2002.

[58] D. Cabric, S. M. Mishra, and R. W. Brodersen, "Implementation issues in spectrum sensing for cognitive radios," in *Conference on Signals, Systems and Computers, Conference Record of the Thirty-Eighth Asilomar*, vol. 1, pp. 772–776, Nov. 2004.

[59] "IEEE 802.22 working group on wireless regional area network enabling broadband wireless access using cognitive radio technology and spectrum sharing in white space," *IEEE Std 802.22-2005*, 2005.

[60] N. Devroye, P. Mitran, and V. Tarokh, "Achievable rates in cognitive radio channels," *IEEE Transactions on Information Theory*, vol. 52, pp. 1813–1827, May 2006.

[61] Y. C. Liang, Y. Zeng, E. C. Y. Peh, and A. T. Hoang, "Sensing-throughput tradeoff for cognitive radio networks," *IEEE Transactions on Wireless Communications*, vol. 7, pp. 1326–1337, April 2008.

[62] K. B. Letaief and W. Zhang, "Cooperative communications for cognitive radio networks," *Proceedings of the IEEE*, vol. 97, pp. 878–893, May 2009.

[63] H. A. Suraweera, P. J. Smith, and M. Shafi, "Capacity limits and performance analysis of cognitive radio with imperfect channel knowledge," *IEEE Transactions on Vehicular Technology*, vol. 59, pp. 1811–1822, May 2010.

[64] Y. C. Liang, K. C. Chen, G. Y. Li, and P. Mahonen, "Cognitive radio networking and communications: an overview," *IEEE Transactions on Vehicular Technology*, vol. 60, pp. 3386–3407, Sept 2011.

[65] E. Axell, G. Leus, E. G. Larsson, and H. V. Poor, "Spectrum sensing for cognitive radio : State-of-the-art and recent advances," *IEEE Signal Processing Magazine*, vol. 29, pp. 101–116, May 2012.

[66] S. Park, H. Kim, and D. Hong, "Cognitive radio networks with energy harvesting," *IEEE Transactions on Wireless Communications*, vol. 12, pp. 1386–1397, March 2013.

[67] X. Hong, J. Wang, C.-X. Wang, and J. Shi, "Cognitive radio in 5g: a perspective on energy-spectral efficiency trade-off," *IEEE Communications Magazine*, vol. 52, pp. 46–53, July 2014.

[68] A. Ahmad, S. Ahmad, M. H. Rehmani, and N. U. Hassan, "A survey on radio resource allocation in cognitive radio sensor networks," *IEEE Communications Surveys Tutorials*, vol. 17, pp. 888–917, Secondquarter 2015.

[69] E. Ahmed, A. Gani, S. Abolfazli, L. J. Yao, and S. U. Khan, "Channel assignment algorithms in cognitive radio networks: Taxonomy, open issues, and challenges," *IEEE Communications Surveys Tutorials,*, vol. 18, pp. 795–823, Firstquarter 2016.

[70] L. Zhang, M. Xiao, G. Wu, S. Li, and Y. C. Liang, "Energy-efficient cognitive transmission with imperfect spectrum sensing," *IEEE Journal on Selected Areas in Communications*, vol. 34, pp. 1320–1335, May 2016.

[71] O. B. Akan, O. Karli, and O. Ergul, "Cognitive radio sensor networks," *IEEE Network*, vol. 23, pp. 34 –40, July-August 2009.

[72] G. Vijay, E. B. A. Bdira, and M. Ibnkahla, "Cognition in wireless sensor networks: A perspective," *IEEE Sensors Journal*, vol. 11, no. 3, pp. 582–592, 2011.

[73] J. Han, W. S. Jeon, and D. G. Jeong, "Energy-efficient channel management scheme for cognitive radio sensor networks," *IEEE Transactions on Vehicular Technology*, vol. 60, no. 4, pp. 1905–1910, 2011.

[74] "IEEE standard definitions and concepts for dynamic spectrum access: Terminology relating to emerging wireless networks, system functionality, and spectrum management," *IEEE Std 1900.1-2008*, pp. 1–62, Oct 2008.

[75] "IEEE standard for information technology– local and metropolitan area networks– specific requirements– part 22: Cognitive wireless ran medium access control (mac) and physical layer (phy) specifications: Policies and procedures for operation in the tv bands," *IEEE Std 802.22-2011*, pp. 1–680, July 2011.

[76] M. Sherman, A. N. Mody, R. Martinez, C. Rodriguez, and R. Reddy, "IEEE standards supporting cognitive radio and networks, dynamic spectrum access and coexistence," *IEEE Communications Magazine*, vol. 46, pp. 72–79, July 2008.

[77] A. Patel, Z. Khan, S. N. Merchant, U. B. Desai, and L. Hanzo, "The achievable rate of interweave cognitive radio in the face of sensing errors," *IEEE Access*, vol. PP, pp. 1–1, Sept 2016.

[78] H. Mu and J. K. Tugnait, "Joint soft-decision cooperative spectrum sensing and power control in multiband cognitive radios," *IEEE Transactions on Signal Processing*, vol. 60, no. 10, pp. 5334–5346, 2012.

[79] R. A. Tannious and A. Nosratinia, "Cognitive radio protocols based on exploiting hybrid arq retransmissions," *IEEE Transactions on Wireless Communications*, vol. 9, no. 9, pp. 2833–2841, 2010.

[80] T. Yucek and H. Arslan, "A survey of spectrum sensing algorithms for cognitive radio applications," *IEEE Communications Surveys and Tutorials*, vol. 11, pp. 116–130, Quarter 2009.

[81] L. Luo and S. Roy, "Efficient spectrum sensing for cognitive radio networks via joint optimization of sensing threshold and duration," *IEEE Transactions on Communications*, vol. 60, no. 10, pp. 2851–2860, 2012.

[82] W. Tang, M. Z. Shakir, M. A. Imran, R. Tafazolli, and M.-S. Alouini, "Throughput analysis for cognitive radio networks with multiple primary users and imperfect spectrum sensing," *IET Communications*, vol. 6, pp. 2787–2795, November 2012.

[83] G. Ozcan and M. C. Gursoy, "Throughput of cognitive radio systems with finite block-length codes," *IEEE Journal on Selected Areas in Communications*, vol. 31, pp. 2541–2554, November 2013.

[84] B. Wang and K. J. R. Liu, "Advances in cognitive radio networks: A survey," *IEEE Journal of Selected Topics in Signal Processing*, vol. 5, pp. 5–23, Feb 2011.

[85] A. A. Khan, M. H. Rehmani, and M. Reisslein, "Cognitive radio for smart grids: Survey of architectures, spectrum sensing mechanisms, and networking protocols," *IEEE Communications Surveys Tutorials*, vol. 18, pp. 860–898, Firstquarter 2016.

[86] A. Ghasemi and E. S. Sousa, "Collaborative spectrum sensing for opportunistic access in fading environments," in *First IEEE International Symposium on New Frontiers in Dynamic Spectrum Access Networks, (DySPAN)*, pp. 131–136, Nov 2005.

[87] R. Umar and A. U. H. Sheikh, "A comparative study of spectrum awareness techniques for cognitive radio oriented wireless networks," *Physical Communication (Elsevier)*, vol. 9, pp. 148–170, 2013.

[88] Y. Xiao and F. Hu, *Cognitive Radio Networks*. Auerbach Publications, Jan 2009.

[89] J. Ma, G. Y. Li, and B. H. Juang, "Signal processing in cognitive radio," *Proceedings of the IEEE*, vol. 97, pp. 805–823, May 2009.

[90] D. Cabric, A. Tkachenko, and R. W. Brodersen, "Spectrum sensing measurements of pilot, energy, and collaborative detection," in *IEEE Military Communications conference MILCOM*, pp. 1–7, IEEE, 2006.

[91] R. Tandra and A. Sahai, "Fundamental limits on detection in low snr under noise uncertainty," in *International Conference on Wireless Networks, Communications and Mobile Computing,*, vol. 1, pp. 464–469 vol.1, June 2005.

[92] D. D. Ariananda, M. K. Lakshmanan, and H. Nikookar, "A survey on spectrum sensing techniques for cognitive radio," in *Second International Workshop on Cognitive Radio and Advanced Spectrum Management, CogART*, pp. 74–79, May 2009.

[93] H. Urkowitz, "Energy detection of unknown deterministic signals," *Proceedings of the IEEE*, vol. 55, no. 4, pp. 523–531, 1967.

[94] F. F. Digham, M.-S. Alouini, and M. K. Simon, "On the energy detection of unknown signals over fading channels," in *IEEE International Conference on Communications, ICC'03*, vol. 5, pp. 3575–3579, IEEE, 2003.

[95] H. Tang, "Some physical layer issues of wide-band cognitive radio systems," in *First IEEE International Symposium on New Frontiers in Dynamic Spectrum Access Networks, 2005. DySPAN 2005.*, pp. 151–159, IEEE, 2005.

[96] T. Yucek and H. Arslan, "Spectrum characterization for opportunistic cognitive radio systems," in *IEEE Military Communications conference, MILCOM*, pp. 1–6, IEEE, 2006.

[97] A. Ghasemi and E. S. Sousa, "Optimization of spectrum sensing for opportunistic spectrum access in cognitive radio networks," in *4th IEEE Consumer Communications and Networking Conference, CCNC*, pp. 1022–1026, 2007.

[98] M. Oner and F. K. Jondral, "Cyclostationarity-based methods for the extraction of the channel allocation information in a spectrum pooling system," in *Radio and Wireless Conference, 2004 IEEE*, pp. 279–282, IEEE, 2004.

[99] M. Ghozzi, F. Marx, M. Dohler, and J. Palicot, "Cyclostatilonarilty-based test for detection of vacant frequency bands," in *1st International Conference on Cognitive Radio Oriented Wireless Networks and Communications*, pp. 1–5, June 2006.

[100] K. Kim, I. A. Akbar, K. K. Bae, J.-S. Um, V. Spooner, and J. H. Reed, "Cyclostationary approaches to signal detection and classification in cognitive radio," in *2007 2nd IEEE International Symposium on New Frontiers in Dynamic Spectrum Access Networks*, pp. 212–215, IEEE, 2007.

[101] A. Sahai, R. Tandra, S. M. Mishra, and N. Hoven, "Fundamental design tradeoffs in cognitive radio systems," in *Proceedings of the first international workshop on Technology and policy for accessing spectrum*, p. 2, ACM, 2006.

[102] M. Gandetto, M. Guainazzo, and C. S. Regazzoni, "Use of time-frequency analysis and neural networks for mode identification in a wireless software-defined radio approach," *EURASIP Journal on Applied Signal Processing*, vol. 2004, pp. 1778–1790, 2004.

[103] R. Tandra and A. Sahai, "Snr walls for feature detectors," in *2nd IEEE International Symposium on New Frontiers in Dynamic Spectrum Access Networks, DySPAN*, pp. 559–570, April 2007.

[104] Y. Zeng, Y. C. Liang, A. T. Hoang, and R. Zhang, "A review on spectrum sensing for cognitive radio: challenges and solutions," *EURASIP Journal on Advances in Signal Processing*, vol. 2010, no. 1, p. 1, 2010.

[105] G. Ganesan and Y. Li, "Cooperative spectrum sensing in cognitive radio networks," in *First IEEE International Symposium on New Frontiers in Dynamic Spectrum Access Networks, DySPAN*, pp. 137–143, 2005.

[106] C. Guo, T. Zhang, Z. Zeng, and C. Feng, "Investigation on spectrum sharing technology based on cognitive radio," in *2006 First International Conference on Communications and Networking in China*, pp. 1–5, IEEE, 2006.

[107] I. F. Akyildiz, B. F. Lo, and R. Balakrishnan, "Cooperative spectrum sensing in cognitive radio networks: A survey," *In Physical Communication*, vol. 4, no. 1, pp. 40–62, 2011.

[108] T. Weiss, J. Hillenbrand, A. Krohn, and F. K. Jondral, "Efficient signaling of spectral resources in spectrum pooling systems," in *Proc. 10th Symposium on Communications and Vehicular Technology (SCVT)*, 2003.

[109] E. Visotsky, S. Kuffner, and R. Peterson, "On collaborative detection of tv transmissions in support of dynamic spectrum sharing," in *First IEEE International Symposium on New Frontiers in Dynamic Spectrum Access Networks, 2005. DySPAN 2005.*, pp. 338–345, IEEE, 2005.

[110] A. F. Cattoni, I. Minetti, M. Gandetto, R. Niu, P. K. Varshney, and C. S. Regazzoni, "A spectrum sensing algorithm based on distributed cognitive models," in *Proc. SDR Forum Technical Conference*, 2006.

[111] M. Gandetto and C. S. Regazzoni, "Spectrum sensing: A distributed approach for cognitive terminals," *IEEE Journal on Selected Areas in Communications*, vol. 25, no. 3, pp. 546–557, 2007.

[112] J. Marinho and E. Monteiro, "Cognitive radio: survey on communication protocols, spectrum decision issues, and future research directions," *Wireless Networks*, vol. 18, no. 2, pp. 147–164, 2012.

[113] J. Zhao, H. Zheng, and G.-H. Yang, "Distributed coordination in dynamic spectrum allocation networks," in *First IEEE International Symposium on New Frontiers in Dynamic Spectrum Access Networks, DySPAN*, pp. 259–268, IEEE, 2005.

[114] S. Krishnamurthy, M. Thoppian, S. Venkatesan, and R. Prakash, "Control channel based mac-layer configuration, routing and situation awareness for cognitive radio networks," in *IEEE Military Communications Conference, (MILCOM)*, pp. 455–460, IEEE, 2005.

[115] L. Giupponi and A. I. Pérez-Neira, "Fuzzy-based spectrum handoff in cognitive radio networks," in *3rd International Conference on Cognitive Radio Oriented Wireless Networks and Communications (CrownCom)*, pp. 1–6, IEEE, 2008.

[116] I. F. Akyildiz, W.-Y. Lee, and K. R. Chowdhury, "CRAHNs: Cognitive radio ad hoc networks," *Ad Hoc Networks*, vol. 7, no. 5, pp. 810–836, 2009.

[117] FCC, "Second memorandum opinion and order (docket no. 08-260), washington, DC, USA," Sept 2010.

[118] FCC, "Auction 97: Advanced wireless services (AWS-3)," Nov 2015. [Online; accessed 26-Sept-2016].

[119] FCC, "Report and order and second furthre notice of proposed rulemaking, washington, dc, USA, (gn docket no. 12-354)," Apr 2015.

[120] FCC, "Notice of proposed rulemaking, washington, DC, USA, et docket no. 13-49)," Feb 2013.

[121] J. Lansford, J. Kenney, P. Ecclesine, T. Yucek, and P. Spaanderman, "Final report of DSRC coexistence tiger team, tech. rep. IEEE 802.11-15/0347r0," March 2015.

[122] *Ofcom Consultation on the U.K. Preparations for the World Radio Communication Conference 2015 (WRC), London, U.K June*, 2014.

[123] *Implementing TV White Spaces, OFCOM, London, U.K, Feb*, 2015.

[124] *Framework for the Use of Certain Non-Broadcasting Applications in the Television Broadcasting Bands Below 698 MHz, SMSE- 012-12, Industry Canada, Oct*, 2012.

[125] *White Space Devices (WSDs) (RSS-222), Industry Canada, Feb*, 2015.

[126] T. Wang, G. Li, J. Ding, Q. Miao, J. Li, and Y. Wang, "5g spectrum: is china ready?," *IEEE Communications Magazine*, vol. 53, pp. 58–65, July 2015.

[127] R. A. Comroe and D. J. Costello, "ARQ schemes for data transmission in mobile radio systems," *IEEE Transactions on Vehicular Technology*, vol. 33, pp. 88–97, Aug 1984.

[128] S. Lin and P. S. Yu, "A hybrid ARQ scheme with parity retransmission for error control of satellite channels," *IEEE Transactions on Communications*, vol. 30, pp. 1701–1719, July 1982.

[129] H. A. Ngo and L. Hanzo, "Hybrid automatic-repeat-request systems for cooperative wireless communications," *IEEE Communications Surveys Tutorials*, vol. 16, pp. 25–45, First 2014.

[130] E. M. Sozer, M. Stojanovic, and J. G. Proakis, "Underwater acoustic networks," *IEEE Journal of Oceanic Engineering*, vol. 25, no. 1, pp. 72–83, 2000.

[131] H. Jianhua, K. R. Subramanian, Y. ZongKai, and C. Wenqing, "Analysis of a new broadcast protocol for satellite communications," *IEEE Communications Letters*, vol. 4, pp. 423–425, Dec 2000.

[132] P. A. Chou, A. E. Mohr, A. Wang, and S. Mehrotra, "Error control for receiver-driven layered multicast of audio and video," *IEEE Transactions on Multimedia*, vol. 3, pp. 108–122, Mar 2001.

[133] B. Zhao and M. C. Valenti, "Practical relay networks: a generalization of hybrid-ARQ," *IEEE Journal on Selected Areas in Communications*, vol. 23, pp. 7–18, Jan 2005.

[134] R. Zhang and L. Hanzo, "Superposition-aided delay-constrained hybrid automatic repeat request," *IEEE Transactions on Vehicular Technology*, vol. 59, pp. 2109–2115, May 2010.

[135] H. Chen, R. G. Maunder, and L. Hanzo, "Low-complexity multiple-component turbo-decoding-aided hybrid ARQ," *IEEE Transactions on Vehicular Technology*, vol. 60, pp. 1571–1577, May 2011.

[136] H. Chen, R. G. Maunder, and L. Hanzo, "Lookup-table-based deferred-iteration aided low-complexity turbo hybrid ARQ," *IEEE Transactions on Vehicular Technology*, vol. 60, pp. 3045–3053, Sept 2011.

[137] H. Chen, R. G. Maunder, and L. Hanzo, "Deferred-iteration aided low-complexity turbo hybrid ARQ relying on a look-up table," in *IEEE Global Telecommunications Conference (GLOBECOM)*, pp. 1–5, Dec 2011.

[138] S. De, A. Sharma, R. Jantti, and D. H. Cavdar, "Channel adaptive stop-and-wait automatic repeat request protocols for short-range wireless links," *IET Communications*, vol. 6, pp. 2128–2137, September 2012.

[139] "IEEE standard for local and metropolitan area networks part 20: Air interface for mobile broadband wireless access systems supporting vehicular mobilityphysical and media access control layer specification," *IEEE Std 802.20-2008*, pp. 1–1039, Aug 2008.

[140] "IEEE standard for local and metropolitan area networks part 16: Air interface for broadband wireless access systems amendment 3: Advanced air interface," *IEEE Std 802.16m-2011(Amendment to IEEE Std 802.16-2009)*, pp. 1–1112, May 2011.

[141] "IEEE standard for wireless man-advanced air interface for broadband wireless access systems," *IEEE Std 802.16.1-2012*, pp. 1–1090, Sept 2012.

[142] B. Harris and K. C. Morgan, "Binary symmetric decision feedback systems," *American Institute of Electrical Engineers, Part I: Communication and Electronics, Transactions of the*, vol. 77, pp. 436–443, Sept 1958.

[143] C. E. Shannon, "Two-way communication channels," in *Proc. 4th Berkeley Symp. Math. Stat. Prob*, vol. 1, pp. 611–644, University of California Press, 1961.

[144] B. Reiffen, W. G. Schmidt, and H. L. Yudkin, "The design of an error-free data transmission system for telephone circuits," *American Institute of Electrical Engineers, Part I: Transactions of the Communication and Electronics*, vol. 80, pp. 224–231, July 1961.

[145] W. R. Cowell and H. O. Burton, "Computer simulation of the use of group codes with retransmission on a gilbert burst channel," *American Institute of Electrical Engineers, Part I: Transactions of the Communication and Electronics*, vol. 80, pp. 577–585, Jan 1962.

[146] R. Benice and A. H. Frey, "Comparisons of error control techniques," *IEEE Transactions on Communication Technology*, vol. 12, pp. 146–154, December 1964.

[147] R. Benice and A. Frey, "An analysis of retransmission systems," *IEEE Transactions on Communication Technology*, vol. 12, pp. 135–145, December 1964.

[148] H. O. Burton and D. D. Sullivan, "Errors and error control," *Proceedings of the IEEE*, vol. 60, pp. 1293–1301, Nov 1972.

[149] R. Stuart, "An insert system for use with feedback communication links," *IEEE Transactions on Communications Systems,*, vol. 11, pp. 142–143, March 1963.

[150] H. Chen, R. G. Maunder, and L. Hanzo, "A survey and tutorial on low-complexity turbo coding techniques and a holistic hybrid ARQ design example," *IEEE Communications Surveys Tutorials*, vol. 15, pp. 1546–1566, Fourth 2013.

[151] E. Rocher and R. Pickholtz, "An analysis of the effectiveness of hybrid transmission schemes," *IBM Journal of Research and Development*, vol. 14, no. 4, pp. 426–433, 1970.

[152] D. Mandelbaum, "An adaptive-feedback coding scheme using incremental redundancy (corresp.)," *IEEE Transactions on Information Theory*, vol. 20, pp. 388–389, May 1974.

[153] S. Kallel, "Complementary punctured convolutional (cpc) codes and their applications," *IEEE Transactions on Communications*, vol. 43, no. 6, pp. 2005–2009, 1995.

[154] Q. Chen and P. Fan, "On the performance of type-iii hybrid ARQ with rcpc codes," in *14th IEEE Proceedings on Personal, Indoor and Mobile Radio Communications (PIMRC)*, vol. 2, pp. 1297–1301, Sept 2003.

[155] C.-X. Wang, H.-G. Ryu, H.-H. Chen, and Y. He, "Hybrid ARQ with rate adaptation in multi-band ofdm uwb systems," in *IEEE International Conference on Communications ICC'09*, pp. 1–5, IEEE, 2009.

[156] Q. Yang and V. Bhargava, "Optimum coding design for type-I hybrid ARQ error control schemes," *Electronics Letters*, vol. 25, pp. 1595–1596, Nov 1989.

[157] H. Liu and M. E. Zarki, "Performance of H.263 video transmission over wireless channels using hybrid ARQ," *IEEE Journal on Selected Areas in Communications*, vol. 15, pp. 1775–1786, Dec 1997.

[158] Q. Zhang and S. A. Kassam, "Hybrid ARQ with selective combining for fading channels," *IEEE Journal on Selected Areas in Communications*, vol. 17, pp. 867–880, May 1999.

[159] E. Malkamaki and H. Leib, "Performance of truncated type-II hybrid ARQ schemes with noisy feedback over block fading channels," *IEEE Transactions on Communications*, vol. 48, pp. 1477–1487, Sep 2000.

[160] S. Marcille, P. Ciblat, and C. J. L. Martret, "Resource allocation for type-I HARQ based wireless ad hoc networks," *IEEE Wireless Communications Letters*, vol. 1, pp. 597–600, December 2012.

[161] K. Xu, W. Ma, L. Zhu, Y. Xu, Y. Gao, D. Zhang, and W. Xie, "NTC-HARQ: Network-turbo-coding based HARQ protocol for wireless broadcasting system," *IEEE Transactions on Vehicular Technology*, vol. 64, pp. 4633–4644, Oct 2015.

[162] C. Zhu, Y. Huo, B. Zhang, R. Zhang, M. El-Hajjar, and L. Hanzo, "Adaptive-truncated-HARQ-aided layered video streaming relying on interlayer FEC coding," *IEEE Transactions on Vehicular Technology*, vol. 65, pp. 1506–1521, March 2016.

[163] A. R. K. Sastry, "Improving automatic repeat request (ARQ) performance on satellite channels under high error rate conditions," *IEEE Transactions on Communications*, vol. 23, pp. 436–439, Apr 1975.

[164] S. Lin, D. J. Costello, and M. J. Miller, "Automatic-repeat-request error-control schemes," *IEEE Communications Magazine*, vol. 22, pp. 5–17, December 1984.

[165] S. Kallel, "Analysis of a type II hybrid ARQ scheme with code combining," *IEEE Transactions on Communications*, vol. 38, pp. 1133–1137, Aug 1990.

[166] L. Hanzo and J. Streit, "Adaptive low-rate wireless videophone schemes," *IEEE Transactions on Circuits and Systems for Video Technology*, vol. 5, pp. 305–318, Aug 1995.

[167] M. Zorzi, R. R. Rao, and L. B. Milstein, "Arq error control for fading mobile radio channels," *IEEE Transactions on Vehicular Technology*, vol. 46, pp. 445–455, May 1997.

[168] G. Caire and D. Tuninetti, "The throughput of hybrid-ARQ protocols for the gaussian collision channel," *IEEE Transactions on Information Theory*, vol. 47, pp. 1971–1988, Jul 2001.

[169] A. C. K. Soong, S.-J. Oh, A. D. Damnjanovic, and Y. C. Yoon, "Forward high-speed wireless packet data service in is-2000 - 1 times;ev-dv," *IEEE Communications Magazine*, vol. 41, pp. 170–177, Aug 2003.

[170] B. Zhao and M. C. Valenti, "Practical relay networks: a generalization of hybrid-ARQ," *IEEE Journal on Selected Areas in Communications*, vol. 23, pp. 7–18, Jan 2005.

[171] K. C. Beh, A. Doufexi, and S. Armour, "Performance evaluation of hybrid ARQ schemes of 3GPP LTE OFDMA system," in *IEEE 18th International Symposium on Personal, Indoor and Mobile Radio Communications*, pp. 1–5, Sept 2007.

[172] D. Kim, Y. Choi, S. Jin, K. Han, and S. Choi, "A mac/phy cross-layer design for efficient ARQ protocols," *IEEE Communications Letters*, vol. 12, pp. 909–911, December 2008.

[173] D. Nguyen, T. Tran, T. Nguyen, and B. Bose, "Wireless broadcast using network coding," *IEEE Transactions on Vehicular Technology*, vol. 58, pp. 914–925, Feb 2009.

[174] M. C. Vuran and I. F. Akyildiz, "Error control in wireless sensor networks: A cross layer analysis," *IEEE/ACM Transactions on Networking*, vol. 17, pp. 1186–1199, Aug 2009.

[175] R. Zhang and L. Hanzo, "A unified treatment of superposition coding aided communications: Theory and practice," *IEEE Communications Surveys Tutorials*, vol. 13, pp. 503–520, Third 2011.

[176] Y. I. Seo and D. K. Sung, "Virtually dedicated resource allocation for VoIP traffic in the downlink mobile wimax system with hybrid ARQ," *IEEE Transactions on Vehicular Technology*, vol. 60, pp. 514–527, Feb 2011.

[177] J. So, "Performance analysis of VoIP services in mobile WiMAX systems with a hybrid ARQ scheme," *IEEE Journal of Communications and Networks*, vol. 14, pp. 510–517, Oct 2012.

[178] B. Zhang, H. Chen, M. El-Hajjar, R. G. Maunder, and L. Hanzo, "Distributed multiple-component turbo codes for cooperative hybrid ARQ," *IEEE Signal Processing Letters*, vol. 20, pp. 599–602, June 2013.

[179] M. Chitre and W. S. Soh, "Reliable point-to-point underwater acoustic data transfer: To juggle or not to juggle?," *IEEE Journal of Oceanic Engineering*, vol. 40, pp. 93–103, Jan 2015.

[180] M. Chitre and W. S. Soh, "Reliable point-to-point underwater acoustic data transfer: To juggle or not to juggle?," *IEEE Journal of Oceanic Engineering*, vol. 40, pp. 93–103, Jan 2015.

[181] N. D. K. Liyanage, C. A. Abeywickrama, P. M. I. U. Kumari, S. A. D. Silva, and C. B. Wavegedara, "Performance investigation of hybrid ARQ in HSDPA systems with AMC," in *Moratuwa Engineering Research Conference (MERCon)*, pp. 126–131, April 2016.

[182] B. Makki, T. Eriksson, and T. Svensson, "On the performance of the relay-ARQ networks," *IEEE Transactions on Vehicular Technology*, vol. 65, pp. 2078–2096, April 2016.

[183] C. Cormio and K. R. Chowdhury, "A survey on MAC protocols for cognitive radio networks," *Ad Hoc Networks*, vol. 7, no. 7, pp. 1315 – 1329, 2009.

[184] A. D. Domenico, E. C. Strinati, and M. D. Benedetto, "A survey on MAC strategies for cognitive radio networks," *IEEE Communications Surveys and Tutorials,*, vol. 14, pp. 21–44, First 2012.

[185] G. Yue, X. Wang, and M. Madihian, "Design of anti-jamming coding for cognitive radio," in *IEEE Global Telecommunications Conference, 2007*, pp. 4190–4194, Nov 2007.

[186] G. Yue and X. Wang, "Design of efficient ARQ schemes with anti-jamming coding for cognitive radios," in *IEEE Wireless Communications and Networking Conference (WCNC)*, pp. 1–6, April 2009.

[187] Y. Liu, Z. Feng, and P. Zhang, "A novel ARQ scheme based on network coding theory in cognitive radio networks," in *IEEE International Conference on Wireless Information Technology and Systems (ICWITS)*, pp. 1–4, Aug 2010.

[188] B. Makki, A. G. I. Amat, and T. Eriksson, "HARQ feedback in spectrum sharing networks," *IEEE Communications Letters*, vol. 16, pp. 1337–1340, September 2012.

[189] B. Makki, T. Svensson, and M. Zorzi, "Finite block-length analysis of spectrum sharing networks using rate adaptation," *IEEE Transactions on Communications*, vol. 63, pp. 2823–2835, Aug 2015.

[190] W. Liang, H. V. Nguyen, S. X. Ng, and L. Hanzo, "Adaptive-TTCM-aided near-instantaneously adaptive dynamic network coding for cooperative cognitive radio networks," *IEEE Transactions on Vehicular Technology*, vol. 65, pp. 1314–1325, March 2016.

[191] J. C. F. Li, W. Zhang, A. Nosratinia, and J. Yuan, "SHARP: Spectrum harvesting with ARQ retransmission and probing in cognitive radio," *IEEE Transactions on Communications*, vol. 61, pp. 951–960, March 2013.

[192] D. Hamza and S. Aissa, "Enhanced primary and secondary performance through cognitive relaying and leveraging primary feedback," *IEEE Transactions on Vehicular Technology*, vol. 63, pp. 2236–2247, Jun 2014.

[193] J. S. Harsini and M. Zorzi, "Transmission strategy design in cognitive radio systems with primary ARQ control and QoS provisioning," *IEEE Transactions on Communications*, vol. 62, pp. 1790–1802, June 2014.

[194] W. C. Ao and K. C. Chen, "End-to-end HARQ in cognitive radio networks," in *IEEE Wireless Communications and Networking Conference (WCNC)*, pp. 1–6, April 2010.

[195] S.Touati, H. Boujemaa, and N. Abed, "Cooperative ARQ protocols for underlay cognitive radio networks," in *Proceedings of the 21st European Signal Processing Conference (EUSIPCO)*, pp. 1–5, Sept 2013.

[196] W. Liang, S. X. Ng, J. Feng, and L. Hanzo, "Pragmatic distributed algorithm for spectral access in cooperative cognitive radio networks," *IEEE Transactions on Communications*, vol. 62, pp. 1188–1200, April 2014.

[197] J. Hu, L. L. Yang, and L. Hanzo, "Maximum average service rate and optimal queue scheduling of delay-constrained hybrid cognitive radio in nakagami fading channels," *IEEE Transactions on Vehicular Technology*, vol. 62, pp. 2220–2229, Jun 2013.

[198] S. Y. Jeon and D. H. Cho, "An ARQ mechanism considering resource and traffic priorities in cognitive radio systems," *IEEE Communications Letters*, vol. 13, pp. 504–506, July 2009.

[199] R. E. Ramos and K. Madani, "A novel generic distributed intelligent re-configurable mobile network architecture," in *53rd IEEE Vehicular Technology Conference, (VTC)*, vol. 3, pp. 1927–1931, May 2001.

[200] D. Cabric and R. W. Brodersen, "Physical layer design issues unique to cognitive radio systems," in *IEEE 16th International Symposium on Personal, Indoor and Mobile Radio Communications*, vol. 2, pp. 759–763 Vol. 2, Sept 2005.

[201] T. Fujii and Y. Suzuki, "Ad-hoc cognitive radio - development to frequency sharing system by using multi-hop network," in *First IEEE International Symposium on New Frontiers in Dynamic Spectrum Access Networks (DySPAN)*, pp. 589–592, Nov 2005.

[202] N. Devroye, P. Mitran, and V. Tarokh, "Limits on communications in a cognitive radio channel," *IEEE Communications Magazine*, vol. 44, pp. 44–49, June 2006.

[203] T. Fujii, Y. Kamiya, and Y. Suzuki, "Multi-band ad-hoc cognitive radio for reducing inter system interference," in *IEEE 17th International Symposium on Personal, Indoor and Mobile Radio Communications*, pp. 1–5, Sept 2006.

[204] P. Mahonen, M. Petrova, J. Riihijärvi, and M. Wellens, "Cognitive wireless networks: your network just became a teenager," in *Proceedings of IEEE INFOCOM*, 2006.

[205] A. Baker, S. Ghosh, A. Kumar, and M. Bayoumi, "Notice of violation of IEEE publication principles LDPC decoder: A cognitive radio perspective for next generation (XG) communication," *IEEE Circuits and Systems Magazine*, vol. 7, pp. 24–37, Third 2007.

[206] T. Weingart, D. C. Sicker, and D. Grunwald, "A statistical method for reconfiguration of cognitive radios," *IEEE Wireless Communications*, vol. 14, pp. 34–40, August 2007.

[207] H. Su and X. Zhang, "Cross-layer based opportunistic MAC protocols for QoS provisionings over cognitive radio wireless networks," *IEEE Journal on Selected Areas in Communications*, vol. 26, pp. 118–129, Jan 2008.

[208] G. Yue, "Antijamming coding techniques," *IEEE Signal Processing Magazine*, vol. 25, pp. 35–45, November 2008.

[209] H. Kushwaha, Y. Xing, R. Chandramouli, and H. Heffes, "Reliable multimedia transmission over cognitive radio networks using fountain codes," *Proceedings of the IEEE*, vol. 96, pp. 155–165, Jan 2008.

[210] S. lun Cheng and Y. Zhen, "Cross-layer combining of power control and adaptive modulation with truncated ARQ for cognitive radios," *The Journal of China Universities of Posts and Telecommunications*, vol. 15, no. 3, pp. 19–23, 2008.

[211] G. Yue and X. Wang, "Anti-jamming coding techniques with application to cognitive radio," *IEEE Transactions on Wireless Communications*, vol. 8, pp. 5996–6007, December 2009.

[212] R. A. Roshid, N. M. Aripin, N. Fisal, S. H. S. Ariffin, and S. K. S. Yusof, "Integration of cooperative sensing and transmission," *IEEE Vehicular Technology Magazine*, vol. 5, pp. 46–53, Sept 2010.

[213] Y. Qi, R. Hoshyar, M. A. Imran, and R. Tafazolli, "H^2-ARQ-Relaying: Spectrum and energy efficiency perspectives," *IEEE Journal on Selected Areas in Communications*, vol. 29, pp. 1547–1558, September 2011.

[214] S. M. Cheng, W. C. Ao, and K. C. Chen, "Efficiency of a cognitive radio link with opportunistic interference mitigation," *IEEE Transactions on Wireless Communications*, vol. 10, pp. 1715–1720, June 2011.

[215] S. Akin and M. C. Gursoy, "Performance analysis of cognitive radio systems under qos constraints and channel uncertainty," *IEEE Transactions on Wireless Communications*, vol. 10, pp. 2883–2895, September 2011.

[216] J. Liu, W. Chen, Z. Cao, and Y. J. Zhang, "Delay optimal scheduling for cognitive radios with cooperative beamforming: A structured matrix-geometric method," *IEEE Transactions on Mobile Computing*, vol. 11, pp. 1412–1423, Aug 2012.

[217] L. Musavian and T. Le-Ngoc, "Cross-layer design for cognitive radios with joint amc and ARQ under delay qos constraint," in *8th International Wireless Communications and Mobile Computing Conference (IWCMC)*, pp. 419–424, Aug 2012.

[218] Y. Yang, H. Ma, and S. Aissa, "Cross-layer combining of adaptive modulation and truncated ARQ under cognitive radio resource requirements," *IEEE Transactions on Vehicular Technology*, vol. 61, pp. 4020–4030, Nov 2012.

[219] J. Wang, A. Huang, L. Cai, and W. Wang, "On the queue dynamics of multiuser multichannel cognitive radio networks," *IEEE Transactions on Vehicular Technology*, vol. 62, pp. 1314–1328, March 2013.

[220] W. C. Ao and K. C. Chen, "Error control for local broadcasting in heterogeneous wireless ad hoc networks," *IEEE Transactions on Communications*, vol. 61, pp. 1510–1519, April 2013.

[221] R. Andreotti, I. Stupia, V. Lottici, F. Giannetti, and L. Vandendorpe, "Goodput-based link resource adaptation for reliable packet transmissions in BIC-OFDM cognitive radio networks," *IEEE Transactions on Signal Processing*, vol. 61, pp. 2267–2281, May 2013.

[222] Y. Wang, P. Ren, F. Gao, and Z. Su, "A hybrid underlay/overlay transmission mode for cognitive radio networks with statistical quality-of-service provisioning," *IEEE Transactions on Wireless Communications*, vol. 13, pp. 1482–1498, March 2014.

[223] G. Ozcan, M. C. Gursoy, and S. Gezici, "Error rate analysis of cognitive radio transmissions with imperfect channel sensing," *IEEE Transactions on Wireless Communications*, vol. 13, pp. 1642–1655, March 2014.

[224] J. S. Harsini and M. Zorzi, "Transmission strategy design in cognitive radio systems with primary ARQ control and qos provisioning," *IEEE Transactions on Communications*, vol. 62, pp. 1790–1802, June 2014.

[225] Y. C. Chen, I. W. Lai, K. C. Chen, W. T. Chen, and C. H. Lee, "Transmission latency and reliability trade-off in path-time coded cognitive radio ad hoc networks," in *IEEE Global Communications Conference*, pp. 1084–1089, Dec 2014.

[226] J. Li, T. Luo, J. Gao, and G. Yue, "A mac protocol for link maintenance in multichannel cognitive radio ad hoc networks," *Journal of Communications and Networks*, vol. 17, pp. 172–183, April 2015.

[227] Y. Zou, J. Zhu, L. Yang, Y. C. Liang, and Y. D. Yao, "Securing physical-layer communications for cognitive radio networks," *IEEE Communications Magazine*, vol. 53, pp. 48–54, September 2015.

[228] B. Makki, T. Svensson, and M. Zorzi, "Finite block-length analysis of spectrum sharing networks: Interference-constrained scenario," *IEEE Wireless Communications Letters*, vol. 4, pp. 433–436, Aug 2015.

[229] D. W. K. Ng, E. S. Lo, and R. Schober, "Multiobjective resource allocation for secure communication in cognitive radio networks with wireless information and power transfer," *IEEE Transactions on Vehicular Technology*, vol. 65, pp. 3166–3184, May 2016.

[230] A. U. Rehman, L. L. Yang, and L. Hanzo, "Performance of cognitive hybrid automatic repeat request: Stop-and-wait," in *IEEE 81st Vehicular Technology Conference (VTC Spring)*, pp. 1–5, May 2015.

[231] A. U. Rehman, C. Dong, L. L. Yang, and L. Hanzo, "Performance of cognitive stop-and-wait hybrid automatic repeat request in the face of imperfect sensing," *IEEE Access*, vol. 4, pp. 5489–5508, July 2016.

[232] A. He, J. Gaeddert, K. K. Bae, T. R. Newman, J. H. Reed, L. Morales, and C.-H. Park, "Development of a case-based reasoning cognitive engine for IEEE 802.22 WRAN applications," *ACM SIGMOBILE Mobile Computing and Communications Review*, vol. 13, no. 2, pp. 37–48, 2009.

[233] G. Ganesan and Y. Li, "Cooperative spectrum sensing in cognitive radio, part I: Two user networks," *IEEE Transactions on Wireless Communications,*, vol. 6, pp. 2204–2213, June 2007.

[234] S. Stotas and A. Nallanathan, "Enhancing the capacity of spectrum sharing cognitive radio networks," *IEEE Transactions on Vehicular Technology*, vol. 60, no. 8, pp. 3768–3779, 2011.

[235] J. Li and Y. Q. Zhao, "Resequencing analysis of stop-and-wait ARQ for parallel multichannel communications," *IEEE/ACM Transactions on Networking*, vol. 17, pp. 817–830, June 2009.

[236] Y. Qin and L. L. Yang, "Throughput analysis of stop-and-wait automatic repeat request scheme for network coding nodes," in *IEEE 71st Vehicular Technology Conference (VTC 2010-Spring)*, pp. 1–5, May 2010.

[237] Y. Qin and L. L. Yang, "Steady-state throughput analysis of network coding nodes employing stop-and-wait automatic repeat request," *IEEE/ACM Transactions on Networking*, vol. 20, pp. 1402–1411, Oct 2012.

[238] J. C. Kao, "Performance analysis of relay-assisted network-coding ARQ with space-time cooperation in wireless relay networks," *IEEE Transactions on Wireless Communications*, vol. 13, pp. 4132–4145, Aug 2014.

[239] S. D. Roy and S. Kundu, "Throughput/delay performance of secondary user in spectrum underlay," in *International Conference on Computer and Communication Technology (ICCCT)*, pp. 800–805, Sept 2010.

[240] S. Akin and M. C. Gursoy, "Performance analysis of cognitive radio systems under qos constraints and channel uncertainty," *IEEE Transactions on Wireless Communications*, vol. 10, pp. 2883–2895, September 2011.

[241] C. Lott, O. Milenkovic, and E. Soljanin, "Hybrid ARQ: Theory, state of the art and future directions," in *IEEE Information Theory Workshop on Information Theory for Wireless Networks*, pp. 1–5, July 2007.

[242] R. Fantacci, "Queuing analysis of the selective repeat automatic repeat request protocol wireless packet networks," *IEEE Transactions on Vehicular Technology*, vol. 45, pp. 258–264, May 1996.

[243] L. Badia, M. Rossi, and M. Zorzi, "SR ARQ packet delay statistics on markov channels in the presence of variable arrival rate," *IEEE Transactions on Wireless Communications*, vol. 5, pp. 1639–1644, July 2006.

[244] R. A. Howard, *Dynamic Probabilistic Systems: Markov models*. New York: John Wiley and Sons, 1971.

[245] R. A. Horn and C. R. Johnson, *Matrix analysis*. Cambridge university press, 2012.

[246] A. U. Rehman, C. Dong, V. A. Thomas, L. L. Yang, and L. Hanzo, "Throughput and delay analysis of cognitive Go-Back-N hybrid automatic repeat request using discrete-time markov modelling," *Accepted in IEEE Access*, Nov 2016.

[247] A. Patel, M. Z. A. Khan, S. N. Merchant, U. B. Desai, and L. Hanzo, "Achievable rates of underlay-based cognitive radio operating under rate limitation," *IEEE Transactions on Vehicular Technology*, vol. 65, pp. 7149–7159, Sept 2016.

[248] W.-Y. Lee and I. F. Akyildiz, "Optimal spectrum sensing framework for cognitive radio networks," *IEEE Transactions on Wireless Communications*, vol. 7, pp. 3845–3857, October 2008.

[249] Y. Saleem and M. H. Rehmani, "Primary radio user activity models for cognitive radio networks: A survey," *Journal of Network and Computer Applications*, vol. 43, pp. 1–16, 2014.

[250] X. Kang, Y. C. Liang, H. K. Garg, and L. Zhang, "Sensing-based spectrum sharing in cognitive radio networks," *IEEE Transactions on Vehicular Technology*, vol. 58, no. 8, pp. 4649–4654, 2009.

[251] Y. Hayashida and M. Komatsu, "Delay performance of Go-back-N ARQ scheme with markovian error channel," in *2nd International Conference on Personal Communications: Gateway to the 21st Century*, vol. 1, pp. 448–452 vol.1, Oct 1993.

[252] M. Zorzi and R. R. Rao, "Performance of ARQ Go-Back-N protocol in markov channels with unreliable feedback: delay analysis," in *IEEE Fourth International Conference on Universal Personal Communications*, pp. 481–485, Nov 1995.

[253] W. Turin, "Throughput analysis of the go-back-n protocol in fading radio channels," *IEEE Journal on Selected Areas in Communications,*, vol. 17, no. 5, pp. 881–887, 1999.

[254] S. S. Chakraborty and M. Liinaharja, "On the performance of an adaptive GBN scheme in a time-varying channel," *IEEE Communications Letters*, vol. 4, pp. 143–145, April 2000.

[255] M. Zorzi, "Some results on error control for burst-error channels under delay constraints," *IEEE Transactions on Vehicular Technology*, vol. 50, pp. 12–24, Jan 2001.

[256] K. Ausavapattanakun and A. Nosratinia, "Analysis of Go-Back-N ARQ in block fading channels," *IEEE Transactions on Wireless Communications*, vol. 6, no. 8, p. 2793, 2007.

[257] C. Dong, L. L. Yang, J. Zuo, S. X. Ng, and L. Hanzo, "Energy, delay, and outage analysis of a buffer-aided three-node network relying on opportunistic routing," *IEEE Transactions on Communications*, vol. 63, pp. 667–682, March 2015.

[258] C. Dong, L. L. Yang, and L. Hanzo, "Performance of buffer-aided adaptive modulation in multihop communications," *IEEE Transactions on Communications*, vol. 63, pp. 3537–3552, Oct 2015.

[259] H. Song, J.-P. Hong, and W. Choi, "On the optimal switching probability for a hybrid cognitive radio system," *IEEE Transactions on Wireless Communications*, vol. 12, pp. 1594–1605, April 2013.

[260] A. U. Rehman, V. A. Thomas, L. L. Yang, and L. Hanzo, "Performance of cognitive selective-repeat hybrid automatic repeat request," *Accepted in IEEE Access*, Nov 2016.

[261] J. Lai, E. Dutkiewicz, R. P. Liu, and R. Vesilo, "Opportunistic spectrum access with two channel sensing in cognitive radio networks," *IEEE Transactions on Mobile Computing*, vol. 14, pp. 126–138, Jan 2015.

[262] E. Axell, G. Leus, E. G. Larsson, and H. V. Poor, "Spectrum sensing for cognitive radio : State-of-the-art and recent advances," *IEEE Signal Processing Magazine*, vol. 29, pp. 101–116, May 2012.

[263] E. Y. Park, M. G. Song, W. Choi, and G. H. Im, "Maximization of long-term average throughput for cooperative secondary system with harq-based primary system in cognitive radio network," *IEEE Communications Letters*, vol. 20, pp. 356–359, Feb 2016.

[264] J. G. Kim and M. M. Krunz, "Delay analysis of selective repeat ARQ for a markovian source over a wireless channel," *IEEE Transactions on Vehicular Technology*, vol. 49, pp. 1968–1981, Sep 2000.

[265] K. Ausavapattanakun and A. Nosratinia, "Analysis of selective-repeat ARQ via matrix signal-flow graphs," *IEEE Transactions on Communications,*, vol. 55, pp. 198–204, Jan 2007.

[266] L. Badia, M. Levorato, and M. Zorzi, "Markov analysis of selective repeat type II hybrid ARQ using block codes," *IEEE Transactions on Communications*, vol. 56, pp. 1434–1441, September 2008.

[267] L. Badia, "A markov analysis of selective repeat ARQ with variable round trip time," *IEEE Communications Letters*, vol. 17, pp. 2184–2187, November 2013.

[268] F. Chiti, R. Fantacci, and A. Tassi, "Evaluation of the resequencing delay for selective repeat ARQ in tdd-based wireless communication systems," *IEEE Transactions on Vehicular Technology*, vol. 63, no. 5, pp. 2450–2455, 2014.

[269] J. G. Proakis, M. Salehi, and G. Bauch, *Contemporary communication systems using MATLAB*. Nelson Education, 2012.

Subject Index

U

V

Author Index

C

D

E

F

G

H

I

J

K

L

M

N

O

P

Q

R

S

T

V

Z